AD_____

Award Number: DAMD17-02-1-0197

TITLE: Targeting of Drugs to ICAM for Treatment of Acute Lung Injury

PRINCIPAL INVESTIGATOR: Vladimir Muzykantov, Ph.D.

CONTRACTING ORGANIZATION: The University of Pennsylvania
Philadelphia, Pennsylvania 19104-6205

REPORT DATE: April 2005

TYPE OF REPORT: Annual

PREPARED FOR: U.S. Army Medical Research and Materiel Command
Fort Detrick, Maryland 21702-5012

REPORT DOCUMENTATION PAGE

Form Approved
OMB No. 074-0188

1. AGENCY USE ONLY (Leave blank)	2. REPORT DATE	3. REPORT TYPE AND DATES COVERED
	April 2005	Annual (11 Mar 2004 - 10 Mar 205)

4. TITLE AND SUBTITLE
Targeting of Drugs to ICAM for Treatment of Acute Lung Injury

5. FUNDING NUMBERS
DAMD17-02-1-0197

6. AUTHOR(S)
Vladimir Muzykantov, Ph.D.

7. PERFORMING ORGANIZATION NAME(S) AND ADDRESS(ES)
The University of Pennsylvania
Philadelphia, Pennsylvania 19104-6205

E-Mail: muzykant@mail.med.upenn.edu

8. PERFORMING ORGANIZATION REPORT NUMBER

9. SPONSORING / MONITORING AGENCY NAME(S) AND ADDRESS(ES)
U.S. Army Medical Research and Materiel Command
Fort Detrick, Maryland 21702-5012

10. SPONSORING / MONITORING AGENCY REPORT NUMBER

11. SUPPLEMENTARY NOTES
Original contains color plates: All DTIC reproductions will be in black and white.

12a. DISTRIBUTION / AVAILABILITY STATEMENT
Approved for Public Release; Distribution Unlimited

12b. DISTRIBUTION CODE

13. ABSTRACT (Maximum 200 Words)

In the third year, we experimentally tested and documented that anti-CAM/SOD and anti-CAM/SOD/catalase tandem conjugates targeted to endothelial cells detoxify diverse reactive oxygen species, thereby protecting cells against oxidative stress and toxicity via apoptotic and necrotic pathways, which permits testing of therapeutic effect of the conjugates in animal models in the fourth year. We designed, synthesized and tested a novel anti-CAM scFv/pro-urokinase recombinant fusion protein construct and documented that it is properly assembled and folded, thereby retaining ability to bind to endothelial cells and be activated by plasmin to produce local fibrinolysis. Further, this fusion protein accumulates in the pulmonary vasculature of naïve, but not PECAM-deficient mice and markedly enhances dissolution of pulmonary thrombi in vivo. We also tested potential adverse effects of accumulation of stable anti-CAM polymer conjugates inside the endothelial cells and detected no signs of cellular injury or compromised uptake and vesicular traffic inside the endothelial cells. These results imply that CAM-targeted delivery of antioxidant and anti-thrombotic drugs, directed to either intracellular or surface compartment of endothelium, provides safe means for treatment ALI/ARDS.

14. SUBJECT TERMS
Endothelium, immunotargeting, oxidant stress, thrombosis, ICAM-1

15. NUMBER OF PAGES
117

16. PRICE CODE

17. SECURITY CLASSIFICATION OF REPORT	18. SECURITY CLASSIFICATION OF THIS PAGE	19. SECURITY CLASSIFICATION OF ABSTRACT	20. LIMITATION OF ABSTRACT
Unclassified	Unclassified	Unclassified	Unlimited

Table of Contents

Targeting of Drugs to ICAM-1 for Treatment of Acute Lung Injury

A. Introduction and brief outline of main research topics pursued in the third year. The main goals of the project are to explore, test, optimize and prepare translation into the clinical domain of a new therapeutic strategy for a more effective containment of the Acute Lung Injury (ALI/ARDS). Both oxidative and thrombotic stresses in the pulmonary vasculature are important pathological factors in the development of ALI/ARDS. The proposed strategy is based on the concept that targeted delivery of antioxidant drugs (e.g., antioxidant enzymes, AOE, such as superoxide dismutase, SOD) and anti-thrombotic drugs (e.g., plasminogen activators, PA, such as urokinase, uPA) to the endothelial cells lining the luminal surface of blood vessels in the lungs would permit more effective and specific therapeutic interventions into developing or ongoing ALI/ARDS. Our results of the first two years of the grant and related studies in the lab indicate that conjugation of AOE and PA with antibodies to surface endothelial determinants functionally involved in ALI/ARDS, Ig-superfamily Cell Adhesion Molecules ICAM-1 and PECAM-1 (CAMs), can provide such a targeting. In agreement with the Statement of Work, in the third year we concentrated our main efforts on the Specific Aims 3 and 4, which both are near to completion now. We have pursued and achieved a substantial progress in the following research topics.

Testing of therapeutic activity of anti-CAM/SOD and anti-CAM/SOD/catalase tandem antioxidant conjugates. Previous reports documented that we have synthesized and characterized size, enzymatic and antigen-binding activities and targeting to endothelial cells in cell cultures and in intact animals of a series of new antioxidant conjugates, namely, anti-PECAM/SOD and tandem anti-PECAM/SOD/catalase. In this year, we characterized in depth models of endothelial oxidative stress (necrosis and apoptosis) and tested protective potential of these conjugates. Our results indicate that conjugates do intercept and detoxify reactive oxygen species (ROS) superoxide anion and H2O2 and protect cells from toxic effects of these ROS.

Design, assembly and testing of endothelial targeting and fibrinolytic activity of anti-CAM/urokinase recombinant fusion construct. In the previous report we described a new, unique affinity carrier for delivery of anti-thrombotic enzymes to the luminal surface of endothelial cells, namely, a single chain of variable fragment of anti-PECAM (scFv). The main effort of this year was focused on design, synthesis and characterization of a novel recombinant fusion protein construct combining anti-PECAM scFv and a pro-drug single chain urokinase plasminogen activator (i.e., anti-PECAM scFv-scuPA, indicated thereafter in the text for simplicity as scFv-uPA). We are proud to report that this state-of-the-art recombinant fusion construct, which can be in theory used in human clinical studies and medical practice, demonstrated highly promising therapeutic activity in an animal model of pulmonary thrombosis, characteristic of ALI/ARDS.

Safety of endothelial targeting of anti-CAM conjugates. We strongly felt that success of our studies demonstrating intracellular delivery of anti-CAM conjugates carrying therapeutic antioxidant enzymes in endothelial cells warrants addressing a question whether such conjugates can cause adverse or harmful in terms of endothelial physiology. We addressed this issue, directly related to the safety of the prospective ALI/ARDS treatments based on the use of anti-CAM conjugates and found that intracellular accumulation of anti-CAM conjugates, even containing non-degradable core, caused no overt acute harmful effect on

endothelium. Results of these cell culture studies, consciously initiated by the PI, provide the first line of evidence for safety of the proposed immunotargeting strategies.

Summary and perspective. Antioxidant and anti-thrombotic anti-CAM conjugates show a promise for improvement of ALI/ARDS containment. Preliminary "acute toxicity" studies support safety of the proposed interventions. In the fourth year, we will pursue experiments projected for the Specific Aim 3 (protection against oxidative stress in vivo) and Specific Aim 5 (combined protective effects of anti-CAM targeting of antioxidants and fibrinolytics).

B. Body of the Report (references to our papers are in *bold Italics*).

B.1. Targeting to endothelial cells and protective effects of anti-CAM/SOD and anti-CAM/SOD/catalase tandem antioxidant conjugates.

B.1.1. Cell culture models of endothelial oxidative stress, apoptosis and lipid peroxidation for testing of protective effects of anti-CAM/SOD and anti-CAM/SOD-catalase tandem conjugates. Anti-PECAM/SOD-catalase is expected to be more effective than individual conjugates against xanthine oxidase (XO) insults, in which both O_2^- and H_2O_2 are formed (O_2^-/H_2O_2 yield may be varied by using hypoxanthine *vs* xanthine). Therefore, in the first part if the study we established this model system in the lab, in order to characterize the duration of the protective effect, kinetics of lysosomal degradation and effects of auxiliary drugs (e.g., chloroquine and nocadozole), using optimal targeting means for SOD and catalase in xanthine/XO model.

In the first series we used a 30 min treatment of endothelial cells (HUVEC) with an organic lipid peroxide 4-HNE as a model oxidant pro-apoptotic agent to as a positive control of apoptosis. After 24 h, cells were washed with PBS, lysed and analyzed by electrophoresis. Caspase-3 activation (a marker of apoptosis) was studied by Western blot analysis using anti-caspase3 antibody. 4-HNE activated procaspase-3 in a dose-dependent manner. In the used concentration range of 4-HNE we found an increase in active caspase3, but not significant drop of total pool of procaspase3 (not shown).

In the next series, we tested endothelial cell necrotic and apoptotic death induced by exposure to hypoxanthine-xanthine oxidase enzymatic syste, HX-XO. HX-XO system is widely-used model of oxidative stress that injure cell by formation of Reactive Oxygen Species (ROS) superoxide anion and hydrogen peroxide. We added HX and XO to cell medium to initiate the production of these ROS. In the first series, necrotic cell death has been determined by release of ^{51}Cr isotope from pre-labeled cells, indicating irreversible damage to the plasma membrane. As Fig 2 below shows, ROS generation by XO from HX caused dose-dependent necrotic death of HUVEC.

In the separate series, in order to detect delayed toxicity, more characteristic of apoptotic pathway, cell viability was analyzed in 24 h after the exposure to oxidative stress by fluorescent microscopy using Live/Dead double staining (Fig. 3, below). XO alone didn't show any cell toxicity. However, addition of HX resulted in significant cell death at HX concentration of 100 μM and higher. Inhibition of XO by allopurinol that was added in the medium along with HX lead to abolishing HX-XO cytotoxicity. Further we analyzed markers of apoptosis, namely conversion of procaspase-3, PARP and ROCK I in treated cells using Western blotting. Procaspase3 level was significantly diminished at 50 μM of HX and higher

indicating that procaspase3 processing appears at lower concentration than detectable cell death (Fig. 3, below). The levels of PARP and ROCK I cleavages followed similar to caspase3 pattern. These findings indicate that ROS generation by XO induces either necrotic or apoptotic endothelial death, depending on dose and time of XO exposure. We used 100 μM HX in experiments on cell protection by immunoconjugates.

B.1.2. Protective effects of anti-CAM/SOD and anti-CAM/SOD-catalase tandem conjugates in HX-XO-model of necrotic endothelial cell death. To study the protection of endothelial cells against HX-XO-induced oxidative stress we first check a protection by free unconjugated SOD. SOD was added in cell culture medium at varied concentration altogether with HX and XO. We did not find any protection by free SOD (not shown).

In the next series, we investigated the protective properties of SOD conjugated to anti-PECAM antibodies. Cells were pretreated with the immunoconjugates for 1 h at 37°C, unbound fraction was removed with fresh medium, and cells were exposed to oxidative stress. We observed that cells treated with anti-CAM/SOD conjugates up to 10 μg of SOD per well were protected compared to cells untreated with the conjugates (Fig.1).

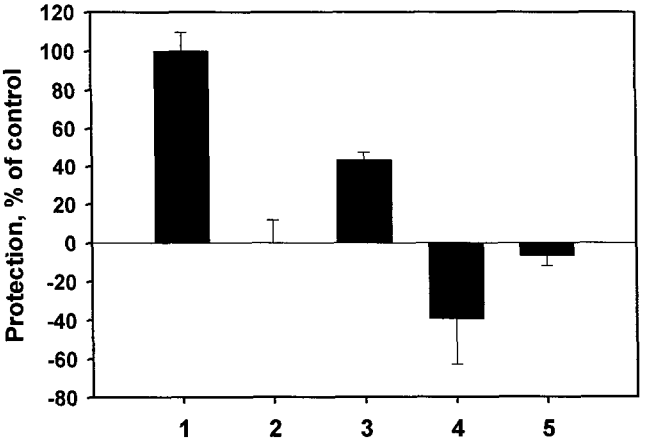

Figure 1. Anti-CAM/SOD conjugate protects endothelial cells from necrotic death induced by 200 μM HX and 25 mU/ml XO. Bar 1, cells treated with 100 μM allopurinol (XO inhibitor that provides complete protection and thus verified that cellular toxicity is induced by enzymatic activity of Xo, generating ROS); bar 2, non-protected cells; bar 3, cells treated with anti-CAM/SOD conjugates (7 μg of SOD/well); bar 4,.cells treated with 10 μg of free SOD/well (no protection); bar 5: cells treated with control IgG/SOD conjugate.

Binding of the conjugates to the endothelial cells directly correlated with initial quantity added (please see Figure 6 in the previous annual report) indicating that endothelial cell surface PECAM was far from saturation in the range used in the experiments. However, the anti-PECAM/SOD conjugates showed bell-shaped protection curve: the maximal protection (~50%) was reached at a dose of 2.5 μg of SOD per well, while further increasing of SOD targeting resulted in lower protection suggesting that excess of SOD may damage cells as it has been demonstrated earlier both in vivo and vitro, due to overproduction of H2O2. To see the importance of hydrogen peroxide we prepared anti-CAM/catalase conjugates as described previously in the pertinent publications (Shuvaev et al, 2004). Cells were pretreated in similar manner as it was done with anti-PECAM/SOD. Binding of anti-CAM/catalase conjugate protected in a dose-depending manner and nearly full protection was reached at a dose of 5-20 μg of catalase per well.

Since these series revealed that both ROS, superoxide anion and H2O2, contribute to toxicity, in the following series, we evaluated protective capacity of a tandem anti-PECAM/SOD/catalase conjugate that, in theory, could combine protective mechanisms provided by both antioxidant enzymes and thus afford maximal protection.

We found that anti-PECAM/SOD/catalase tandem conjugate protects EC against oxidative stress caused by xanthine oxidase. Figure 2, below, shows protection against necrotic cell

death induced by a large dose of XO. In pilot studies, both anti-PECAM/catalase and anti-PECAM/SOD provided partial protection against XO/X, yet did not protect as effectively as the tandem conjugates. However, level of XO-generated H_2O_2 did not exceed 15-20 uM, which is far from cytotoxic levels. This result, taken in the context of the known ability of O_2- and H_2O_2 to produce hydroxyl radical via the direct Haber-Weiss reaction that is not effective in pure systems, but is markedly accelerated in the presence of trace amounts of transient metals, implies that single AOE conjugates reduce toxicity of XO/X system by intercepting the individual reactants of the Haber-Weiss reaction. Hence, the targeting of tandem SOD/catalase will afford the most effective protection via interception of both ROS, prevention of $OH^{\cdot}$ formation and protection against H_2O_2.

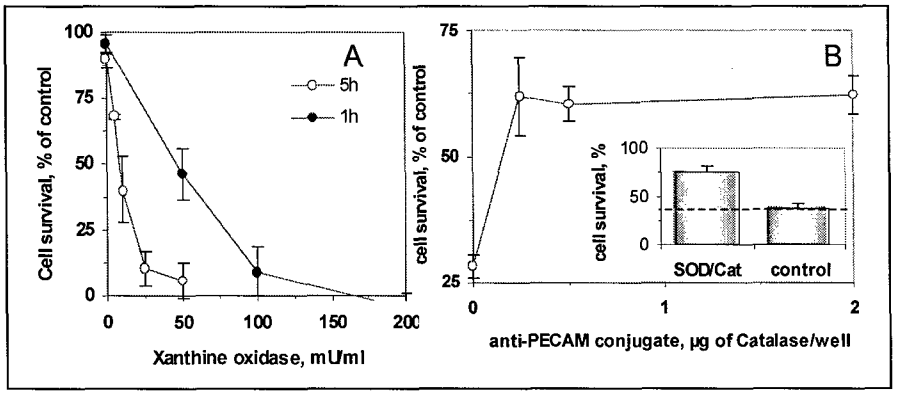

Fig.2. Toxicity of xanthine/XO system to cells and protection by tandem anti-PECAM/SOD/catalase conjugate. (A) The HUVEC medium was replaced by RPMI+20 mM HEPES+20 µM xanthine. Cell death was measured by ^{51}Cr release 1 and 5 h after addition of indicated dose of XO. (B) Protection of HUVEC against xanthine/XO-induced oxidative stress. Cells were treated with SOD/Catalase conjugate, washed and exposed to 20 µM xanthine/25 mU/ml XO. Cell death was determined 5 h later as in A. Insert: effects of anti-PECAM/SOD-catalase *vs* control anti-PECAM conjugated with an inert protein. Dash line shows survival of control HUVEC exposed to xanthine/XO.

B.1.3. Anti-PECAM/SOD/catalase conjugate protects endothelial cells against apoptosis induced by xanthine oxidase (XO). Results of determination of enzymatic activity presented in the previous annual report indicated that both enzymes in anti-PECAM/SOD/catalase are active (Fig.5). Since this conjugate protect EC against toxicity caused by XO-produced O_2- and H_2O_2 assay (Fig. 2), we tested whether it protects against apoptotic death as well. Depending on dose of hypoxanthine and time of incubation, XO induces nearly 100% lethality in HUVEC (Fig. 3a), accompanied by degradation of ROCK-1, characteristic of apoptotic activation of caspases (Fig.3b). Anti-PECAM/SOD/catalase attenuated apoptotic degradation of ROCK-1 in a dose dependent manner (Fig. 3c), confirming effective antioxidant protection by the tandem AOE conjugate. Therefore, ROS detoxification attained by SOD and catalase targeted to endothelial cell adhesion molecule affords protection against both necrotic (see above) and apoptotic pathways of ROS toxicity.

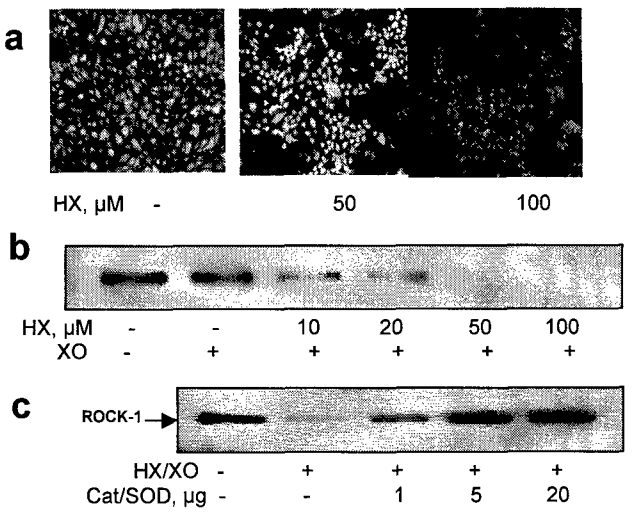

Figure 3 Anti-PECAM/SOD/catalase protects EC against apoptosis. Cells were treated with 25 mU/ml XO in the presence of hypoxanthine (HX). (a) Cell viability 24 h after exposure to HX/XO examined by Live/Dead kit (Molecular Probe). Live cells: green, dead cells: red. (b) Induction of apoptosis by HX/XO: Western blot analysis of ROCK-1 degradation, a marker for activation of apoptotic caspases. (c) Anti-PECAM/SOD/catalase blocks ROCK-1 degradation in EC treated with 25 mU/ml XO and 100 µM HX.

B.1.4. Targeting of anti-CAM antioxidants alleviates oxidative stress induced by ROS produced by endothelial cells in response to ischemia. Encouraged by these positive

results of antioxidant protection attained by anti-CAM/SOD and anti-CAM/SOD/catalase tandem conjugate in static culture of endothelial cells exposed to chemically generated external ROS, we advanced our experiments into a greatly more physiological model, in which flow-adapted endothelial cells grown in hollow fibers cartridges are challenged with an abrupt cessation of perfusion. Our previous studies (Wei, 1999; Al-Mehdi, 2000) showed that this leads to activation of intracellular ROS-generating enzymatic system(s) in endothelial cells, first of all, endothelial NDAPH-oxidase, leading to oxidative stress. To date, models of perfused and flow-adapted endothelial cells represent the most advanced and physiologically relevant in vitro correlate to human vascular physiology and pathology.

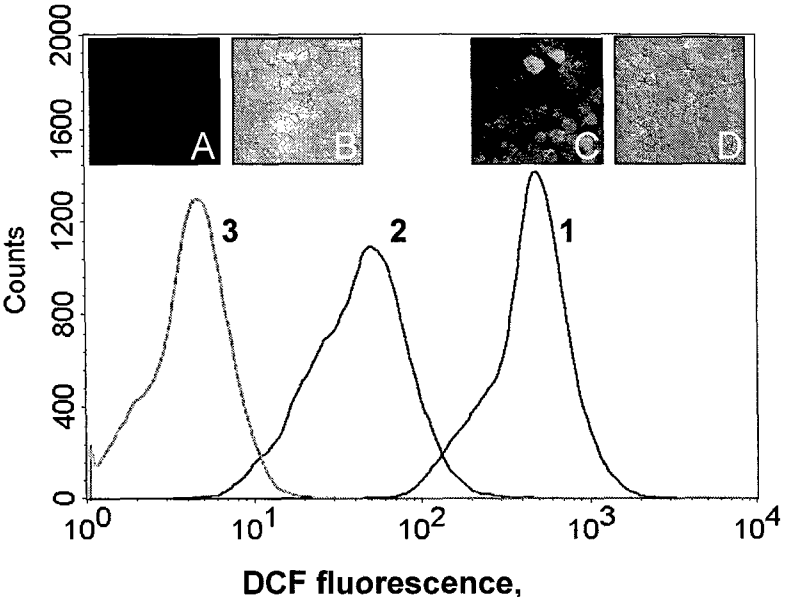

Fig.4. Protection of endothelial cells against ischemia-mediated ROS generation. Histogram shows FACS analysis of DCF fluorescence in control ischemic cells (trace 1) and in cells treated with mixture of free catalase, SOD and anti-PECAM (trace 2) and equal amount of PECAM/SOD/catalase conjugate (trace 3). Inset, fluorescent microscopy (A and C) and phase contrast images (B and D) of untreated (A-B) and conjugate-treated cells (C-D).

In order to test whether AOE immunotargeting intercepts endogenous ROS produced by endothelial cells, we utilized a model of flow-adapted HUVEC, which produce O_2- or/and H_2O_2 via NADPH-oxidase dependent pathway in response to ischemia. To detect ROS, we preloaded cells with DCF, a probe that fluoresces in response to over-production of ROS. Perfusion of a mixture of non-conjugated SOD and catalase afforded only partial reduction of DCF fluorescence, while anti-PECAM/SOD/catalase conjugate abolished fluorescence induced by ischemia (Fig. 4).

B.1.5. Summary of testing of anti-CAM targeting antioxidant conjugates. Taken together, our data obtained in the third year of the grant unequivocally support our hypothesis that CAM-directed targeting of antioxidant enzymes into endothelial cells might provide an effective maneuver for protection of pulmonary vasculature against oxidative stress, a key pathological component of ALI/ARDS. In particular, we found that anti-CAM/SOD and anti-CAM/SOD/catalase tandem conjugate effectively intercept and detoxify their ROS substrates, superoxide anion and H2H2 (both diffusing into endothelium from outside or generated by the cells itself) and thus protect against both necrotic and apoptotic pathways of ROS toxicity. Protective potency of anti-CAM/SOD/catalase tandem conjugate exceeds that of conjugates possessing individual activities, such as anti-CAM/SOD. Based on the achieved progress, the Specific Aim 3 is currently ~75% complete. In the next year, protective features of these novel treatments will be tested in animal models.

B.2. Design, synthesis and characterization of anti-CAM/urokinase recombinant fusion construct, anti-PECAM scFv/scuPA. In the year 2, we designed a single chain fragment of anti-PECAM in order to design a fusion protein combining the features of CAM

targeting and activation of thrombolysis. This section describes our work in this direction. Figures to this section are attached to the text.

B.2.1. Introduction. It is critically important that anti-thrombotic activity be maintained on the surface of endothelium. Endothelial cells do not internalize antibodies to PECAM and ICAM [Muzykantov 1999; Murciano, 2003]. However, multivalent conjugates, formed by chemical coupling of drugs to anti-PECAM or anti-ICAM, cross-link target adhesion molecules and initiate endothelial endocytosis [Muro 2003; 2004]. Ensuing internalization of conjugates would limit their utility, despite high enzymatic potency and targeting to endothelial cells *in vivo* [Muzykantov 1996; Murciano 2003]. Fc-fragment-mediated side effects (e.g., activation of leukocytes or complement) and technological hurdles in production and quality control also represent potential downsides of chemical conjugates. To circumvent these problems, we have developed recombinant constructs that fuse PAs with monovalent single chain antibody fragments (scFv).

In this study we used urokinase (uPA) to create a prototype modular fusion construct for vascular immunotargeting to the endothelial luminal surface. Urokinase is produced as a 54 kDa single-chain molecule (scuPA) that has little constitutive protease activity and its cleavage by plasmin at Lys^{158}-Ile^{159} generates a disulfide-linked two-chain molecule (tcuPA) with a much higher plasminogen activating rate. Low-molecular-weight (lmw)-scuPA is generated by specific hydrolysis of the Glu^{143}-Leu^{144} peptide bond and demonstrated identical plasminogen activating potency compared with full-length scuPA. Thus, targeting lmw-scuPA construct(s) offers a potential advantage of plasmin-mediated activation of a latent pro-drug into a fully active fibrinolytic agent in sites of thrombosis. In addition, lmw-scuPA, lacking the receptor-binding domain, does not bind to the widely expressed urokinase receptor (uPAR, CD87) capable of altering cell adhesion and migration, among other effects on cell behavior. Thus, endothelial binding and activity of the anti-PECAM/scuPA construct driven primarily by the antibody component enhance delivery specificity and safety.

B.2.2. Cloning synthesis and biochemical characteristics of anti-PECAM scFv-scuPA. The variable regions of the P-390 antibody heavy and light chains were cloned into the plasmid pww152. The variable heavy chain and light chain were assembled into a scFv fragment by overlap extension PCR and cloned into the expression plasmid pswc4. 390scFv was amplified for cloning into the expression plasmid pMT/Bip/V5 using the upstream primer sen390 (5'-GGACTAGTCAGGTTACTCTGAAAGCGTCTGGCCC-3'), which introduces a restriction site for *Spe*I at the 5' end, and the downstream primer rev390 (5'-ATAAGAATGCGGCCGCGCCGGAAGAGCTACTACCCGATGAGGAAGAACGCAATTCCACCTTGG-3'), which appends the sequence of a short peptide linker $(Ser_4Gly)_2$ and a *Not*I restriction site. lmw-scuPA (Leu^{144}-Leu^{411}) was amplified with the primers senUK (5'-ATAAGAATGCGGCCGCATTAAAATTTCAGTGTGGCC-3'), which introduces a *Not*I restriction site at the 5' end, and downstream revUK (5'-CCGCTCGAGTCAGAGGGCCAGGCCATTC-3') to introduce an *Xho*I restriction site at the 3' end. The 390 scFv-lmw scuPA construct was assembled as follows: first, two PCR products were purified and digested with *Spe*I, *Not*I and *Not*I, *Xho*I, respectively. Second, the two digested fragments were ligated and cloned into *Spe*I and *Xho*I sites of the drosophila expression vector pMT/Bip/V5. Successful cloning was confirmed by restriction analysis of recombinant plasmids and by automated genetic sequencing.

An expression vector for the generation of anti-PECAM single chain variable fragment (scFv)-uPA was designed as illustrated in Figure 5A and cloned as follows. Anti-PECAM scFv was assembled from PCR-amplified cDNAs encoding the variable heavy and light chain regions of the rat monoclonal antibody directed against mouse PECAM-1 using hybridoma clone mAb 390 and a $(Gly_4Ser)_3$ linker sequence (Fig. 5B). An additional construct, a scFv with a tag encoding soluble human recombinant tissue factor (sTF-tag), was produced and expressed in *E.coli* to test binding.

DNA encoding scFv was fused with the cDNA encoding lmw-scuPA using a $(Ser_4Gly)_2Ala_3$ linker, yielding the plasmid pMT-BD1 that encodes for the full-length fusion protein scFv-uPA (scFv-uPA, unless specified otherwise) (Fig. 5C). scFv-uPA expression was induced in S2 drosophila cells as previously described, and the fusion protein was purified from cell culture medium using an uPA antibody affinity column with a yield of 5 mg/L. The identity of the protein was confirmed by Western Blotting using an anti-uPA antibody, revealing a single uPA-antigen containing band of a predicted size ~60kD (Fig. 5D). SDS-PAGE of purified scFv-uPA also revealed a single band migrating with a predicted molecular weight of 60 kDa (Fig. 5E). Plasmin converted the lmw-scuPA moiety in the fusion construct into its two-chain derivative lmw-tcuPA, evident on SDS-PAGE under reducing conditions (Fig. 5E): the construct was cleaved into two nearly identical fragments, the N-terminal portion of fusion comprising scFv linked to amino acids Leu^{144}-Lys^{158} of uPA (30 kD) and the B-chain of uPA (amino acids Ile^{159}-Leu^{411}, MW 30 kD), co-migrating as a single band.

B.2.3. Binding of scFv and scFv-uPA to PECAM-expressing cells. Fluorescent microscopy using biotinylated scFv-uPA fusion protein and FITC-labeled streptavidin showed that scFv-uPA bound to a human mesothelioma cell line (REN) transfected with cDNA encoding murine PECAM-1 (REN/PECAM), but not to control REN cells (Fig. 6B). Specific binding of scFv-uPA to PECAM-expressing cells was also confirmed by ELISA, in which half-maximal binding was reached at 38 nM, consistent with the FACS analysis (Fig. 6C). Addition of free anti-PECAM IgG inhibited scFv-uPA binding to PECAM-expressing cells, confirming the specificity of targeting (Fig. 6D).

B.2.4. Enzymatic and fibrinolytic activity of anti-PECAM scFv-uPA. Plasmin converted the scFv-uPA fusion protein into a construct containing two-chain urokinase (Fig. 6E). To verify that this produces an active urokinase from a latent pro-drug, we tested its enzymatic activity by a chromogenic substrate specific for plasminogen activators, but not for plasmin itself. Plasmin induced a marked, dose dependent increase in the scFv-uPA amidolytic activity, from a basal level of ≤ 5,040 IU/mg to 46,590 IU/mg (Fig. 7A). Further, scFv-uPA lysed preformed fibrin clots containing plasminogen to the same extent as free lmw-scuPA (Fig. 7B). Therefore, N-terminal fusion of the scFv to scuPA did not compromise its folding, ability to become activated by plasmin or its ability to initiate fibrinolysis.

To test whether the antibody fragment delivers functionally active urokinase to the cell surface, we tested the amidolytic activity of scFv-uPA in culture wells containing REN/PECAM *vs* control REN cells. The chromogenic activity assay showed that the fusion protein developed enzymatic activity after binding to REN/PECAM cells, nut not REN cells (Fig. 7C), and that addition of the parental anti-PECAM IgG inhibited the delivery of uPA activity, confirming the specificity of targeting (Fig. 7D).

B.2.5. Vascular immunotargeting of scFv-uPA in mice. To test the biodistribution and PECAM targeting of our constructs, they were radiolabeled with ^{125}I and injected into mice. One hour after IV injection, free ^{125}I-lmw-scuPA showed a similar distribution in wild type and PECAM KO mice (Fig. 8A). Notably, the organ-to-blood ratio, a parameter that reflects preferential uptake in organs of interest, did not exceed 1 in any organ, except for the liver, which serves as a clearance site for IgG and plasminogen activators from blood. This result shows that free lmw-scuPA injected in circulation does not bind specifically to endothelial cells (Fig. 8B).

PECAM KO mice provide an *in vivo* test of immunotargeting specificity. Accordingly, the organ distribution of ^{125}I-labeled scFv-uPA in PECAM KO mice was nearly identical to that of non-targeted lmw-scuPA (Fig. 8A). In contrast, the fusion protein accumulated preferentially in the lungs and, to somewhat lesser extent, in other highly vascularized organs of wild type mice expressing PECAM on the surface of endothelium (Fig. 8A). The scFv-uPA immunospecificity index (ISI, ratio of tissue uptake of targeted *vs* non-targeted counterparts, a marker of targeting specificity) attained 10 in the lungs and 5 in the heart of wild type mice (Fig. 8C). In contrast, scFv-uPA ISI did not exceed 1 in the PECAM KO mice, showing no specific accumulation in organs in the absence of endothelial targeting.

Anti-PECAM scFv-uPA was cleared from the circulation more rapidly than non-targeted lmw-scuPA (Fig. 8A, 9A). This was likely due to endothelial targeting leading to depletion of circulating pool, since blood level of scFv-uPA and scuPA was identical in PECAM KO mice (Fig. 8A). However, 15 min after injection in WT mice, the level of both formulations decreased to <5% ID per gram of blood (Fig. 9A). Consistent with this observation, uptake of the fusion protein in the lung of WT mice was rapid and reached its maximum 5 min post injection (Fig. 9B). After an initial 30% decline, the pulmonary level of scFv-uPA was relatively stable over several hours. Due to blood clearance, the lung/blood ratio reached its peak 15-30 min after injection and remained stably elevated for the duration of the study.

B.2.6. Endothelial targeting of anti-PECAM scFv-uPA facilitates lysis of pulmonary emboli. Given these favorable targeting and kinetic characteristics, we tested the effect of scFv-uPA delivery to endothelial PECAM in a mouse model of acute pulmonary thrombosis induced by injecting radiolabeled fibrin emboli (3-5 μm in diameter). After IV injection these emboli form aggregates that lodge preferentially in the pre-capillary bed of the lungs[38] [Murciano, 2002]. To model prophylactic fibrinolysis, we injected various doses of scFv-uPA *versus* non-targeted lmw-scuPA 10 min prior to injecting ^{125}I-emboli and measured the residual isotope in the lungs 1 hr later. At all doses tested, the fusion protein produced significantly more effective dissolution of pulmonary emboli than enzymatically identical doses of non-targeted lmw-scuPA ($P < 0.025$) (Fig. 10). This effect could not be attributed to the potential benefit of blocking of PECAM-1, since a mixture of lmw-scuPA and anti-PECAM produced the same fibrinolysis as lmw-scuPA.

B.2.7. Legends to figures for the section B2 (please see attachment #10).

Figure 5. Molecular design, expression and characterization of anti-PECAM scFv-lmw scuPA. (A) Schematic diagram of the cloning strategy for the fusion construct pMT-BD1. Variable domains of heavy chain and light chain were linked by a $(Gly_4Ser)_3$ linker, and then fused to the N-terminus of lmw-scuPA by a $(Ser_4Gly)_2Ala_3$ linker. (B) Variable domains of heavy chain (H chain) and light chain (L chain) of P-390 were amplified and

assembled into full-length scFv. M, DNA standards. (C) lmw-scuPA and anti-PECAM scFv were ligated and cloned into *Spe*I and *Xho*I sites of the pMT expression vector. *Xho*I and *Spe*I digestion of the fusion construct (fusion). (D) Western blot analysis of 40 µl of culture medium alone or after induction by 0.5 mM $CuSO_4$. 50 ng and 200 ng of purified fusion protein were blotted to compare the expression level. (E) 10-15 % gradient SDS-PAGE analysis of purified fusion protein with or without plasmin treatment under non-reduced or reduced conditions.

Figure 6. Anti-PECAM scFv and scFv-scuPA fusion proteins bind specifically to cells expressing mouse PECAM. (A) FACS analysis of dose-dependent binding of parental anti-PECAM IgG mAb 390 (upper panel) and anti-PECAM scFv tagged with soluble tissue factor (lower panel) to mouse endothelial cells bEnd3. Black line: cells only; green line: cells with secondary and tertiary antibody; red line: cells incubated with tagged scFv and secondary/tertiary antibody. sTF-tag alone did not bind to bEnd3 cells (not shown). (B) FITC-streptavidin staining of REN/PECAM (left) *vs* control REN (right) cells after incubation with biotinylated anti-PECAM scFv-scuPA (40X magnification). (C) ELISA using urokinase antibody reveals binding curves of anti-PECAM scFv-scuPA fusion protein to REN/PECAM (closed circles) vs REN (open circles) cells. (D) Inhibition of binding of fusion protein to REN/PECAM cells by parental anti-PECAM IgG mAb 390, determined by ELISA.

Figure 7. Urokinase activity of free and cell-bound anti-PECAM scFv-lmw scuPA. (A) Amidolytic activities of fusion protein generated at different molar ratios of plasmin to scFv-uPA (mean of two preparations). (B) Fibrinolytic activity using a fibrin plate. Equal doses (from left: 200, 100, 50 and 0 ng) of lmw-tcuPA, lmw-scuPA and scFv-lmw scuPA fusion protein were incubated on a fibrin-coated plate at 37 °C and areas of lysis were identified after staining fibrin with Trypan blue. (C) Amidolytic activity associated with the cell surface of PECAM-negative REN (open circles) and PECAM-transfected (closed circles) REN cells was determined by conversion of chromogenic substrate after incubation with various amounts of fusion proteins. (D) Pre-incubation of REN/PECAM cells with parental anti-PECAM IgG, mAb 390, reduces binding of enzymatically active scFv-uPA.

Figure 8. *In vivo* biodistribution of anti-PECAM scFv-lmw scuPA and lmw-scuPA. 10 µg of fusion protein or lmw-scuPA were mixed with 0.25 µg of radiolabeled tracer protein and injected i.v. to wild type or PECAM KO mice, respectively. One hour later, tissue uptake was determined. (A) Percentage of injected dose per gram tissue (%ID/g). Note that scFv-uPA, but not scuPA, shows preferential uptake in the lungs and other vascularized organs of WT, but not of PECAM KO mice. (B) Organ-to-blood ratio for various organs. Broken line: blood level, ratio equal to 1. (C) Immunospecificity index (ISI), calculated as ratio of organ-to-blood ratios of targeted and non-targeted counterpart. The broken line shows an ISI equal to 1, reflecting equal tissue levels of targeted and non-targeted counterparts.

Figure 9. Kinetics of *in vivo* pulmonary targeting and blood clearance of anti-PECAM scFv-scuPA. (A) Kinetics of blood clearance of targeted fusion construct (closed circles) and non-targeted scuPA (open circles). (B) Kinetics of the targeted fusion protein levels in lungs (closed circles) and blood (open circles). Fusion protein exhibited a rapid and prolonged accumulation in lung tissues. Lung-to-blood ratios at indicated time points were calculated (inset).

Figure 10. Accumulation of fusion protein in pulmonary vasculature facilitates local fibrinolysis. (A) Dissolution of ^{125}I-labeled microemboli lodged in mouse pulmonary vasculature by bolus injection of fusion protein, the amidolytically equivalent amount of lmw-scuPA and a mixture of lmw-scuPA and parental antibody, respectively. Thrombolytic potency was expressed as percent lysis *vs.* dose administrated. (B). Simplified model for a proposed strategy of thromboprophylaxis by vascular immunotargeting of genetically engineered anti-PECAM scFv-uPA fusion protein.

B.2.8. Summary of anti-thrombotic fusion protein targeting to the pulmonary endothelium. Our data accumulated in the third year of funding and shown above indicate that: i) molecular design, recombinant assembly and expression of scFv-uPA yields a properly folded fusion construct of correct size (60 kD) possessing both antigen-binding and plasminogen-activating activities; ii) lmw scuPA moiety of the construct is a pro-drug that can be cleaved and thereby activated by plasminogen into a fully active fibrinolytic that exerts high enzymatic activity and lysis of fibrin clots; iii) the fusion construct specifically binds to endothelial cells in culture and in naïve animals, but not in the vasculature of PECAM-deficient animals; iv) the fusion protein accumulates in the pulmonary vasculature; v) it does facilitate dissolution of pulmonary thrombi in animals. Taken together, these data support our hypothesis that anti-PECAM scFv-uPA construct can be used to improve management of pulmonary thrombosis and fibrin deposition in ALI/ARDS. This hypothesis will be further tested in animal models of ALI/ARDS in the fourth year of the grant. Based on this progress, the Specific Aim 4 is currently ~75% complete.

B3. Targeting of anti-CAM conjugates does not cause overt pathological alterations in the endothelial cells. A body of evidence accumulated so far in this project and in other studies in the lab that explore strategies for CAM-directed immunotargeting of therapeutics to and into endothelial cells indicate that this approach indeed might provide a basis for a new, highly specific and effective therapeutic interventions for containment of ALI/ARDS (and, likely in many other human pathologies). However, one cannot ignore a question, whether binding and, further, intracellular delivery and accumulation of anti-CAM conjugates will damage endothelial cells or compromise their functions and comfort? In this section we describe first series of experiments designed specifically to address these safety-related issues. Color versions of the figures shown in the section can be seen in the attached paper by Muro et al, Blood 2005 (please see this paper for more detailed explanations of this study).

B.3.1. Introduction and design of the study. In order to prepare swift and effective translation of our research into pre-clinical and clinical domains, we consciously decided to initiate a pilot "early phase" toxicity study of anti-CAM conjugates. We determined whether intracellular accumulation of anti-CAM/conjugates cause cell death or disrupts constitutive endothelial vesicular transport, e.g. due to overload of this compartment by residing conjugates. In this study we utilized a non-degradable polymer carriers conjugated with anti-ICAM (anti-ICAM/nanocarriers, or anti-ICAM/NC), thus augmenting potentially harmful effects of a prolonged intracellular residence of targeted cargoes, which could be not as evident in case of protein conjugates that are degraded in endothelial lysosomes within a few hours.

B.3.2. Intracellular accumulation of anti-CAM conjugates does not affect constitutive fluid uptake and vesicular traffic in endothelial cells. To evaluate the effect of

nanocarriers on the uptake of Texas Red dextran, HUVEC were incubated with either mock or green-labeled anti-ICAM/NC for 30 min at 4°C, then washed and warmed to 37°C for 3 h, to enable trafficking of the internalized nanocarriers to lysosomes. The cells were then incubated with Texas Red dextran for 15 min at 37°C, washed and fixed in cold. The number of dextran-labeled vesicles and the percentage of these that trafficked to lysosomal compartments preloaded with nanocarriers were determined from merged fluorescent micrographs. Trafficking of Texas Red dextran to FITC-labeled anti-LAMP-1 positive compartments by unloaded cells was used as a control. Also, HUVEC were incubated for 48 h after internalization of anti-ICAM/NC, then cells were stained using the Live/Dead kit as described bellow to determine the fraction of cells retaining intracellular nanocarriers, morphological appearance of the cell monolayer, total number of cells per sample, and cell viability.

To test whether anti-ICAM/NC affect constitutive endocytosis and lysosomal traffic, we used fluorescent dextran as a fluid phase marker. HUVEC treated with either single or double combinations of pharmacological inhibitors of internalization via clathrin-coated pits (MDC), caveoli (filipin), or macropinocytosis (amiloride) were still able to internalize dextran (Fig. 11A). The fact that dextran uptake could only be inhibited by simultaneous treatment with drugs affecting all three pathways, confirms that it enters EC through all these endocytic mechanisms. Furthermore, dextran was similarly internalized and delivered to lysosomes by control cells and cells that had internalized a saturating dose of anti-ICAM/NC (Fig. 11B and 11C). Therefore, anti-ICAM/NC internalization via CAM-mediated endocytosis does not affect other endocytotic pathways in endothelial cells.

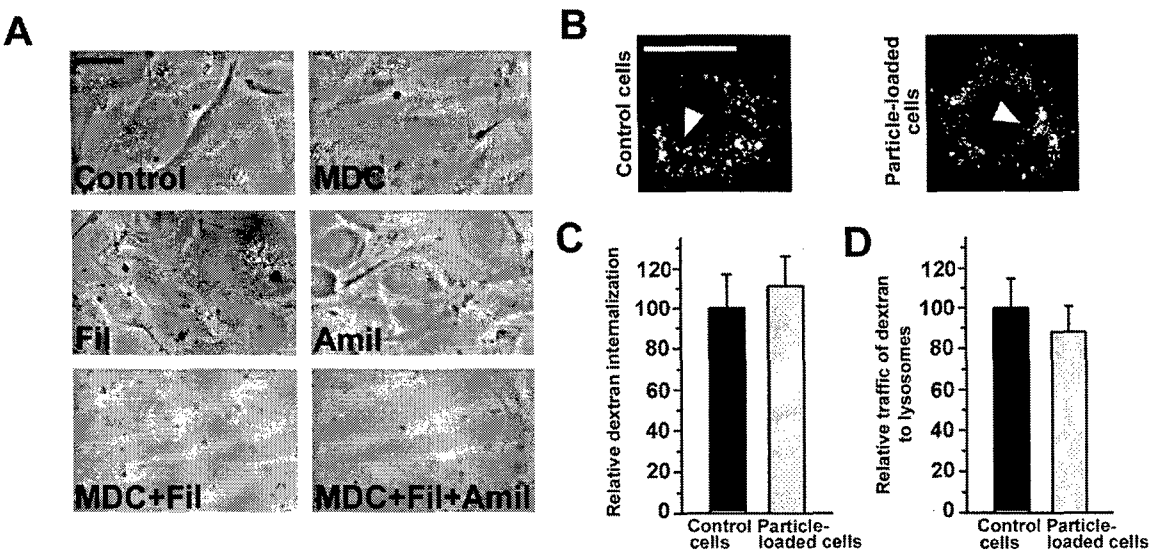

Figure 11. Loading cells with anti-ICAM/NC does not affect endocytosis and trafficking of dextran. (A) Internalization of the fluid phase marker, fluorescent Texas Red Dextran, by either control HUVEC or cells treated with pharmacological inhibitors of internalization by clathrin-coated pits (MDC), caveoli (Filipin = Fil), or macropicocytosis (Amiloride = Amil). Note that TR Dextran enters cells via diverse endocytic pathways. (B) HUVEC, either control or pre-loaded with a saturating dose anti-ICAM/NC, were incubated with TR Dextran, and traffics to lysosomes. Yellow color (arrowhead): co-localization of TR Dextran with lysosomes labeled in green by FITC-anti-LAMP-1 (control cells) or FITC-anti-ICAM/NC (particle-loaded cells). Bar = 10 μm. (C) The number of TR Dextran-labeled endocytic vesicles per cell and (D) percent of these localizing to lysosomal compartments was determined by fluorescence microscopy. Data are mean ± SEM from n > 10 cells.

B.3.3. Prolonged retention of anti-CAM conjugates does not compromise viability and proliferation of endothelial cells. Anti-ICAM/NC still resided in intracellular vesicular compartments 48 h after uptake by HUVEC (Fig. 12A); 97 ± 12 % of the cells still contained nanoparticles at this time (Fig. 12B). Neither cell number, nor morphology of the endothelial monolayer, nor cellular viability was affected by the prolonged intracellular retention of nanocarriers (Fig. 12B-C). Interestingly, an almost equal share of intracellular nanoparticles could be identified in dividing endothelial cells (insert in Fig. 12A).

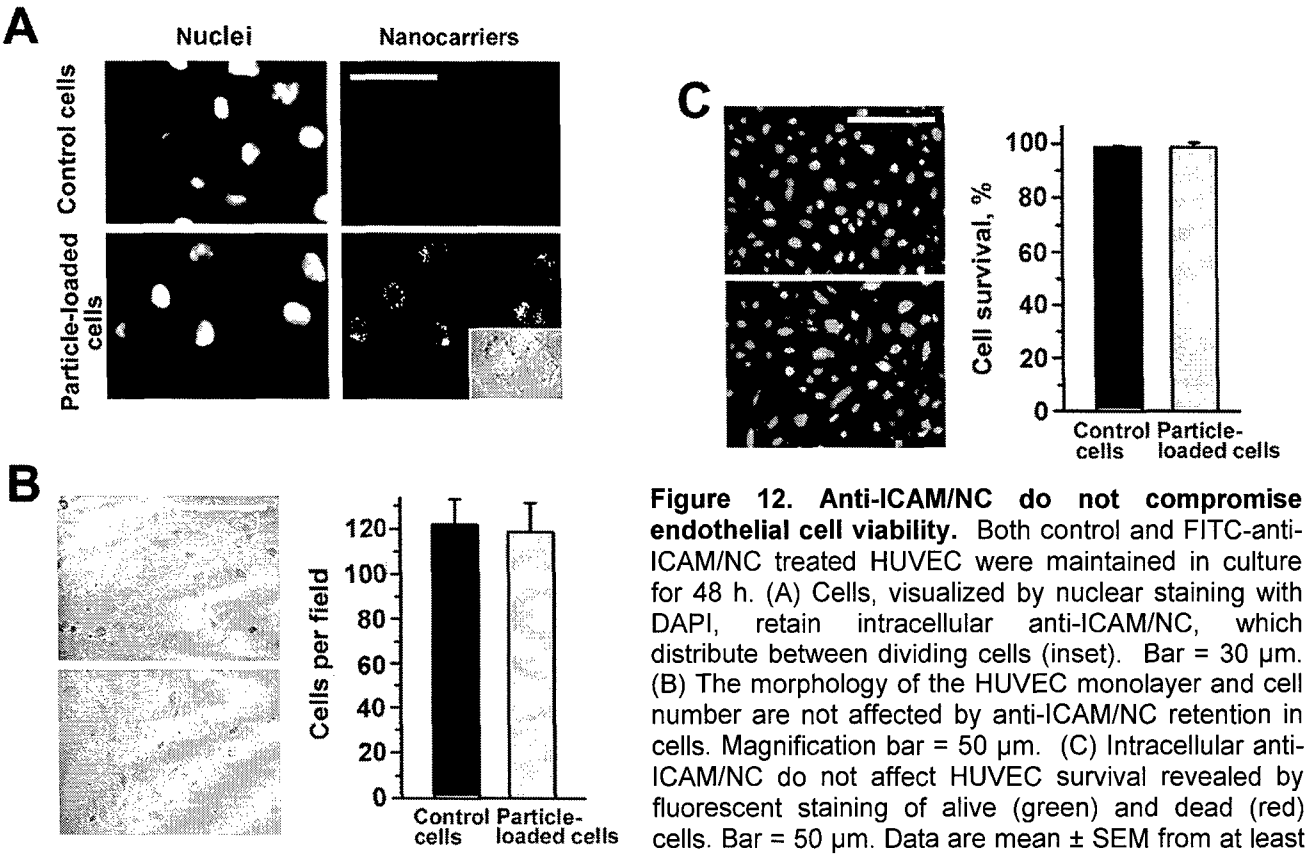

Figure 12. Anti-ICAM/NC do not compromise endothelial cell viability. Both control and FITC-anti-ICAM/NC treated HUVEC were maintained in culture for 48 h. (A) Cells, visualized by nuclear staining with DAPI, retain intracellular anti-ICAM/NC, which distribute between dividing cells (inset). Bar = 30 μm. (B) The morphology of the HUVEC monolayer and cell number are not affected by anti-ICAM/NC retention in cells. Magnification bar = 50 μm. (C) Intracellular anti-ICAM/NC do not affect HUVEC survival revealed by fluorescent staining of alive (green) and dead (red) cells. Bar = 50 μm. Data are mean ± SEM from at least 500 cells per condition.

B3.3. Summary: anti-ICAM conjugates do not induce overt acute toxicity in endothelial cells. Results shown in the section B3 indicate that: i) Endothelial cells retain internalized non-degradable anti-ICAM conjugates for a prolonged time (days in cell culture) without detectable cellular toxicity; ii) Loading of endothelial cells with saturating doses of such anti-ICAM conjugates does not block constitutive endothelial endocytotic and vesicular traffic pathways; iii) Conjugate-loaded endothelial cells retain normal morphology and ability to divide. Taken together, these results support the notion of high safety of using anti-CAM conjugates and provide an impetus for a more systematic toxicity studies in cultures and animals, which should be performed in collaboration with industrial partners.

C. Key Research Accomplishments. In the third year, our studies have been focused on the testing of therapeutic anti-CAM conjugates, with major focus on pulmonary targeting of plasminogen activators. Our new results indicate that anti-CAM antioxidant conjugates targeted to endothelial cells detoxify diverse ROS and thus protect endothelial cells against oxidative stress and that anti-CAM urokinase fusion protein represents a highly promising candidate for further translation into pre-clinical and clinical studies of management pulmonary thrombosis. We report the following key research results achieved in pursuing the Specific Aims 3 and 4 (both are currently ~75% completed).

- Models of endothelial oxidative stress (necrotic and apoptotic versions) induced by diverse extracellular or intracellular ROS including superoxide anion and H2O2 have been established.
- Protective activity of anti-CAM/SOD and tandem anti-CAM/SOD/catalase conjugates has been demonstrated and characterized in these models;
- Anti-CAM/SOD/catalase tandem conjugate shows greater protective potency against necrotic and apoptotic pathways of oxidative stress in all tested models, including ischemia-induced ROS generation within flow adapted endothelial cells.
- A recombinant fusion construct combining anti-PECAM scFv and lmw scuPA has been designed, synthesized and purified;
- Its proper size, folding and antigen-binding and enzymatic activities have been documented;
- Anti-PECAM scFv-scuPA is a pro-drug that can be converted into a fully active plasminogen activator by plasmin that cleaves a scuPA moiety of the fusion construct and endows it with high enzymatic and fibrinolytic activity. This makes anti-PECAM scFv-scuPA construct an ideal candidate for local interventions into supra-mural vascular thrombosis;
- Anti-PECAM scFv-scuPA specifically binds to endothelial cells in cell cultures and in intact animals;
- After injection in animals, scFv-scuPA preferentially accumulates in the pulmonary vasculature and, at lesser extent, in other highly vascularized organs;
- Anti-PECAM scFv-scuPA markedly facilitates dissolution of pulmonary thrombi in animal models of lung embolism;
- Anti-PECAM scFv-scuPA construct is an ideal candidate for industrialization and translation into pre-clinical and clinical studies, since it represents highly homogeneous standard stable entity lacking Fc-fragment related side effects and is amenable a large-scale GMP-level production and use;
- Internalizable stable anti-CAM conjugates accumulating within endothelial cells do not affect their viability and division;
- Stable anti-CAM conjugates reside for a prolonged time within endothelial cells without marked pathological changes in cellular endocytotic and traffic pathways.

D. Reportable Outcomes

We organized this section in a way that permits to maintain confluence of reported publications that naturally overlaps between the grant years, such as "in press" in year 2 *vs* "published" in year 3. We show *publications reported in the previous years of the grant in Italics,* followed by an extra-space and a list of publications submitted or published within the current funding year.

The total number of publications during the first three years of funding is:
Full-size papers and chapters - 14;
Published abstracts of scientific conferences and meetings - 28;
Lectures in scientific meetings and research seminars - 13.

D.1. Full-size publications (papers in which the PI is senior author):*

1. S.Muro, R.Wiewrodt, A.Thomas, L.Koniaris, S.Albelda, ***V.Muzykantov**** *and M.Koval (2003) A novel endocytic pathway induced by clustering endothelial ICAM-1 or PECAM-1. J Cell Sci. 2003;116(Pt 8):1599-1609*

2. ***V.Muzykantov*** *(2003) Targeting pulmonary endothelium. in: "Biomedical Aspects of Drug Targeting",* ***Vladimir Muzykantov*** *and Vladimir Torchilin,* Eds., *Kluwer Academic Publishers, Boston-Dodrecht-London, pages 129-148*

3. J.C.Murciano, S.Muro, L.Koniaris, M.Christofidou-Solomidou, D.Harshaw, S.Albelda, D.Granger, D.Cines and ***V.R.Muzykantov**** *(2003) ICAM-directed vascular immunotargeting of anti-thrombotic agents to the endothelial luminal surface. Blood, 101:3977-1984*

4. *S.Muro, X.Cui, C.Gajewski,* ***V.Muzykantov**** *and M.Koval (2003) Slow intracellular trafficking of catalase nanoparticles targeted to ICAM-1 protects endothelial cells from oxidative stress. Am.J.Physiol., Cell Physiol., 285(5):C1339-47.*

5. V.Shuvaev, T.Dziubla, R.Wiewrodt, and **V.Muzykantov*** (2004) Streptavidin-biotin cross-linking of therapeutic enzymes with carrier antibodies: nanoconjugates for protection against endothelial oxidative stress. "*Methods in Molecular Biology. Bioconjugation Protocols: Strategies and Methods*", C.M.Niemeyer, Ed., Humana Press, Totowa, NJ, Chapter 1, pp 3-18

6. S.Muro, **V.Muzykantov*** and J.Murciano (2004) Characterization of endothelial internalization and targeting of antibody-enzyme conjugates in cell cultures and in laboratory animals "*Methods in Molecular Biology. Bioconjugation Protocols: Strategies and Methods*", C.M.Niemeyer, Ed., Humana Press, Totowa, NJ, Chapter 2, pp 21-36

7. S.Muro, M.Koval and **V.Muzykantov*** (2004) Endothelial endocytic pathways: gates for vascular drug delivery. *Current Vascular Pharmacology*, 2:281-299

8. S.Muro, C.Gayewsky, M.Koval and **V.Muzykantov** (2005) ICAM-1 recycling in endothelial cells: a novel pathway for sustained intracellular delivery and prolonged effects of drugs. *Blood*, 105:650-658

9. S.Muro and **V.Muzykantov*** (2005) Targeting of antioxidant and anti-thrombotic drugs to endothelial cell adhesion molecules. *Current Pharmacological Design* (in press)

10. **V.Muzykantov*** and M.Christofidou-Solomidou (2005) Antioxidant strategies in the respiratory medicine. *Am.J.Respiratory Medicine* (in press)
11. **V.Muzykantov*** and S.Danilov (2005) Delivery of drugs and genes to vascular endothelium. "*Encyclopedia of the Microvasculature*" (D.Sherpo and J.Garcia Ed.), in press
12. T.Dziubla, S. Muro, **V.R.Muzykantov** and M. Koval (2005) Nanoscale Antioxidant Therapeutics. In *Oxidative Stress, Disease and Cancer*, Keshav K. Singh, Editor, Imperial College Press, London., in press
13. **V.Muzykantov** (2005) Targeting drugs to pulmonary endothelium. *Expert Opinion on Drug Delivery*, under revision, provisionally accepted
14. T.Dziubla and **V.Muzykantov** (2005) Delivery of nanoparticles to the lungs. "Nanoparticles as drug carriers" (V.Torchilin, Editor), submitted

D.2. Published presentations at international and national scientific conferences.

1. *S.Muro, A.Thomas, **V.Muzykantov**, M.Koval (2002) PKc-mediated endocytosis of conjugates targeted to ICAM-1. Abstracts of Experimental Biology 2002 Meeting, New Orleans, LA, April 20-24, 2002 (A.382.12) FASEB J., 2002, 16(4), p A439*
2. *A.Scherpereel, J.C.Murciano, R.Wiewerodt, S.Kennel, **V.Muzykantov**, M.Christofidou-Solomidou (2002) Glucose oxidase vascular immunotargeting to pulmonary endothelium enhances luminal expression of ICAM-1 and P-selectin in the lung. Abstracts of Experimental Biology 2002 Meeting, New Orleans, LA, April 20-24, 2002 (A.382.13) FASEB J., 2002, 16(4), p A439*
3. *S. Muro, M.Koval, A.Thomas and **V.Muzykantov** (2002) Affinity carriers targeted ICAM-1: trafficking into endothelial cells. Abstracts of American Thoracic Society International Conference, Atlanta, GA, May 17-22, 2002; Am.J.Resp.Crit.Care Med., 2002; 165 (4):A101*
4. *A.Thomas, T.Sweitzer, R.Wiewrodt, S.Muro, M.Koval and **V.Muzykantov** (2002) Size-dependent intracellular targeting of immunoconjugates directed against endothelial surface adhesion molecules. Abstracts of XIV World Congress of Pharmacology, San Francisco, CA July 7-12, 2002; Pharmacologist, 2002, 44, #2 (suppl. 1), 61.2*
5. *S.Muro, T.Sweitzer, R.Wiewrodt, L.Koniaris, A.Thomas, S.Albelda, M.Koval and **V.Muzykantov** (2002) Kinetics of intracellular immunotargeting to endothelium via adhesion molecules. Ibid, 61.3*
6. ***V.Muzykantov** (2002) Catalase immunotargeting: protection against oxidative stress in the pulmonary vasculature. Abstr. Int.Symposium "Reactive Oxygen and Nitrogen Species", St.Petersburg-Kizhi, Russia, 8-12 July, 2002, Palma Press, Moscow, p.58*
7. *M.Christofidou, S.Muro, J.Murciano, M.Barry, A.Thomas, V.Shuvaev, S.Albelda, D.Cines and **V.R.Muzykantov** (2003) Targeting endothelial surface adhesion molecules. Abstr. Symposium of Vector Targeting, Cold Spring Harbor, NY, March 20-22, 2003, page 19)*
8. *M.Christofidou, A.Scherpereel, A.Boyen, E.Arguiri, V.Shuvaev, S.Kennel and **V.Muzykantov** (2003) Hyperoxia potentiates oxidative injury in murine lungs induced by glucose oxidase targeted to thrombomodulin. Abstr., Experimental Biology Meeting, San Diego, CA, April 11-15, 2003; FASEB J., 2003; 17(4) part I, page A247*

9. *S.Muro, X.Cui, C.Gajewski, M.Koval,* ***V.Muzykantov*** *(2003) Pharmacological Modulation of Intracellular Trafficking and Lysosomal Degradation Prolongs the Anti-oxidant Effect of Catalase Conjugates Delivered into Endothelial Cells via ICAM-1. Abstr. 11th Intern.Symp. Recent Advances in Drug Delivery Systems, Salt Lake City, UT, March 3-6, 2003 (#014)*
10. *M.Christofidou-Solomiudou, B.Kozower, A.Scherpereel, T.Szeitzer,, S.Muro, R.Wiewrodt, V.Shuvaev, A.Thomas, M.Koval, A.Patterson, S.Albelda and* ***V.Muzykantov****. Targeting of antioxidants to adhesion molecules (2003) Inflammation Research, 52, Suppl.2, p.S81 (Abstracts of 6th World Congress on Inflammation, Vancouver, Canada, August 2-6, 2003)*
11. *E.Berk,* ***V.Muzykantov*** *and S.Muro (2003) Binding and uptake of anti-ICAM-1 coated nanoparticles by flow-adapted endothelial cells. Abstr. 9th Annual Respiration Research Retreat of the University of Pennsylvania, Sugarloaf Conference Center, Philadelphia, PA, June 20, 2003, #9*
12. *M.Christofidou-Solomidou, A.Scherpereel, A.Bohen, E.Arguiri, V.Shuvaev, S.Kennel,* ***V.Muzykantov*** *(2003) Hyperoxia potentiates oxidative injury in murine lungs induced by glucose oxidase targeted to thrombomodulin. Ibid, #16*
13. *S.Muro, C.Gajewsky, M.Koval,* ***V.Muzykantov*** *(2003) Slow intracellular degradation of ICAM-1 or PECAM-1 targeted catalase nanoparticles protects endothelial cells from oxidative stress. Ibid, #49*
14. *V.Shuvaev, S.Tliba, T.Dziubla,* ***V.Muzykantov*** *(2003) Combined immunoconjugate delivery of CuZnSOD and catalase to human endothelial cells and their protection against oxidative stress. Ibid, #55*

15. M.Christofidou-Solomiudou, V.Shuvaev, A.Scherpereel, E.Arguiri, S.Tliba and **V.Muzykantov.** (2004) Vascular immunotargeting of catalase as SOD using an anti-PECAM carrier ameliorates oxidative lung injury in double hit mouse model. Abstr. International ATS Conference, May 21-26, 2004, Orlando FL, *Am.J.Resp.Ctric.Care Med.*, 169, page A874
16. V.Shuvaev, S.Tliba, K.Laude, D.Harrison, V.Muzykantov (2004) PECAM-targeted delivery of superoxide dismutase to endothelium protects against xanthine oxidase induced oxidant stress and Ang II-induced hypertension. *Abstr. 10th Annual Respiration Research Retreat of the University of Pennsylvania*, Sugarloaf Conference Center, Philadelphia, PA, June 11, 2004, p.41
17. S.Muro, C.Gajewski, M.Koval, V.Muzykantov (2004) Sustained endothelial delivery of catalase via ICAM-1 recycling pathway. Ibid, p.33
18. K.Laude, V.Shuvaev, A.Bikineyeva, S.Dikalov, **V.Muzykantov**, D.Harrison. Endothelial immunotargeting of superoxide dismutase corrects endothelial dysfunction in angiotensin II-induced hypertension. *Hypertension*, 2004, vol. 44, #4 Abstr. 58th AHA Conference on High Blood Pressure Research, Chicago, IL, October 9-12, 2004, page 555
19. S.Muro and V.Muzykantov (2004) Sustained drug delivery into endothelium via ICAM-1. *Abstr. of AHA Grover Conference on Pulmonary Circulation*, Lost Valley Ranch, CO, September 1-12, 2004, Abstr.#12
20. S.Muro, C.Gajewsky, M.Koval and **V.Muzykantov** (2004) Sustained drug delivery into endothelial cells via recycling ICAM-1. *Abstr. of International*

Symposium on Molecular Design in Drug Development and Discovery, Toronto, Canada July 8-10, 2004, Abst.#9

21. M.Christofidou-Solomidou, V.Shuvaev, A.Scherpereel, E.Arguiri, S.Tliba and **V.Muzykantov.** (2004) Vascular immunotargeting of catalase as SOD using an anti-PECAM carrier ameliorates oxidative lung injury in double hit mouse model. Abstr. International ATS Conference, May 21-26, 2004, Orlando FL, *Am.J.Resp.Ctric.Care Med.*, 169, page A874
22. S.Muro, J.C.Murciano and **V.R.Muzykantov** (2004) Targeting of drugs to cell adhesion molecules for treatment of acute lung injury. *Proceedings of the DOD PRMRP Military Health Research Forum*, San Juan, Puerto Rico, 25-28 April, 2004, Page 16
23. S.Muro, C.Gajewsky, M.Koval and **V.Muzykantov** (2004) Sustained endothelial delivery of catalase via ICAM-1 recycling pathway. *Ibid.*, p 23
24. B.Ding, C.Gottstein, D.Cines, A.Kuo, S.Zaitsev, T.Krasik, K.Ganguly, V.Muzykantov (2004) A genetically engineered anti-PECAM/urokinase fusion construct for targeting fibrinolysis to pulmonary vasculature. *Abstr. of 21st Annual Pharmacological Sciences Student Symposium of University of Pennsylvania*, Gregg Center, Bryrn Mawr, PA, 8 October 2004, p.17
25. C.Gajewsky, S.Muro, M.Koval and **V.Muzykantov** (2004) Sustained endothelial delivery of catalase via ICAM-1 recycling pathway. *Ibid.*, p 18
26. V.Muzykantov, S.Muro, T.Dziubla, V.Shuvaev (2004) Endothelial adhesion molecules as therapeutic targets. *Abstr. of Institute of Medical Engineering Symposium, University of Pennsylvania*, December 2, 2004, p.8
27. W.Qui, S.Muro, T.Dziubla, V.Muzykantov (2004) Characterization of surface-adsorbed antibody particle binding to endothelium. *Ibid*, p.70
28. V.Shuvaev, S.Tliba, K.Laude, D.Harrison, V.Muzykantov (2004) Targeted delivery of SOD via immunoconjugation to endothelium protects against xanthine oxidase-induced oxidant stress and angiotensin II-induced hypertension. *Ibid*, p.71

D. 3. Unpublished presentations at scientific conferences and invited seminars.

Dr. V.Muzykantov presented the results of this project in the following invited lectures:

05/24/02 *Invited Speaker, ATS International Conference, Atlanta, GA:*
"Targeting antioxidant enzymes to the pulmonary vasculature"

07/10/02 *Invited Speaker, International Symposium "Reactive Oxygen Species", St.Petersburg, Russia,*
"Intracellular delivery of catalase to endothelium"

09/31/02 *University of Cologne, Germany*
"Delivery of therapeutics to the pulmonary vasculature"

10/01/02 *University of Mainz, Germany*
"Targeting endothelial cell adhesion molecules"

10/03/02 *Urbino University, Italy*
"Novel strategies for vascular delivery of anti-thrombotic agents"

12/16/02 *Centocor, Radnor, PA*
"Perspectives for translation of the vascular immunotargeting into the clinical domain"

02/24/03 Harvard University/MGH, Department of Radiology "Targeting of enzymes to surface adhesion molecules"

03/05/03 Invited Speaker, International Symposium of Controlled Release and Advanced Drug Delivery Systems, Salt Lake City, Utah: "Vascular Immunotargeting of Antioxidant Enzymes to Endothelial Cells"

04/04/03 Department of Pharmacogenetics, Pittsburgh University, PA: "Delivery of antioxidants to pulmonary endothelium".

06/24/03 Department of Cardiology, Emory University School of Medicine, Atlanta, GA: "Targeting antioxidant enzymes via cell adhesion molecules"

07/30/03 Department of Pharmaceutical Sciences, University of Nebraska, Omaha: "Molecular design of drug delivery systems for targeting endothelium".

08/10/03 Invited Speaker, 6th World Congress on Inflammation (International Association Inflammation Societies Congress, IAIS), August 2-6th, Vancouver, Canada: "Targeting endothelial cell adhesion molecules"

09/12/03 Keynote Speaker, 4th Annual Colloqium "Cellular and Molecular *Biomechanics", University of Virginia, Charlottesville, VA: "New horizons in targeting endothelial cell adhesion molecules"*

10/02/03 Cardio-Pulmonary Research Institute, Winthrop University Hospital, SUNY at Stony Brook School of Medicine, Mineola, NY: "Novel strategies for protection against oxidant pulmonary stress".

11/21/03 Department Molecular Cardiology, Cleveland Clinic Foundation, Cleveland, OH: "Drug targeting to endothelial cells"

01/21/04 Invited Discussant, Transatlantic Airway Conference "Gene and Drug Therapies of Airway Diseases", Lucerne, Switzerland

04/10/04 Drexel University, Department of Bioengineering, Philadelphia, PA: "Targeting endothelial cell adhesion molecules"

08/26/04 Invited Speaker, **Gordon Research Conference** "Endothelial cell phenotypes in health and diseases", Andover, NH: "Targeted drug delivery to endothelium"

10/06/04 Department of Physiology, John Hopkins University, School of Health: "Delivery of antioxidant enzymes to pulmonary vasculature"

11/03/04 Division of Cardiovascular Medicine, University of Michigan, Ann Arbor, MI: "Endothelial cell adhesion molecules: therapeutic targets"

11/16/04 Department of Bioengineering, Ohio University, Athens, OH: "Delivery of anti-thrombotic agents to endothelial surface determinants"

12/02/04 Symposium of the University of Pennsylvania Institute for Medical Engineering: "Targeted drug delivery to defined cellular compartments in endothelial cells"

D.4. Graduate Students Training

Mr. Rudy Fuentes, a Graduate Student of the University of Pennsylvania Pharmacology Graduate Group, completed 2003 fall semester rotation training in the Muzykantov's lab. Mr. Fuentes studied effects of biotinylation and conjugation with anti-CAM on biochemical properties of SOD.

Ms. Anu Thomas, a Graduate Student of the Philadelphia University of Science, enlisted for her Ph.D. Thesis experimental studies in Muzykantov's lab since fall

semester of 2004. Ms. Thomas studies mechanisms of internalization of anti-CAM conjugates in endothelial cells.

Mr. Armen Karamajan, a Graduate Student of the University of Pennsylvania Pharmacology Graduate Group, completed 2004 fall semester rotation training in the Muzykantov's lab. His rotation project involved experiments with flow-adapted endothelial cells.
Ms. Weining Qui, a Graduate Student of the University of Pennsylvania Bioengineering Graduate Group, completed 2004 summer-fall semesters rotation training in Muzykantov's lab. Her rotation projects involved quantitative analysis of binding anti-ICAM conjugates to endothelial cells. She passed the first qualifying exam and currently works on Ph.D. thesis proposal on analysis of anti-ICAM conjugates binding to endothelium in Muzykantov's lab.
Mr. Bisen Ding, a Graduate Student of the of the University of Pennsylvania Pharmacology Graduate Group, completed 2004 fall semester rotation training in the Muzykantov's lab. Mr Ding is a key researcher involved in design and testing of recombinant fusion anti-CAM scFv-scuPA construct and will pursue his Ph.D. project on targeted delivery of anti-thrombotic agents in Muzykantov's lab.

D.5. Special Honors and Recognition by the Scientific Community.
1. Dr. Muzykantov has been invited to the ***Gordon Research Conference*** *"Oxygen Radicals in Biology" (Ventura, CA, February 8-13, 2004) to give a talk: "Targeting antioxidant enzymes to vascular endothelium". Traditionally, talks at GRC (that is regarded as the highest-level scientific forum) are not published in order to permit unlimited sharing of fresh research data with peers.*

2. Dr. Muzykantov organized and chaired a Symposium on Targeted Drug Delivery at 6th World Congress on Inflammation (International Association Inflammation Societies Congress, IAIS), August 2-6th, Vancouver, Canada

3. Dr. Muzykantov has been invited as a Keynote Speaker to 4th Annual Colloqium "Cellular and Molecular Biomechanics", University of Virginia, Charlottesville, VA (September 12th, 2003).

4. Dr. Muzykantov has been invited to give a talk "Targeted drug delivery to endothelium" at the **Gordon Research Conference** "Endothelial cell phenotypes in health and diseases", Andover, NH, August 22-27, 2004.

5. Dr. Muzykantov served as a chair of session on targeted drug delivery at the Gordon Research Conference on Drug Delivery, Big Sky, MT, 09/08/04

E. Conclusions.

We have characterized cellular models of acute oxidant injury (treatment of cells with xanthine-xanthine oxidase superoxide anion generating system, exposure to H2O2, and reactive oxygen species production by flow-adapted endothelial cells in response to ischemia). We defined markers of cellular oxidation and toxicity via necrotic and apoptotic pathways.

We have tested protective effects of anti-CAM/SOD and anti-CAM/SOD/catalase tandem conjugates in these models of apoptotic and necrotic death of endothelial cells induced by ROS. We found that these conjugates detoxify diverse ROS (including those generated within endothelial cells in response to ischemia) and thus protect endothelium against the toxicity and that the tandem conjugate affords a more complete protective effect.

Using a recombinant gene engineering techniques we designed a fusion protein construct combining anti-PECAM scFv with low molecular weight single chain urokinase plasminogen activator (scFv-scuPA) and verified its proper assembly, size and folding using biochemical methods.

Testing of functional activities of the resultant scFv-scuPA fusion protein construct showed that its scFv moiety retains uncompromised antigen-binding activity, whereas its scuPA moiety retains capacity to be activated by plasmin from a pro-drug form into an enzymatically active fibrinolytic agent.

We characterized blood clearance, biodistribution and endothelial targeting of radiolabeled anti-PECAM scFv-scuPA fusion construct in naïve mice using genetically modified PECAM-deficient mice as a negative control. This state-of-the-art study documented that the fusion construct specifically targets endothelial cells in vivo and accumulates in the pulmonary vasculature and, at lesser extent, in other highly vascularized organs after IV injection in naïve animals.

Using a model of pulmonary thrombosis developed in the lab, we demonstrated that pulmonary accumulation of anti-PECAM scFv-scuPA provides a significant improvement of thrombolysis in the lungs. This result, taken together with other characteristics of scFv-scuPA indicates that we produced a novel, highly promising targeted anti-thrombotic agent that can be tested for containment of pulmonary thrombosis in ALI/ARDS in animals and likely in human studies.

Internalizable stable anti-CAM conjugates accumulating within endothelial cells do not affect their viability and division. Further, stable anti-CAM conjugates reside for a prolonged time within endothelial cells without marked pathological changes in cellular endocytotic and traffic pathways. These results support a preliminary notion of safety of these conjugates.

The general conclusion is that the achieved research progress: i) corresponds to the SOW and research plan projected for first three years of the grant; ii) indicates that the Specific Aims (Tasks) 3 and 4 are currently ~75% completed; indicates a high probability of success of the rest of the studies projected these Aims and Specific Aim 5 within year 4 and general success of the project.

G. References. In this section we provide exclusively references to the published studies from our group. Other publications pertinent to this report can be found in the original grant and attached appendix items.

1. S.Muro, R.Wiewrodt, A.Thomas, L.Koniaris, S.Albelda, **V.Muzykantov*** and M.Koval (2003) A novel endocytic pathway induced by clustering endothelial ICAM-1 or PECAM-1. J Cell Sci. 2003 Apr 15;116(Pt 8):1599-1609
2. R.Wiewrodt, A.Thomas, L.Cipelletti, M.Christofidou-Solomidou, D.Weitz, S.I.Feinstein, D.Schaffer, S.M.Albelda, M.Koval and **V.Muzykantov*** (2002) Size-dependent immunotargeting of cargo materials into endothelial cells. *Blood*, 99: 912-922.
3. A.Scherpereel, J.C.Murciano, R.Wiewerodt, S.Kennel, **V.Muzykantov**, M.Christofidou-Solomidou (2002) Glucose oxidase vascular immunotargeting to pulmonary endothelium enhances luminal expression of ICAM-1 and P-selectin in the lung. Abstracts of Experimental Biology 2002 Meeting, New Orleans, LA, April 20-24, 2002 (A.382.13) FASEB J., 2002, 16(4), p A439
4. S. Muro, M.Koval, A.Thomas and **V.Muzykantov** (2002) Affinity carriers targeted ICAM-1: trafficking into endothelial cells. Abstracts of American Thoracic Society International Conference, Atlanta, GA, May 17-22, 2002; Am.J.Resp.Crit.Care Med., 2002; 165 (4):A101
5. J.C.Murciano, S.Muro, L.Koniaris, M.Christofidou-Solomidou, D.Harshaw, S.Albelda, D.Granger, D.Cines and **V.R.Muzykantov*** (2003) ICAM-directed vascular immunotargeting of anti-thrombotic agents to the endothelial luminal surface. *Blood*, 101:3977-1984
6. S.Muro, X.Cui, C.Gajewski, **V.Muzykantov*** and M.Koval (2003) Slow intracellular trafficking of catalase nanoparticles targeted to ICAM-1 protects endothelial cells from oxidative stress. *Am.J.Physiol., Cell Physiol.*, 285(5):C1339-47.
7. V.Shuvaev, T.Dziubla, R.Wiewrodt, and **V.Muzykantov*** (2004) Streptavidin-biotin cross-linking of therapeutic enzymes with carrier antibodies: nanoconjugates for protection against endothelial oxidative stress. "*Methods in Molecular Biology. Bioconjugation Protocols: Strategies and Methods*", C.M.Niemeyer, Ed., Humana Press, Totowa, NJ, Chapter 1, pp 3-18
8. S.Muro, **V.Muzykantov*** and J.Murciano (2004) Characterization of endothelial internalization and targeting of antibody-enzyme conjugates in cell cultures and in laboratory animals "*Methods in Molecular Biology. Bioconjugation Protocols: Strategies and Methods*", C.M.Niemeyer, Ed., Humana Press, Totowa, NJ, Chapter 2, pp 21-36
9. S.Muro, M.Koval and **V.Muzykantov*** (2004) Endothelial endocytic pathways: gates for vascular drug delivery. *Current Vascular Pharmacology*, 2:281-299
10. S.Muro, C.Gayewsky, M.Koval and **V.Muzykantov** (2005) ICAM-1 recycling in endothelial cells: a novel pathway for sustained intracellular delivery and prolonged effects of drugs. *Blood*, 105:650-658

Appendices
Attached are:

1. Set of figures for the Section B2 (figures 5-10, report pages 27-32).
2. V.Shuvaev, T.Dziubla, R.Wiewrodt, and **V.Muzykantov*** (2004) Streptavidin-biotin cross-linking of therapeutic enzymes with carrier antibodies: nanoconjugates for protection against endothelial oxidative stress. "*Methods in Molecular Biology. Bioconjugation Protocols: Strategies and Methods*", C.M.Niemeyer, Ed., Humana Press, Totowa, NJ, Chapter 1, pp 3-18
3. S.Muro, **V.Muzykantov*** and J.Murciano (2004) Characterization of endothelial internalization and targeting of antibody-enzyme conjugates in cell cultures and in laboratory animals "*Methods in Molecular Biology. Bioconjugation Protocols: Strategies and Methods*", C.M.Niemeyer, Ed., Humana Press, Totowa, NJ, Chapter 2, pp 21-36
4. S.Muro, M.Koval and **V.Muzykantov*** (2004) Endothelial endocytic pathways: gates for vascular drug delivery. *Current Vascular Pharmacology*, 2:281-299
5. S.Muro, C.Gayewsky, M.Koval and **V.Muzykantov** (2005) ICAM-1 recycling in endothelial cells: a novel pathway for sustained intracellular delivery and prolonged effects of drugs. *Blood*, 105:650-658
6. M.Christofidou-Solomidou, V.Shuvaev, A.Scherpereel, E.Arguiri, S.Tliba and **V.Muzykantov.** (2004) Vascular immunotargeting of catalase as SOD using an anti-PECAM carrier ameliorates oxidative lung injury in double hit mouse model. Abstr. International ATS Conference, May 21-26, 2004, Orlando FL, *Am.J.Resp.Ctric.Care Med.*, 169, page A874
7. V.Shuvaev, S.Tliba, K.Laude, D.Harrison, V.Muzykantov (2004) PECAM-targeted delivery of superoxide dismutase to endothelium protects against xanthine oxidase induced oxidant stress and Ang II-induced hypertension. *Abstr. 10th Annual Respiration Research Retreat of the University of Pennsylvania*, Sugarloaf Conference Center, Philadelphia, PA, June 11, 2004, p.41
8. S.Muro, C.Gajewski, M.Koval, V.Muzykantov (2004) Sustained endothelial delivery of catalase via ICAM-1 recycling pathway. Ibid, p.33
9. K.Laude, V.Shuvaev, A.Bikineyeva, S.Dikalov, **V.Muzykantov**, D.Harrison. Endothelial immunotargeting of superoxide dismutase corrects endothelial dysfunction in angiotensin II-induced hypertension. *Hypertension*, 2004, vol. 44, #4 Abstr. 58th AHA Conference on High Blood Pressure Research, Chicago, IL, October 9-12, 2004, page 555
10. S.Muro and V.Muzykantov (2004) Sustained drug delivery into endothelium via ICAM-1. *Abstr. of AHA Grover Conference on Pulmonary Circulation*, Lost Valley Ranch, CO, September 1-12, 2004, Abstr.#12
11. S.Muro, C.Gajewsky, M.Koval and **V.Muzykantov** (2004) Sustained drug delivery into endothelial cells via recycling ICAM-1. *Abstr. of International Symposium on Molecular Design in Drug Development and Discovery*, Toronto, Canada July 8-10, 2004, Abst.#9
12. M.Christofidou-Solomidou, V.Shuvaev, A.Scherpereel, E.Arguiri, S.Tliba and **V.Muzykantov.** (2004) Vascular immunotargeting of catalase as SOD

using an anti-PECAM carrier ameliorates oxidative lung injury in double hit mouse model. Abstr. International ATS Conference, May 21-26, 2004, Orlando FL, *Am.J.Resp.Ctric.Care Med.*, 169, page A874

13. S.Muro, J.C.Murciano and **V.R.Muzykantov** (2004) Targeting of drugs to cell adhesion molecules for treatment of acute lung injury. *Proceedings of the DOD PRMRP Military Health Research Forum*, San Juan, Puerto Rico, 25-28 April, 2004, Page 16
14. S.Muro, C.Gajewsky, M.Koval and **V.Muzykantov** (2004) Sustained endothelial delivery of catalase via ICAM-1 recycling pathway. *Ibid.*, p 23
15. B.Ding, C.Gottstein, D.Cines, A.Kuo, S.Zaitsev, T.Krasik, K.Ganguly, V.Muzykantov (2004) A genetically engineered anti-PECAM/urokinase fusion construct for targeting fibrinolysis to pulmonary vasculature. *Abstr. of 21st Annual Pharmacological Sciences Student Symposium of University of Pennsylvania*, Gregg Center, Bryrn Mawr, PA, 8 October 2004, p.17
16. C.Gajewsky, S.Muro, M.Koval and **V.Muzykantov** (2004) Sustained endothelial delivery of catalase via ICAM-1 recycling pathway. *Ibid.*, p 18
17. V.Muzykantov, S.Muro, T.Dziubla, V.Shuvaev (2004) Endothelial adhesion molecules as therapeutic targets. *Abstr. of Institute of Medical Engineering Symposium, University of Pennsylvania*, December 2, 2004, p.8
18. W.Qui, S.Muro, T.Dziubla, V.Muzykantov (2004) Characterization of surface-adsorbed antibody particle binding to endothelium. *Ibid*, p.70
19. V.Shuvaev, S.Tliba, K.Laude, D.Harrison, V.Muzykantov (2004) Targeted delivery of SOD via immunoconjugation to endothelium protects against xanthine oxidase-induced oxidant stress and angiotensin II-induced hypertension. *Ibid*, p.71

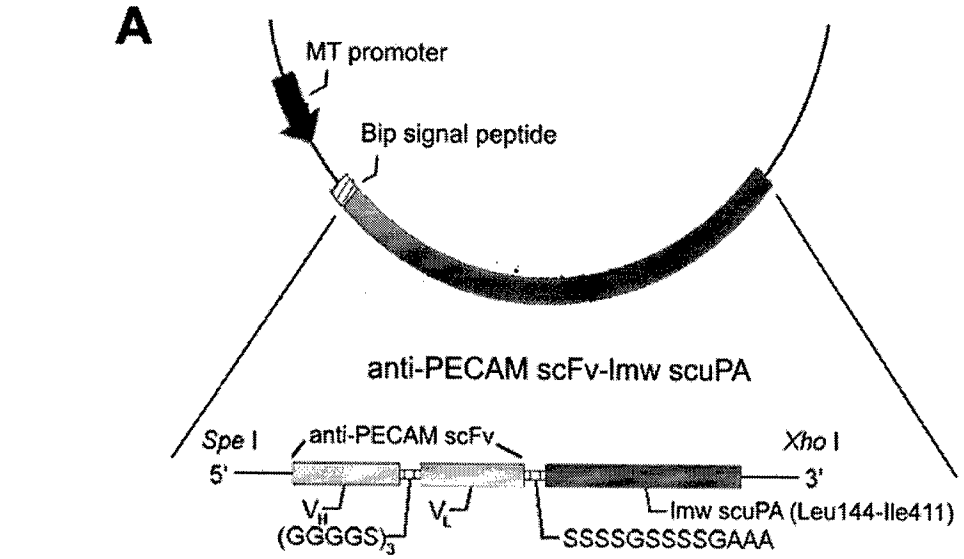
A
MT promoter
Bip signal peptide
anti-PECAM scFv-lmw scuPA
Spe I
anti-PECAM scFv
Xho I
5'
3'
V_H
V_L
(GGGGS)$_3$
lmw scuPA (Leu144-Ile411)
SSSSGSSSSGAAA

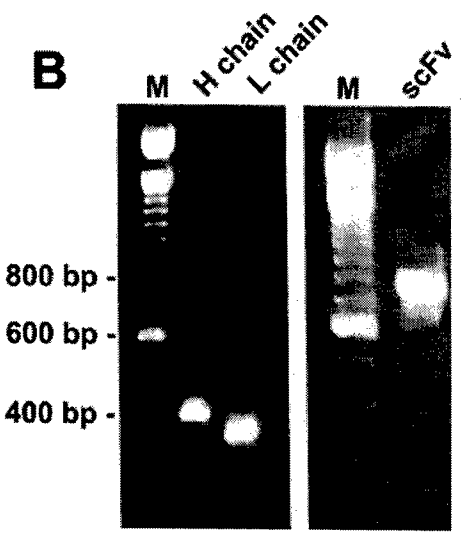
B
M
H chain
L chain
M
scFv
800 bp -
600 bp -
400 bp -

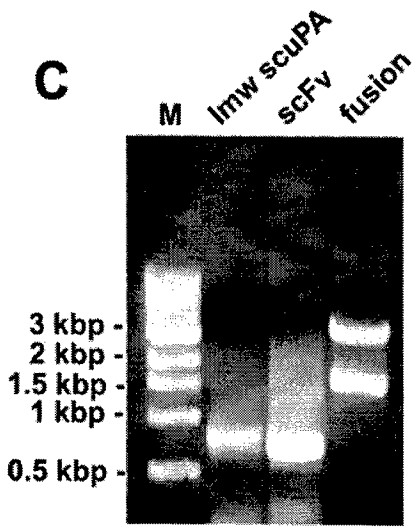
C
M
lmw scuPA
scFv
fusion
3 kbp -
2 kbp -
1.5 kbp -
1 kbp -
0.5 kbp -

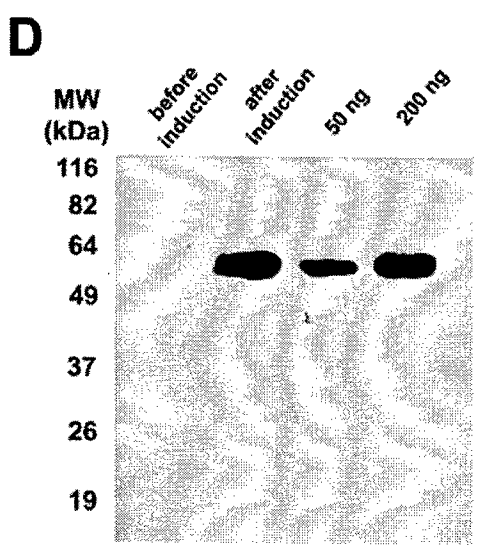
D
MW
(kDa)
before induction
after induction
50 ng
200 ng
116
82
64
49
37
26
19

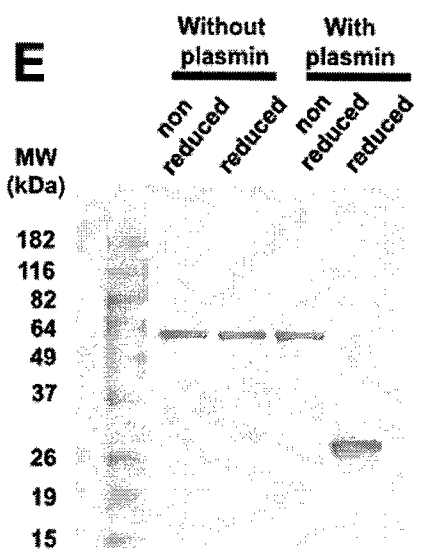
E
Without plasmin
With plasmin
non reduced
reduced
non reduced
reduced
MW
(kDa)
182
116
82
64
49
37
26
19
15

A

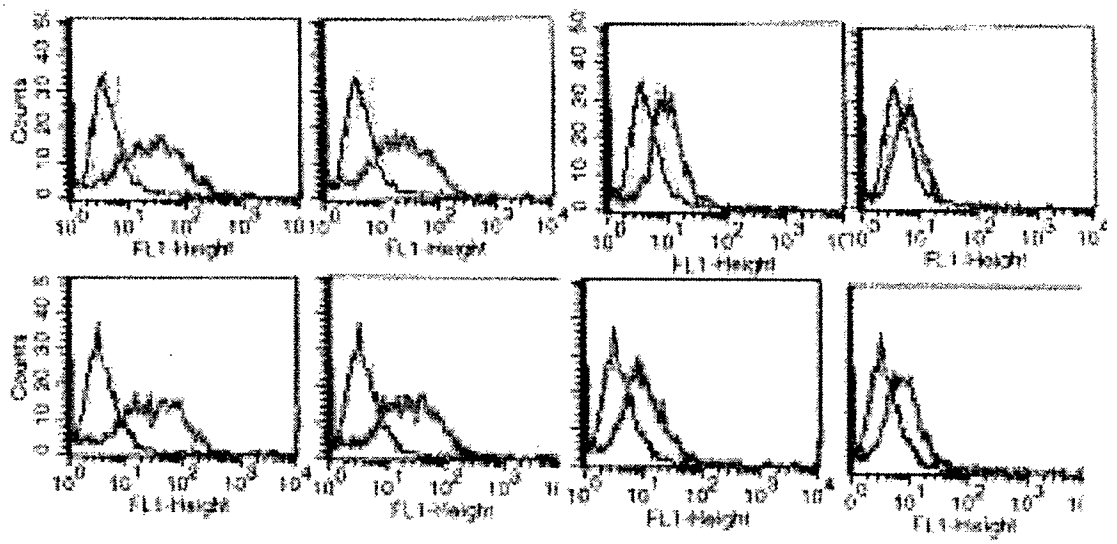

B

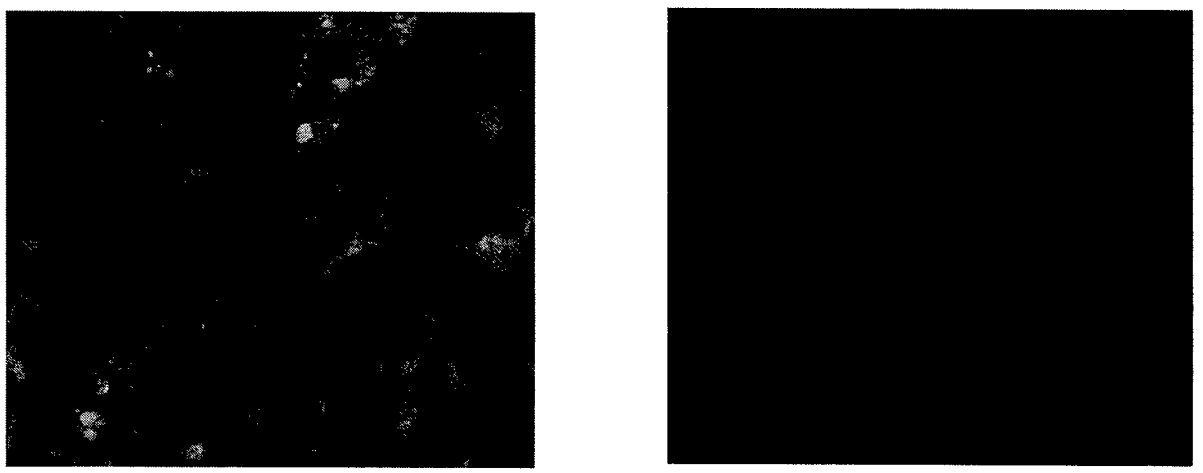

REN/mouse PECAM-1

REN

C

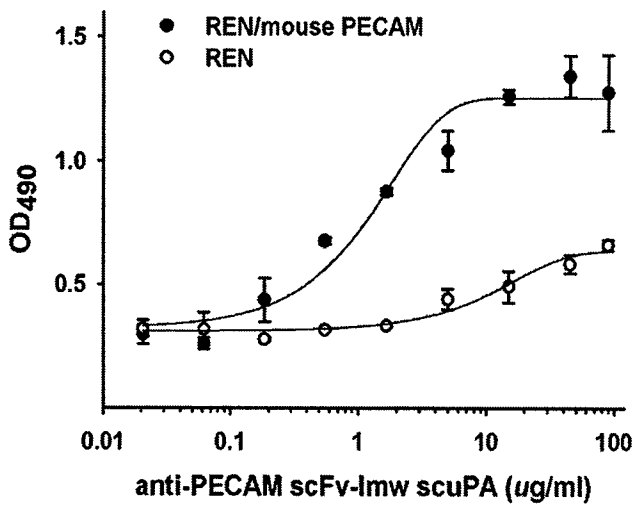

D

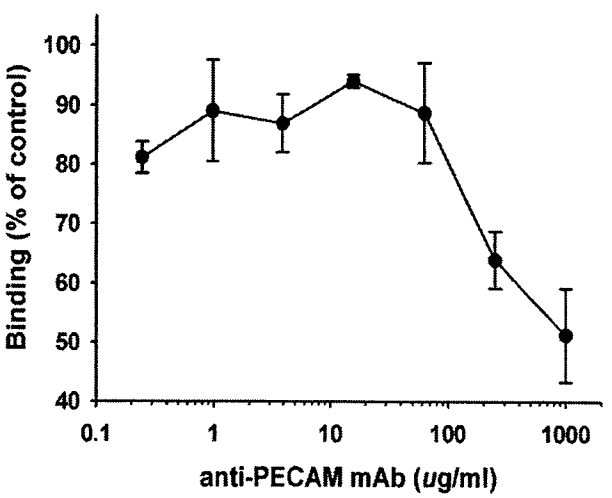

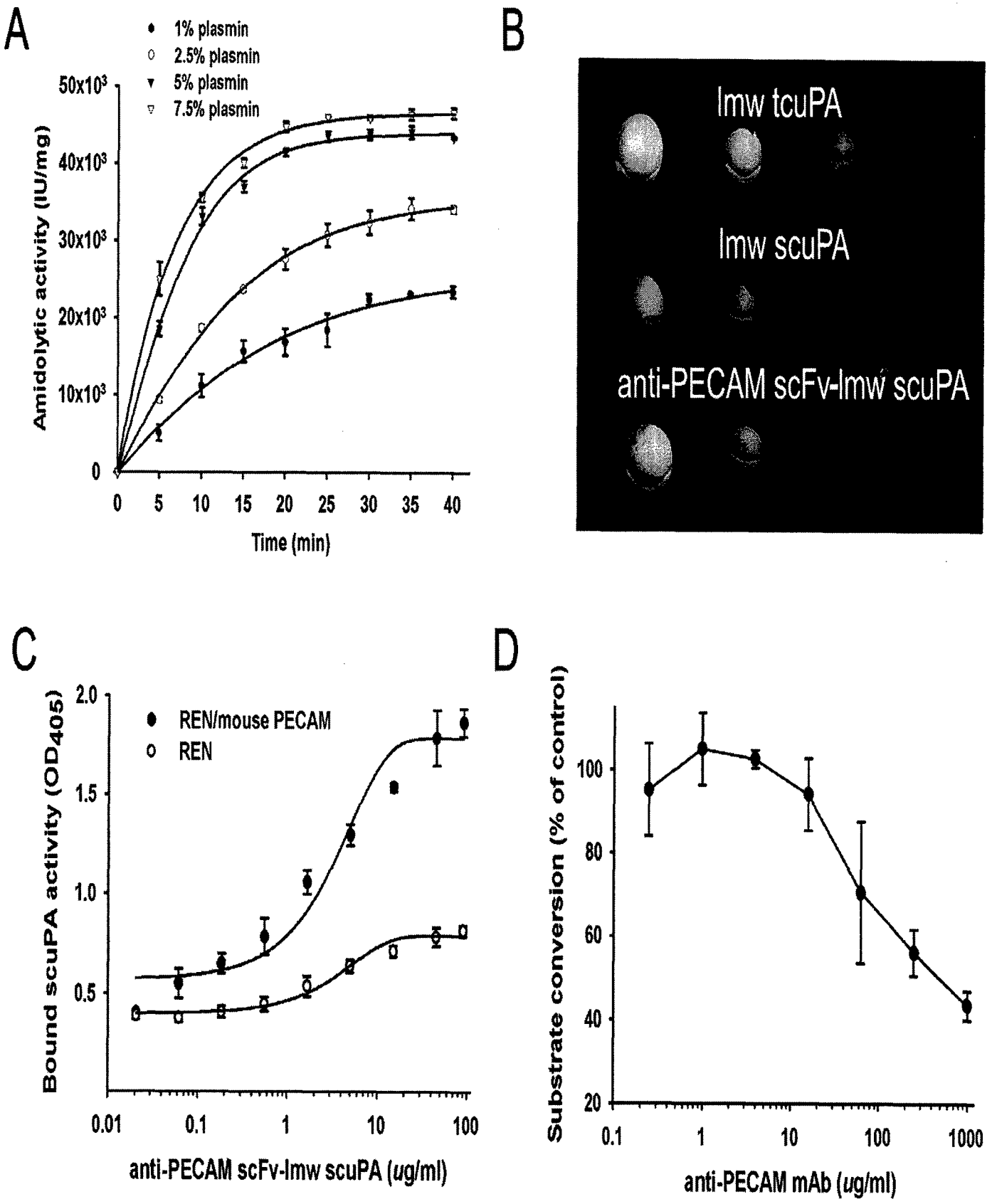
A
1% plasmin
2.5% plasmin
5% plasmin
7.5% plasmin
Amidolytic activity (IU/mg)
50x10³
40x10³
30x10³
20x10³
10x10³
0
0 5 10 15 20 25 30 35 40
Time (min)
B
lmw tcuPA
lmw scuPA
anti-PECAM scFv-lmw scuPA
C
REN/mouse PECAM
REN
Bound scuPA activity (OD405)
2.0
1.5
1.0
0.5
0.01 0.1 1 10 100
anti-PECAM scFv-lmw scuPA (ug/ml)
D
Substrate conversion (% of control)
100
80
60
40
20
0.1 1 10 100 1000
anti-PECAM mAb (ug/ml)

A

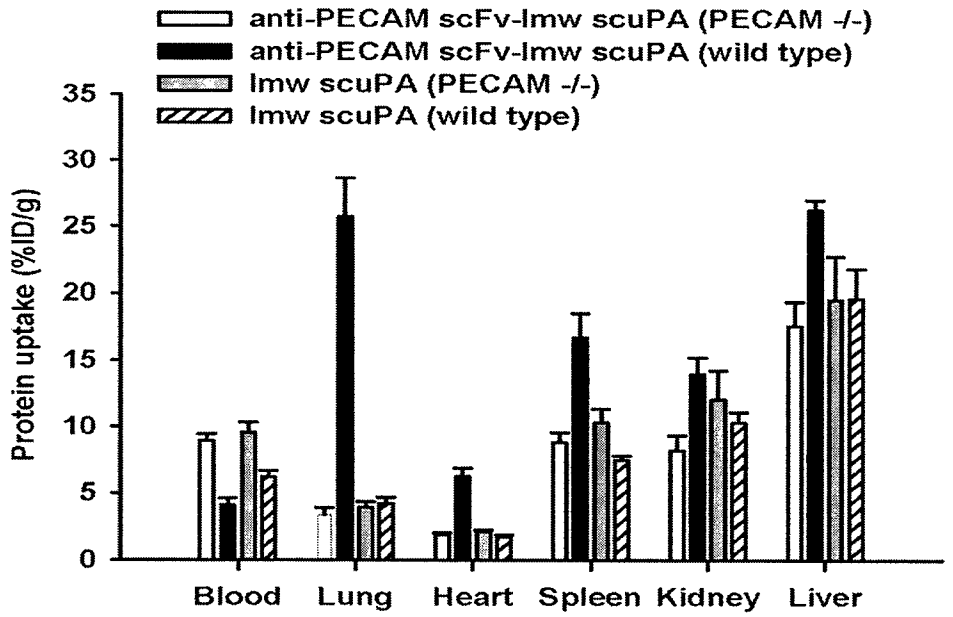
anti-PECAM scFv-lmw scuPA (PECAM -/-)
anti-PECAM scFv-lmw scuPA (wild type)
lmw scuPA (PECAM -/-)
lmw scuPA (wild type)
Protein uptake (%ID/g)
35
30
25
20
15
10
5
0
Blood
Lung
Heart
Spleen
Kidney
Liver

B

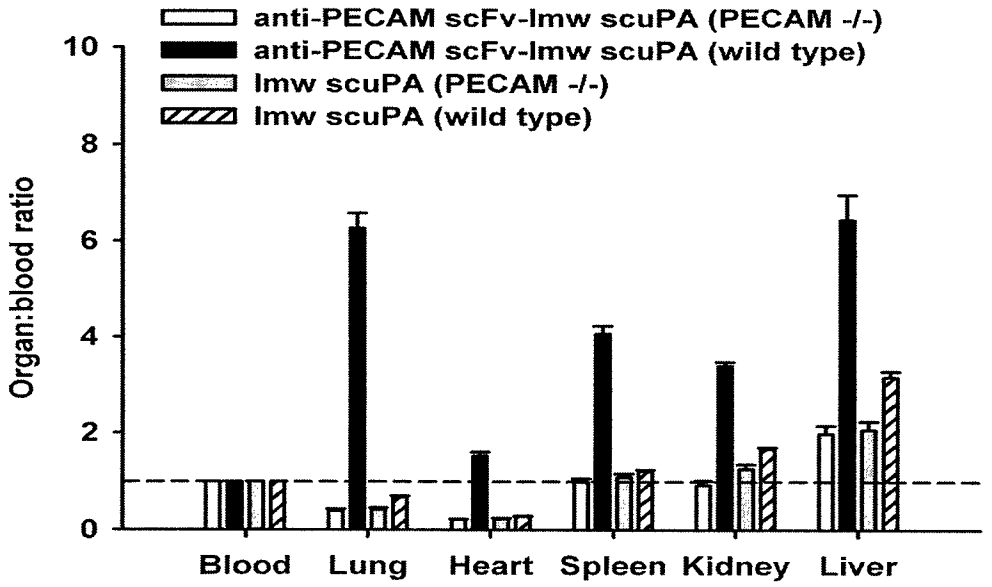
anti-PECAM scFv-lmw scuPA (PECAM -/-)
anti-PECAM scFv-lmw scuPA (wild type)
lmw scuPA (PECAM -/-)
lmw scuPA (wild type)
Organ:blood ratio
10
8
6
4
2
0
Blood
Lung
Heart
Spleen
Kidney
Liver

C

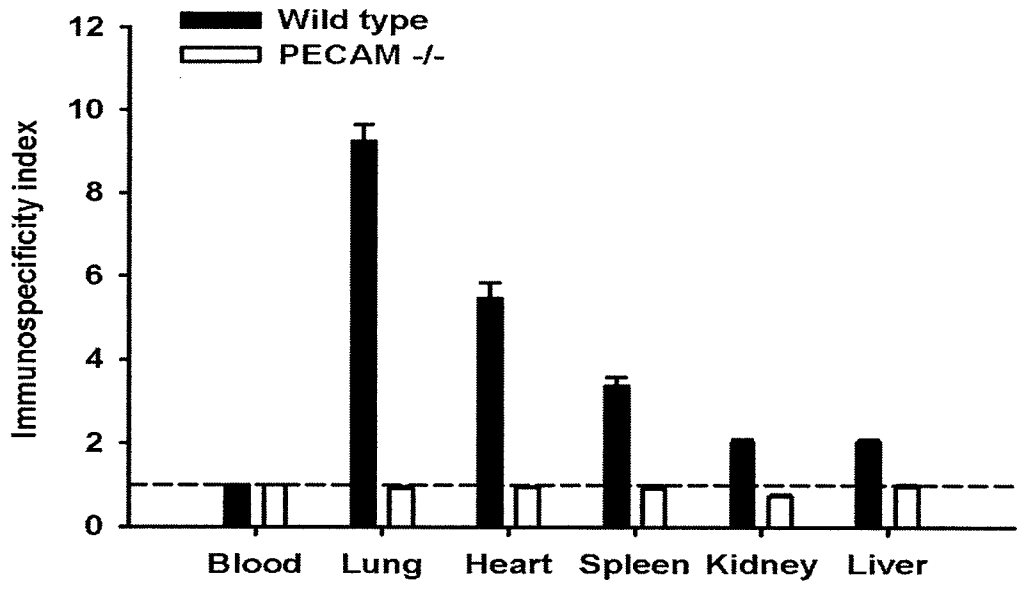
Wild type
PECAM -/-
Immunospecificity index
12
10
8
6
4
2
0
Blood
Lung
Heart
Spleen
Kidney
Liver

Figure 9

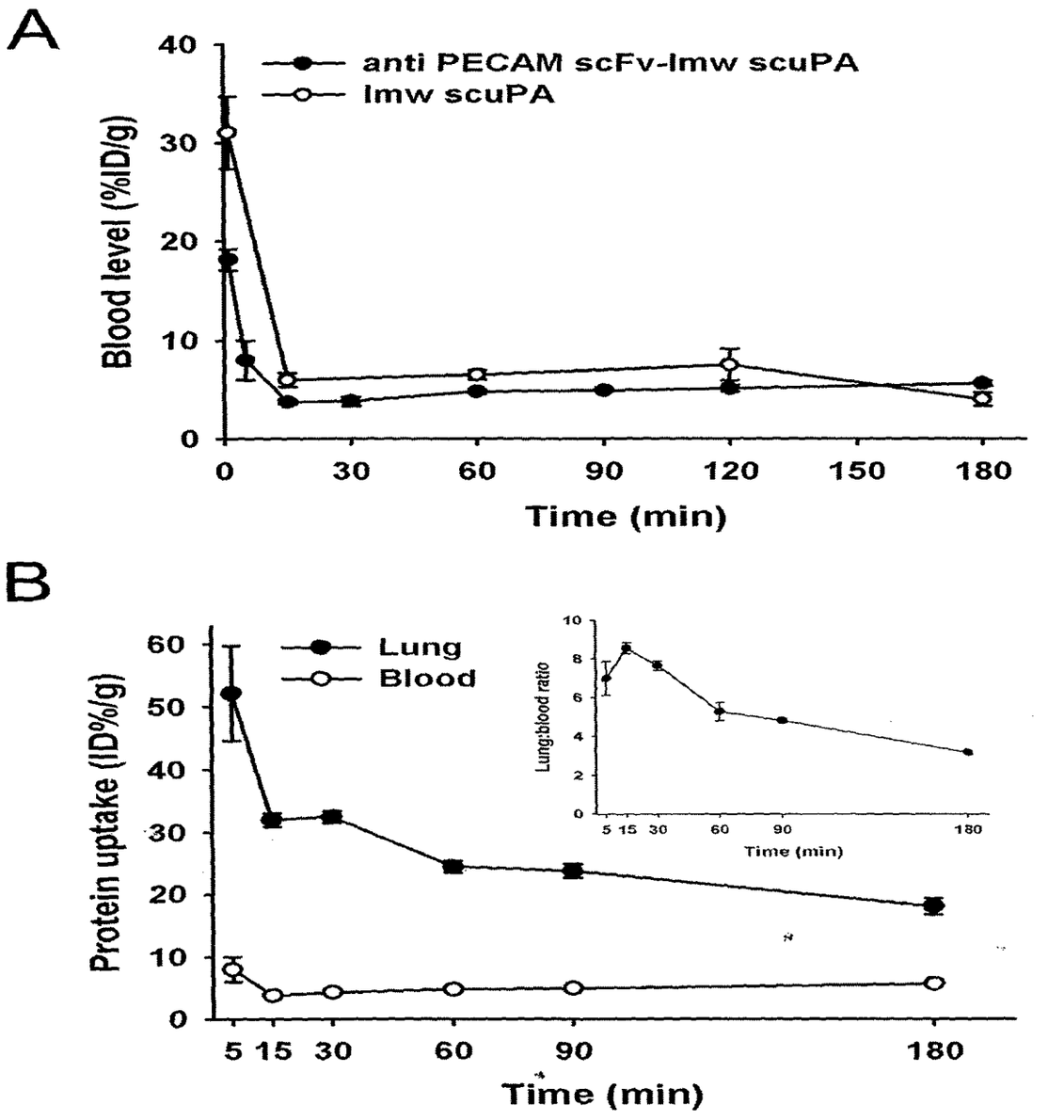
A
anti PECAM scFv-lmw scuPA
lmw scuPA
Blood level (%ID/g)
40
30
20
10
0
0
30
60
90
120
150
180
Time (min)
B
Lung
Blood
Protein uptake (ID%/g)
60
50
40
30
20
10
0
5 15 30 60 90 180
Time (min)
Lung:blood ratio
10
8
6
4
2
0
5 15 30 60 90 180
Time (min)

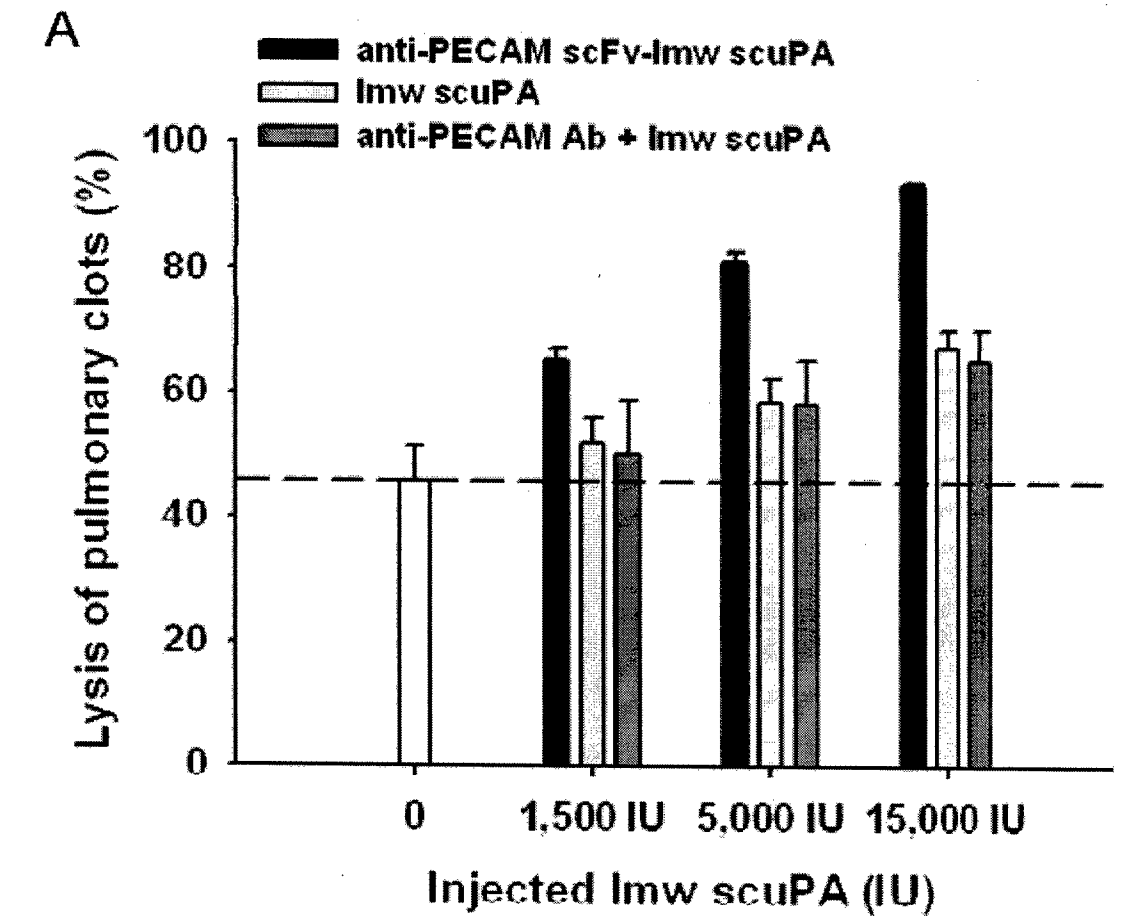
A
anti-PECAM scFv-lmw scuPA
lmw scuPA
anti-PECAM Ab + lmw scuPA
Lysis of pulmonary clots (%)
100
80
60
40
20
0
0
1,500 IU
5,000 IU
15,000 IU
Injected lmw scuPA (IU)

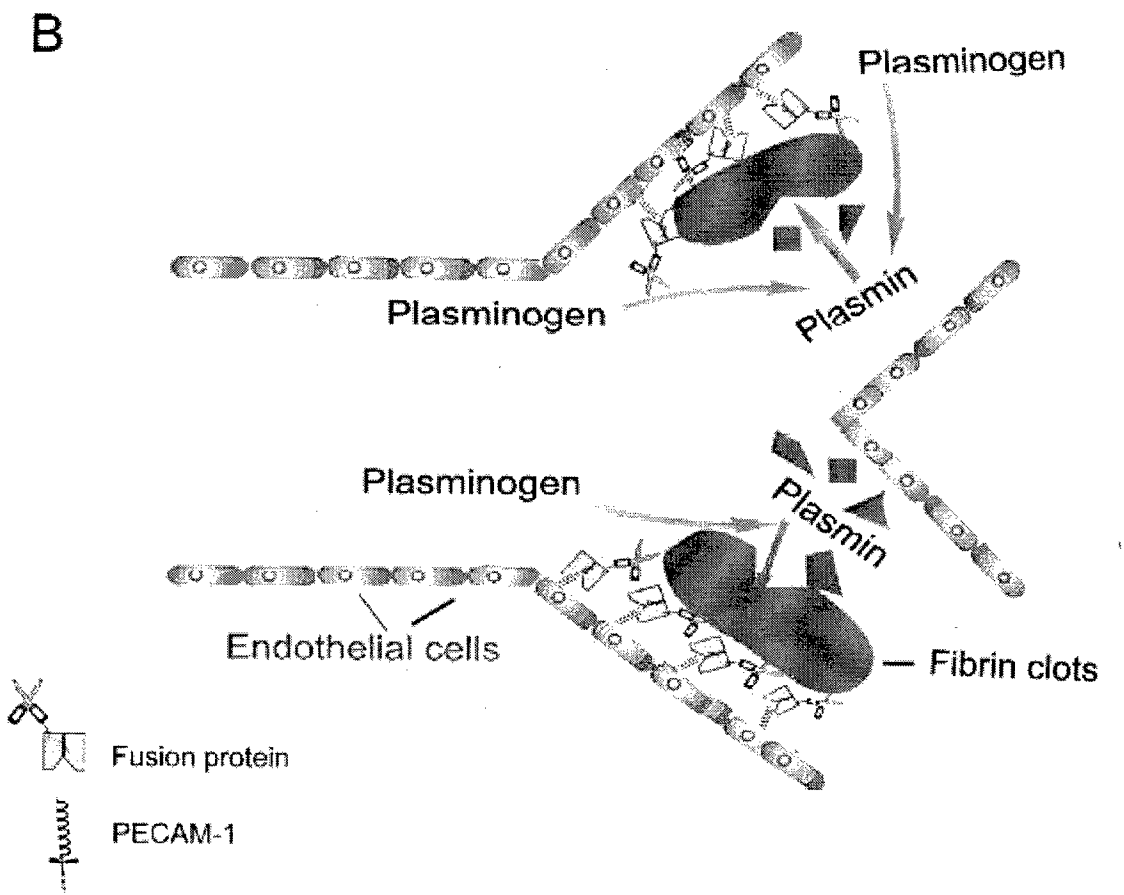
B
Plasminogen
Plasminogen
Plasmin
Plasminogen
Plasmin
Endothelial cells
Fibrin clots
Fusion protein
PECAM-1

1

Streptavidin–Biotin Crosslinking of Therapeutic Enzymes With Carrier Antibodies

Nanoconjugates for Protection Against Endothelial Oxidative Stress

Vladimir V. Shuvaev, Thomas Dziubla, Rainer Wiewrodt, and Vladimir R. Muzykantov

Summary

The streptavidin–biotin system may be used to synthesize immunoconjugates for targeted delivery of drugs, including therapeutic enzymes. The size of antibody–enzyme conjugates, which is controlled by the extent of biotinylation and molar ratio between the conjugate components, represents an important parameter that in some cases dictates subcellular addressing of drugs. This chapter describes the methodology of formation and characterization of polymeric immunoconjugates in the nanoscale range. A theoretical model of streptavidin conjugation based on general principles of polymer chemistry is considered. Factors that influence size and functional characterization of resulting polymer conjugates, as well as advantages and limitations of this approach, are described in detail. The protocols describe the formation of immunoconjugates possessing an antioxidant enzyme, catalase, directed to endothelial cells by anti-platelet endothelial cell adhesion molecule antibodies. However because of the modular nature of the streptavidin–biotin crosslinker system, the techniques herein can be easily adapted for the preparation of nanoscale immunoconjugates delivering other protein drugs to diverse cellular antigens.

Key Words: Immunoconjugates; vascular immunotargeting; polymerization; nanoscale carrier; catalase; streptavidin; biotin; dynamic light scattering; drug delivery.

1. Introduction

Targeted drug delivery, as attained by conjugating therapeutic enzymes with affinity carrier antibodies, promises a significant improvement over the current therapeutic means and, therefore, has remained the focus of intense research

From: *Methods in Molecular Biology, vol. 283: Bioconjugation Protocols: Strategies and Methods*
Edited by: C. M. Niemeyer © Humana Press Inc., Totowa, NJ

for several decades. For example, endothelial cells lining the luminal surface of the vasculature represent an important target for delivery of antithrombotic, anti-inflammatory, antioxidant agents and genetic materials. Cell adhesion molecules (e.g., platelet endothelial cell adhesion molecule [PECAM] and intercellular adhesion molecule [ICAM]) represent very attractive endothelial determinants for vascular immunotargeting, for example, in the context of inflammation. Some drugs require intracellular uptake. Recent studies revealed that although endothelial cells do not internalize monomeric antibodies against PECAM and ICAM, one can facilitate intracellular delivery of therapeutic cargoes by controlling size of the anti-PECAM and anti-ICAM immunoconjugates in the nanoscale range *(1–3)*.

The biotin–streptavidin system can be used to synthesize nanoscale therapeutic immunoconjugates, providing an interesting alternative to other commonly pursued intravenous drug targeting strategies, such as liposomes and polymeric nanocarriers *(4–7)*. These immunoconjugates are typically characterized by (1) their high drug incorporation efficiency, (2) high drug to carrier ratio, (3) a wide tunable range of particles sizes with the same or similar composition, and (4) a relatively rigid and biodegradable structure. In optimal conditions, the degree of drug inclusion is so high that the level of free drug becomes negligible and a separation step may often be omitted. Several reporter and therapeutic enzymes conjugated with anti-PECAM and anti-ICAM have been successfully delivered in therapeutic levels to pulmonary endothelium *(1,2,8–11)*.

This chapter describes the methodology and detail protocols for the generation of nanoscale immunoconjugates using the polymeric form of the streptavidin–biotin system in addition to methods to control their size and shows examples of targeted delivery of an antioxidant therapeutic enzyme, catalase, to vascular endothelium in cell culture.

The distinguishing feature of the streptavidin–biotin system is the extraordinary affinity ($K_d = 10^{-15}$ *M*) of this noncovalent interaction. It may be compared only with systems involving liganded metal ions either as partial covalent bonds or chelates. This extremely specific almost irreversible reaction is widely used in biology and medicine *(12)*. If a biotin derivative is covalently linked to proteins, these biotinylated proteins will bind to streptavidin and form a conjugate. These conjugates can be categorized into two types depending on protein biotinylation level: oligomeric and polymeric conjugates. Oligomeric conjugates, which are readily used in many labeling techniques, occur when the protein contains less than two biotin residues per protein (**Fig. 1A**). However, when the average biotinylation level of the proteins (e.g., biotinylated antibody and enzyme) is equal to or exceeds 2, polymer structures can be formed (**Fig. 1B,C**). Because the linkage occurs through the paired coupling of spe-

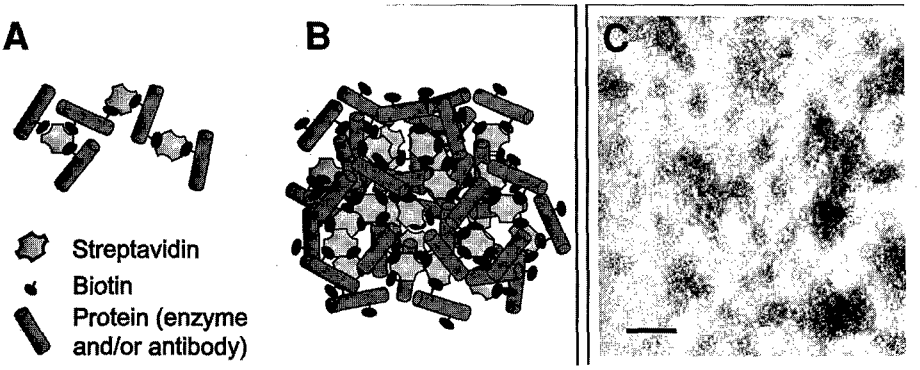

Fig. 1. Scheme of protein conjugation with streptavidin–biotin system. Proteins with less than 2 biotin/molecule form an oligomeric structure (**A**). Higher biotinylated proteins can switch polymerization reactions in the presence of streptavidin as a crosslinker with formation of polymeric structure (**B**). Polymer size depends on reactive conditions, probably a result of the high rate of streptavidin–biotin reaction and formation of internal core inaccessible for free copolymers. (**C**) Electron micrograph of negatively stained immunoconjugates. Conjugates were placed on grids precoated with thin carbon films, and negative staining was performed with uranyl acetate. Images were taken from representative areas at an original magnification of ×50,000 and enlarged to ×440,000. Scale bar = 100 nm.

cific subunits isolated on separate molecular species, it is convenient to relate these conjugates to the classic step (condensation) polymerization chemistry *(13)*. In this circumstance, the modified Carathor's equation applies to this reaction scheme.

$$X_n = \frac{1 + r}{1 + r - frp}$$

where X_n is the average number of monomer residues (both streptavidin and protein) per conjugate, r is the ratio of streptavidin molecules to protein molecules, f is the number of proteins that can bind to streptavidin, and p is the extent of reaction (number of available linkage sites that are actually linked). From this equation, it is noted that polymerization occurs only when the denominator approaches zero. Hence, it is possible to approximately know *a priori* what protein:streptavidin ratio, r, will provide the maximum conjugate size for a given biotinylation level. Also, because of the high sensitivity of the extent of reaction on X_n, small changes in polymerization procedures can have a large impact upon the final size of the conjugate.

2. Materials

2.1. Equipment

1. Dynamic light scattering apparatus 90Plus Particle Sizer (Brookhaven Instruments Corp., Holtsville, NY) or similar apparatus.
2. UV-VIS spectrophotometer.
3. Microplate reader.
4. Gamma-counter.
5. Fluorescent microscope.

2.2. Reagents and Proteins

1. Succinimidyl-6-(biotinamido) hexanoate (NHS-LC-Biotin; Pierce, Rockford, IL).
2. 2-(4'-hydroxyazobenzene) benzoic acid (HABA; Pierce).
3. *O*-Phenylenediamine (OPD, in tablets of 60 mg; Sigma, St. Louis, MO).
4. $Na^{51}CrO_4$ (Perkin Elmer, Boston, MA).
5. Dimethylformamide (DMF).
6. Hydrogen peroxide (H_2O_2).
7. Glycerol.
8. Catalase from bovine liver (Calbiochem, CA).
9. Streptavidin from *Streptomyces avidinii* (Calbiochem).
10. Avidin (Pierce).
11. Horseradish peroxidase (HRP).
12. Monoclonal anti-PECAM antibody (clone 62 was generously provided by Dr. Nakada; Centocor, Malvern, PA).
13. Mouse IgG (Calbiochem, San Diego, CA).

2.3. Buffers, Media, and Cells

1. Phosphate-buffered saline (PBS): 0.1 *M* sodium phosphate, 0.15 *M* sodium chloride, pH 7.2.
2. HABA stock solution: 10 m*M* HABA in 10 m*M* NaOH. Add 24.2 mg to 10 mL of 10 m*M* NaOH. The solution may be stored at 4°C.
3. HABA/avidin working solution: dissolve 10 mg of avidin in 19.4 mL PBS and add 600 µL of 10 m*M* HABA stock solution.
4. Cell culture medium: M199 medium (Gibco, Grand Island, NY), 10% fetal calf serum (Gibco) supplemented with 100 µg/mL heparin (Sigma), 2 m*M* L-glutamine (Gibco), 15 µg/mL endothelial cell growth supplement (Upstate, Lake Placid, NY), 100 U/mL penicillin, and 100 µg/mL streptomycin.
5. RPMI 1640 medium without phenol red (Gibco).
6. Human umbilical vein endothelial cells (HUVEC; Clonetics, San Diego, CA).

3. Methods

3.1. Biotinylation of IgG Antibodies and Catalase

1. Dissolve IgG (anti-PECAM antibody or any other mouse IgG) and catalase in 0.1 *M* PBS to concentrations of 3.5 and 5.0 mg/mL, respectively. Considering

that molecular masses of IgG and catalase are 150 and 240 kDa, respectively, their molar concentrations are 23.3 μ*M* and 20.8 μ*M*, respectively (*see* **Notes 1** and **2**).

2. Prepare fresh 0.1 *M* NHS-LC-biotin in DMF, that is, dissolve 4.5 mg NHS-LC-biotin in 100 μL of anhydrous DMF. Keep solutions of proteins and NHS-LC-biotin on ice.
3. Add appropriate volume of 0.1 *M* NHS-LC-biotin to protein solution to have 5-, 10-, and 15-fold biotin:protein molar excess using the following equation:

$$V_{NHS\text{–}Biotin} = kV_{protein}\left(\frac{C_{protein}}{C_{NHS\text{–}Biotin}}\right)$$

where $V_{NHS\text{–}biotin}$ and $V_{protein}$ are the volumes of NHS-LC-biotin and protein (antibody or catalase), respectively in μL; $C_{NHS\text{–}biotin}$ and $C_{protein}$ are the molar concentrations of NHS-LC-biotin and protein (antibody or catalase), respectively in m*M*; *k* is molar excess of biotin label. Thus, add 1.2, 2.3, and 3.5 μL of 0.1 *M* NHS-LC-biotin to 1 mL of antibody solution and 1.0, 2.1, and 3.1 μL of 0.1 *M* NHS-LC-biotin to 1 mL of catalase solution. Vortex the samples.

4. Incubate the samples on ice for 2 h.
5. Remove unbound biotin derivatives by dialysis against 1.0 L of PBS with three changes.
6. Measure protein concentration in catalase and antibody preparations by A_{280} absorbance using following coefficients: A(0.1%) 1.04 for catalase and 1.7 for IgG. Bradford assay (Bio-Rad) or other protein assays may be used as well.
7. Split antibody preparation in Eppendorf tubes 100 μL/tube and store at –80°C (or –20°C) because IgG at 4°C can easily aggregate and even partial aggregation of IgG may significantly affect further conjugation. Catalase may be stored in PBS at 4°C during several months without significant loss of its activity.

3.2. Estimation of Protein Biotinylation Level

1. Add 450 μL of HABA/avidin working solution into plastic spectrophotometric cuvet and measure absorbance at 500 nm Å. Add 50 μL of sample, mix it in cuvet and measure A'_{500}. Biotin competes with HABA for same binding sites on avidin and releases HABA in free solution that in turn decreases the absorbance of the dye. Because the reaction may require 2–5 min to be complete, check the absorbance several times and take into calculation only the value after absorbance was stabilized for at least 15 s (*see* **Notes 3–5**).
2. Calculate molar concentration of biotin using following equation:

$$[biotin, \mu M] = \frac{(D' \times A^{\circ} - A') \times D'' \times 10^6}{\varepsilon_{HABA}}$$

where *D'* is dilution coefficient for HABA/avidin working solution *D'* = 0.9; *D'* is dilution coefficient of the sample *D"* = 50 μL/500 μL = 10;
10^6 is a coefficient to express biotin concentration in μ*M*; ε_{HABA} is molar extinction coefficient of HABA bound to avidin at 500 nm that equals 34000 AU × $M^{-1}cm^{-1}$.

Considering all known parameters the equation may be easily transformed into a simple formula:

$$[biotin, \mu M] = (0.9 \times \mathring{A} - A') \times 294$$

3. Calculate protein biotinylation using following equation:

$$\text{Protein Biotinylation} = \frac{[biotin, \mu M]}{[Protein, \mu M]}$$

3.3. Conjugation

Immunoconjugates may be prepared by a one-step or two-step procedure. In both cases, the molar ratio between biotinylated protein that should be specifically delivered (i.e., catalase) and biotinylated antibody that targets specific antigen on cell surface (i.e., anti-PECAM) is kept constant. As a rule, the catalase:anti-PECAM ratio is 1:1 mol/mol. In contrast, an optimal concentration of streptavidin (with respect to the desired conjugation size) varies and should be determined for each preparation of biotinylated ligands. In the one-step procedure, biotinylated proteins (enzyme and antibody) are premixed and then streptavidin is added to conjugate them. In two-step procedure, biotinylated enzyme is first conjugated with streptavidin and then antibody is added to form the larger secondary conjugate (*see* **Note 6**).

3.3.1. One-Step Procedure

3.3.1.1. Streptavidin Titration

1. Prepare 110 µL of catalase/antibody mixture with the molar ratio 1:1 in PBS. For that, mix 58 µL of 5.0 mg/mL catalase and 52 µL of 3.5 mg/mL anti-PECAM. All components for conjugation are to be kept on ice.
2. Split the mixture into 5 aliquots of 20 µL each in 1.5-mL transparent Eppendorf tubes.
3. Add 10.0 mg/mL streptavidin solution in PBS to have final molar ratio streptavidin:(catalase + antibody) 0.5, 1.0, 1.5, 2.0, and 2.5 (i.e., add 1.3, 2.6, 4.0, 5.3, and 6.6 µL of streptavidin, respectively). The conjugation should be performed while vortexing. Continuous and regular mixing is critical for correct conjugation.
4. Measure the mean effective diameter of the obtained conjugates by dynamic light scattering (DLS). Add 180 µL of PBS to each conjugate sample, mix it well, and transfer the diluted sample into NMR tube for the analysis on DLS apparatus 90Plus Particle Sizer. Count rate should be from 100 kcps to 1 Mcps. Run the sample for at least 3 min and determine effective diameter (*see* **Note 7**).
5. Plot the effective diameter of conjugates as a function of streptavidin/(catalase + antibody) molar ratio. Make additional points if necessary. The standard streptavidin titration curve is bell shaped, similar to the classical antigen–antibody precipitation titration curves. Higher biotinylated component(s) produces larger conjugates (*see* **Subheading 3.5.1.**).

3.3.1.2. Preparation of Conjugate Stock

1. Chose optimal streptavidin:(catalase + antibody) molar ratio that gives you the required size of conjugate (*see* **Subheading 3.3.1.1., step 5**).
2. Prepare 100 µL of catalase + antibody mixture with the molar ratio 1:1 in PBS. Mix 53 µL of 5.0 mg/mL catalase and 47 µL of 3.5 mg/mL anti-PECAM.
3. Calculate the volume of 10 mg/mL streptavidin that should be added to reach a specific molar ratio. For example, if you found that the optimal molar ratio is 2, add 26.4 µL of 10.0 mg/mL streptavidin.
4. Add 5 µL of the conjugate preparation to 195 µL of PBS. Transfer the diluted sample into NMR tube and measure the effective diameter of obtained conjugates by DLS. Upscaling may change the size of conjugate. If this occurs, then adjustment in volume of streptavidin should be done to correct optimal streptavidin:protein molar ratio.

3.3.2. Two-Step Procedure

3.3.2.1. Titration by Streptavidin

1. Transfer 10.6-µL aliquots of 5.0 mg/mL biotinylated catalase into five 0.5-mL Eppendorf tubes.
2. In the first conjugation step, add 1.3, 2.6, 4.0, 5.3, and 6.6 µL of 10 mg/mL streptavidin per tube. Addition of streptavidin solution should be as fast as possible while the sample is at constant vortexing. Keep vortexing for several seconds after streptavidin was added. Spin it down briefly.
3. Incubate 5 min on ice.
4. In the second conjugation step, add 9.4 µL of 3.5 mg/mL anti-PECAM to all five samples in a similar way as in first conjugation step. Final streptavidin:(catalase + antibody) molar ratios are 0.5, 1.0, 1.5, 2.0, and 2.5, respectively.
5. Measure the effective diameter of obtained conjugates by DLS (*see* **Subheading 3.3.1.1., step 4,** and **Note 7** for details).
6. Plot the effective diameter of conjugates as a function of streptavidin:(catalase + antibody) molar ratio. Make additional points if necessary. Higher biotinylated component(s) produces larger conjugates (*see* **Subheading 3.5.1.**, for example).

3.3.2.2. Preparation of Conjugate Stock

1. Chose optimal streptavidin:(catalase + antibody) molar ratio that gives you required size of the conjugate (*see* plot obtained in **Subheading 3.3.2.1., step 6**).
2. Transfer 53 µL of 5.0 mg/mL biotinylated catalase into 1.5-mL transparent Eppendorf tubes.
3. In the first conjugation step, add specified quantity of streptavidin. For example, if you found that the final streptavidin:(catalase + antibody) molar ratio has to be 2, add 26.4 µL of 10 mg/mL streptavidin. Addition of streptavidin solution should be as fast as possible while the sample is at constant vortexing. Keep vortexing for several seconds after streptavidin was added, spin it down and incubate sample during 5 min on ice.

4. In the second conjugation step, add 47 µL of 3.5 mg/mL anti-PECAM to primary conjugate in a similar way as in first conjugation step.
5. Mix 5 µL of the final conjugate preparation with 195 µL of PBS. Transfer the diluted sample into NMR tube and measure an effective diameter of obtained conjugates by DLS. Upscaling may slightly change the size of conjugate compared with results of streptavidin titration using small volumes. In this case adjustment in volume of streptavidin should be done to correct optimal streptavidin:protein molar ratio.

3.3.3. Storage of Conjugate

Because conjugates tend to aggregate, keeping them at 4°C for longer than several hours is not recommended. Freezing is also not recommended for the same reason of material aggregation after thawing. To store conjugate for further use, add glycerol to 50% and keep the preparation at –20°C. Under these conditions, no significant changes in conjugate size, catalase enzymatic activity, and antibody binding occur for at least 1 wk (*see* **Note 8**).

3.4. Characterization of Conjugates In Vitro

To be therapeutically functional, immunoconjugates should preserve both its activities: enzymatic activity of catalase and antibody binding to cell antigen. Because the conjugation process may affect both protein components, functional activity of the conjugates must be tested in vitro before more expensive and challenging in vivo studies. For example, protection assay against H_2O_2-induced injury of endothelial cell culture reveals functional activity of the catalase conjugate.

3.4.1. Catalase Activity

1. Prepare 10X stock solution of assay buffer: 50 m*M* sodium phosphate, pH 7.0.
2. Prepare working solution: dilute 75 µL of 3% H_2O_2 in 10 mL 1X assay buffer.
3. Take 1 mL of working solution and add catalase (as free enzyme or conjugate) to final concentration of 0.1–1.0 µg of catalase/mL.
4. Place the sample immediately in a quartz cuvet into UV-VIS spectrophotometer and follow the kinetics of H_2O_2 degradation at 242 nm.
5. Measure the slope of the curve ΔA/min using initial linear fragment and calculate catalase activity as follows:

$$\text{Catalase activity, U/mg} = 23.0(\Delta A/\text{min})/\text{mg of catalase}$$

3.4.2. Protection Against Hydrogen Peroxide Cytotoxicity

1. Pretreat a 24-well plate with 0.5 mL/well of 1% gelatin for 1 h, remove the solution ,and allow it to dry out for 1 h. Plate HUVEC (4th passage) in the plate at a cell density of 50,000–100,000 cell/well in cell culture medium. Grow cells for

3–4 d until confluent culture. One day before the experiment, replace the medium with a fresh one containing 200,000 cpm/mL of [^{51}Cr] as $Na^{51}CrO_4$.

2. The next day, wash out free [^{51}Cr] with fresh cell culture medium and add 0.25 mL/well of catalase/anti-PECAM immunoconjugates (*see* **Subheading 3.3.1.2.**) diluted with the medium at a concentration of 5–10 μg of catalase/well. Incubate cells for 1 h at 37°C. Wash out unbound conjugates first with fresh cell culture medium and then with phenol red-free RPMI medium.
3. Induce oxidative stress by addition of 5 m*M* H_2O_2 in RPMI (i.e., 257 μL/50 mL of RPMI) and incubate cells at 37°C for 5 h.
4. Place an aliquot of 20 μL of supernatant into 96-well low-binding plate at 0, 15, 30, 45, and 60 min for the H_2O_2 degradation assay. In the meantime, prepare calibration curve by placing 0, 5, 10, 15, and 20 μL of 5 m*M* H_2O_2 in duplicates and adjust the volume with RPMI.
5. For the H_2O_2 degradation assay, prepare fresh OPD/HRP working solution: dissolve one 60-mg tablet of OPD in 17.5 mL of PBS on rotating platform or orbital shaker and add 100 μL of 1 mg/mL HRP. Add 180 μL of OPD/HRP working solution to sample-containing wells on 96-well plate. Incubate the plate on ELISA shaker for 15 min. Stop the reaction by addition of 50 μL/well of 50% H_2SO_4. Read the absorbance in microplate reader at 490 nm. Calculate the H_2O_2 concentration in the samples using calibration curve.
6. To detect of [^{51}Cr] release, after a 5-h incubation take 100 μL of cell culture supernatant into tubes for gamma-counter. Pool the rest of supernatant and cell lysate with 0.5 mL of 1% Triton X-100, 1.0 *M* NaOH. Measure radioactivity in the samples and calculate the % of released [^{51}Cr].

3.5. Results

3.5.1. Conjugate Preparation

Catalase was biotinylated to a level of 3.25 biotin/catalase monomer (or approx 12–13 biotin/catalase tetramer) and monoclonal anti-PECAM antibody was biotinylated to 3.5 biotin/IgG. Both proteins were mixed at a molar ratio 1:1, and streptavidin was added to form conjugates. The titration curve of the conjugation is shown in **Fig. 2A** as a dependence of conjugate effective diameter determined by DLS on molar ratio streptavidin:biotinylated proteins. The curve demonstrates a continuous increase of the conjugate size at relative excess of biotinylated proteins (**Fig. 2A**, right shoulder of the curve). The maximum is reached at equimolar ratio between accessible biotin-binding sites on streptavidin and available biotins on proteins. Thus the position of the maximum will depend on effective number and flexibility of biotins on the proteins, size and structure of the proteins and mixing conditions. Further increase of streptavidin concentration results in relative excess of streptavidin and decreasing of conjugate size (**Fig 2A**, left shoulder). Noteworthy, the left shoulder has a plateau supposedly because the

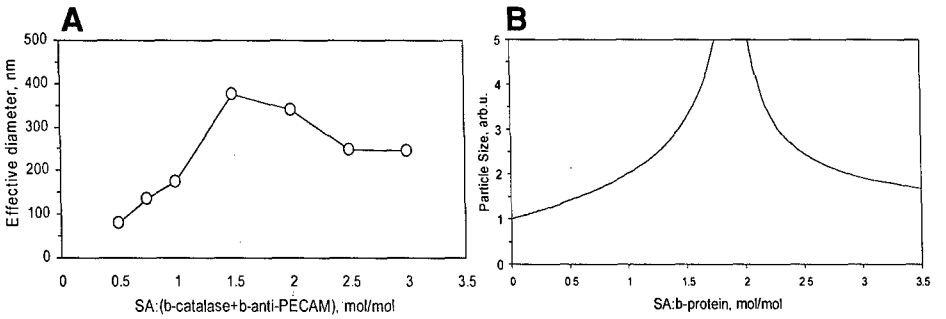

Fig. 2. Titration of biotinylated proteins (catalase and anti-PECAM antibody) with streptavidin. **A,** Catalase was mixed with antibody, and streptavidin was added as a bulk to conjugate both proteins. Size was measured by DLS. **B,** Modeling of conjugation reaction. Parametric addition of Carathor's equation with streptavidin as the limiting reagent (streptavidin:protein < 1.0) and protein as the limiting reagent (streptavidin:protein > 1). The extent of reaction was selected such that these two equations converged to a maximum value. Degree of polymerization was related to particle size through the r^2 relationship of conjugate molecular weight to radius of gyration.

reaction between biotin and streptavidin is so fast that a rate of mixing of two these components is always a limiting step.

Based on the Carathor's equation, the relative concentration of the two reagents (streptavidin and biotinylated protein) is one of the key determinants in the ultimate number of proteins per conjugate. As such, by varying the ratio of streptavidin to biotinylated protein, it is theoretically possible to control the size of particle. If we use the average biotinylation of catalase and antibody at a converging extent of reaction, a theoretical titration curve with a maximum at 1.95 streptavidin:proteins molar ratio is obtained (**Fig. 2B**). This is very close to the actual maximum obtained in experiment (compare with **Fig. 2A**). Deviations from theory are most likely the result of the presence of proteins with two distinct biotinylation levels (i.e., catalase and antibody). Also, the extent of reaction is dependent upon size of conjugate, which is not considered in the model presented. Although this model is limiting in its ability to account for varying accessible functionality with extent of reaction, it still demonstrates the sensitivity of size on reaction conditions.

The size of resulting conjugate depends on biotinylation level of protein(s). Biotinylated catalase was mixed with antibody biotinylated at different extents (**Fig. 3A**). Higher biotinylated antibody formed larger conjugates. The rate of streptavidin addition is another important parameter that affects the size of conjugate. Slow addition of streptavidin leads to increased size of forming conjugates compared to instant mixing (**Fig. 3B**). This dependence of particle

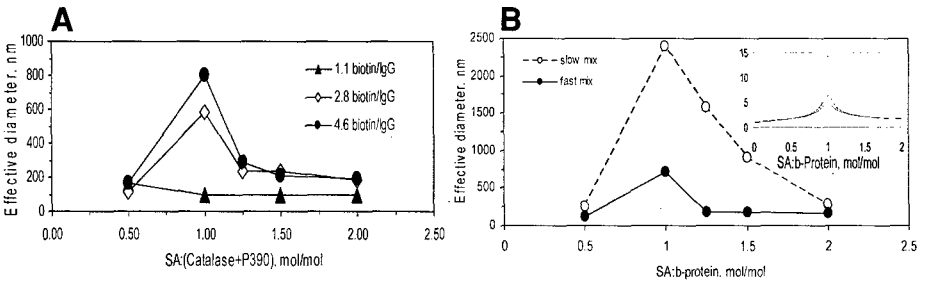

Fig. 3. Effects of biotinylation level and mixing conditions on size of immunoconjugate. **(A)** Catalase at a level of biotinylation of 12 biotin/tetramer was mixed with antibody of indicated biotinylation at a molar ratio 1:1. Streptavidin was added as a bulk. **(B)** The rate of streptavidin addition affects the size of conjugate. Streptavidin was added as a bulk (closed circles) or at slow rate of about 5 μL/min. Insert shows theoretical modeling of this effect. An increase in the extent of reaction results in an increase in the maximum of the titration curve. It is hypothesized that by adding reactants slowing, the likelihood of steric shielding of binding sites is reduced. This results in an overall increase in the extent of reaction and the conjugate size.

size on mixing conditions can also be accounted for by the extent of reaction in the Carathor's. Because the reaction rate proceeds nearly instantaneously, mixing conditions will greatly affect the extent of reaction. As such, experiment agrees well with theory that the increase in reaction mixing results in a decrease in extent of reaction, and therefore results in smaller maximum particle sizes (**Fig. 3B**, insert).

3.5.2. Conjugate Characterization

We prepared catalase/anti-PECAM immunoconjugates for further characterization. The conjugates were analyzed by high-performance liquid chromatography gel filtration. We could detect only trace amounts of free catalase in conjugate preparation, whereas practically all streptavidin and antibody were apparently included in conjugates (**Fig. 4A**). Thus use of the conjugates does not require additional step of conjugate separation from free component. Conjugation only slightly decreased activity of catalase. Its activity in the conjugate was measured to be 80% of initial catalase activity in free solution. Furthermore, the binding of the conjugates was visualized by immunofluorescence microscopy using fluorescein isothiocyanate-labeled antimouse IgG antibody. The conjugates readily bound to cultured human endothelial cells (**Fig. 4B**). Interestingly, they are mostly localized on cell-cell borders in accordance to PECAM distribution in confluent culture ***(14)***.

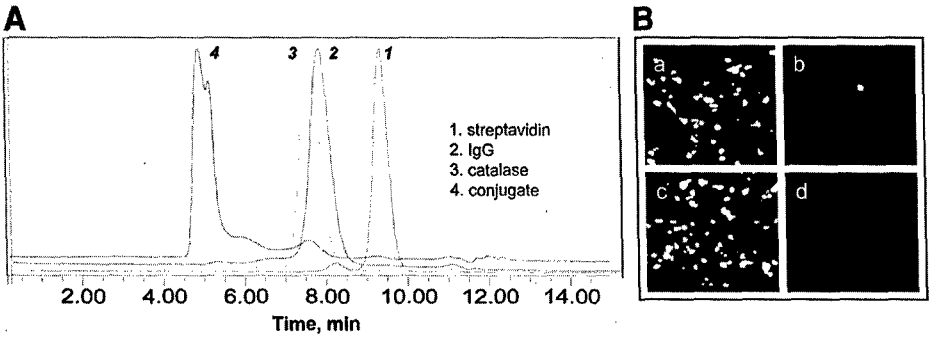

Fig. 4. Characterization of immunoconjugates. (**A**) High-performance liquid chromatography analysis of catalase/anti-PECAM immunoconjugates on SW-300 gel-filtration column (Waters, MA). The conjugation was performed by the one-step procedure. The immunoconjugate and its individual components were injected in phosphate buffer. Normalized chromatograms are shown. (**B**) Binding of the immunoconjugates to HUVECs. Catalase/anti-PECAM (a and c) or catalase/nonimmune IgG (b and d) 300-nm immunoconjugates at a concentration of 5 μg of catalase/well were incubated with confluent cell culture. Cells were fixed without (a and b) or with (c and d) after permeabilization and conjugates were stained using fluorescein isothiocyanate-labeled anti mouse IgG. Samples were analyzed by fluorescence microscopy.

The conjugates were used for protecting endothelial cells against oxidative stress (**Fig. 5**). HUVECs were preincubated with catalase/anti-PECAM antibody at different doses of catalase (0.1–5.0 μg of catalase/well as indicated) and protective properties of the bound conjugates were analyzed by H_2O_2 degradation assay, [^{51}Cr] release, and visually by phase-contrast microscopy. Enzymatic activity of the bound conjugates estimated by H_2O_2 degradation assay showed dose-dependent response up to 5 μg of catalase/well (**Fig. 5A**). However, only doses of 1.0 and 5.0 μg of catalase/well were protective as detected by [^{51}Cr] release (**Fig. 5B**). Phase-contrast microscopy also demonstrated that those doses protected cells against oxidative stress compared to cells untreated with the conjugates (**Fig. 5C**).

4. Notes

4.1. Biotinylation

1. It is important to remember that biotinylation depends on initial concentration of protein. The level of biotinylation is increased at a higher concentration of protein even at same NHS-LC-biotin:protein molar ratio.
2. Biotinylation efficiency and its effects on protein activities vary significantly from protein to protein. In case of catalase, biotinylation does not change the catalytic activity at up to a level of 4–5 biotin/catalase monomer.

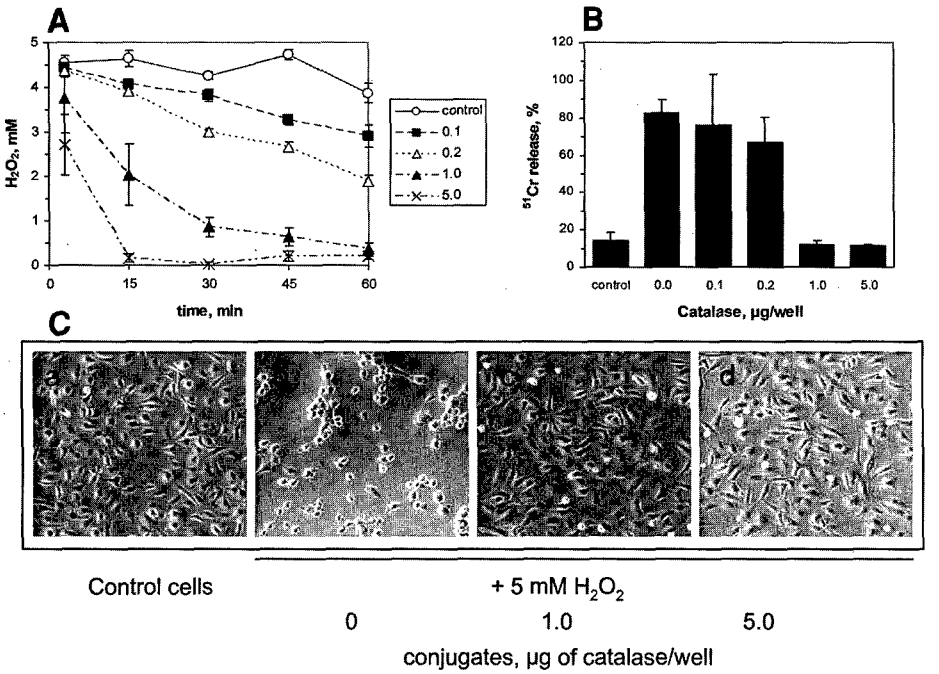

Fig. 5. Cell protection against H_2O_2-induced oxidative stress by catalase/anti-PECAM immunoconjugates. Cells were treated with the immunoconjugates as described in **Subheading 3.4.2.** at several concentrations. **(A)** Degradation of H_2O_2 by bound catalase-containing conjugates. Initial concentrations of immunoconjugates used for cell treatment are indicated in micrograms of catalase/well. **(B)** Cell death as a result of severe oxidative stress was analyzed by release of [^{51}Cr]. Cells were incubated with 5 m*M* H_2O_2 for 5 h. Release of [^{51}Cr] in control cells shows level of passive diffusion whereas practically complete [^{51}Cr] release in the absence of immunoconjugates demonstrates significant cell death. **(C)** Phase-contrast microscopy of control and treated cells.

4.2. Estimation of Protein Biotinylation Level

3. HABA is not readily soluble in 10 m*M* NaOH and requires 10–20 min of intense vortexing.
4. HABA will change its color from yellow to amber because the dye instantly interacts with avidin. HABA/avidin working solution may be stored during 2–4 wk at 4°C. Absorbance of the solution at 500 nm should be 0.9–1.3 AU (we recommend to adjust it to 0.95–1.05 AU with HABA appropriately diluted in PBS to keep constant concentration of HABA).
5. Absorbance of working solution after addition of biotin should be no less than 0.35–0.4. Otherwise the sample of biotinylated protein will have to be diluted.

4.3. Conjugation

6. A number of factors are important in conjugation and may affect a size of particles:
   a. Streptavidin:protein ratio is the most important parameter. A titration curve is required for each new preparation of biotinylated catalase or antibody.
   b. The optimal biotinylation level should be estimated experimentally for every protein. To produce 150- to 400-nm conjugates, proteins have to be biotinylated to a level of 3–4 biotin/catalase monomer or IgG. Under-biotinylated protein may form too small particles and does not reach desired size. It may be rebiotinylated. Overbiotinylated protein will form precipitates and titration curve does not show a visible maximum. Such proteins cannot be used for conjugation.
   c. Reaction between streptavidin and biotin is so fast that mixing conditions are able to change size of formed conjugates. Instant addition of streptavidin is recommended because it is easier to control. However, you can prepare larger conjugates if you inject streptavidin slower. It can be useful tool for preparation conjugates of different size and essentially same composition.
   d. Although we usually look on the left shoulder of the titration curve to find the optimal condition for conjugation, it is possible to use right steep shoulder as well. An advantage of using the right shoulder is that streptavidin may be added in several steps with control of the conjugate size after each step.
7. DLS is an attractive technique in measuring conjugate size because this is an absolute method that does not require preliminary calibration or standards. It is fast, reliable, direct technique and the easiest method to measure particles sizes in the 20- to 1000-nm range. However, DLS is based on the principle of light scattering of moving objects that implies specific limitations on preparation of sample and its reading. There are a number of important issues that should always be taken into consideration to obtain meaningful values. First of all, it is important to possess a rudimentary knowledge of the theory to effectively use the machine. Briefly, at a moment in time, particles in solution will scatter light with a particular intensity at a set angle (at 90° in case of 90Plus Particle Sizer). If we wait for some time (Δt) and then check the scattering intensity, the intensity will change as a result in the change of particle orientation. If Δt is very small, then the intensity will not change very much, because the particles have not had enough time to move around in solution. However, as Δt increases, the chances of the intensity being the same (autocorrelating) will decrease dramatically. This dependence of intensity autocorrelation on time is directly related to the ability of particles to randomly move. If we assume the particles move according to the rules of Brownian motion, we can obtain equations that describe the speed of particle motion as a function of particle size. Hence, we can relate the decay in the autocorrelation directly to particle size. When the assumptions built into the math equations are accurate, then the DLS provides a rapid reliable means of measurement. In practical circumstances, the following points should be kept in mind when analyzing data:

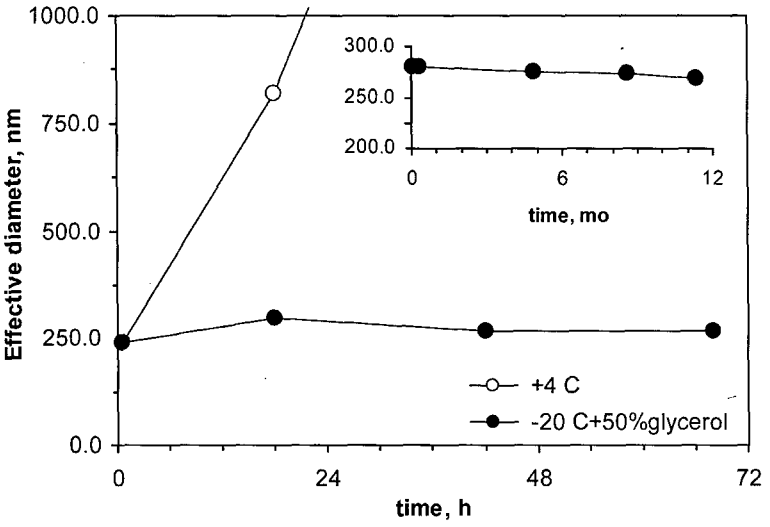

Fig. 6. Effects of viscosity on conjugate aggregation. Storage of conjugate at +4°C in PBS results in significant aggregation and imminent precipitation of immunoconjugate (open circles), whereas 50% glycerol at –20°C prevents their change in size for both short-term (closed circles) and long-term storage (insert).

a. Monitor the count rate to insure that samples are not too dilute or too concentrated for calculations (100 kcps to 1 Mcps). If the count rate is too small, then random fluctuations (e.g., dust particles) will impose very large error in the readings, and very long measurement times will be necessary to average out these occurrences. However, if concentration is too large, then particle–particle interactions become significant, and the Brownian motion is no longer valid.
b. Check at least four different fitting functions to verify particle size. To account for particle size distributions, the autocorrelator can impose different distribution functions to calculate a size and dispersity (linear, quadratic, and so on). Particle sizes calculated from each of these functions should agree seemingly well with each other. If they do not, or if dispersities are rather large (>0.2), then keep in mind that measured particle sizes are not guaranteed.
c. A simple way to evaluate homogeneity in the sample is by monitoring the shape of the decay curve at the point where the autocorrelation goes to zero. If this curve is smooth, and drops down to zero, then particles are nicely dispersed. If the curve is other than exponential and does not go to zero, particle sizes are very high and not well distributed. Typically we consider a reading is good when the autocorrelation curve is linear for 2 logs, which is rare for conjugates larger than 300–400 nm.

8. Appropriate storage of conjugates may be critical for experiments that have to be performed at a different time or location. In this case, the major obstacle is the general tendency of immunoconjugates to aggregate with time. We found that

aggregation of conjugates can be slowed down or prevented by increasing viscosity of the solution. Good results were obtained by storage of conjugates in 30% or 50% at –20°C. Under these conditions, 30% glycerol was enough to slow down aggregation for 1–2 d. However, longer incubation revealed some aggregation. Storage in 50% glycerol apparently completely prevents aggregation, as size of conjugates was stable for at least 1 yr (**Fig. 6**). Protective and enzymatic activities of catalase/anti-PECAM conjugates were practically intact after at least 1 wk. It is important to remember that glycerol affects DLS reading by changing the viscosity of solution. Thus, effects of storage in glycerol should always be compared vs. freshly prepared samples in the same concentration of glycerol.

Acknowledgments

We thank Drs. Thomas Sweitzer, Arnaud Scherpereel, and Ms. Anu P. Thomas for critically important contributions to the previous studies, which provided experimental background for development of the protocols outlined in this chapter. This work was supported by NIH SCOR in Acute Lung Injury (NHLBI HL 60290, Project 4), NHLBI RO1 HL/GM 71175-01, and the Department of Defense Grant (PR 012262) to VRM.

References

1. Muzykantov, V. R., Christofidou-Solomidou, M., Balyasnikova, I., Harshaw, D. W., Schultz, L., Fisher, A. B., et al. (1999) Streptavidin facilitates internalization and pulmonary targeting of an anti-endothelial cell antibody (platelet-endothelial cell adhesion molecule 1): a strategy for vascular immunotargeting of drugs. *Proc. Natl. Acad. Sci. USA* **96,** 2379–2384.
2. Wiewrodt, R., Thomas, A. P., Cipelletti, L., Christofidou-Solomidou, M., Weitz, D. A., Feinstein, S. I., et al. (2002) Size-dependent intracellular immunotargeting of therapeutic cargoes into endothelial cells. *Blood* **99,** 912–922.
3. Muro, S., Wiewrodt, R., Thomas, A., Koniaris, L., Albelda, S. M., Muzykantov, V. R., et al. (2003) A novel endocytic pathway induced by clustering endothelial ICAM-1 or PECAM-1. *J. Cell Sci.* **116,** 1599–1609.
4. Lasic, D. D. (1998) Novel applications of liposomes. *Trends Biotechnol.* **16,** 307–321.
5. Panyam, J. and Labhasetwar, V. (2003) Biodegradable nanoparticles for drug and gene delivery to cells and tissue. *Adv. Drug Deliv. Rev.* **55,** 329–347.
6. Muzykantov, V. R. (1997) Conjugation of catalase to a carrier antibody via a streptavidin-biotin cross-linker. *Biotechnol. Appl. Biochem.* **26,** 103–109.
7. Muzykantov, V. R. (2001) Delivery of antioxidant enzyme proteins to the lung. *Antioxid. Redox. Signal.* **3,** 39–62.
8. Atochina, E. N., Balyasnikova, I. V., Danilov, S. M., Granger, D. N., Fisher, A. B., and Muzykantov, V. R. (1998) Immunotargeting of catalase to ACE or ICAM-1 protects perfused rat lungs against oxidative stress. *Am. J. Physiol.* **275,** L806–L817.

9. Sweitzer, T. D., Thomas, A. P., Wiewrodt, R., Nakada, M. T., Branco, F., and Muzykantov, V. R. (2003) PECAM-directed immunotargeting of catalase: specific, rapid and transient protection against hydrogen peroxide. *Free Radic. Biol. Med.* **34,** 1035–1046.
10. Murciano, J. C., Muro, S., Koniaris, L., Christofidou-Solomidou, M., Harshaw, D. W., Albelda, S. M., et al. (2003) ICAM-directed vascular immunotargeting of anti-thrombotic agents to the endothelial luminal surface. *Blood*, **101,** 3977–3984.
11. Kozower, B. D., Christofidou-Solomidou, M., Sweitzer, T. D., Muro, S., Buerk, D. G., Solomides, C. C., et al. (2003) Immunotargeting of catalase to the pulmonary endothelium alleviates oxidative stress and reduces acute lung transplantation injury. *Nat. Biotechnol.* **21,** 392–398.
12. Wilchek, M. and Bayer, E. A., eds. (1990) *Avidin-Biotin Technology.* Academic Press, Inc., San Diego, CA.
13. Odian, G. (1991) *Principles of Polymerization.* John Wiley and Sons, Inc., New York, NY.
14. Osawa, M., Masuda, M., Kusano, K., and Fujiwara, K. (2002) Evidence for a role of platelet endothelial cell adhesion molecule-1 in endothelial cell mechanosignal transduction: is it a mechanoresponsive molecule? *J. Cell Biol.* **158,** 773–785.

2

Characterization of Endothelial Internalization and Targeting of Antibody–Enzyme Conjugates in Cell Cultures and in Laboratory Animals

Silvia Muro, Vladimir R. Muzykantov, and Juan-Carlos Murciano

Summary

Streptavidin–biotin conjugates of enzymes with carrier antibodies provide a versatile means for targeting selected cellular populations in cell cultures and in vivo. Both specific delivery to cells and proper subcellular addressing of enzyme cargoes are important parameters of targeting. This chapter describes methodologies for evaluating the binding and internalization of labeled conjugates directed to endothelial surface adhesion molecules in cell cultures using anti-intercellular adhesion molecule/catalase or antiplatelet endothelial cell adhesion molecule/catalase conjugates as examples. It also describes protocols for characterization of biodistribution and pulmonary targeting of radiolabeled conjugates in rats using anti-intercellular adhesion molecule/tPA conjugates as an example. The experimental procedures, results, and notes provided may help in investigations of vascular immunotargeting of reporter, experimental, diagnostic, or therapeutic enzymes to endothelial and, perhaps, other cell types, both in vitro and in vivo.

Key Words: Endothelium; cell adhesion molecules; catalase; plasminogen activators; lung targeting.

1. Introduction

Streptavidin crosslinking of reporter and therapeutic enzymes with antibodies to endothelial cell adhesion molecules provides nanoscale conjugates useful for experimental and, perhaps, diagnostic or therapeutic vascular immunotargeting (*see* Chapter 1 and **refs. *1–3***). Binding and appropriate subcellular addressing of antibody–enzyme conjugates to and/or into the target cells are key components for optimal design of drug-delivery systems. The size of the conjugates is an important parameter that determines the rate of intracellular uptake and, perhaps, subcellular trafficking of the conjugates ***(4,5)***.

From: *Methods in Molecular Biology, vol. 283: Bioconjugation Protocols: Strategies and Methods*
Edited by: C. M. Niemeyer © Humana Press Inc., Totowa, NJ

This chapter outlines basic experimental protocols useful in the characterization of these relevant conjugates parameters. The first part (**Subheading 3.1.**) describes protocols for cell culture experiments that use fluorescent and radioisotope labeling as means to trace binding, internalization, and fate of anti-platelet endothelial cell adhesion molecule (PECAM)/catalase and anti-intercellular adhesion molecule (ICAM)/catalase conjugates. The second part (**Subheading 3.2.**) describes protocols for in vivo experiments in intact anesthetized rats using anti-ICAM/tissue-type plasminogen activator (tPA) conjugate labeled with radioisotopes. Thus, particular immunoconjugates described in this chapter are potentially useful for vascular targeting of either antioxidant (e.g., catalase to detoxify H_2O_2, **ref. *6***) or antithrombotic enzymes (e.g., tPA to dissolve fibrin, **ref. *3***). However, because of the modular nature of the conjugation and labeling procedures used, the described protocols can be used for the characterization of endothelial targeting and uptake of diverse reporter and therapeutic enzyme cargoes conjugated with a variety of carrier antibodies *(7)*. Furthermore, cell culture protocols given here for endothelial cells can be applied to other cell types of interest.

2. Materials

2.1. Equipment

1. Gamma-counter.
2. Fluorescence microscope equipped with ×40 or ×60 magnification objectives; filters compatible with fluorescein isothiocyanate (FITC; green), Texas Red (red), and UV or Alexa Fluor 350 (blue) fluorescence; digital camera; and image analysis software (ImagePro).

2.2. Reagents, Proteins, and Antibodies

1. Standard phosphate buffer, PBS, (NaH_2PO_4 20 m*M*, 150 m*M* NaCl, pH 7.4).
2. Glycine solution (50 m*M* glycine, 100 m*M* NaCl, pH 2.5) is used for elution of conjugates or antibodies bound to antigen expressed in the cells.
3. Lysis buffer (PBS containing 2% Triton X-100) is used to lyse cells and differentiate the internalized from the surface retained fractions of conjugates or antibodies.
4. PBS containing 5% bovine serum albumin (PBS-BSA) is used to increase the protein content in the analysis of free iodine label released from damaged proteins.
5. PBS containing 10% fetal bovine serum (PBS-FBS) is used to block the unspecific binding of conjugates or antibodies to the cells while providing the cell necessary nutrients.
6. Antibodies: human anti-ICAM-1 (MAb R6.5) or rat anti-ICAM-1 (MAb 1A29); human anti-PECAM-1 (MAb 62); and goat anti-mouse IgG conjugated to FITC, Texas Red, or Alexa Fluor 350.

7. Other reagents: Concentrated (100% w/v) trichloroacetic acid solution (TCA); goat serum; FITC-labeled streptavidin; tPA; catalase; paraformaldehyde; mowiol; [^{125}]iodine.

2.3. Immunoconjugates

^{125}I-labeled and nonlabeled immunoconjugates synthesized and characterized by dynamic light scattering as described in Chapter 1, where radioisotope is coupled to the cargo enzyme, not the carrier antibody, were used. In some cases, anti-ICAM/catalase conjugates based on FITC-labeled polymer were used *(4,5)*.

2.4. Cells and Media

1. Human umbilical vein endothelial cells (HUVECs, Clonetics).
2. Endothelial cell growth medium (*see* Chapter 1 for details on medium composition) free of antibiotics.

3. Methods

3.1. Characterization of Immunoconjugates in Cell Culture

3.1.1. Quantitative Tracing of Radiolabeled Conjugates in HUVECs

1. Seed the cells in 24-well plates. Cultivate to confluence (approx 48 h) in the appropriate medium. Replace by fresh antibiotic-free medium 24 h before the experiment.
2. Wash cells twice by warm (37°C) culture medium. Add 0.5 µg to 1 µg of conjugate per well (i.e., specific activity 0.03 µCi/µg to 0.1 µCi/µg) in 0.5 mL of medium supplemented with 10% FBS. Incubate cells for 1–2 h at 37°C in the presence of the immunoconjugates.
3. Wash cells three times by medium to remove nonbound conjugates. Incubate cells with a glycine solution (15 min, room temperature [RT]) to elute noninternalized immunoconjugates bound to the cell surface. Using a gamma-counter, determine radioactivity in glycine-eluted fraction (*see* **Note 5**).
4. Wash cells three times by medium and incubate them for 15 min at RT with 0.5 mL of lysis buffer. Add 0.1 mL of the obtained cell lysates to 0.5 mL of PBS-BSA and sequentially add 0.2 mL of TCA and incubate 20 min at RT to precipitate proteins. Centrifuge TCA–lysate mixture (3000*g*, 10 min) and determine radioactivity in pellet and supernatant fractions.
5. Determine protein concentration in a fraction of cell lysates to normalize radioactivity values in samples per gram of total cell protein. Relative and absolute binding, internalization, and/or degradation of the immunoconjugates can be calculated as follows:

$$\textit{Total binding} = \frac{\textit{cpm in glycine fraction} + \textit{cpm in lysate pellet fraction} + \textit{cpm in lysate supernatant fraction}}{\textit{specific activity (cpm/ng of conjugate)}}$$

$$\text{Internalization percentage (if applicable)} = 100 \times \frac{\text{cpm in lysate fraction}}{\text{cpm in lysate fraction} + \text{cpm in glycine-eluted fraction}}$$

$$\text{Total internalization (if applicable)} = \frac{\text{cpm in lysate fraction}}{\text{specific activity (cpm/ng of conjugate)}}$$

$$\text{Degradation percentage} = 100 \times \frac{\text{cpm in supernatant fraction}}{\text{cpm in glycine} + \text{cpm in lysate supernatant} + \text{cpm in lysate pellet fractions}}$$

$$\text{Total degradation} = \frac{\text{cpm supernatant fraction}}{\text{specific activity (cpm/ng of conjugate)}}$$

3.1.2. Subcellular Detection of Immunoconjugates by Immunofluorescence

3.1.2.1. Binding of Immunoconjugates to Target Cells

1. Seed the cells onto 12-mm^2 glass coverslips coated with 1% gelatin in 24-well plates. Allow cells to grow for 48 h to confluence (**Note 2**). Replace medium by fresh antibiotic-free medium 24 h before the experiment. Incubate cells for 5 min at 4°C before the experiment. Wash cells twice and replace by medium containing 10% FBS and a conjugate (1–1.5 µg of per well). Incubate cells for 30 min at 4°C to permit binding.
2. Wash cells three times with cold medium to eliminate nonbound conjugates. Fix cell by a cold solution 2% paraformaldehyde in PBS (15 min) (**Note 3**).
3. Wash cells three times with PBS and stain surface-bound conjugates by incubating fixed cells for 30 min at RT with a 4 µg/mL solution of Texas Red-labeled goat anti-mouse IgG in PBS-FBS (alternatively, use fluorescently labeled antibodies against the enzyme cargo) (**Note 1**). Wash cells three times with PBS.
4. Mount cell-containing coverslips on glass microscope slides using mowiol and incubate overnight at RT to allow the mounting media to polymerize. Observe samples by fluorescence microscopy using ×40 or ×60 objectives. Compare images of fluorescence and phase-contrast fields to confirm location of the immunoconjugate to the cell surface.

3.1.2.2. Internalization of Immunoconjugates Into Target Cells

1. Seed and grow cells to confluence as described in **Subheading 3.1.2.1.**
2. Wash cells twice with 37°C prewarmed medium and add immunoconjugate and incubate with cells for 1 h at 37°C to permit binding and internalization. Fix cells and stain surface-bound conjugates as described in **Subheading 3.1.2.1.**
3. Wash cells three times with PBS and permeabilize them by 15-min incubation with a cold solution 0.2% Triton X-100 in PBS. Stain internalized conjugates by incubating permeabilized cells with FITC-labeled goat anti-mouse IgG (4 µg/mL in PBS serum).
4. Wash cells and mount coverslips on microscope slides as described in **Subheading 3.1.2.1.**

5. Take images using filters compatible with Texas Red (red) and FITC (green) in a fluorescence microscope (×40 or ×60 objective) and merge them. Surface-bound conjugates will appear yellow (double-labeled), whereas internalized conjugates will be single-labeled in green. Imaging software can be programmed to quantify relative conjugate internalization, following the formula:

$$\text{Internalization percentage} = 100 \times \frac{(\text{number of green conjugates} - \text{number of red conjugates})}{\text{number of green conjugates}}$$

3.1.2.3. Fate of Intracellularly Delivered Immunoconjugates

1. For this type of experiments, use fluorescently labeled conjugates (i.e., based on FITC-labeled nondegradable polymer beads; *see* **Note 4**) prepared as previously described in detail ***(4,5)***. First, incubate cells in the presence of conjugates at 4°C to permit binding to the cell surface. Then, wash nonbound immunoconjugates with cold medium, add FBS-supplemented medium, and incubate cells for the time period of interest at 37°C to permit endocytosis and intracellular trafficking of the immunoconjugates previously bound to the cell surface.
2. Wash and fix cells as in **Subheading 3.1.2.1.** followed by staining of the noninternalized conjugates for 30 min at RT with a solution 4 μg/mL goat anti-mouse IgG (i.e., labeled with Alexa Fluor 350) in PBS serum.
3. Wash the preparations three times with PBS and permeabilize cells for 15 min with a cold solution 0.2 % Triton X-100 in PBS. Incubate permeabilized cells with a solution 4 μg/mL goat anti-mouse IgG (i.e., labeled with Texas Red) in PBS serum.
4. Wash cells and mount coverslips on microscope slides as described in **Subheading 3.1.2.1.**

Inspect in a fluorescence microscope using filters compatible with FITC (green), Alexa Fluor 350 (blue), and Texas Red (red) and merge images. Immunoconjugates bound to the cell surface will appear triple-labeled as white. Nondegraded internalized conjugates will appear as double-labeled in yellow, whereas internalized counterparts with degraded protein component will be single-labeled as green.

3.2. Characterization of Immunoconjugates In Vivo

3.2.1. Biodistribution of Radiolabeled Conjugates After Intravenous Administration

1. Anesthetize rats (Sprague–Dawley) weighing 250 g using an intraperitoneal injection of 300 μL of Nembutal solution (70 mg/kg of body weight) and wait 5 min until animals are fully anesthetized (i.e., they do not react to their legs being squeezed with forceps).
2. Inject ^{125}I-labeled conjugates (approx 1–5 μg of the conjugate, 100,000–300,000 cpm per animal) via a tail vein in 0.2 mL of PBS using an insulin syringe with a

27.5-gage needle. Warming up the tail by using hot water makes the vein more visible and easy to inject.

3. One hour after injection, sacrifice anesthetized animals by dissection of the descending aorta, collect 1 mL of blood from the peritoneal cavity, and place it in a heparin-containing tube. Excise internal organs, including lung, liver, kidney, spleen, and heart; rinse in saline; blot in filter paper; weigh; and analyze for radioactivity in a gamma-counter.
4. Use radiotracing data to calculate the following parameters of conjugates behavior in vivo (for more information, *see* **refs. *3***, ***8***, and ***9***):
   a. Percent of injected dose (%ID) characterizes total uptake in a given organ and thus it shows biodistribution and effectiveness of the immunoconjugate targeting. However, this parameter does not take into account organ sizes; thus, uptake in the liver (approx 10 g in a rat) might appear far greater than the uptake in smaller organs (e.g., lung, ~1 g).
   b. To evaluate tissue selectivity of the uptake (and compare the data obtained in different animal species, as well as organs with different sizes), calculate %ID per gram (%ID/g).
   c. The ratio between %ID/g in an organ of interest and that in blood gives the localization ratio (LR) that compensates for a difference in the blood level of circulating conjugates and allows comparison of targeting between different carriers, which may have different rates of blood clearance.
   d. By dividing the LR of a specific antibody conjugate in an organ by that of the control IgG counterpart, calculate the immunospecificity index (ISI = LR_{MAb}/LR_{IgG}), the ratio between the tissue uptake of immune and nonimmune counterparts normalized to their blood level. ISI is the most objective parameter of the targeting specificity.

3.3. Results

3.3.1. Characterization of Immunoconjugates in Cell Culture

3.3.1.1. Analysis of Binding and Fate of Radiolabeled Conjugates

Site-specific binding and degradation of the conjugates by cells was determined by measuring ^{125}I in fractions of glycine elution, TCA pellet, and supernatant of cell lysates obtained from HUVECs incubated with anti-PECAM/^{125}I-catalase and IgG/^{125}I-catalase conjugates as described in **Subheading 3.1.1.** The sum of the recovered ^{125}I shows total amount of catalase associated with cells and reveals the specificity of binding of anti-PECAM conjugates, using as negative control nonspecific IgG conjugates (**Fig. 1A**). A relatively minor fraction of ^{125}I was found in the supernatant after TCA precipitation of cell lysates, indicating that catalase undergoes very modest degradation within 1 h of incubation at 37°C in endothelial cells (**Fig. 1B**).

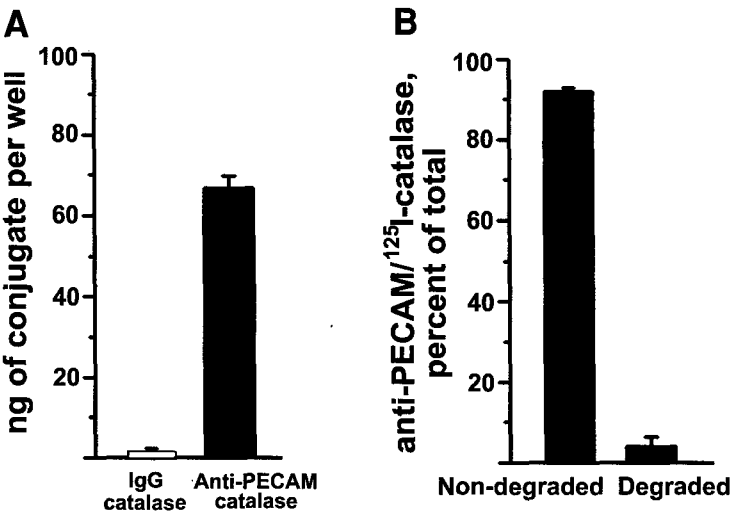

Fig. 1. Quantitative analysis of binding and degradation of radiolabeled anti-PECAM/catalase conjugates in HUVECs. HUVECs were incubated for 90 min at 37°C with anti-PECAM/^{125}I-catalase or control IgG counterpart conjugates, washed, and lysed to determine the TCA-soluble fraction of cell-bound radioactivity. The absolute amount of conjugate in the different fractions is calculated based on its specific activity as described in **Subheading 3.1.1.**

3.3.1.2. Imaging of Binding, Internalization, and Fate of Immunoconjugates by Immunofluorescence

Figure 2 shows that anti-PECAM/catalase but not IgG/catalase conjugates bind to HUVECs at 4°C, thus confirming the data obtained with ^{125}I tracing (*see* **Fig. 1**). Comparison of fluorescence and phase-contrast images indicates that anti-PECAM/catalase conjugates are located in the cell periphery, consistent with the predominant expression of PECAM-1 to the cell borders.

Moreover, in cells incubated for 1 h at 37°C with anti-PECAM/catalase conjugates, only a fraction of the conjugate was labeled before permeabilization by Texas Red-labeled secondary antibody, whereas FITC-labeled secondary antibody applied after permeabilization reveals abundant immunostaining (**Fig. 3A**). Single FITC-labeled (green) internalized conjugates are localized in the perinuclear region of the cell, whereas noninternalized double-labeled (yellow) conjugates tend to localize to the cell periphery. Semiquantitative analysis of double-labeled and single-labeled images shows that endothelial cells internalize 50% of cell-bound anti-PECAM/catalase conjugates.

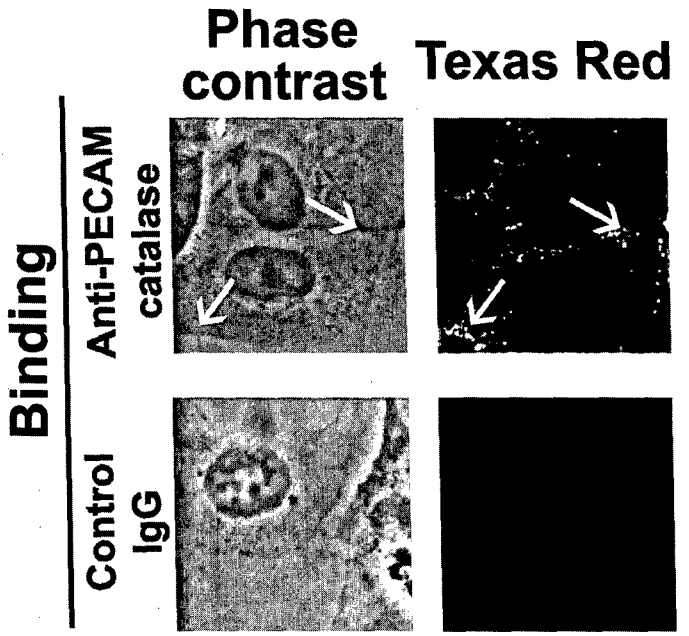

Fig. 2. Fluorescent detection of binding of anti-PECAM/catalase conjugates to HUVECs. HUVECs were incubated for 30 min at 4°C with anti-PECAM/catalase or nonspecific IgG conjugates, washed, fixed, and surface-bound anti-PECAM was stained with Texas Red goat anti-mouse IgG. The samples were analyzed by phase contrast and fluorescence microscopy. The arrows show conjugates bound to the cell surface.

To visualize and estimate degradation of internalized cargoes by fluorescence microscopy, one can retreat to use fluorescently-labeled conjugates, for example, based on FITC-labeled synthetic nanobeads used as carriers for both targeting antibodies and enzyme cargoes *(4,5)*. The advantage of this carrier is that it permits direct tracing of the conjugates in cellular compartments, including lysosomes. FITC-labeled regular immunoconjugates can also be used for this purpose, (e.g., conjugates containing FITC–streptavidin; *see* **Note 4**). A pulse-chase incubation (initial incubation 30 min at 4°C followed by removal of nonbound conjugates and incubation at 37°C), permits one to separate phases of binding, internalization, and intracellular trafficking. After internalization and fixation, surface-bound particles are counterstained using goat anti-mouse IgG conjugated to Alexa Fluor 350, followed by cell permeabilization and incubation with Texas Red-labeled goat anti-mouse IgG. This staining method

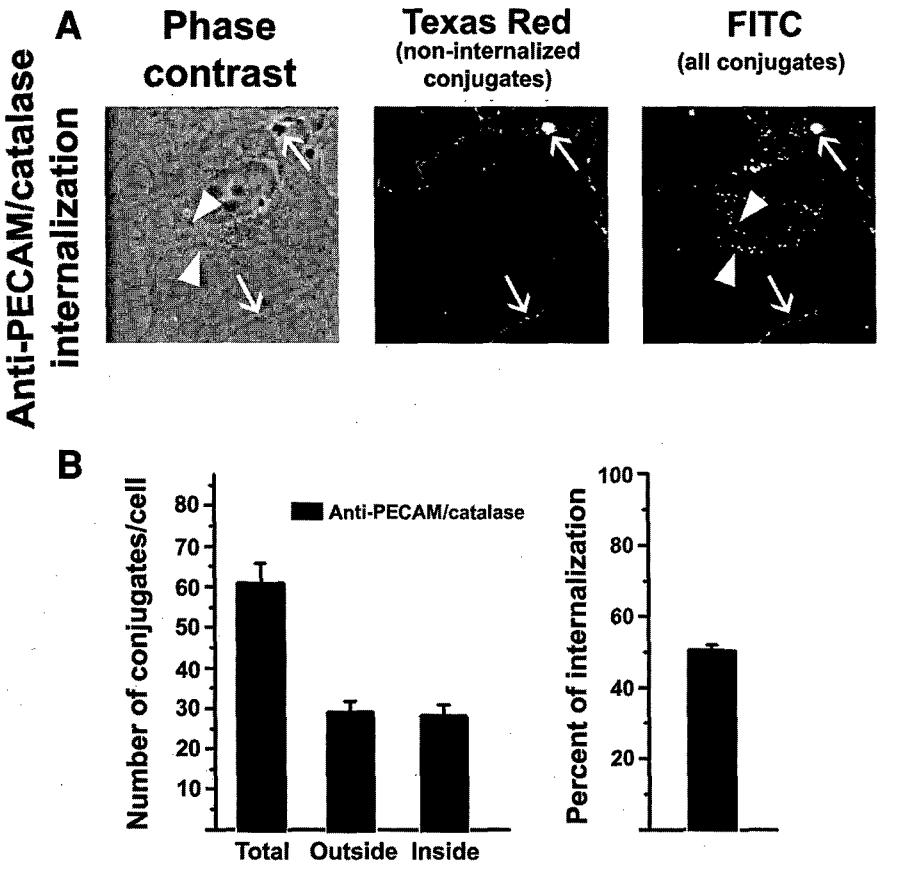

Fig. 3. Fluorescence microscopy of the uptake of anti-PECAM/catalase conjugates by HUVECs. HUVECs were incubated for 1 h at 37°C in the presence of anti-PECAM/catalase conjugates, washed, fixed, and noninternalized conjugates were stained with Texas Red-labeled goat anti-mouse IgG, followed by cell permeabilization and staining with FITC-labeled goat anti-mouse IgG. **A,** The arrows show double-labeled conjugates on the cell surface. The arrowheads show single FITC-labeled conjugates, internalized within the cell. **B,** Quantification of the experiment described above, expressed as mean and standard error (n = 10 fields, from two independent experiments).

(**Fig. 4**) distinguishes surface-bound (triple-stained, white), as well as internalized nondegraded (double-stained, yellow) and degraded conjugates (single-stained, green). The results of the particular experiment shown in **Fig. 4** indicate that conjugates are stable within the cell for 1–2 h and degrade 3 h after internalization.

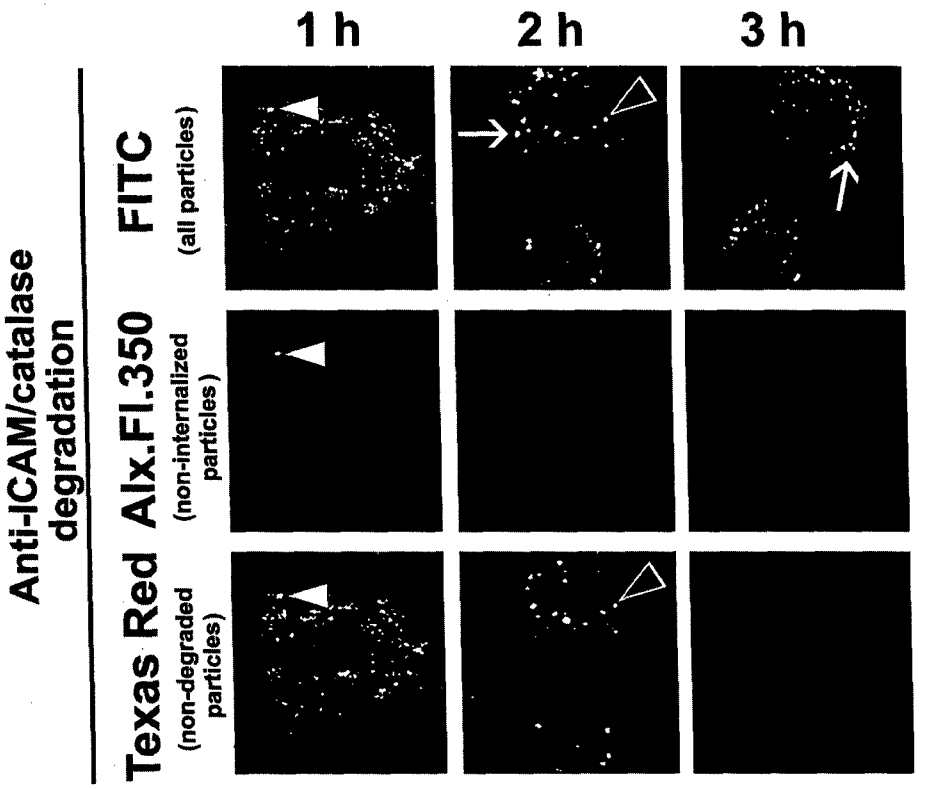

Fig. 4. Imaging of the stability of anti-ICAM/catalase nanoparticles internalized in HUVECs. HUVECs were incubated for 30 min at 4°C in the presence of FITC-labeled anti-ICAM/catalase nanoparticles to permit binding of these to the surface antigen. Then, nonbound particles were washed and the cells were incubated either for 1 h, 2 h, or 3 h at 37°C, to permit internalization and intracellular trafficking of the anti-ICAM/catalase particles. After cell fixation, noninternalized particles were stained with Alexa Fluor 350 goat anti-mouse IgG. Thereafter, the cells were permeabilized and incubated with Texas Red goat anti-mouse IgG. The samples were analyzed by fluorescence microscopy. Closed arrowheads show a triple FITC+Alexa Fluor 350+Texas Red-labeled particle, located to the cell surface. Open arrowheads show a double FITC+Texas Red-labeled particle, which indicates that the targeting antibody was not degraded after internalization within the cell. The arrow shows single FITC-labeled particles, indicating that the targeting antibody in the internalized particles has been degraded.

3.3.2. Characterization of Immunoconjugates In Vivo

3.3.2.1. Biodistribution and Pulmonary Targeting of tPA Conjugated With Anti-ICAM

Experiments with tPA conjugated with an ICAM-1 monoclonal antibody illustrate analysis of vascular immunotargeting in vivo. **Figure 5A** shows comparison of biodistribution of radiolabeled anti-ICAM/^{125}I-tPA conjugate and its components, either ^{125}I-anti-ICAM or ^{125}I-tPA, 1 h after intravenous injection in rats. Anti-ICAM and anti-ICAM/tPA conjugate display preferential uptake in the pulmonary vasculature and significant uptake in hepatic and splenic vasculature. These highly vascularized organs (especially lungs that possess about 30% of endothelial surface in the body) represent privileged targets in agreement with the fact that ICAM is constitutively expressed on the endothelial surface ***(10)***. Nonconjugated tPA shows no pulmonary targeting; in fact, its extremely rapid clearance (its half-life in rats is around 1–5 min; **ref. *11***) leads to disappearance of the tracer from blood and major organs within 1 h after injection.

3.3.2.2. Comparison of Biodistribution Attained Using Different Injection Routes

High levels of pulmonary uptake of conjugates directed against pan-endothelial determinants, such as ICAM-1, might be to the result of several reasons: (1) an extremely extended endothelial surface in the alveolar capillaries; (2) the fact that lung receives 100% of the heart blood output; or (3) the phenomenon of first-pass blood after intravenous injection. **Figure 5B** shows that injection of anti-ICAM/tPA conjugate via the left ventricle, which obviates the first pass in the lungs, produces less effective pulmonary targeting, suggesting that indeed first-pass phenomenon contributes to the pulmonary targeting. However, a high level of pulmonary uptake after left ventricle administration confirms the specificity of anti-ICAM conjugates targeting in vivo.

3.3.2.3. Evaluation of the Targeting Specificity of Immunoconjugates

Figure 6 illustrates the analysis of immunoconjugates biodistribution and targeting in rats 1 h after intravenous injection. A comparison of %ID/g in organs reveals that anti-ICAM/tPA conjugate but not IgG/tPA counterpart accumulates in the pulmonary vasculature. However, the blood level of anti-ICAM/tPA is lower than that of the nonimmune IgG/tPA counterpart, likely because of depletion of circulating blood pool by endothelial binding. The LR that compensates for differences in blood level reveals very high selectivity of anti-ICAM/tPA uptake in highly vascularized organs including liver (LR close to 3), spleen (LR exceeds 7), and especially lungs (LR close to 30). Calculation

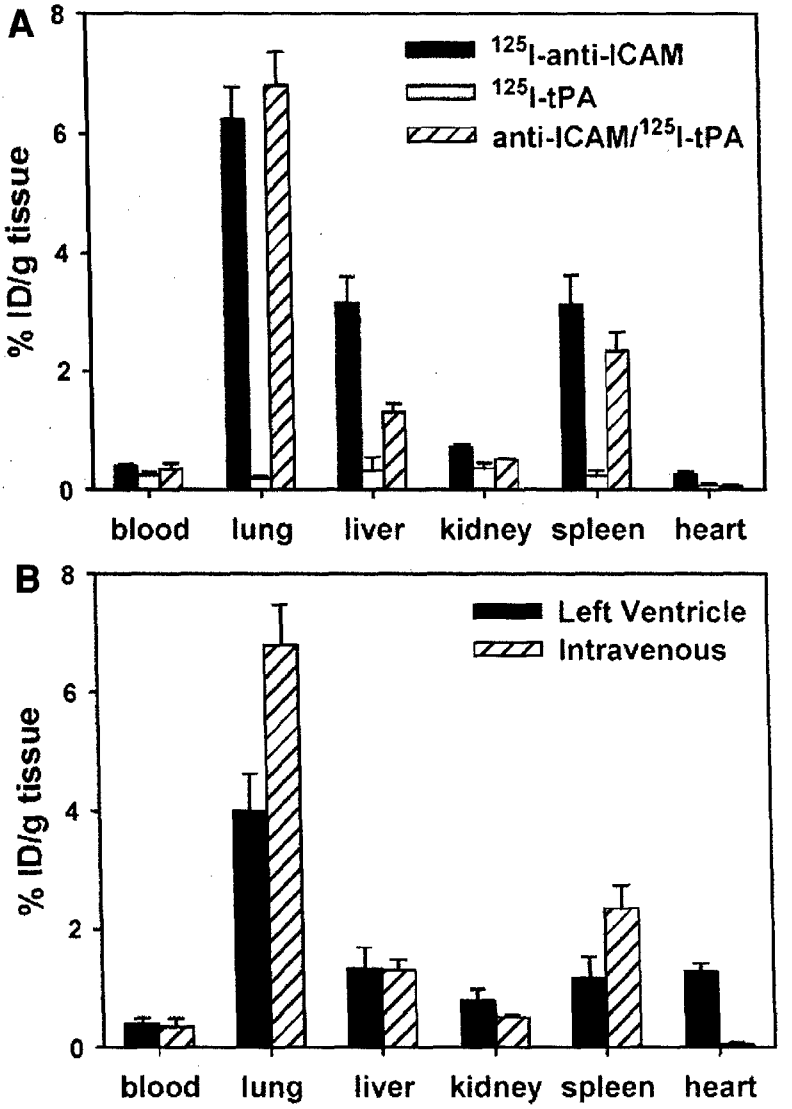

Fig. 5. Biodistribution of immunoconjugates and free components in vivo. Tracer amounts of radiolabeled proteins (approx 1 μg of radioactive material per sample) were injected intravascularly in anesthetized rats. After 1 h, animals were sacrificed and blood and organs extracted and analyzed for radioactivity. **A,** ^{125}I-anti-ICAM (black bars) or anti-ICAM/125I-tPA (hatched bars), but not free ^{125}I-tPA (white bars) accumulate in the lung, liver, and spleen after intravenous injection. **B,** Comparison of biodistribution of anti-ICAM/^{125}I-tPA after injections via the tail vein (hatched bars) or the left ventricle (black bars). Data are presented as mean ± SD, n = 4–9 animals per determination.

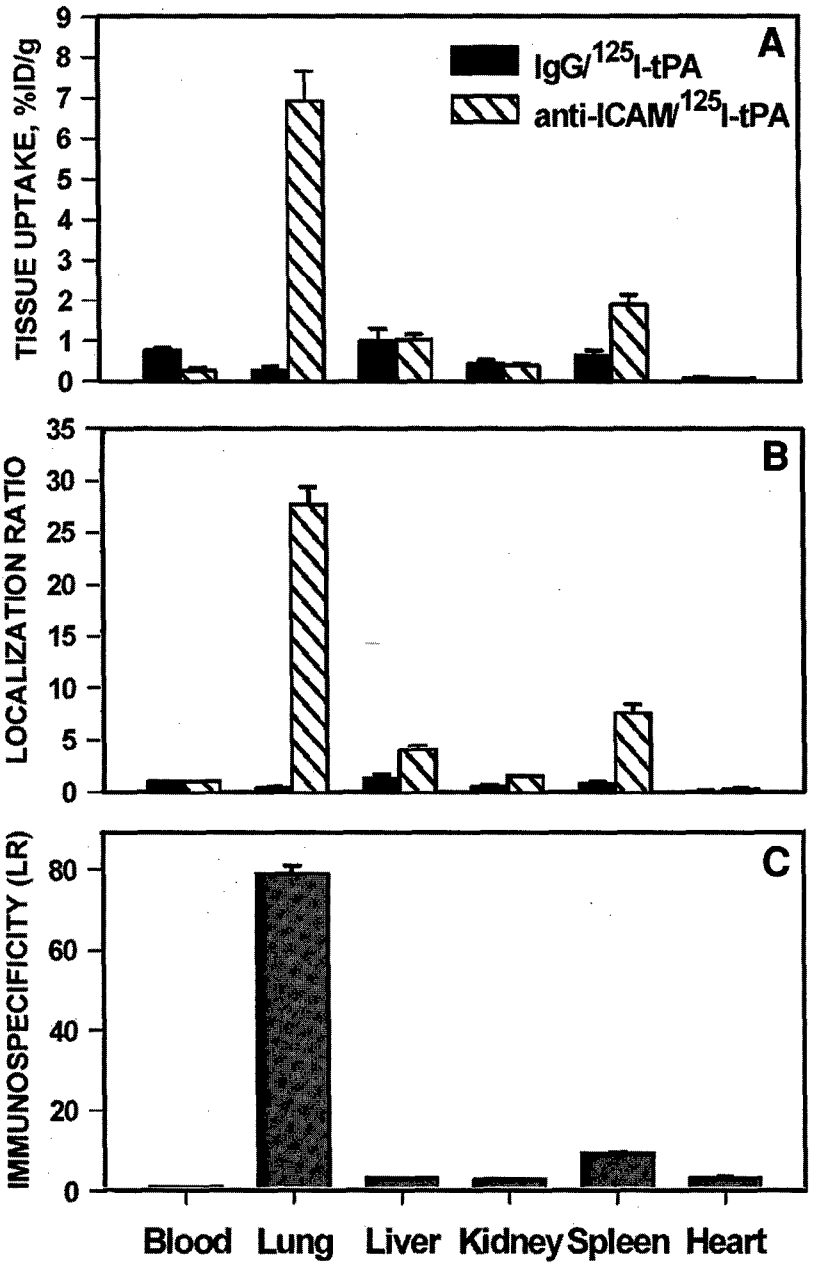

Fig. 6. Analysis of anti-ICAM/tPA biodistribution in vivo. Radioactivity in organs was analyzed 1 h after intravenous injection anti-ICAM/^{125}I-tPA (hatched bars) or control nonspecific IgG/^{125}I-tPA (black bars). The data (mean ± SD, n = 4–9) is presented as: **(A)** % ID/g of tissue; **(B)** LR; and **(C)** ISI. Adapted from **ref. *3***.

of ISI reveals that anti-ICAM/tPA accumulates in the lungs almost 100 times higher than IgG/tPA counterpart, thus confirming high specificity of targeting.

4. Notes

1. Uptake and trafficking of immunoconjugates within the target cells can be studied by tracing the antibody carrier, the enzymatic cargo, or both moieties. The protocols described in **Subheadings 3.1.2.1., 3.1.2.2.**, and **3.1.2.3.** trace antibody moieties using secondary antibodies against murine IgG. The same protocols can be used to trace enzyme cargo, for example, using an antibody to catalase. Moreover, conjugates directly labeled with a fluorescent probe, such as the ones based on fluorescent-labeled nanobeads or streptavidin crosslinker, are optimal because they can be visualized without additional staining. There are some specific factors that may require adjustment and optimization of the described protocols to be applied to particular conjugates and target cells of interest. Some general considerations are given below.
2. Many cell types do not adhere well to glass surfaces. Coating coverslips with a proadhesive protein (i.e., fibronectin, vitronectin, collagen) before cell seeding helps to solve this problem. A 1-h incubation with 1% gelatin solution in PBS followed by a 1-h incubation to dry coverslips up is a generic choice. The density of seeding of each cell type must be adjusted to reach confluence within the first 48 h after seeding to avoid repeated division cycles that can lead to detachment. For example, optimal density for HUVEC is 7×10^4 cell per 24 wells when seeded 48 h before the experiment. Moreover, cells tend to detach from any substrate at 4°C; thus, cold incubation should be minimal to permit binding of the conjugates. To avoid excessive detachment, pour washing medium gently and slowly on the well wall rather than directly on the cells. Glycine elution of membrane-bound conjugates may also provoke cell detachment and incubation time must be minimal (do not exceed 15 min). Inspect cell morphology and monolayer integrity by phase contrast microscopy and terminate "high-risk" exposures at the first signs of cell retraction, rounding or detachment.
3. Fixation of cells with 2% paraformaldehyde solution (10–15 min) is generally used when preparing samples for immunofluorescence, but the concentration must be optimized and can be lowed to 0.5 % to 1% if necessary to avoid disruption of the plasma membrane and partial cell permeabilization. In addition, the concentrations and incubation times of labeled antibodies given above are arbitrary and should be adjusted for particular preparations. To block nonspecific binding of labeled antibodies, preincubate fixed cells with a solution 10–20% serum of a corresponding animal species before immunostaining. To reduce nonspecific binding of the immunoconjugates (e.g., to control cells that do not express a target antigen), use incubation media containing 2–4% BSA.
4. Adjust settings for acquisition and processing of fluorescence images to optimize visualization. For instance, in the case that fluorescent signal was low, rational increase of the exposure time or brightness postacquisition can be performed, although preserving the specificity of the signal and the legitimacy of the image.

This approach helps to colocalize fluorescent signals obtained from different objects when labeled with fluorescent probes at different intensity, such as staining of a highly fluorescent FITC-labeled conjugate using secondary antibody that is relatively poorly labeled with Texas Red. Merging the images taken under similar acquisition parameters will show FITC signal masking Texas Red on the same object, not permitting visualization of a real double-labeled object and, therefore, leading to misinterpretation of the result. In addition, the choice of the fluorescent probes to reveal colocalizing objects should be made such that colors resulting from merged images permit an easy interpretation of the results. For instance, colocalization of green and red results in yellow and the three colors can be readily interpreted. However, colocalization of green and blue results in a light, bluish shade, not clearly distinguishable from the two parental colors.

5. Finally, the data on internalization and degradation of the radiolabeled conjugates should be analyzed and interpreted cautiously. For instance, multimeric conjugates can bind to cells with such high avidity that resulting large antibody/antigen clusters are difficult to disrupt by glycine elution, providing false-positive internalization result. Visualization of the uptake using double-fluorescence based techniques permits to circumvent this artifact.

Acknowledgments

The authors thank Drs. Michael Koval and Steven Albelda for contributions to the previous studies, which provided experimental background for the development of the protocols outlined in this chapter. This work was supported by NIH SCOR in Acute Lung Injury (NHLBI HL 60290, Project 4), NHLBI RO1 HL/GM 71175–01, and the Department of Defense Grant (PR 012262) to VRM.

References

1. Muzykantov, V. R., Christofidou-Solomidou, M., Balyasnikova, I., Harshaw, D. W., Schultz, L., Fisher, A. B., et al. (1999) Streptavidin facilitates internalization and pulmonary targeting of an anti-endothelial cell antibody (platelet-endothelial cell adhesion molecule 1): a strategy for vascular immunotargeting of drugs. *Proc. Natl. Acad. Sci. USA* **96,** 2379–2384.
2. Scherpereel, A., Wiewrodt, R., Christofidou-Solomidou, M., Gervais, R., Murciano, J. C., Albelda, S. M., et al. (2001) Cell-selective intracellular delivery of a foreign enzyme to endothelium in vivo using vascular immunotargeting. *FASEB J.* **15,** 416–426.
3. Murciano, J. C., Muro, S., Koniaris, L., Christofidou-Solomidou, M., Harshaw, D. W., Albelda, S. M., et al. (2003) ICAM-directed vascular immunotargeting of antithrombotic agents to the endothelial luminal surface. *Blood* **101,** 3977–3984.
4. Wiewrodt, R., Thomas, A. P., Cipelletti, L., Christofidou-Solomidou, M., Weitz, D. A., Feinstein, S. I., et al. (2002) Size-dependent intracellular immunotargeting of therapeutic cargoes into endothelial cells. *Blood* **99,** 912–922.

5. Muro, S., Wiewrodt, R., Thomas, A., Koniaris, L., Albelda, S. M., Muzykantov, V. R., et al. (2003) A novel endocytic pathway induced by clustering endothelial ICAM-1 or PECAM-1. *J. Cell Sci.* **116,** 1599–1609.
6. Kozower, B. D., Christofidou-Solomidou, M., Sweitzer, T. D., Muro, S., Buerk, D. G., Solomides, C. C., et al. (2003) Immunotargeting of catalase to the pulmonary endothelium alleviates oxidative stress and reduces acute lung transplantation injury. *Nat. Biotechnol.* **21,** 392–398.
7. Muzykantov, V. R., Atochina, E. N., Ischiropoulos, H., Danilov, S. M., and Fisher, A. B. (1996) Immunotargeting of antioxidant enzyme to the pulmonary endothelium. *Proc. Natl. Acad. Sci. USA* **93,** 5213–5218.
8. Danilov, S. M., Gavrilyuk, V. D., Franke, F. E., Pauls, K., Harshaw, D. W., et al. (2001) Lung uptake of antibodies to endothelial antigens: key determinants of vascular immunotargeting. *Am. J. Physiol. Lung Cell Mol. Physiol.* **280,** L1335–L1347.
9. Murciano, J. C., Harshaw, D., Neschis, D. G., Koniaris, L., Bdeir, K., Medinilla, S., et al. (2002) Platelets inhibit the lysis of pulmonary microemboli. *Am. J. Physiol. Lung Cell Mol. Physiol.* **282,** L529–L539.
10. Panes, J., Perry, M. A., Anderson, D. C., Manning, A., Leone, B., Cepinskas, G., et al. (1995) Regional differences in constitutive and induced ICAM-1 expression in vivo. *Am. J. Physiol.* **269,** H1955–H1964.
11. Kuiper, J., Otter, M., Rijken, D. C., and van Berkel, T. J. (1988) Characterization of the interaction in vivo of tissue-type plasminogen activator with liver cells. *J. Biol. Chem.* **263,** 18,220–18,224.

Endothelial Endocytic Pathways: Gates for Vascular Drug Delivery

Silvia Muro[1], Michael Koval[2] and Vladimir Muzykantov[1,3,*]

[1]*Institute for Environmental Medicine, Departments of* [2]*Physiology and* [3]*Pharmacology, University of Pennsylvania, School of Medicine, 1 John Morgan Building, 3620 Hamilton Walk, Philadelphia, PA 19104-6068, USA*

Abstract: Vascular endothelium plays strategic roles in many drug delivery paradigms, both as an important therapeutic target itself and as a barrier for reaching tissues beyond the vascular wall. Diverse means are being developed to improve vascular drug delivery including stealth liposomes and polymer carriers. Affinity carriers including antibodies or peptides that specifically bind to endothelial surface determinants, either constitutive or pathological, enhance targeting of drugs to endothelial cells (EC) in diverse vascular areas. In many cases, binding to endothelial surface determinants facilitates internalization of the drug/carrier complex. There are several main endocytic pathways in EC, including clathrin- and caveoli-mediated endocytosis, phagocytosis and macropinocytosis (these two are less characteristic of generic EC) and the recently described Cell Adhesion Molecule (CAM)-mediated endocytosis. The latter may be of interest for intracellular drug delivery to EC involved in inflammation or thrombosis. The metabolism and effects of internalized drugs largely depend on the routes of intracellular trafficking, which may lead to degrading lysosomal compartments or other organelles, recycling to the plasma membrane or transcytosis to the basal surface of endothelium. The latter route, characteristic of caveoli-mediated endocytosis, may serve for trans-endothelial drug delivery. Paracellular trafficking, which can be enhanced under pathological conditions or by auxiliary agents, represents an alternative for transcytosis. Endothelial surface determinants involved in endocytosis, mechanisms of the latter and trafficking pathways, as well as specific characteristics of EC in different vascular areas, are discussed in detail in the context of modern paradigms of vascular drug delivery.

Keywords: Drug delivery, Vascular endothelium, Endocytosis, Transcytosis, Paracellular transport, Intracellular trafficking.

1. INTRODUCTION

VASCULAR ENDOTHELIUM: A BARRIER AND TARGET FOR DRUG DELIVERY

The inner surface of blood vessels is lined with endothelial cells (EC) strategically positioned to control vascular physiology. EC control numerous vital functions and represent an extremely important target and barrier for drug delivery.

For instance, numerous vasoactive factors secreted by EC and including (yet most likely not limited to) NO, prostacyclin and endothelium-derived hyperpolarizing factor (EDHF), suppress contractility of the vascular smooth muscle cells and therefore control vascular tone [1, 2].

EC help to control thrombosis [1]. For example, in concert with plasma protein C, endothelial transmembrane glycoprotein thrombomodulin converts thrombin into an anti-coagulant enzyme [3]. Among other anti-thrombotic factors, EC secrete NO and prostacyclin, which suppress platelet aggregation, as well as urokinase and tissue type plasminogen activators that dissolve blood clots *via* generation of the fibrin-degrading protease plasmin.

The endothelium is also involved in inflammation, a process that is often intertwined with thrombosis [4, 5]. Under normal circumstances, EC provide very limited, if any, support for activities of pro-inflammatory cells (e.g., white blood cells, WBC). However, pathological mediators, including cytokines, reactive oxygen species (ROS), growth factors and abnormal shear stress, induce endothelial secretion of chemoattractants and exposure of adhesion molecules leading to leukocyte attraction, adhesion and transmigration [6-9].

Furthermore, EC play an important role in normal and pathological vascular redox mechanisms [10]. They produce ROS (superoxide anion O_2^- and H_2O_2) *via* enzymatic pathways that can be further activated by pathological mediators [11]. ROS apparently play an important role in cellular signaling. However, ROS overproduction by EC or by activated WBC leads to vascular oxidant stress, inactivation of NO by O_2^-, lipid peroxidation and tissue injury [12].

EC function is modulated by exposure to dynamic environmental factors such as blood flow shear stress, aggressive inflammatory cells and compounds in the circulation, including lipids, proteases, oxidants and xenobiotics. Disruption of normal endothelial function can exacerbate the pathology of a number of diseases including atherosclerosis, hypertension, thrombosis, diabetes, acute lung injury and sepsis. Improper EC function can also lead to defects in angiogenesis, which in turn, could either inhibit vascularization during wound repair resulting in tissue necrosis or cause inappropriate blood vessel formation, which can lead to tumor vascularization. Therefore, EC

*Address correspondence to this author at the IFEM, University of Pennsylvania Medical Center, 1 John Morgan Building, 3620 Hamilton Walk, Philadelphia, PA 19104-6068, USA; Tel: 215-898-9823; Fax: 215-898-0868; E-mail: muzykant@mail.med.upenn.edu

1570-1611/04 $45.00+.00

represent an important potential target for delivery of therapeutic agents including, but not limited to, antioxidants to protect against oxidative stress, anticoagulants and fibrinolytics to manage thrombotic stress, NO donors to reduce vessel tone and blood pressure, and anti-inflammatory agents to suppress vascular inflammation.

The total surface area of vascular endothelium in the human body approaches the size of a tennis court (~ 240 m^2), making it a large and highly accessible target for drugs circulating in the bloodstream. Most therapeutic agents, however, have no specific affinity to this target. Therefore, only a small fraction of injected drugs produces a therapeutic effect in endothelium, whereas the major fraction is handled as a waste product, or worse, produces deleterious side effects. Furthermore, binding to target cells is necessary, but not sufficient, for effective action of many drugs, which require internalization and proper sub-cellular addressing. Thus, it is a key issue in the design of drug delivery vehicles to create carriers that are targeted to EC and also are trafficked by the target cells to destinations where they can have maximal efficacy. Recognizing this problem, more and more groups are focusing their research efforts on the design of novel strategies for targeted delivery of therapeutics to EC [13-26].

With other layers of the blood vessel wall, the endothelium forms a barrier for delivery of drugs to extravascular targets, such as tumors, brain and myocardium. Understanding the mechanisms involved in trans-cellular and paracellular endothelial transport may permit more effective delivery of these drugs. Among other parameters, endothelial uptake and transcytosis depend on the size of a transported agent. Barrier function of endothelium is especially restrictive for large therapeutic molecules (e.g., proteins or genetic materials) and drug delivery systems that employ carrier nanoparticles, liposomes, or high molecular mass polymers.

Therefore, the endothelium is an extremely important tissue in the context of vascular drug delivery, either as a target itself for therapeutic interventions by a delivered drug or as a barrier on route to peripheral tissues [27, 28]. Targeted delivery of drugs to endothelium and control of their internalization, sub-cellular addressing and transendothelial transport are critically important components for the rational design of safe, effective and specific therapies. The goal of this article is to review these issues in the context of drug delivery systems designed for targeting of drugs to and beyond EC.

2. A BRIEF OVERVIEW OF VASCULAR DRUG DELIVERY SYSTEMS

Most known drugs lack specific binding and uptake by target organs. On the other hand, many drugs undergo rapid inactivation in the body by aggressive components of blood and special cellular detoxifying systems. In addition, some drugs including therapeutic enzymes (e.g., proteases), have specific inhibitors in the blood. Also, drugs can be eliminated through a number of mechanisms, including clearance from the bloodstream by non-specific targets (e.g., red blood cells and hepatocytes) and specific clearance systems (e.g., reticuloendothelial system and renal filtration). This often dictates that administration of large doses is required for efficacy, also increasing potentially dangerous side effects.

Elimination and inactivation of pharmacological agents is decreased when a therapeutic "cargo" is loaded into or conjugated with natural or artificial carriers increasing bioavailability of a drug (e.g., liposomes, polymer nanoparticles, lipoproteins, blood cells or proteins) [27, 29-37]. Coating of drugs or their carriers by activated polyethylene glycol, PEG, forms an aqueous shell masking against natural protective mechanisms including macrophages, complement and immune cells, a strategy sometimes referred to as "stealth" technology [38-40]. PEG-coating markedly prolongs circulation of drugs and reduces side effects associated with the immune response and systemic activation of host defense including complement and leukocytes.

In addition, many delivery systems such as liposomes or conjugation with carrier lipoproteins, facilitate intracellular uptake of drugs [41]. The mechanisms of this phenomenon are complex and depend on specific cell type and carrier (see below). However, there are several mechanisms employed by currently available drug carriers to facilitate intracellular uptake.

First, drugs conjugated with ligands of cellular receptors can be internalized *via* vesicle-mediated pathways. Endocytosed carriers usually follow the natural itinerary their receptors would normally traverse to the point of dissociation or degradation in intracellular compartments such as lysosomes. For example, cells expressing transferrin receptor internalize drugs conjugated or genetically fused with transferrin *via* clathrin-mediated endocytosis [42]. Second, fusion-competent liposomes can be designed to enter the cells *via* endocytic pathways, leading to delivery and fusion with intracellular membrane organelles, or to fuse with lipids in the plasma membrane, thus injecting their content directly into the cytosol. In an attempt to control the extent and specificity of cytosolic delivery, liposome carriers have been designed that are destabilized after internalization at acidic pH in endocytic compartments prior to release of a drug or fusion with cell membranes [43]. Third, antibodies and their derivatives with multivalent binding sites facilitate cellular entry of liposomes [44-48]. Fourth, a more recent approach to cytosol delivery has been to couple proteins and sub-micron particles with the TAT-peptide from HIV virus, which in some instances can enter cells in an energy independent manner, although they may require endocytosis in other cases [49, 50]. This and some other charged peptides enriched with lysine and/or arginine promiscuously permeate cell membranes and enable cytosolic delivery to diverse cell types *in vitro* and *in vivo* [51, 52].

Therefore, diverse natural carriers (e.g., lipoproteins or transferrin) or synthetic carriers (e.g., liposomes) can facilitate vascular drug delivery and intracellular uptake. In the next section we consider how these means can be employed in the context of specific drug targeting to EC.

3. ENDOTHELIAL SURFACE DETERMINANTS: POTENTIAL TARGETS FOR DRUG DELIVERY

Stealth liposomes, protein carriers and other delivery systems prolong the circulation time of drugs and may enhance their cellular uptake, but do not confer an affinity to

EC. Unless drugs are coupled to high-affinity carriers, the circulation removes drugs and their derivatives rapidly, even after local infusion *via* vascular catheters. In these instances, the major fraction of injected materials ends up in the liver and not in EC. Devices allowing a transient cessation of blood flow in the site of catheter placement have been designed in order to attain a high local concentration and a more effective prolonged interaction of the infused material with endothelium, but blood flow interruption may lead to ischemia and vascular injury.

Viable means for effective, rapid, and safe targeting of therapeutic molecules to EC are beginning to emerge to address this important and persisting biomedical problem. In order to facilitate targeting, cargoes or their carriers can be conjugated (chemically or genetically) with affinity moieties that bind to EC. Antibodies directed against endothelial surface determinants and small antigen-binding fragments of these antibodies represent one of the most useful classes of affinity carriers for targeted drug delivery to EC. Indeed, coupling drugs with carrier antibodies permits targeted delivery to EC (vascular immunotargeting) [19, 53].

Immunostaining of tissues, *in vivo* selection of peptide ligands using phage display and tracing labeled antibodies in animals have been used to identify several EC antigens that potentially can be used as targets [14, 15, 20, 21, 54-57]. However, no universal or ideal carrier suits all therapeutic needs. Specific therapeutic goals require different secondary effects mediated by binding to EC, drug targeting to different sub-populations of EC (e.g., resting *vs.* inflammation-engaged EC), and to diverse cellular compartments. Also, targeted delivery of antioxidants or NO-donors to normal or resting EC can be useful for either prophylaxis or therapies. On the other hand, specific recognition and drug delivery to abnormally activated or pathologically altered EC might permit more specific means for treatment of such maladies as localized tumor growth and inflammation. Table **1** shows some endothelial determinants useful for experimental vascular targeting to EC, which may have therapeutic potential.

Several surface determinants are potentially useful for targeting either normal and/or pathologically altered EC. For example, antibodies to thrombomodulin (TM), a constitutively expressed EC antigen, can be used for targeting of diverse cargoes to the endothelium [58]. Unfortunately, TM is functionally "untouchable" for therapies, because its inhibition by anti-TM may cause thrombosis [59]. However, TM antibodies are being successfully utilized for delivery of reporter or toxic compounds to the pulmonary EC in animal models [60].

Angiotensin-converting enzyme (ACE) is a transmembrane glycoprotein expressed on the endothelial luminal surface, which converts Ang I into Ang II to induce vasoconstricting, pro-oxidant and pro-inflammatory activities [61-63]. Pulmonary vasculature is enriched in

Table 1. Endothelial Determinants: Selected Candidate Targets for Drug Delivery

Target	Function and Localization	Targeting Advantages	Potential Problems
ACE	Peptidase, converts Ang I into Ang II and cleaves bradykinin. ACE enriched in the lung capillaries.	Selective targeting to lung EC. Intracellular delivery. Vasodilating and anti-inflammatory effects of ACE inhibition.	Inflammation suppresses targeting. ACE inhibition may be dangerous.
TM	Binds thrombin and converts it into an anti-coagulant enzyme. Enriched in the lungs.	Intracellular delivery to EC useful for modeling of lung injury in animals.	Inflammation suppresses targeting. Thrombosis due to TM inhibition.
PECAM	Facilitates transmigration of leukocytes. Stably expressed in EC borders.	Intracellular delivery of anti-PECAM conjugate may also suppress inflammation	PECAM-signaling and side effects are not understood
ICAM	Mediates leukocyte adhesion to EC. Stably expressed by EC, and up-regulated by pathological agents.	Similar to PECAM, but inflammation enhances targeting.	Similar to PECAM
E-selectin	Supports leukocytes adhesion. Expressed only on altered EC.	Intracellular targeting to EC in inflammation	Targeting is not robust. Transient expression.
P-selectin	Similar to E-selectin	Similar to E-selectin	Similar to above. Targeting platelets
gp90	Function unknown. Localized in EC cavoli.	Transendothelial targeting.	Human analogue and side effects are not known.
gp85	Function unknown. EC avesicular zone in alveolar capillaries.	Targeting to the EC surface	Similar to above
gp60	Albumin-binding protein in EC caveoli	Transendothelial targeting	Side effects and specificity of targeting are not known

EC – endothelial cells, ACE – angiotensin-converting enzyme, TM - thrombomodulin, PECAM - platelet-endothelial adhesion molecule, ICAM - intercellular adhesion molecule; gp – glycoproteins.

ACE: nearly 100% of EC in the alveolar capillaries are ACE-positive *vs* <15% ACE-positive EC in the extra-pulmonary capillaries [64]. Radiolabeled anti-ACE accumulates in the pulmonary vasculature after intravascular and intraperitoneal injections in rats, cats, primates and humans [14, 17]. Diverse reporter compounds and drugs conjugated with anti-ACE accumulate selectively in the lungs after intravenous injection in rats [14, 17, 65]. Recently, anti-ACE has been used successfully for re-targeting of viruses to pulmonary EC in rats [25, 26].

ACE also inactivates bradykinin, a peptide stimulating NO production, although Ang II may stimulate NO production by EC [66]. Some anti-ACE antibodies block its active site and/or facilitate ACE shedding from the endothelium by specific secretases regulated by metalloproteases [67-69]. However, other ACE antibodies enable ACE to retain its function. Therefore, using ACE antibodies directed to different epitopes enables targeting strategies to be developed that either retain or inhibit ACE activity, enhancing flexibility and therapeutic applicability of the strategy. ACE inhibition may be beneficial in conditions associated with vascular oxidant stress, ischemia and inflammation.

Pro-inflammatory agents (e.g., ROS) suppress endothelial expression of ACE [70, 71] which may inhibit therapeutic targeting. However, anti-ACE is a good candidate for targeting to the pulmonary endothelium for a prophylactic use; it does not cause acute harmful reactions in animals and humans [17]. EC internalize anti-ACE that may deliver drugs intracellularly [65]. Anti-ACE-conjugated antioxidant enzymes such as catalase, accumulates in rat lungs *in vivo* [72] and protect perfused rat lungs against H_2O_2 [73].

Platelet-Endothelial Cell Adhesion Molecule-1 (PECAM, CD31) is a pan-endothelial transmembrane Ig superfamily glycoprotein (m.w. 130 kD), predominantly localized in the sites of cellular contacts in the endothelial monolayer [74]. Platelets and WBC also express PECAM, but at levels that are orders of magnitude lower than EC. PECAM is abundant in EC, which express millions of anti-PECAM binding sites [75]. In addition, PECAM is a stable EC antigen: cytokines and ROS do not down regulate its expression and surface density on the endothelium. This promises a robust PECAM-targeted drug delivery to either normal or pathologically altered vasculature, for either prophylaxis or therapies.

PECAM is involved in the cellular recognition, adhesion, signaling, and trans-endothelial migration of leukocytes [74]. Adhesion and transmigration of leukocytes is involved in pathogenesis of many disease conditions including inflammation, sepsis, atherosclerosis, acute lung injury and diabetes [76-78]. Animal studies showed that blocking PECAM by administration of anti-PECAM suppresses inflammation and protects organs against leukocyte-mediated oxidant stress [77, 79]. Therefore, anti-PECAM targeting may provide secondary benefits for management of inflammation, perhaps by attenuation of leukocyte transmigration.

EC bind anti-PECAM without internalization, but anti-PECAM conjugation (e.g., by streptavidin) provides multimeric anti-PECAM complexes that are readily internalized by endothelium and accumulate in animal lungs in perfusion or after IV administration [64, 75]. An active reporter enzyme, beta-galactosidase, conjugated to anti-PECAM has been shown to accumulate intracellularly in the pulmonary endothelium as soon as 10 min after IV injection in mice and pigs [80, 81].

InterCellular Adhesion Molecule-1 (ICAM-1, CD54) is another Ig superfamily surface glycoprotein with a short cytoplasmic domain, transmembrane domain and large extracellular domain [6, 82-84]. It is normally expressed by EC at relatively high surface density ($2x10^4$-$2x10^5$ surface copies per cell). Some other cell types also express ICAM-1 (e.g., alveolar epithelial cells, macrophages). However, the major fraction of blood-accessible ICAM-1 is exposed on the luminal surface of EC. Several laboratories demonstrated robust and specific binding of radiolabeled ICAM antibodies and anti-ICAM conjugates to vascular endothelium after intravenous administration in diverse laboratory animals [64, 73, 85-87].

Pathological stimuli, such as ROS, cytokines, abnormal shear stress and hypoxia stimulate surface expression of ICAM-1 by EC *via* signaling mechanisms involving activation of MAP kinases and nuclear translocation of NF-kappaB [88, 89]. ROS and cytokines elevate the ICAM-1 surface density in pulmonary EC [90, 91]. Therefore, in contrast with some other constitutive endothelial determinants (e.g., TM and ACE), immunotargeting to ICAM-1 is not suppressed, but instead is markedly facilitated in inflammation and other pathological conditions [85-87, 92-96].

ICAM-1, a counter-receptor for integrins on WBC, supports their firm adhesion to EC and thus contributes to inflammation [97-100]. In addition, ICAM-1 serves as a natural ligand for certain viruses [101]. ICAM-1 may also serve as a signaling molecule, yet the exact mechanisms, specificity and significance of this signaling in different cell types remains to be more fully elucidated. Antibodies (including humanized murine mAbs) directed against ICAM-1 suppress leukocytes adhesion to EC, thus producing anti-inflammatory effects in animal models and clinical pathological settings associated with vascular injury, such as acute inflammation, ischemia/reperfusion and oxidant stress [102-106]. Blocking of endothelial ICAM-1 by targeting may inhibit leukocyte adhesion to EC and thus suppress inflammation, a benefit for treatment of vascular oxidant and thrombotic stress. The anti-inflammatory effect of anti-ICAM conjugates may be even more potent due to their potentially higher affinity/valency and down regulation of surface ICAM-1 *via* internalization (see below).

Antibodies directed against constitutive cell adhesion molecules PECAM and ICAM described above do not discriminate between EC in different vascular areas, thus providing "pan-endothelial targeting". Anti-PECAM and anti-ICAM directed conjugates accumulate preferentially in the lungs after intravenous administration (due to the fact that pulmonary vasculature represents about 30% of the total vascular surface in the body and receives 100% cardiac first pass venous blood output), whereas injecting *via* catheters inserted in a conduit artery facilitates local delivery in the downstream vascular area [64, 81]. Local delivery may also

be enhanced by surface endothelial determinants enriched in particular vascular areas or in focal pathological processes.

For example, glycoprotein gp85 identified by Ghitescu [107] is predominantly localized in the thin part of EC body that separates alveolar and vascular compartments and lacks main organelles ("avesicular zone"); gp85 monoclonal antibodies accumulate in rat pulmonary vasculature without internalization [108]. On the other hand, animal studies showed that the pulmonary endothelium in rats contains surface determinants localized to cholesterol-enriched plasma membrane microdomains, including caveoli. Ligands of determinants localized to caveoli such as gp60 and gp90 also accumulate in the pulmonary vasculature after intravenous injection in rats, enter EC and traverse endothelial barrier [57]. The functions and human counterparts of these endothelial determinants are not known and, thus their potential utility as targets for drug delivery is not clear. However, caveoli-localized determinants might provide an exciting opportunity for trans-endothelial drug delivery (see Section 6).

Endothelium in the cerebral vasculature represents a specially important and difficult target. Recent animal studies showed that carrier antibodies and peptides directed to several surface determinants relatively enriched in EC in the brain, including receptors for transferrin, insulin, putrescin and some growth factors, permit delivery of the reporter compounds and genes into the brain [109-111]. Importantly, some of these endothelial receptors apparently permit transendothelial drug delivery into the brain tissue and neurons (see in Section 6).

EC exposed to inflammatory mediators and abnormal shear stress show cell surface expression of P-selectin, normally stored intracellularly and mobilized rapidly to the surface, and E-selectin, which is newly synthesized by activated EC [7]. Therefore, selectins are transiently exposed on the surface of stressed EC [112, 113]. Experiments in cell cultures and limited animal studies show that selectins may permit targeting of drugs to cytokine-activated endothelium [16, 114-118].

EC in solid tumors also represent a specially important and challenging target for delivery of agents designed to visualize tumors, inhibit angiogenesis, or eradicate malignant cells [119-121]. Tumor vasculature is characterized by numerous morphological abnormalities [122, 123]. EC in tumor vessels expose abnormal determinants including selectins (see above), integrins, apoptosis markers and receptors for growth factors [124-128]. Targeting these determinants in tumors might be useful to accomplish two goals: i) inflict damage in the tumor vasculature leading to thrombosis, infarction and starvation of malignant cells [18, 129] and, ii) delivery of anti-tumor agents to the proper malignant cells using, for example, PEG-immunoliposomes or polymers loaded with taxol or doxorubicin [130, 131]. The latter approach involves permeation of the endothelial barrier, mostly *via* paracellular pathways (see Section 6). EC seem to internalize protein carriers modified with peptides containing RGD sequence to provide recognition of integrins over-expressed on tumor endothelium [132].

In summary, affinity carriers directed to diverse determinants presented on surface of normal or pathologically altered EC, permit targeted delivery of reporters and, perhaps, therapeutic cargoes to the vascular endothelium. In addition to this delivery function, affinity carriers may provide additional means to control the rate of internalization and sub-cellular or trans-cellular traffic. This subject will be considered in more detail in the following sections.

4. MECHANISMS OF ENDOTHELIAL ENDOCYTOSIS

Endocytosis is a complex and delicately coordinated process, which involves an extensive cellular machinery to mediate the formation of membrane transport vesicles to enable the internalization of extracellular material (reviewed in [133-135]). In endothelium, which is strategically positioned at the interface between blood vessels and interstitial milieu, endocytosis has a prime role in the maintenance of body homeostasis by regulating transendothelial gradients and the transport of macromolecules (reviewed by [136, 137]). Depending upon the ultimate fate of the internalized vesicles, endocytic events in EC have been categorized as either endocytosis, i.e., the uptake of fluids, biomolecules and other ligands that sort to endothelial processing pathways, or transcytosis that reflects transport across the cells to the subendothelial space [138-140]. EC employ multiple mechanisms for vesicle-mediated membrane transport (see Fig. **1** and Table **2**). The mechanism of endocytosis is frequently dictated by membrane receptors used by extracellular ligands to bind to the plasma membrane as a prerequisite to internalization.

Caveolar-mediated uptake plays an important role in endothelial transport functions (reviewed by [141-144]). Caveolar-mediated endocytosis is preferentially inhibited by chelators of cholesterol (e.g., filipin or cyclodextrin) and is mediated by interactions of the coat protein caveolin with cell signaling and cytoskeletal molecules. Internalization *via* caveoli is involved in the uptake of glycolipids, GPI-anchored proteins, and chemokines [145-148], dynamic recycling of brain microvascular EC membranes [149], constitutive turnover of TM [150], potocytosis of folate and other solutes [151], and can participate in the regulation of the vascular permeability [152]. Importantly, caveolar-mediated endocytosis serves as an entry point for transcytosis of many compounds through the endothelial monolayer from the bloodstream to sub-endothelial tissues (see Section 6).

Clathrin-mediated endocytosis, which is the predominant form of receptor-mediated endocytosis in most cell types, is less prominent in EC than caveolar-mediated endocytosis. Nonetheless, numerous cases of clathrin-mediated endocytosis have been reported among EC, particularly, in EC in hepatic sinusoids, which participate in clathrin-mediated internalization of IgG immune complexes *via* Fc receptors [153]. Mannose-terminated glycoproteins or lactosilated albumin particles are internalized through mannose or galactose-specific receptors [154, 155]. Also, colloidal gold coated with mannan, albumin, or thrombospondin aggregates on coated pits and is taken up by EC in sinusoids in liver [156-159]. This is also the case for chondroitin sulphate proteoglycan attached to gold particles,

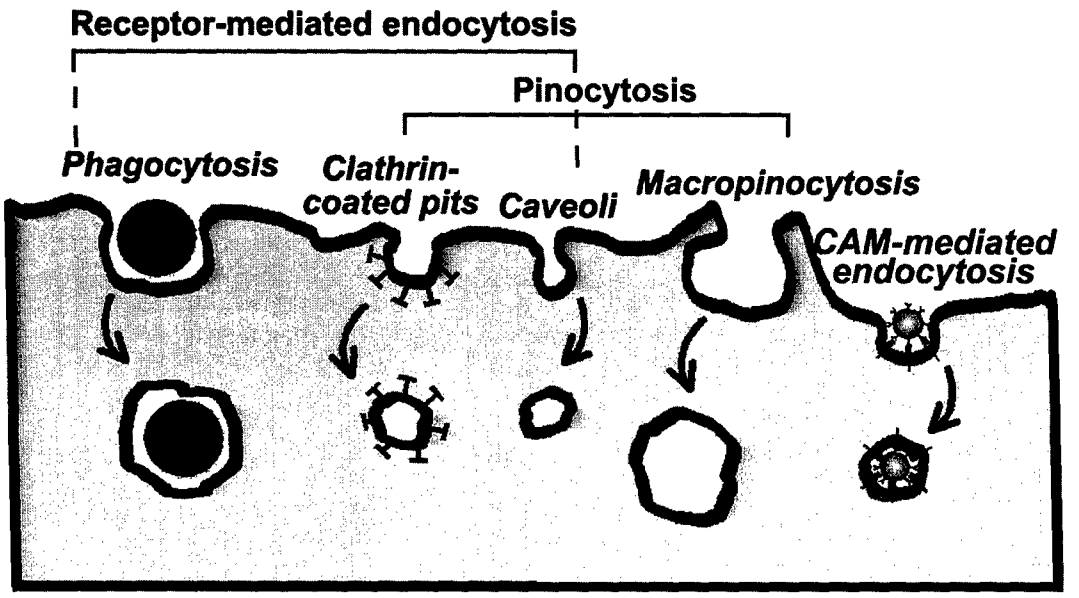

Fig. (1). *Endocytic pathways*: Endocytosis accounts for the internalization of extracellular material into cells, mediated by formation of transport vesicles derived from the plasma membrane. The terms "phagocytosis" and "pinocytosis" refer to the uptake of large particulate ligands and extracellular medium, respectively. In addition, macromolecular ligands can bind to specific receptors at the plasma membrane, triggering their internalization by what is known as "receptor-mediated endocytosis". This term contrasts with "macropinocytosis", which consists in the non-adsorptive bulk uptake of extracellular fluids. Cell adhesion molecule (CAM)-mediated endocytosis is stimulated by clustering Ig superfamily CAMs. "Clathrin-" and "caveoli"-mediated pathways are ubiquitous endocytic mechanisms, whereas "phagocytosis" and "macropinocytosis" are most typically presented by specialized cells (e.g., macrophages, dendritic cells). The five different pathways depicted have been found to some extent in EC, yet "caveoli"-mediated endocytosis seems to be the most active process.

Table 2. Endocytic Pathways and Inhibitors

Internalization pathway	Inhibitor	Molecular target
Clathrin-mediated	Potasium depletion	Clathrin dissociation
Clathrin-mediated	MDC	Protein interaction at latices
Clathrin-mediated	Amantadine	Vesicle budding
Caveoli	Genistein	Tyrosine kinases
Caveoli	Filipin	Cholesterol sequestration
Caveoli	Cyclodextrin	Cholesterol extraction
Multiple	Dynamin K44A, PH*	Dynamin
Macropinocytosis/Phagocytosis	Cytochalasin	Actin filaments
Multiple	Latrunculin	Monomeric actin
Macropinocytosis	Amiloride	Na^+/H^+ exchanger
Macropinocytosis	BIM-1, H7, staurosporin	Protein kinase C
EGF/BCR receptor uptake	Radicicol	Src kinase
Rho dependent uptake	Y27632	ROCK
Macropinocytosis/Phagocytosis	Wortmannin	PI3 kinase

MDC – Monodansyl cadaverine. Dynamin K44A – dominant negative dynamin affected at the ATPase site. Dynamin PH* - dominant negative dynamin affected at the plecktrin homology domain. BIM-1 – Bisindolylmaleimide-1. H7 - 1-(5-Isoquinolinesulfonyl)-2-methylpiperazine. ROCK – Rho dependent kinase. PI 3 kinase – phosphatidyl inositol 3 kinase.

which bind to hyaluronic acid/chondroitin sulphate receptor at the plasma membrane and undergo internalization by coated pits in rat liver EC [160].

The endothelium in many organs (i.e. spleen, bone marrow, thymus, or brain) has been shown to internalize ligands through clathrin-mediated endocytosis, as is the case for acetoacetylated or acetylated LDL [161], gold-coated LDL or insulin [162], and transferrin [163, 164]. Also, EC likely internalize lipoprotein lipase (LPL) by clathrin-related mechanisms. LPL synthesized and secreted by EC is retained on the abluminal side, being further transported across the cell to the apical space [165], where it provides intravascular hydrolysis of triacylglycerol-rich lipoproteins [166] and also contributes to LDL-holoparticle turnover and selective uptake of LDL-associated lipids [167]. Internalization of LPL within the cell might occur as a consequence of its interaction with heparan sulphate proteoglycans during turnover or recycling of the latter [168]. For instance, LPL stimulates endocytosis of LDL upon binding of membrane-associated heparan sulphate [169] and also enhances binding, uptake and degradation of glycated LDL in a manner independent of LDL receptor and LDL-receptor related protein [170]. Additionally, LPL has been found to bind with high affinity to the glycoprotein gp330 in microvascular EC [171, 172]. Although the localization of gp330 in EC remains unclear, this is typically concentrated to clathrin-coated areas in epithelial cells, indicating that LPL internalization might be mediated by a clathrin-related pathway [173]. However, lipoprotein interactions with the syndecan family of endothelial proteoglycans also can lead to internalization *via* a clusterization-induced pathway distinct from coated pits endocytosis [174].

Clathrin-coated pits also mediate constitutive internalization of plasma membrane proteins, as is the case for E- and P-selectins, two inducible endothelial adhesion molecules whose recycling and/or surface expression is regulated by clathrin-mediated uptake [112, 175]. The inducible expression of selectins has been used as a means to enable intracellular delivery to activated EC. For instance, anti-E-selectin targeted liposomes or conjugates have been found to internalize *via* clathrin-coated pits within EC, to enable intracellular delivery of anti-inflammatory drugs [176, 177].

Another membrane internalization process represented in EC, although to a low extent, is phagocytosis (reviewed in [178, 179]). Phagocytosis, which is typically displayed by macrophages and antigen presenting cells, accounts for the internalization of large (> 1μm) particulate ligands [180]. This requires initial binding of the particle to specific receptors (i.e. scavenger receptor, C3R, FcγR, etc), with subsequent activation of a battery of signaling cascades (i.e. phosphatidyl inositol 3 kinase and Rho family GTPases, among others) (reviewed by [181]). In many instances, these events drive a major redistribution of the actin cytoskeleton. As a consequence of the cortical actin polymerization, either pseudopods or large invaginations form at the cell surface, where the plasma membrane surrounds the particulate ligand in a zipper-like mechanism [182], finally resulting in a cup-shape invagination. This is the case of vascular EC, which have been reported to uptake aged red blood cells and apoptotic cells with phosphatidylserine exposed in the outer layer of the cell surface, upon binding of these to the lectin-like oxidized LDL receptor 1 (LOX-1) [183]. *Neisseria meningitidis* induces the formation of cellular protrusions *via* activation of Rho and Cdc42 and recruitment of ezrin and moesin to the cortical membrane, which mediate bacterial entrance in EC [184].

In contrast to caveoli-mediated, clathrin-mediated endocytosis and phagocytosis, macropinocytosis [185, 186] is generally considered a non-receptor mediated process, where cells uptake large volumes of extracellular fluids and solutes (classical macropinosomes are > 1μm in diameter), during a mechanism that involves active formation of membrane ruffles and protrusions at the plasma membrane [187-189]. This is reminiscent of phagocytosis, where macropinocytosis requires large re-arrangements of the actin cytoskeleton, with involvement of protein kinases C and Rho family small GTPases as central signal transduction players [190-194]. In general, however, macropinocytosis is constitutive in highly specialized cells (i.e. macrophages and dendritic cells) and can be induced by growth factors in epithelial cells [195-197], but does not seem to be a principal endocytic pathway in EC. Nevertheless, it has recently been found that human immunodeficiency virus (HIV) can access brain microvascular EC by a macropinocytic mechanism, apparently involving endothelial ICAM-1 [198].

However, neither phagocytosis, macropinocytosis nor classical clathrin-mediated endocytosis seem to be principal endocytic pathways in vascular endothelium. In fact, coated-pits are much less abundant than non-coated vesicles in capillary endothelium in lung [199]. For example, hormones like insulin or gonadotropin [200, 201], long chain fatty acids such as oleate [202], or ligands for TM [203, 204], have been described to enter vascular EC *via* coated pits as a minor fraction, whereas caveoli account for the internalization of the main pool.

Interestingly, two adhesion molecules constitutively expressed in EC, ICAM-1 and PECAM-1, present the capability to drive internalization of small multivalent ligands, although neither these molecules nor their monomeric ligands (i.e. antibodies) have been found to be internalized by endothelium [75, 87, 205, 206]. However, major group human rhinovirus and respiratory syncytial virus use ICAM-1 as a receptor during cell invasion, although the mechanism of cell uptake remains uncertain [207, 208]. Also, PECAM-1 is required for binding of malaria infected red blood cells to EC in culture [209] and homophilic PECAM-1 interaction displays a signaling role during recognition and phagocytic ingestion of apoptotic leukocytes by macrophages [210].

This offers a pathway for intracellular delivery of therapeutic cargoes, by using small multimeric conjugates of ICAM-1 and PECAM-1 antibodies. These have been recently shown to enter EC by a non-classical endocytic mechanism, CAM-mediated endocytosis, which is distinct from classical clathrin- or caveolar-mediated uptake as well as from phagocytic and macropinocytic processes [206]. In particular, internalization of anti-ICAM-1 or anti-PECAM-1 conjugates was dependent on antigen clustering, and a critical parameter for internalization was conjugate size (100

- 300 nm in diameter). CAM-mediated endocytosis also required Rho kinase- and protein kinase C- mediated rearrangements of the actin cytoskeleton [206].

Anti-PECAM/DNA conjugates provide specific transfection of EC in culture [205] and in mice [22]. Furthermore, anti-PECAM-conjugated glucose oxidase generates H_2O_2 in cultured EC intracellularly in cell culture [211] and induces acute oxidative endothelial injury in murine lungs after IV injection [212]. Recent studies indicate that anti-CAM/catalase conjugates bind to and enter EC, which protects endothelium against oxidant stress in cell cultures [75, 213] and in animals [214].

5. INTRACELLULAR TRAFFICKING AND FATE OF INTERNALIZED MATERIALS

The endocytic pathways reviewed above can be used for the intracellular or transcellular delivery of therapeutic cargoes in EC. Therefore, control of the cellular processes driving the internalization of site-specific therapeutics is important in order to achieve their optimal effects. Intracellular trafficking of a drug can be dictated by its entry pathway; hence determining its final destination and degradation rate. For instance, internalized membranes and/or contents can be selected for recycling to the cell surface, transported through the cell body and exocytosed by transcytosis, sorted to other sub-cellular destinations such as Golgi, trans-Golgi network (TGN) or endoplasmic reticulum (ER), or most typically processed for delivery to specialized intracellular compartments responsible for degradation of internalized materials (see Fig. 2 and Table 3).

In this context, there are three main systems accounting for protein degradation in mammalian cells. Cytosolic proteins are degraded by proteosomes or calpains, whereas lysosomal proteases digest proteins within the lumen of endocytic vesicles. Calpains are cysteine proteases localized

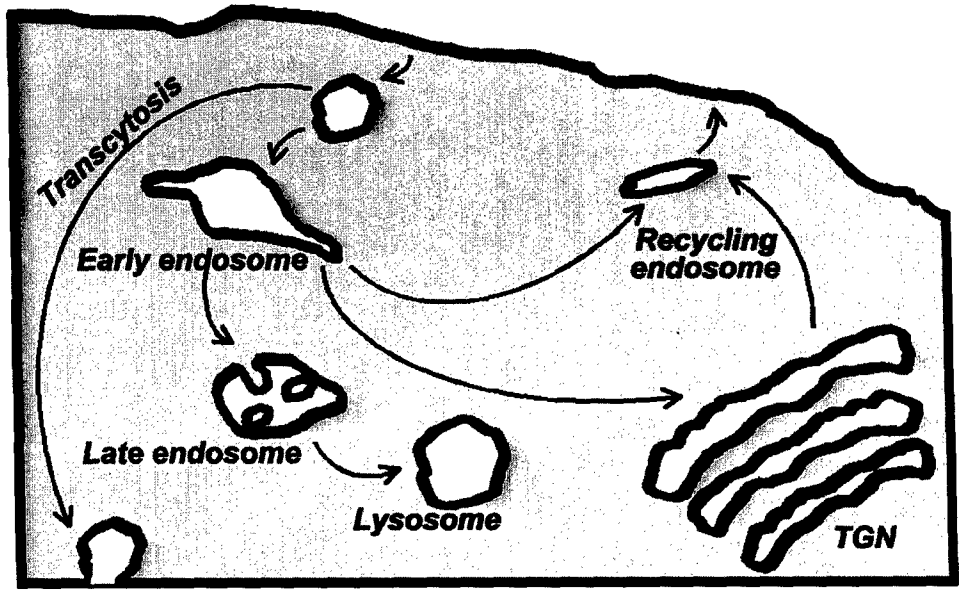

Fig. (2). *Intracellular trafficking*: Endocytic vesicles, containing membrane receptors and their respective ligands or other contents, can be selected for sorting to different sub-cellular compartments. For instance, these can recycle to the cell surface by "recycling endosomes" (e.g., directly or through Trans Golgi Network (TGN) compartments) or transported through the cell body and exocytosed to the abluminal space by "transcytosis". Internalized material can also be processed for delivery to endocytic compartments for degradation (e.g., by trafficking through "early endosomes", "late endosomes" and "lysosomes"), or sorted to other sub-cellular destinations such as Golgi or the Endoplasmic Reticulum.

Table 3. Intracellular Trafficking and Inhibitors

Trafficking pathway	Inhibitor	Molecular target
Trans Golgi network (TGN) trafficking	Brefeldin	TGN/ER-Arf1
Receptor recycling	Chlorpromazine	Recycling
Trafficking to lysosomes and recycling	Monensin	Na^+/H^+ exchange at the endosome
Lysosomal degradation	Ammonium chloride, chloroquine	Vesicle acidification
Lysosomal degradation	Bafilomycin	Vacuolar H^+-ATPase
Endosome-lysosome trafficking	Nocodazole, colchicine	Microtubular network

to the cytoplasm and nucleus of all cell types studied (reviewed by [215]). They undergo activation by Ca^{2+} and phospholipids, which promote targeting of calpains to membranes. In this situation, calpains can exert proteolytic activity, resulting in modification of enzyme [216] and receptor function [217, 218]. Also, cytoskeleton-related proteins can undergo modification by calpain activity, as is the case for calpain-dependent disruption of integrin/ cytoskeleton interactions [216, 219-221].

Another cytosolic degradation system, the proteosome, is also primarily located in the cytosol of all eukaryotic cells. Proteosomes are multisubunit complexes (i.e., 20S, 26S, the immunoproteosome, and the hybrid proteosome), which contain a common core and different additional regulatory subunits (reviewed by [222]). For instance, cytokine-dependent immunoproteosome activation has been related to the production of peptides that will act as ligands of MHC-I [223]. On the other hand, activation of the hybrid proteosome (depending on ATP but not on ubiquitin) generates peptides that are targeted to ER lumen [224]. The function of the proteosome 26S containing subunits that confer this complex the ability to selectively recognize, bind and cleave ubiquitin-tagged proteins has been extensively studied [222]. The process of protein degradation by the ubiquitin system requires initial attachment of ubiquitin residues to the protein substrate by ubiquitin-protein ligases, which recognize particular post-translational modifications in the target proteins. Subsequently, the ubiquitin-tagged proteins will be degraded by the 26S proteosome complex, concomitantly with the release of reusable ubiquitin residues.

However, most typically lysosomes are responsible for proteolysis of internalized material, since most endocytic traffic merges with lysosomal compartments. The endolysosomal system contains a series of differentiated vesicles including early endosomes, late endosomes and lysosomes. Early endosomes are the first compartment where sorting of materials to recycling, degradation pathways or other subcellular organelles is decided [225-229]. In this context, H^+-ATPases and Na^+, K^+-ATPases favor acidification of the endosomal lumen, whereas Na^+/H^+-exchangers help to generate a positive potential that inhibits proton influx [230]. These combined actions regulate the pH at the early endosome lumen, which becomes to be around 6.3-6.5. This mildly acidic pH favors separation of some ligands from their receptors, being the latter typically recycled to the plasma membrane, whereas ligands tend to traffic to late endosomes, as is the case of LDL-R or transferrin-R (reviewed by [231]). Alternatively, the receptor/ligand complex can also be recycled as a unit, or the complex can be entirely targeted to degradation [232].

When sorted to lysosomal compartments, materials traffic to late endosomes. Here, the vacuolar-ATPase pumps H^+ to the vesicle lumen [233], being responsible for the further acidification of this compartment to a pH around 5-5.5 [234]. Regulation of pH also depends on Cl^- channels directed inwardly to counteract the positive membrane potential created by the vacuolar-ATPase activity [235]. The compartments continue to acidify to very low pH (pH 4.8) and materials traffic to lysosomes, the terminal compartment in the degradation pathway. Lysosomes appear as electron dense bodies, where the entrapped materials can be then rapidly degraded by lysosomal acidic proteases [236].

Lysosomal hydrolysis is regulated by proton ATPases and cysteine transporters, as mentioned above, and also by lysosome-associated membrane proteins, the main protein constituent of endolysosomal membranes (reviewed by [237]). The latter are heavily glycosylated transmembrane proteins, referred to as LAMPs, which protect lysosomes from the action of degradative enzymes [238]. Hydrolysis at lysosomal compartments is carried out by proteases (i.e. cathepsins), including both exopeptidases (cysteine and serine proteases) and endopeptidases (cystein and aspartic proteases) [237, 239]. These proteases are extensively glycosylated, which facilitates their trafficking to lysosomes and helps confer resistance to low pH [236].

An example of a typical endocytic pathway, which delivers the internalized materials to the endolysosomal system, is clathrin-mediated internalization, although this can also sort the internalized contents to recycling or transcytotic pathways, after rapid removal of the clathrin coat from the membrane of the vesicles. For instance, transferrin-R or P-selectin can transit from the cell surface to endosomes and TGN, following by trafficking back to the EC surface [163, 175]. However, rapid degradation of P-selectin in lysosomes can also occur as a consequence of its frequent passage through endosomal compartments [175].

Also, a variety of ligands such as IgG immune complexes, glycoproteins, ferritin, thrombospondin, or colloidal gold coated with albumin, insulin, LDL or chondroitin sulphate proteoglycans are transported within minutes to lysosomal compartments in hepatic endothelial sinusoids [153, 154, 157-160, 162, 240]. Moreover, site-specific delivery vehicles targeted to endothelium through E-selectin (i.e. anti-E-selectin liposomes and conjugates) traffic rapidly to multivesicular bodies and other acidic compartments [176, 177], which could considerably reduce the half-life of potential cargoes. In epithelial cells, IgA is internalized by clathrin-mediated endocytosis and subsequently transcytosed from the basolateral to the apical plasma membrane [241]. Whether this pathway also operates in EC remains to be determined, however, some ligands internalized by EC through caveolae are transcytosed (see Section 6).

Phagocytosis typically results in lysosomal delivery. Phagosomes rapidly undergo uncoating of the actin-based machinery after internalization, with recycling of the plasma membrane proteins and degradation of receptors and content by sequential fusion with endosomes and lysosomes [109, 242-244]. Similarly, during macropinocytosis, the internalized contents can be recycled to the cell surface, but more typically are processed by delivery to the endosome-lysosome system. The first case can occur by tubulation of macropinosomes with fission into small vesicular intermediates [245], whereas classically, macropinosomes mature to acidic degradation vesicles by sequential interactions with pre-existing compartments [185, 246].

Ligands internalized by caveolar-mediated endocytosis can be sorted to several intracellular compartments using a variety of sorting pathways, with an interesting capability of

avoiding lysosomal compartments. For instance, cholera toxin traffic through early and late endosomes [145, 146], and SV40 is sorted from early endosomes to Golgi and finally ER [247, 248]. Some ligands, such as folate, can be delivered to the cytoplasm during a process called potocytosis, where folate is transported across the plasma membrane while folate receptor remains associated with caveolae at the plasma membrane [249]. Others, such as alkaline phosphatase, bradykinin, acetylcholine and endothelin, are returned to the cell surface after their internalization [147, 250-252]. Therefore, internalization *via* caveoli tends to favor sorting to sub-cellular compartments other than lysosomes and thus may be useful to avoid rapid degradation pathways. Also caveolar-mediated uptake provides a rapid mechanism for membrane turnover in EC, where plasma membrane components traffic through tubular endosomes and TGN in a constant influx-efflux cycle [149].

As mentioned above, EC can also use a ligand-induced endocytic pathway known as CAM-mediated endocytosis [206]. This internalization pathway delivers materials to lysosomal compartments with unusually slow kinetics (around 3 h) [253]. Conjugation of catalase to anti-ICAM-1 or anti-PECAM-1 antibodies permits intracellular delivery of the active enzyme to EC, and provides anti-oxidant protection for a relatively prolonged window time due to the slow kinetics of delivery to lysosomes [214, 253].

The protective effect of anti-CAM delivered catalase can be further prolonged either in the presence of drugs acting on the microtubular-network (i.e. nocodazole) [253], which is involved in traffic to lysosomes [254], or using weak bases (i.e. chloroquine), which impair acid-dependent activation of degradation enzymes in these compartments [253].

6. TRAVERSING ENDOTHELIAL BARRIERS *VIA* TRANSCYTOSIS AND PARACELLULAR TRANSPORT

In cases when a drug must be delivered to malignant cells in tumors, across the Blood Brain Barrier (BBB) or cardiomyocytes in the heart and other extravascular targets, endothelium represents a barrier that must be traversed for the therapeutic effect. In theory, drugs and macromolecules can extravasate *via* two pathways: transcytosis (i.e., endocytosis on the apical surface followed by traffic through the EC body to the basolateral surface) or diffusion *via* intercellular junctions (paracellular transport). The role and contribution of these two pathways in migration of macromolecules from the bloodstream into tissues is a subject of intense research and ongoing discussions. The theoretical concept of endothelial transcytosis of macromolecules involving dynamic or stable trans-cellular vesicular channels has been postulated by Majno and Palade in the 1960s [255, 256]. However, even today the mechanisms, regulation, significance and therapeutic utility of this pathway remain very much elusive [257].

Numerous studies from several groups including experiments in perfused organs and intact animals strongly indicate that transcytosis represents a significant route across the vascular endothelial barrier [57, 258-263]. When considering transcytosis for the purposes of drug delivery, ligands are endocytosed by the apical (lumenal) aspect of the endothelial plasma membrane, followed by transport through a series of intracellular compartments and delivery to the basolateral (ablumenal) plasma membrane where they are secreted.

An alternate model for transcytosis is through the formation of an organelle, called the vesiculo-vacuolar organelle (VVO) that may form dynamic or stable channels through cells [264]. Both morphological and functional evidence including studies of transendothelial transfer of labeled compounds in animal models show the presence of a VVO in EC [57, 264]. However, relatively little is known about mechanisms of VVO formation and how it can be manipulated pharmacologically. For example, histamine and VEGF seem to stimulate transport *via* VVO formation [264], but the specificity of this functional modulation is difficult to interpret, because these vasoactive agents also facilitate paracellular transport (see below).

Endothelial transcytosis often originates from the caveolar endocytotic pathway, where plasma solutes and macromolecules are taken up from the bloodstream in bulk by fluid phase adsorption (glycogen, dextran, ferritin, etc) or by binding to specific receptors (LDL, ceruloplasmin, etc) and reach the abluminal space [138, 258, 260, 265-267]. Plasma proteins such as albumin, TM, chorionic gonadotropin, insulin and growth factors can be transported to the abluminal surface of the EC *via* caveoli-mediated transcytosis [200, 201, 266, 268]. The levels of plasma lipoproteins and cholesterol homeostasis are believed to be maintained largely by endothelium in arteries which, due to continuous caveolar uptake, serves to reconstitute the levels of cholesterol in the vessel wall and permits the transit and subsequent accessibility of cholesterol-carrying lipoproteins to sub-endothelial layers of the vessel wall and peripheral tissues [269, 270].

Several studies indicated that interaction of a protein ligand leading to receptor clustering in caveoli and activation of specific signaling pathways plays a critical role in initiation of transcytosis [260, 261]. For example, caveolar clustering of endothelial albumin binding protein gp60 has been shown to increase transendothelial permeability by mediation of phosphorylation events including signaling through the Src family of tyrosine kinases [271]. Interestingly, chemical modifications of caveolar ligands, such as albumin nitration (that may take place in oxidant stress and inflammation) even further stimulate transcytosis [272].

Caveolar transcytosis pathways are envisioned as means for transcellular delivery of therapeutics, which could be achieved by targeting caveolae-located receptors. For example, active reporter compounds conjugated with antibodies directed against specific antigen (gp90) localized in pulmonary endothelial caveolae undergo transendothelial and transepithelial transport through pulmonary endothelium from the blood stream to the alveolar space after injection *in vivo* [57]. Although the function of gp90 and potential effects of its inhibition by targeting are unknown, it is tempting to speculate that caveolar targeting will permit more effective extravascular drug delivery.

In this context, transcytosis through the BBB represents a specific interest. The paracellular pathways (see below) in

this vascular area are relatively restricted, yet the BBB endothelium is not all that impermeable and yet can be traversed *via* a plethora of agents (for reviews see [273, 274]). From a biological standpoint, this can be illustrated by the fact that *Escherichia coli* invades the central nervous system by transmigration through brain microvascular EC using an actin- and microtubule-dependent phagocytic mechanism, although this pathway was inactive in systemic EC [275]. From a drug delivery standpoint, it is important that ligands of insulin, putrescine and transferrin receptors are expressed on the BBB endothelium. Also, antibodies and high-affinity binding peptides defined using a BBB endothelial phage-display library show an encouraging ability to accumulate in the brain tissue [32, 276]. Moreover, proteins and genetic "drugs" or reporter compounds conjugated with these affinity carriers display their activities in the brain tissue after systemic administration, suggesting transmission across the BBB [110, 111, 277].

In addition to transcytosis mechanisms, the density and permeability between cells of the endothelial monolayer varies between different organs; in this respect, endothelium can be roughly categorized into three types. The first type is fenestrated endothelium, which is localized to organs of the reticuloendothelial system, including hepatic and spleenic sinuses and bone marrow. Fenestrae is Latin for "windows" and refers to the relatively large pores between the fenestrated EC. These pores can be up to several microns in diameter and thus permit the relatively unhindered extravasation of blood components, including red and WBC in these tissues. A second type is continuous endothelium, which is present in most of other organs such as cardiac, pulmonary and mesenterial blood vessels. Continuous endothelium is relatively tighter than fenestrated endothelium and has fewer pores with 100 nm diameters. Although this can permit passage of macromolecules to tissues, in most cases, filtration through the continuous endothelium is restricted to small molecules and solutes such as glucose and small hormones. The third type is microvascular endothelium, which is the most restricted in permeability. In particular, brain microvascular EC form an extremely dense monolayer, resulting in an extremely tight BBB, which lacks significant permeability for plasma proteins and possesses specific enzymatic systems (glycoprotein P, e.g.) to facilitate reverse transport of molecules from the brain tissue to the circulation [274]. Clearly, due to these differences in vascular permeability, BBB endothelium represents the most formidable biological barrier for the extravascular drug delivery, while fenestrated endothelium does not restrict extravasation of even large carriers such as liposomes, polymer particles and viruses [278].

However, in many organs (e.g., liver) and types of vasculature (e.g., venules) the mainstream of transendothelial transport for nano-scale drug delivery vehicles such as liposomes and polymer carriers follows paracellular pathways. Paracellular endothelial permeability is controlled by proteins which form the tight junction complex localized to contact sites between EC. Proteins in the claudin family form the basis for regulating paracellular permeability [279, 280]. Claudins are not a simple barrier, per se, since many claudins form paracellular channels that enable selective ion permeability. Also, different tissues express different claudins, suggesting at least some regulation at the level of transcription. Recently, a definitive role for claudin-5 in regulating the BBB was demonstrated since substrates less than 1 kD molecular mass were freely permeable across the BBB in claudin-5 deficient mice [281]. Moreover, claudin function and paracellular permeability is also regulated by associated transmembrane proteins (occludin, junction adhesion molecule (JAM), connexins, VE-cadherin) and peripheral proteins, which tether it to the actin cytoskeleton such as ZO-1, ZO-2, ZO-3 and PATJ [282-284]. For instance, HGF/SF treated vascular EC show increased permeability due to ZO-1 phosphorylation, with no effect on claudin expression levels, suggesting a change in barrier function due to disruption of the ZO-1/claudin-1 complex [285]. The ability of VEGF and thrombin to increase endothelial permeability may also be due to a comparable upstream effect on signaling cascades that alter tight junction organization. Hormone activation and cross talk between these different classes of junction proteins and the regulation of claudin function is just beginning to be elucidated and is an active area of research.

The array of different tight junction associated proteins suggests many avenues for pharmacological manipulations of vascular permeability (see [286]). Studies using clostridium toxin, which binds to the extracellular domains of claudin-3 and claudin-4 and disrupts intestinal epithelial barrier function provide a basis for the notion that tight junction interfaces can be disrupted by targeting claudins. Thus, it seems plausible that another class of small molecules or perhaps claudin antibodies might provide an alternative strategy for preferential and transient disruption of EC tight junctions. In particular, the selective change in BBB paracellular permeability exhibited by claudin-5 deficient mice suggests that specific modulation of claudin-5 may have potential as a method to temporarily alter BBB permeability [281]. Conversely, blockade of junction proteins may help increase endothelial barrier function, as indicated above, where anti-ICAM-1 conjugates appear to inhibit leukocyte transmigration.

Many pathological mediators and conditions including hypoxia, hyperoxia, histamine, VEGF, thrombin, hyperthermia, abnormal shear stress, cytokines and ROS elevate vascular permeability [287-291]. However, some compounds (e.g., adenosine) tend to restrict endothelial permeability in cell cultures [292]. Some permeability-enhancing agents (histamine, VEGF) apparently stimulate both transcytosis [122] and paracellular transport [291, 293]. Vasoactive agents inducing paracellular permea-bility cause elevation of cytosolic Ca^{2+} in EC [294], activation of kinases leading to myosin light chain phosphorylation and subsequent endothelial contraction and reorganization of adhesion contacts [77, 288, 295, 296].

Vascular cells, including the endothelium itself, can regulate vascular permeability *via* the action of diverse vasoactive substances, which regulate porosity of endothelial monolayer and blood pressure (the higher intravascular pressure, the more effective extravascular transport). Interestingly, one modality of a vasoactive agent (e.g., its effect on blood pressure) frequently is balanced by its other

modality (effect on permeability). For example, endothelial ACE converts Ang I into Ang II, which induces vasoconstriction, yet ACE also inactivates bradykinin and substance P [61], peptides that increase vascular permeability. EC produce a potent vasodilating agent NO that may reduce vascular permeability at low levels [297].

Due to activities of substance P, thrombin, ROS, VEGF, bradykinin and other kinins endothelial permeability is usually enhanced under pathological conditions including inflammation, which can exacerbate edema [257]. Both these factors and morphological alterations (fenestrations) enhance permeability of tumor vasculature and cause tumor vascular leakiness [123, 290, 298]. This phenomenon is being actively exploited in design of liposomal and polymer carrier-based strategies for drug delivery to tumors (enhanced permeability and retention effect, EPR) [299].

The role of transcytosis *vs* paracellular transport of particular compounds under normal and pathological conditions is controversial and is the subject of continuing discussions. For example, although liposomes can undergo endothelial transcytosis in cell cultures, they likely leave the vasculature *via* paracellular pathways in animals [278]. Experiments in perfused organs showed that albumin extravasation is independent on temperature, suggesting that this process represents a passive diffusion *via* intercellular pores rather than *via* energy-dependent endocytotic pathways [137]. Mice genetically deficient in caveolin, a critical component of caveolar endocytotic pathway, do not show overt abnormalities of tissue transport of plasma components [300, 301]. However, both transcellular and paracellular pathways can and should be employed for rational design of modern drug delivery systems. In theory, paracellular pathways may be more useful for extravasation of drugs in tumors and inflammation foci, whereas endothelial transcytosis might serve as a pathway for drug delivery through the BBB.

CONCLUSION AND PERSPECTIVES

Recent years have produced a wealth of knowledge of molecular mechanisms regulating pathways for endothelial entry, intracellular traffic, degradation or recycling and transcytosis of diverse materials, including therapeutic agents. Optimal endothelial and transendothelial drug delivery promises substantial improvements of effectiveness and safety of therapeutic strategies for treatment of cardiovascular (e.g., atherosclerosis, hypertension, ischemia-reperfusion syndrome), pulmonary (e.g., acute lung injury, hyperoxia, pulmonary hypertension), and metabolic diseases (e.g., diabetes), inflammation (e.g., sepsis and endotoxemia) and tumor growth. One key to effective treatment of these distinct pathologies is the ability to control the rates and precise destinations of endothelial drug delivery. There is a plethora of potential avenues for achieving this challenging and exciting goal.

Optimal selection of endothelial surface determinants and design of drug delivery system molecular characteristics such as valency of binding to endothelium, charge and size will be likely used to control the uptake and fate of drugs. Utilization of cross-linkers sensitive to minute changes in pH or specific cellular proteases (e.g., lysosomal cathepsin G) can be employed for the release of active drugs at selected stages of their intracellular traffic. Conjugation of drugs or drug vehicles with membrane fusion and chaperone peptides will help to achieve yet even more precise sub-cellular localization in organelles such as mitochondria, nucleus or peroxysomes.

In some cases, therapeutic needs might require methods to decelerate or avoid endothelial internalization such as in case of delivery of anti-thrombotic and other agents, which need to exert their activity in the vascular lumen. Therefore, using non-internalizable determinants (e.g., monomeric anti-ICAM-1) or deceleration of natural endocytotic pathways (e.g., by using vehicles with diameter exceeding the limit of internalization) could be used for this goal. Transcytotic and paracellular transport mechanisms could be employed in the cases when a drug should be delivered beyond the EC.

In summary, binding, entry and traffic of drugs into and through EC represent central paradigms of many drug delivery strategies serving diverse therapeutic goals. Future progress in understanding the control of these processes will provide more effective and safe therapeutic means.

ACKNOWLEDGEMENTS

This work was supported by NIH SCOR in Acute Lung Injury (NHLBI HL 60290, Project 4), NHLBI RO1 (HL/GM 71175-01) and Department of Defense Grant (PR012262) to VRM. SM was supported in part by a fellowship from Fundación Ramón Areces (Spain). M.K. was supported by NIH grants GM61012 and P01 HL019737-26, Project 3.

ABBREVIATIONS

ACE	=	Angiotensin-Converting Enzyme
Ang I	=	Angiotensin 1
Ang II	=	Angiotensin 2
BBB	=	Blood Brain Barrier
CAM	=	Cellular Adhesion Molecule
EDHF	=	Endothelium-Derived Hyperpolarizing Factor
ER	=	Endoplasmic Reticulum
EGF	=	Epithelial Growth Factor
EC	=	Endothelial Cell(s)
GPI	=	Glycosyl Phosphatidyl Inositol
HGF	=	Human Growth Factor
ICAM-1	=	Intercellular Adhesion Molecule-1
JAM	=	Junction Adhesion Molecule
LOX-1	=	Lectin-like Oxidized LDL receptor-1
LPL	=	Lipoprotein Lipase
LAMP	=	Lysosomal Associated Membrane Protein 1
LDL	=	Low Density Lipoprotein
LDL-R	=	Low Density Lipoprotein Receptor
NO	=	Nitric Oxide

PEG	=	Polyethylene Glycol
PECAM	=	Platelet EC Adhesion Molecule-1
ROS	=	Reactive Oxygen Species
ROCK	=	Rho-dependent Kinase
RBC	=	Red Blood Cell
Transferrin-R	=	Transferrin Receptor
TM	=	Thrombomodulin
TGN	=	Trans-Golgi Network
VVO	=	Vesiculo-Vacuolar Organelle
VEGF	=	Vascular Endothelial Growth Factor
WBC	=	White Blood Cells

REFERENCES

[1] Cines DB, Pollak ES, Buck CA, Loscalzo J, Zimmerman GA, McEver RP, et al. Endothelial cells in physiology and in the pathophysiology of vascular disorders. Blood 1998; 91(10): 3527-61.

[2] Gimbrone MA, Jr. Vascular endothelium, hemodynamic forces, and atherogenesis. Am J Pathol 1999; 155(1): 1-5.

[3] Esmon CT. The roles of protein C and thrombomodulin in the regulation of blood coagulation. J Biol Chem 1989; 264(9): 4743-6.

[4] Carlos TM, Harlan JM. Leukocyte-endothelial adhesion molecules. Blood 1994; 84(7): 2068-101.

[5] Muller WA. Leukocyte- endothelial cell interactions in the inflammatory response. Lab Invest 2002; 82(5): 521-33.

[6] Springer TA. Adhesion receptors of the immune system. Nature 1990; 346(6283): 425-34.

[7] Bevilacqua MP, Nelson RM. Endothelial-leukocyte adhesion molecules in inflammation and metastasis. Thromb Haemost 1993; 70(1): 152-4.

[8] Ley K, Tedder TF. Leukocyte interactions with vascular endothelium. New insights into selectin-mediated attachment and rolling. J Immunol 1995; 155(2): 525-8.

[9] Zimmerman GA, McIntyre TM, Prescott SM. Adhesion and signaling in vascular cell-cell interactions. J Clin Invest 1996; 98(8): 1699-702.

[10] Vanhoutte PM. Endothelium-derived free radicals: for worse and for better. J Clin Invest 2001; 107(1): 23-5.

[11] Zulueta JJ, Sawhney R, Yu FS, Cote CC, Hassoun PM. Intracellular generation of reactive oxygen species in endothelial cells exposed to anoxia-reoxygenation. Am J Physiol 1997; 272(5 Pt 1): L897-902.

[12] Rubbo H, Tarpey M, Freeman BA. Nitric oxide and reactive oxygen species in vascular injury. Biochem Soc Symp 1995; 61: 33-45.

[13] Kennel SJ, Lee R, Bultman S, Kabalka G. Rat monoclonal antibody distribution in mice: an epitope inside the lung vascular space mediates very efficient localization. Int J Rad Appl Instrum B 1990; 17(2): 193-200.

[14] Danilov SM, Muzykantov VR, Martynov AV, Atochina EN, Sakharov I, Trakht IN, et al. Lung is the target organ for a monoclonal antibody to angiotensin-converting enzyme. Lab Invest 1991; 64(1): 118-24.

[15] Jacobson BS, Schnitzer JE, McCaffery M, Palade GE. Isolation and partial characterization of the luminal plasmalemma of microvascular endothelium from rat lungs. Eur J Cell Biol 1992; 58(2): 296-306.

[16] Keelan ET, Harrison AA, Chapman PT, Binns RM, Peters AM, Haskard DO. Imaging vascular endothelial activation: an approach using radiolabeled monoclonal antibodies against the endothelial cell adhesion molecule E-selectin. J Nucl Med 1994; 35(2): 276-81.

[17] Muzykantov VR, Danilov SM. Targeting of radiolabeled monoclonal antibody against ACE to the pulmonary endothelium. In: V. Torchilin, editor. Targeted Delivery of Imaging Agents. Roca Baton, Florida: CRC Press; 1995; p. 465-485.

[18] Huang X, Molema G, King S, Watkins L, Edgington TS, Thorpe PE. Tumor infarction in mice by antibody-directed targeting of tissue factor to tumor vasculature. Science 1997; 275(5299): 547-50.

[19] Schnitzer JE. Vascular targeting as a strategy for cancer therapy. N Engl J Med 1998; 339(7): 472-4.

[20] Rajotte D, Arap W, Hagedorn M, Koivunen E, Pasqualini R, Ruoslahti E. Molecular heterogeneity of the vascular endothelium revealed by *in vivo* phage display. J Clin Invest 1998; 102(2): 430-7.

[21] Stan RV, Ghitescu L, Jacobson BS, Palade GE. Isolation, cloning, and localization of rat PV-1, a novel endothelial caveolar protein. J Cell Biol 1999; 145(6): 1189-98.

[22] Li S, Tan Y, Viroonchatapan E, Pitt BR, Huang L. Targeted gene delivery to pulmonary endothelium by anti-PECAM antibody. Am J Physiol Lung Cell Mol Physiol 2000; 278(3): L504-11.

[23] Nicklin SA, White SJ, Watkins SJ, Hawkins RE, Baker AH. Selective targeting of gene transfer to vascular endothelial cells by use of peptides isolated by phage display. Circulation 2000; 102(2): 231-7.

[24] Ranney DF. Biomimetic transport and rational drug delivery. Biochem Pharmacol 2000; 59(2): 105-14.

[25] Reynolds PN, Zinn KR, Gavrilyuk VD, Balyasnikova IV, Rogers BE, Buchsbaum DJ, et al. A targetable, injectable adenoviral vector for selective gene delivery to pulmonary endothelium *in vivo*. Mol Ther 2000; 2(6): 562-78.

[26] Reynolds PN, Nicklin SA, Kaliberova L, Boatman BG, Grizzle WE, Balyasnikova IV, et al. Combined transductional and transcriptional targeting improves the specificity of transgene expression *in vivo*. Nat Biotechnol 2001; 19(9): 838-42.

[27] Poznansky MJ, Juliano RL. Biological approaches to the controlled delivery of drugs: a critical review. Pharmacol Rev 1984; 36(4): 277-336.

[28] Drexler H, Hornig B. Endothelial dysfunction in human disease. J Mol Cell Cardiol 1999; 31(1): 51-60.

[29] Semple G, Ashworth DM, Batt AR, Baxter AJ, Benzies DW, Elliot LH, et al. Peptidomimetic aminomethylene ketone inhibitors of interleukin-1 beta-converting enzyme (ICE). Bioorg Med Chem Lett 1998; 8(8): 959-64.

[30] Bangham AD. Surrogate cells or Trojan horses. The discovery of liposomes. Bioessays 1995; 17(12): 1081-8.

[31] Tamada JA, Langer R. Erosion kinetics of hydrolytically degradable polymers. Proc Natl Acad Sci USA 1993; 90(2): 552-6.

[32] Jeong B, Bae YH, Lee DS, Kim SW. Biodegradable block copolymers as injectable drug-delivery systems. Nature 1997; 388(6645): 860-2.

[33] Bartus RT, Tracy MA, Emerich DF, Zale SE. Sustained delivery of proteins for novel therapeutic agents. Science 1998; 281(5380): 1161-2.

[34] Luo D, Saltzman WM. Synthetic DNA delivery systems. Nat Biotechnol 2000; 18(1): 33-7.

[35] Shen ZR, Zhu JH, Ma Z, Wang F, Wang ZY. Preparation of biodegradable microspheres of testosterone with poly(D,L-lactide-co-glycolide) and test of drug release *in vitro*. Artif Cells Blood Substit Immobil Biotechnol 2000; 28(1): 57-64.

[36] Yang YY, Chung TS, Ng NP. Morphology, drug distribution, and *in vitro* release profiles of biodegradable polymeric microspheres containing protein fabricated by double-emulsion solvent extraction/evaporation method. Biomaterials 2001; 22(3): 231-41.

[37] Siepmann J, Gopferich A. Mathematical modeling of bioerodible, polymeric drug delivery systems. Adv Drug Deliv Rev 2001; 48(2-3): 229-47.

[38] Abuchowski A, McCoy JR, Palczuk NC, van Es T, Davis FF. Effect of covalent attachment of polyethylene glycol on immunogenicity and circulating life of bovine liver catalase. J Biol Chem 1977; 252(11): 3582-6.

[39] Phillips WT, Klipper RW, Awasthi VD, Rudolph AS, Cliff R, Kwasiborski V, et al. Polyethylene glycol-modified liposome-encapsulated hemoglobin: a long circulating red cell substitute. J Pharmacol Exp Ther 1999; 288(2): 665-70.

[40] Liu TH, Beckman JS, Freeman BA, Hogan EL, Hsu CY. Polyethylene glycol-conjugated superoxide dismutase and catalase reduce ischemic brain injury. Am J Physiol 1989; 256(2 Pt 2): H589-93.

[41] Freeman BA, Turrens JF, Mirza Z, Crapo JD, Young SL. Modulation of oxidant lung injury by using liposome-entrapped superoxide dismutase and catalase. Fed Proc 1985; 44(10): 2591-5.

[42] Lee HJ, Engelhardt B, Lesley J, Bickel U, Pardridge WM. Targeting rat anti-mouse transferrin receptor monoclonal antibodies through blood-brain barrier in mouse. J Pharmacol Exp Ther 2000; 292(3): 1048-52.

[43] Adlakha-Hutcheon G, Bally MB, Shew CR, Madden TD. Controlled destabilization of a liposomal drug delivery system enhances mitoxantrone antitumor activity. Nat Biotechnol 1999; 17(8): 775-9.

[44] Raso V. Immunotargeting intracellular compartments. Anal Biochem 1994; 222(2): 297-304.

[45] Caron PC, Laird W, Co MS, Avdalovic NM, Queen C, Scheinberg DA. Engineered humanized dimeric forms of IgG are more effective antibodies. J Exp Med 1992; 176(4): 1191-5.

[46] Pardridge WM, Buciak J, Yang J, Wu D. Enhanced endocytosis in cultured human breast carcinoma cells and *in vivo* biodistribution in rats of a humanized monoclonal antibody after cationization of the protein. J Pharmacol Exp Ther 1998; 286(1): 548-54.

[47] Becerril B, Poul MA, Marks JD. Toward selection of internalizing antibodies from phage libraries. Biochem Biophys Res Commun 1999; 255(2): 386-93.

[48] Nielsen UB, Marks JD. Internalizing antibodies and targeted cancer therapy: direct selection from phage display libraries. Pharm Sci Technol 2000; 3(8): 282-291.

[49] Schwartz JJ, Zhang S. Peptide-mediated cellular delivery. Curr Opin Mol Ther 2000; 2(2): 162-7.

[50] Jin LH, Bahn JH, Eum WS, Kwon HY, Jang SH, Han KH, et al. Transduction of human catalase mediated by an HIV-1 TAT protein basic domain and arginine-rich peptides into mammalian cells. Free Radic Biol Med 2001; 31(11): 1509-19.

[51] Lewin M, Carlesso N, Tung CH, Tang XW, Cory D, Scadden DT, et al. Tat peptide-derivatized magnetic nanoparticles allow *in vivo* tracking and recovery of progenitor cells. Nat Biotechnol 2000; 18(4): 410-4.

[52] Torchilin VP, Rammohan R, Weissig V, Levchenko TS. TAT peptide on the surface of liposomes affords their efficient intracellular delivery even at low temperature and in the presence of metabolic inhibitors. Proc Natl Acad Sci USA 2001; 98(15): 8786-91.

[53] Muzykantov V. Immunotargeting of drugs to the pulmonary vascular endothelium as a therapeutic strategy. Pathophysiology 1998; 5: 15-33.

[54] Greenwalt TJ, Steane EA. Evaluation of methods for quantitating erythrocyte antibodies and description of a new method using horseradish peroxidase-labelled antiglobulin. Haematologia (Budap) 1980; 13(1-4): 33-48.

[55] Vainio O, Dunon D, Aissi F, Dangy JP, McNagny KM, Imhof BA. HEMCAM, an adhesion molecule expressed by c-kit+ hemopoietic progenitors. J Cell Biol 1996; 135(6 Pt 1): 1655-68.

[56] Goetz DJ, el-Sabban ME, Hammer DA, Pauli BU. Lu-ECAM-1-mediated adhesion of melanoma cells to endothelium under conditions of flow. Int J Cancer 1996; 65(2): 192-9.

[57] McIntosh DP, Tan XY, Oh P, Schnitzer JE. Targeting endothelium and its dynamic caveolae for tissue-specific transcytosis *in vivo*: a pathway to overcome cell barriers to drug and gene delivery. Proc Natl Acad Sci USA 2002; 99(4): 1996-2001.

[58] Kennel SJ, Lankford TK, Foote LJ, Davis IA, Boll RA, Mirzadeh S. Combination vascular targeted and tumor targeted radioimmunotherapy. Cancer Biother Radiopharm 1999; 14(5): 371-9.

[59] Esmon CT. Thrombomodulin as a model of molecular mechanisms that modulate protease specificity and function at the vessel surface. Faseb J 1995; 9(10): 946-55.

[60] Christofidou-Solomidou M, Kennel S, Scherpereel A, Wiewrodt R, Solomides CC, Pietra GG, et al. Vascular immunotargeting of glucose oxidase to the endothelial antigens induces distinct forms of oxidant acute lung injury: targeting to thrombomodulin, but not to PECAM-1, causes pulmonary thrombosis and neutrophil transmigration. Am J Pathol 2002; 160(3): 1155-69.

[61] Erdos EG. Angiotensin I converting enzyme and the changes in our concepts through the years. Lewis K. Dahl memorial lecture. Hypertension 1990; 16(4): 363-70.

[62] Laursen JB, Rajagopalan S, Galis Z, Tarpey M, Freeman BA, Harrison DG. Role of superoxide in angiotensin II-induced but not catecholamine-induced hypertension. Circulation 1997; 95(3): 588-93.

[63] Heitsch H, Brovkovych S, Malinski T, Wiemer G. Angiotensin-(1-7)-Stimulated Nitric Oxide and Superoxide Release From Endothelial Cells. Hypertension 2001; 37(1): 72-76.

[64] Danilov SM, Gavrilyuk VD, Franke FE, Pauls K, Harshaw DW, McDonald TD, et al. Lung uptake of antibodies to endothelial antigens: key determinants of vascular immunotargeting. Am J Physiol Lung Cell Mol Physiol 2001; 280(6): L1335-47.

[65] Muzykantov VR, Atochina EN, Kuo A, Barnathan ES, Notarfrancesco K, Shuman H, et al. Endothelial cells internalize monoclonal antibody to angiotensin-converting enzyme. Am J Physiol 1996; 270(5 Pt 1): L704-13.

[66] Olson SC, Dowds TA, Pino PA, Barry MT, Burke-Wolin T. ANG II stimulates endothelial nitric oxide synthase expression in bovine pulmonary artery endothelium. Am J Physiol 1997; 273(2 Pt 1): L315-21.

[67] Danilov S, Jaspard E, Churakova T, Towbin H, Savoie F, Wei L, et al. Structure-function analysis of angiotensin I-converting enzyme using monoclonal antibodies. Selective inhibition of the amino-terminal active site. J Biol Chem 1994; 269(43): 26806-14.

[68] Sadhukhan R, Santhamma KR, Reddy P, Peschon JJ, Black RA, Sen I. Unaltered cleavage and secretion of angiotensin-converting enzyme in tumor necrosis factor-alpha-converting enzyme-deficient mice. J Biol Chem 1999; 274(15): 10511-6.

[69] Balyasnikova IV, Karran EH, Albrecht RF 2nd, Danilov SM. Epitope-specific antibody-induced cleavage of angiotensin-converting enzyme from the cell surface. Biochem J 2002; 362(Pt 3): 585-95.

[70] Muzykantov VR. Delivery of antioxidant enzyme proteins to the lung. Antioxid Redox Signal 2001; 3(1): 39-62.

[71] Atochina EN, Hiemisch HH, Muzykantov VR, Danilov SM. Systemic administration of platelet-activating factor in rat reduces specific pulmonary uptake of circulating monoclonal antibody to angiotensin-converting enzyme. Lung 1992; 170(6): 349-58.

[72] Muzykantov VR, Atochina EN, Ischiropoulos H, Danilov SM, Fisher AB. Immunotargeting of antioxidant enzyme to the pulmonary endothelium. Proc Natl Acad Sci USA 1996; 93(11): 5213-8.

[73] Atochina EN, Balyasnikova IV, Danilov SM, Granger DN, Fisher AB, Muzykantov VR. Immunotargeting of catalase to ACE or ICAM-1 protects perfused rat lungs against oxidative stress. Am J Physiol 1998; 275(4 Pt 1): L806-17.

[74] Newman PJ. The biology of PECAM-1. J Clin Invest 1997; 99(1): 3-8.

[75] Muzykantov VR, Christofidou-Solomidou M, Balyasnikova I, Harshaw DW, Schultz L, Fisher AB, et al. Streptavidin facilitates internalization and pulmonary targeting of an anti- endothelial cell antibody (platelet-endothelial cell adhesion molecule 1): a strategy for vascular immunotargeting of drugs. Proc Natl Acad Sci USA 1999; 96(5): 2379-84.

[76] Rinaldo J, Christman, J. ARDS: pathogenesis. In: Fishman A, editor. Fishman's Pulmonary Diseases and Disorders. New York: McGraw and Hill; 1998. p. 2537-2548.

[77] Mulligan MS, Miyasaka M, Tamatani T, Jones ML, Ward PA. Requirements for L-selectin in neutrophil-mediated lung injury in rats. J Immunol 1994; 152(2): 832-40.

[78] Meyrick BO. Endotoxin-mediated pulmonary endothelial cell injury. Fed Proc 1986; 45(1): 19-24.

[79] Vaporciyan AA, DeLisser HM, Yan HC, Mendiguren, II, Thom SR, Jones ML, et al. Involvement of platelet- endothelial cell adhesion molecule-1 in neutrophil recruitment *in vivo*. Science 1993; 262(5139): 1580-2.

[80] Scherpereel A, Wiewrodt R, Christofidou-Solomidou M, Gervais R, Murciano JC, Albelda SM, et al. Cell-selective intracellular delivery of a foreign enzyme to endothelium *in vivo* using vascular immunotargeting. FASEB J 2001; 15(2): 416-26.

[81] Scherpereel A, Rome JJ, Wiewrodt R, Watkins SC, Harshaw DW, Alder S, et al. Platelet-endothelial cell adhesion molecule-1-directed immunotargeting to cardiopulmonary vasculature. J Pharmacol Exp Ther 2002; 300(3): 777-86.

[82] Bevilacqua MP, Stengelin S, Gimbrone MA Jr, Seed B. Endothelial leukocyte adhesion molecule 1: an inducible receptor for neutrophils related to complement regulatory proteins and lectins. Science 1989; 243(4895): 1160-5.

[83] Albelda SM. Endothelial and epithelial cell adhesion molecules. Am J Respir Cell Mol Biol 1991; 4(3): 195-203.

[84] Kishimoto TK, Rothlein R. Integrins, ICAMs, and selectins: role and regulation of adhesion molecules in neutrophil recruitment to inflammatory sites. Adv Pharmacol 1994; 25: 117-69.

[85] Panes J, Perry MA, Anderson DC, Muzykantov VR, Carden DL, Miyasaka M, et al. Portal hypertension enhances endotoxin-induced intercellular adhesion molecule 1 up-regulation in the rat. Gastroenterology 1996; 110(3): 866-74.

[86] Komatsu S, Panes J, Russell JM, Anderson DC, Muzykantov VR, Miyasaka M, et al. Effects of chronic arterial hypertension on constitutive and induced intercellular adhesion molecule-1 expression *in vivo*. Hypertension 1997; 29(2): 683-9.

[87] Murciano JC, Muro S, Koniaris L, Christofidou-Solomidou M, Harshaw DW, Albelda SM, et al. ICAM-directed vascular immunotargeting of anti-thrombotic agents to the endothelial surface. Blood 2003; 101(10): 3977-84.

[88] Dustin ML, Rothlein R, Bhan AK, Dinarello CA, Springer TA. Induction by IL 1 and interferon-gamma: tissue distribution, biochemistry, and function of a natural adherence molecule (ICAM-1). J Immunol 1986; 137(1): 245-54.

[89] Hubbard AK, Rothlein R. Intercellular adhesion molecule-1 (ICAM-1) expression and cell signaling cascades. Free Radic Biol Med 2000; 28(9): 1379-86.

[90] Mulligan MS, Vaporciyan AA, Miyasaka M, Tamatani T, Ward PA. Tumor necrosis factor alpha regulates *in vivo* intrapulmonary expression of ICAM-1. Am J Pathol 1993; 142(6): 1739-49.

[91] Doerschuk CM, Quinlan WM, Doyle NA, Bullard DC, Vestweber D, Jones ML, et al. The role of P-selectin and ICAM-1 in acute lung injury as determined using blocking antibodies and mutant mice. J Immunol 1996; 157(10): 4609-14.

[92] Amano J, Hiroe M, Ohta Y, Ishiyama S, Nishikawa T, Tanaka H, et al. Uptake of indium-111-anti-intercellular adhesion molecule-1 monoclonal antibody in the allografted rat lung during acute rejection. J Heart Lung Transplant 1996; 15(10): 1027-33.

[93] Sasso DE, Gionfriddo MA, Thrall RS, Syrbu SI, Smilowitz HM, Weiner RE. Biodistribution of indium-111-labeled antibody directed against intercellular adhesion molecule-1. J Nucl Med 1996; 37(4): 656-61.

[94] Villanueva FS, Jankowski RJ, Klibanov S, Pina ML, Alber SM, Watkins SC, et al. Microbubbles targeted to intercellular adhesion molecule-1 bind to activated coronary artery endothelial cells. Circulation 1998; 98(1): 1-5.

[95] Weiner RE, Sasso DE, Gionfriddo MA, Syrbu SI, Smilowitz HM, Vento J, et al. Early detection of bleomycin-induced lung injury in rat using indium-111-labeled antibody directed against intercellular adhesion molecule-1. J Nucl Med 1998; 39(4): 723-8.

[96] Klibanov AL, Hughes MS, Villanueva FS, Jankowski RJ, Wagner WR, Wojdyla JK, et al. Targeting and ultrasound imaging of microbubble-based contrast agents. Magma 1999; 8(3): 177-84.

[97] Diamond MS, Staunton DE, Marlin SD, Springer TA. Binding of the integrin Mac-1 (CD11b/CD18) to the third immunoglobulin-like domain of ICAM-1 (CD54) and its regulation by glycosylation. Cell 1991; 65(6): 961-71.

[98] Kunkel EJ, Jung U, Bullard DC, Norman KE, Wolitzky BA, Vestweber D, et al. Absence of trauma-induced leukocyte rolling in mice deficient in both P-selectin and intercellular adhesion molecule 1. J Exp Med 1996; 183(1): 57-65.

[99] Steeber DA, Campbell MA, Basit A, Ley K, Tedder TF. Optimal selectin-mediated rolling of leukocytes during inflammation *in vivo* requires intercellular adhesion molecule-1 expression. Proc Natl Acad Sci USA 1998; 95(13): 7562-7.

[100] Jun CD, Shimaoka M, Carman CV, Takagi J, Springer TA. Dimerization and the effectiveness of ICAM-1 in mediating LFA-1-dependent adhesion. Proc Natl Acad Sci USA 2001; 98(12): 6830-5.

[101] Staunton DE, Merluzzi VJ, Rothlein R, Barton R, Marlin SD, Springer TA. A cell adhesion molecule, ICAM-1, is the major surface receptor for rhinoviruses. Cell 1989; 56(5): 849-53.

[102] Rothlein R, Mainolfi EA, Kishimoto TK. Treatment of inflammation with anti-ICAM-1. Res Immunol 1993; 144(9): 735-9; discussion 754-62.

[103] DeMeester SR, Molinari MA, Shiraishi T, Okabayashi K, Manchester JK, Wick MR, et al. Attenuation of rat lung isograft reperfusion injury with a combination of anti-ICAM-1 and anti-beta2 integrin monoclonal antibodies. Transplantation 1996; 62(10): 1477-85.

[104] Lefer DJ, Flynn DM, Anderson DC, Buda AJ. Combined inhibition of P-selectin and ICAM-1 reduces myocardial injury following ischemia and reperfusion. Am J Physiol 1996; 271(6 Pt 2): H2421-9.

[105] Murohara T, Delyani JA, Albelda SM, Lefer AM. Blockade of platelet endothelial cell adhesion molecule-1 protects against myocardial ischemia and reperfusion injury in cats. J Immunol 1996; 156(9): 3550-7.

[106] Kumasaka T, Quinlan WM, Doyle NA, Condon TP, Sligh J, Takei F, et al. Role of the intercellular adhesion molecule-1(ICAM-1) in endotoxin-induced pneumonia evaluated using ICAM-1 antisense oligonucleotides, anti-ICAM-1 monoclonal antibodies, and ICAM-1 mutant mice. J Clin Invest 1996; 97(10): 2362-9.

[107] Ghitescu L, Jacobson BS, Crine P. A novel, 85 kDa endothelial antigen differentiates plasma membrane macrodomains in lung alveolar capillaries. Endothelium 1999; 6(3): 241-50.

[108] Murciano JC, Harshaw DW, Ghitescu L, Danilov SM, Muzykantov VR. Vascular immunotargeting to endothelial surface in a specific macrodomain in alveolar capillaries. Am J Respir Crit Care Med 2001; 164(7): 1295-302.

[109] Muller WA, Steinman RM, Cohn ZA. The membrane proteins of the vacuolar system. II. Bidirectional flow between secondary lysosomes and plasma membrane. J Cell Biol 1980; 86(1): 304-14.

[110] Song BW, Vinters HV, Wu D, Pardridge WM. Enhanced neuroprotective effects of basic fibroblast growth factor in regional brain ischemia after conjugation to a blood-brain barrier delivery vector. J Pharmacol Exp Ther 2002; 301(2): 605-10.

[111] Zhang Y, Schlachetzki F, Pardridge WM. Global non-viral gene transfer to the primate brain following intravenous administration. Mol Ther 2003; 7(1): 11-8.

[112] von Asmuth EJ, Smeets EF, Ginsel LA, Onderwater JJ, Leeuwenberg JF, Buurman WA. Evidence for endocytosis of E-selectin in human endothelial cells. Eur J Immunol 1992; 22(10): 2519-26.

[113] Kuijpers TW, Raleigh M, Kavanagh T, Janssen H, Calafat J, Roos D, et al. Cytokine-activated endothelial cells internalize E-selectin into a lysosomal compartment of vesiculotubular shape. A tubulin-driven process. J Immunol 1994; 152(10): 5060-9.

[114] Kiely JM, Cybulsky MI, Luscinskas FW, Gimbrone MA, Jr. Immunoselective targeting of an anti-thrombin agent to the surface of cytokine-activated vascular endothelial cells. Arterioscler Thromb Vasc Biol 1995; 15(8): 1211-8.

[115] Spragg DD, Alford DR, Greferath R, Larsen CE, Lee KD, Gurtner GC, et al. Immunotargeting of liposomes to activated vascular endothelial cells: a strategy for site-selective delivery in the cardiovascular system. Proc Natl Acad Sci USA 1997; 94(16): 8795-800.

[116] Fujise K, Revelle BM, Stacy L, Madison EL, Yeh ET, Willerson JT, et al. A tissue plasminogen activator/P-selectin fusion protein is an effective thrombolytic agent. Circulation 1997; 95(3): 715-22.

[117] Harari OA, Wickham TJ, Stocker CJ, Kovesdi I, Segal DM, Huehns TY, et al. Targeting an adenoviral gene vector to cytokine-activated vascular endothelium via E-selectin. Gene Ther 1999; 6(5): 801-7.

[118] Lindner JR, Song J, Christiansen J, Klibanov AL, Xu F, Ley K. Ultrasound assessment of inflammation and renal tissue injury with microbubbles targeted to P-selectin. Circulation 2001; 104(17): 2107-12.

[119] McDevitt MR, Ma D, Lai LT, Simon J, Borchardt P, Frank RK, et al. Tumor therapy with targeted atomic nanogenerators. Science 2001; 294(5546): 1537-40.

[120] Folkman J. Angiogenesis inhibitors generated by tumors. Mol Med 1995; 1(2): 120-2.

[121] Jain RK. Delivery of molecular and cellular medicine to solid tumors. Adv Drug Deliv Rev 2001; 46(1-3): 149-68.

[122] Dvorak HF, Nagy JA, Dvorak AM. Structure of solid tumors and their vasculature: implications for therapy with monoclonal antibodies. Cancer Cells 1991; 3(3): 77-85.

[123] Hashizume H, Baluk P, Morikawa S, McLean JW, Thurston G, Roberge S, et al. Openings between defective endothelial cells explain tumor vessel leakiness. Am J Pathol 2000; 156(4): 1363-80.

[124] Brooks PC, Clark RA, Cheresh DA. Requirement of vascular integrin alpha v beta 3 for angiogenesis. Science 1994; 264(5158): 569-71.

[125] Burrows FJ, Derbyshire EJ, Tazzari PL, Amlot P, Gazdar AF, King SW, et al. Up-regulation of endoglin on vascular endothelial cells in human solid tumors: implications for diagnosis and therapy. Clin Cancer Res 1995; 1(12): 1623-34.

[126] St Croix B, Rago C, Velculescu V, Traverso G, Romans KE, Montgomery E, et al. Genes expressed in human tumor endothelium. Science 2000; 289(5482): 1197-202.

[127] Molema G. Tumor vasculature directed drug targeting: applying new technologies and knowledge to the development of clinically relevant therapies. Pharm Res 2002; 19(9): 1251-8.

[128] Arap W, Pasqualini R, Ruoslahti E. Cancer treatment by targeted drug delivery to tumor vasculature in a mouse model. Science 1998; 279(5349): 377-80.

[129] Ran S, Gao B, Duffy S, Watkins L, Rote N, Thorpe PE. Infarction of solid Hodgkin's tumors in mice by antibody-directed targeting of tissue factor to tumor vasculature. Cancer Res 1998; 58(20): 4646-53.

[130] Duncan R. Polymer-drug conjugates: targeting cancer. In: Muzykantov V and Torchilin V, editors. Biomedical aspects of drug targeting. Boston/Dodrecht/London.: Kluwer Academic Publishers; 2003; p. 193-209.

[131] Sugano M, Egilmez NK, Yokota SJ, Chen FA, Harding J, Huang SK, et al. Antibody targeting of doxorubicin-loaded liposomes suppresses the growth and metastatic spread of established human lung tumor xenografts in severe combined immunodeficient mice. Cancer Res 2000; 60(24): 6942-9.

[132] Schraa AJ, Kok RJ, Berendsen AD, Moorlag HE, Bos EJ, Meijer DK, et al. Endothelial cells internalize and degrade RGD-modified proteins developed for tumor vasculature targeting. J Control Release 2002; 83(2): 241-51.

[133] Riezman H, Woodman PG, van Meer G, Marsh M. Molecular mechanisms of endocytosis. Cell 1997; 91(6): 731-8.

[134] Conner SD, Schmid SL. Regulated portals of entry into the cell. Nature 2003; 422(6927): 37-44.

[135] Mukherjee S, Ghosh RN, Maxfield FR. Endocytosis. Physiol Rev 1997; 77(3): 759-803.

[136] Simionescu M, Gafencu A, Antohe F. Transcytosis of plasma macromolecules in endothelial cells: a cell biological survey. Microsc Res Tech 2002; 57(5): 269-88.

[137] Rippe B, Rosengren BI, Carlsson O, Venturoli D. Transendothelial transport: the vesicle controversy. J Vasc Res 2002; 39(5): 375-90.

[138] Simionescu M, Simionescu N. Endothelial transport of macromolecules: transcytosis and endocytosis. A look from cell biology. Cell Biol Rev 1991; 25(1): 5-78.

[139] Predescu D, Palade GE. Plasmalemmal vesicles represent the large pore system of continuous microvascular endothelium. Am J Physiol 1993; 265(2 Pt 2): H725-33.

[140] Minshall RD, Tiruppathi C, Vogel SM, Malik AB. Vesicle formation and trafficking in endothelial cells and regulation of endothelial barrier function. Histochem Cell Biol 2002; 117(2): 105-12.

[141] Stan RV. Structure and function of endothelial caveolae. Microsc Res Tech 2002; 57(5): 350-64.

[142] Schnitzer JE, Liu J, Oh P. Endothelial caveolae have the molecular transport machinery for vesicle budding, docking, and fusion including VAMP, NSF, SNAP, annexins, and GTPases. J Biol Chem 1995; 270(24): 14399-404.

[143] Schnitzer JE, McIntosh DP, Dvorak AM, Liu J, Oh P. Separation of caveolae from associated microdomains of GPI-anchored proteins. Science 1995; 269(5229): 1435-9.

[144] Schnitzer JE. Caveolae: from basic trafficking mechanisms to targeting transcytosis for tissue-specific drug and gene delivery *in vivo*. Adv Drug Deliv Rev 2001; 49(3): 265-80.

[145] Montesano R, Roth J, Robert A, Orci L. Non-coated membrane invaginations are involved in binding and internalization of cholera and tetanus toxins. Nature 1982; 296(5858): 651-3.

[146] Tran D, Carpentier JL, Sawano F, Gorden P, Orci L. Ligands internalized through coated or noncoated invaginations follow a common intracellular pathway. Proc Natl Acad Sci USA 1987; 84(22): 7957-61.

[147] Parton RG, Joggerst B, Simons K. Regulated internalization of caveolae. J Cell Biol 1994; 127(5): 1199-215.

[148] Vilhardt F, Nielsen M, Sandvig K, van Deurs B. Urokinase-type plasminogen activator receptor is internalized by different mechanisms in polarized and nonpolarized Madin-Darby canine kidney epithelial cells. Mol Biol Cell 1999; 10(1): 179-95.

[149] Raub TJ, Audus KL. Adsorptive endocytosis and membrane recycling by cultured primary bovine brain microvessel endothelial cell monolayers. J Cell Sci 1990; 97 (Pt 1): 127-38.

[150] Teasdale MS, Bird CH, Bird P. Internalization of the anticoagulant thrombomodulin is constitutive and does not require a signal in the cytoplasmic domain. Immunol Cell Biol 1994; 72(6): 480-8.

[151] Anderson RG, Kamen BA, Rothberg KG, Lacey SW. Potocytosis: sequestration and transport of small molecules by caveolae. Science 1992; 255(5043): 410-1.

[152] Hofman P, Blaauwgeers HG, Tolentino MJ, Adamis AP, Nunes Cardozo BJ, Vrensen GF, et al. VEGF-A induced hyperpermeability of blood-retinal barrier endothelium *in vivo* is predominantly associated with pinocytotic vesicular transport and not with formation of fenestrations. Vascular endothelial growth factor-A. Curr Eye Res 2000; 21(2): 637-45.

[153] Kosugi I, Muro H, Shirasawa H, Ito I. Endocytosis of soluble IgG immune complex and its transport to lysosomes in hepatic sinusoidal endothelial cells. J Hepatol 1992; 16(1-2): 106-14.

[154] Stang E, Kindberg GM, Berg T, Roos N. Endocytosis mediated by the mannose receptor in liver endothelial cells. An immunocytochemical study. Eur J Cell Biol 1990; 52(1): 67-76.

[155] Dini L, Kolb-Bachofen V. Preclustered receptor arrangement is a prerequisite for galactose-specific clearance of large particulate ligands in rat liver. Exp Cell Res 1989; 184(1): 235-40.

[156] Kempka G, Kolb-Bachofen V. Binding, uptake, and transcytosis of ligands for mannose-specific receptors in rat liver: an electron microscopic study. Exp Cell Res 1988; 176(1): 38-48.

[157] Geoffroy JS, Becker RP. Endocytosis by endothelial phagocytes: uptake of bovine serum albumin-gold conjugates in bone marrow. J Ultrastruct Res 1984; 89(3): 223-39.

[158] Volker W, Schon P, Vischer P. Binding and endocytosis of thrombospondin and thrombospondin fragments in endothelial cell cultures analyzed by cuprolinic blue staining, colloidal gold labeling, and silver enhancement techniques. J Histochem Cytochem 1991; 39(10): 1385-94.

[159] Yoshioka T, Yamamoto K, Kobashi H, Tomita M, Tsuji T. Receptor-mediated endocytosis of chemically modified albumins by sinusoidal endothelial cells and Kupffer cells in rat and human liver. Liver 1994; 14(3): 129-37.

[160] Smedsrod B, Malmgren M, Ericsson J, Laurent TC. Morphological studies on endocytosis of chondroitin sulphate proteoglycan by rat liver EC. Cell Tissue Res 1988; 253(1): 39-45.

[161] Pitas RE, Boyles J, Mahley RW, Bissell DM. Uptake of chemically modified low density lipoproteins *in vivo* is mediated by specific EC. J Cell Biol 1985; 100(1): 103-17.

[162] Stitt AW, Anderson HR, Gardiner TA, Bailie JR, Archer DB. Receptor-mediated endocytosis and intracellular trafficking of insulin and low-density lipoprotein by retinal vascular endothelial cells. Invest Ophthalmol Vis Sci 1994; 35(9): 3384-92.

[163] Roberts RL, Fine RE, Sandra A. Receptor-mediated endocytosis of transferrin at the blood-brain barrier. J Cell Sci 1993; 104 (Pt 2): 521-32.

[164] Roberts RL, Sandra A. Transport of transferrin across the blood-thymus barrier in young rats. Tissue Cell 1994; 26(5): 757-66.

[165] Stins MF, Maxfield FR, Goldberg IJ. Polarized binding of lipoprotein lipase to endothelial cells. Implications for its physiological actions. Arterioscler Thromb 1992; 12(12): 1437-46.

[166] Stein O, Halperin G, Leitersdorf E, Olivecrona T, Stein Y. Lipoprotein lipase mediated uptake of non-degradable ether analogues of phosphatidylcholine and cholesteryl ester by cultured cells. Biochim Biophys Acta 1984; 795(1): 47-59.

[167] Goti D, Balazs Z, Panzenboeck U, Hrzenjak A, Reicher H, Wagner E, et al. Effects of lipoprotein lipase on uptake and transcytosis of low density lipoprotein (LDL) and LDL-associated alpha-tocopherol in a porcine *in vitro* blood-brain barrier model. J Biol Chem 2002; 277(32): 28537-44.

[168] Stins MF, Sivaram P, Sasaki A, Goldberg IJ. Specificity of lipoprotein lipase binding to endothelial cells. J Lipid Res 1993; 34(11): 1853-61.

[169] Schonherr E, Zhao B, Hausser H, Muller M, Langer C, Wagner WD, et al. Lipoprotein lipase-mediated interactions of small proteoglycans and low-density lipoproteins. Eur J Cell Biol 2000; 79(10): 689-96.

[170] Zimmermann R, Panzenbock U, Wintersperger A, Levak-Frank S, Graier W, Glatter O, et al. Lipoprotein lipase mediates the uptake

of glycated LDL in fibroblasts, endothelial cells, and macrophages. Diabetes 2001; 50(7): 1643-53.

[171] Schnitzer JE, Shen CP, Palade GE. Lectin analysis of common glycoproteins detected on the surface of continuous microvascular endothelium in situ and in culture: identification of sialoglycoproteins. Eur J Cell Biol 1990; 52(2): 241-51.

[172] Kounnas MZ, Chappell DA, Strickland DK, Argraves WS. Glycoprotein 330, a member of the low density lipoprotein receptor family, binds lipoprotein lipase *in vitro*. J Biol Chem 1993; 268(19): 14176-81.

[173] Le Panse S, Galceran M, Pontillon F, Lelongt B, van de Putte M, Ronco PM, et al. Immunofunctional properties of a yolk sac epithelial cell line expressing two proteins gp280 and gp330 of the intermicrovillar area of proximal tubule cells: inhibition of endocytosis by the specific antibodies. Eur J Cell Biol 1995; 67(2): 120-9.

[174] Fuki IV, Kuhn KM, Lomazov IR, Rothman VL, Tuszynski GP, Iozzo RV, et al. The syndecan family of proteoglycans. Novel receptors mediating internalization of atherogenic lipoproteins *in vitro*. J Clin Invest 1997; 100(6): 1611-22.

[175] Straley KS, Green SA. Rapid transport of internalized P-selectin to late endosomes and the TGN: roles in regulating cell surface expression and recycling to secretory granules. J Cell Biol 2000; 151(1): 107-16.

[176] Kessner S, Krause A, Rothe U, Bendas G. Investigation of the cellular uptake of E-Selectin-targeted immunoliposomes by activated human EC. Biochim Biophys Acta 2001; 1514(2): 177-90.

[177] Everts M, Kok RJ, Asgeirsdottir SA, Melgert BN, Moolenaar TJ, Koning GA, et al. Selective intracellular delivery of dexamethasone into activated endothelial cells using an E-selectin-directed immunoconjugate. J Immunol 2002; 168(2): 883-9.

[178] Stossel TP. The early history of phagocytosis. In: Tartakoff AM, editor. In Advances in cell and molecular biology of membranes and organelles. Stamford. Connecticut: JAI Press Inc.; 1999; p. 3-18.

[179] Caron E, Hall A. Phagocytosis: Oxford University Press; 2001.

[180] Koval M, Preiter K, Adles C, Stahl PD, Steinberg TH. Size of IgG-opsonized particles determines macrophage response during internalization. Exp Cell Res 1998; 242(1): 265-73.

[181] Hall A. Phagocytosis. In: Marsh M, editor. Endocytosis. Oxford. UK: Oxford University Press; 2001; p. 58-77.

[182] Griffin FM Jr, Griffin JA, Leider JE, Silverstein SC. Studies on the mechanism of phagocytosis. I. Requirements for circumferential attachment of particle-bound ligands to specific receptors on the macrophage plasma membrane. J Exp Med 1975; 142(5): 1263-82.

[183] Oka K, Sawamura T, Kikuta K, Itokawa S, Kume N, Kita T, et al. Lectin-like oxidized low-density lipoprotein receptor 1 mediates phagocytosis of aged/apoptotic cells in EC. Proc Natl Acad Sci USA 1998; 95(16): 9535-40.

[184] Eugene E, Hoffmann I, Pujol C, Couraud PO, Bourdoulous S, Nassif X. Microvilli-like structures are associated with the internalization of virulent capsulated Neisseria meningitidis into vascular endothelial cells. J Cell Sci 2002; 115(Pt 6): 1231-41.

[185] Swanson JA, Watts C. Macropinocytosis. Trends Cell Biol 1995; 5: 424-81.

[186] Lewis. Pinocytosis. Johns Hopkins Hosp Bull 1931; 49: 17-36.

[187] Machesky LM, Reeves E, Wientjes F, Mattheyse FJ, Grogan A, Totty NF, et al. Mammalian actin-related protein 2/3 complex localizes to regions of lamellipodial protrusion and is composed of evolutionarily conserved proteins. Biochem J 1997; 328 (Pt 1): 105-12.

[188] Machesky LM, Mullins RD, Higgs HN, Kaiser DA, Blanchoin L, May RC, et al. Scar, a WASp-related protein, activates nucleation of actin filaments by the Arp2/3 complex. Proc Natl Acad Sci USA 1999; 96(7): 3739-44.

[189] Saito T, Lamy F, Roger PP, Lecocq R, Dumont JE. Characterization and identification as cofilin and destrin of two thyrotropin- and phorbol ester-regulated phosphoproteins in thyroid cells. Exp Cell Res 1994; 212(1): 49-61.

[190] Veithen A, Cupers P, Baudhuin P, Courtoy PJ. v-Src induces constitutive macropinocytosis in rat fibroblasts. J Cell Sci 1996; 109 (Pt 8): 2005-12.

[191] Ridley AJ, Hall A. The small GTP-binding protein rho regulates the assembly of focal adhesions and actin stress fibers in response to growth factors. Cell 1992; 70(3): 389-99.

[192] Bar-Sagi D, Feramisco JR. Induction of membrane ruffling and fluid-phase pinocytosis in quiescent fibroblasts by ras proteins. Science 1986; 233(4768): 1061-8.

[193] Swanson JA. Phorbol esters stimulate macropinocytosis and solute flow through macrophages. J Cell Sci 1989; 94 (Pt 1): 135-42.

[194] Wennstrom S, Siegbahn A, Yokote K, Arvidsson AK, Heldin CH, Mori S, et al. Membrane ruffling and chemotaxis transduced by the PDGF beta-receptor require the binding site for phosphatidylinositol 3' kinase. Oncogene 1994; 9(2): 651-60.

[195] Willingham MC, Haigler HT, Fitzgerald DJ, Gallo MG, Rutherford AV, Pastan IH. The morphologic pathway of binding and internalization of epidermal growth factor in cultured cells. Studies on A431, KB, and 3T3 cells, using multiple methods of labelling. Exp Cell Res 1983; 146(1): 163-75.

[196] Mellstrom K, Heldin CH, Westermark B. Induction of circular membrane ruffling on human fibroblasts by platelet-derived growth factor. Exp Cell Res 1988; 177(2): 347-59.

[197] Brunk U, Schellens J, Westermark B. Influence of epidermal growth factor (EGF) on ruffling activity, pinocytosis and proliferation of cultivated human glia cells. Exp Cell Res 1976; 103(2): 295-302.

[198] Liu NQ, Lossinsky AS, Popik W, Li X, Gujuluva C, Kriederman B, et al. Human immunodeficiency virus type 1 enters brain microvascular endothelia by macropinocytosis dependent on lipid rafts and the mitogen-activated protein kinase signaling pathway. J Virol 2002; 76(13): 6689-700.

[199] Gil J. Number and distribution of plasmalemmal vesicles in the lung. Fed Proc 1983; 42(8): 2414-8.

[200] Ghinea N, Mai TV, Groyer-Picard MT, Milgrom E. How protein hormones reach their target cells. Receptor-mediated transcytosis of hCG through endothelial cells. J Cell Biol 1994; 125(1): 87-97.

[201] Roberts RL, Sandra A. Receptor-mediated endocytosis of insulin by cultured endothelial cells. Tissue Cell 1992; 24(5): 603-11.

[202] Ring A, Pohl J, Volkl A, Stremmel W. Evidence for vesicles that mediate long-chain fatty acid uptake by human microvascular endothelial cells. J Lipid Res 2002; 43(12): 2095-104.

[203] Conway EM, Nowakowski B, Steiner-Mosonyi M. Thrombomodulin lacking the cytoplasmic domain efficiently internalizes thrombin via nonclathrin-coated, pit-mediated endocytosis. J Cell Physiol 1994; 158(2): 285-98.

[204] Conway EM, Boffa MC, Nowakowski B, Steiner-Mosonyi M. An ultrastructural study of thrombomodulin endocytosis: internalization occurs via clathrin-coated and non-coated pits. J Cell Physiol 1992; 151(3): 604-12.

[205] Wiewrodt R, Thomas AP, Cipelletti L, Christofidou-Solomidou M, Weitz DA, Feinstein SI, et al. Size-dependent intracellular immunotargeting of therapeutic cargoes into endothelial cells. Blood 2002; 99(3): 912-22.

[206] Muro S, Wiewrodt R, Thomas A, Koniaris L, Albelda SM, Muzykantov VR, et al. A novel endocytic pathway induced by clustering endothelial ICAM-1 or PECAM-1. J Cell Sci 2003; 116(Pt 8): 1599-1609.

[207] Behera AK, Matsuse H, Kumar M, Kong X, Lockey RF, Mohapatra SS. Blocking intercellular adhesion molecule-1 on human epithelial cells decreases respiratory syncytial virus infection. Biochem Biophys Res Commun 2001; 280(1): 188-95.

[208] Schober D, Kronenberger P, Prchla E, Blaas D, Fuchs R. Major and minor receptor group human rhinoviruses penetrate from endosomes by different mechanisms. J Virol 1998; 72(2): 1354-64.

[209] Treutiger CJ, Heddini A, Fernandez V, Muller WA, Wahlgren M. PECAM-1/CD31, an endothelial receptor for binding Plasmodium falciparum-infected erythrocytes. Nat Med 1997; 3(12): 1405-8.

[210] Brown S, Heinisch I, Ross E, Shaw K, Buckley CD, Savill J. Apoptosis disables CD31-mediated cell detachment from phagocytes promoting binding and engulfment. Nature 2002; 418(6894): 200-3.

[211] Gow AJ, Branco F, Christofidou-Solomidou M, Black-Schultz L, Albelda SM, Muzykantov VR. Immunotargeting of glucose oxidase: intracellular production of H_2O_2 and endothelial oxidative stress. Am J Physiol 1999; 277(2 Pt 1): L271-81.

[212] Christofidou-Solomidou M, Pietra GG, Solomides CC, Arguiris E, Harshaw D, Fitzgerald GA, et al. Immunotargeting of glucose oxidase to endothelium *in vivo* causes oxidative vascular injury in the lungs. Am J Physiol Lung Cell Mol Physiol 2000; 278(4): L794-805.

[213] Sweitzer TD, Thomas AP, Wiewrodt R, Nakada MT, Branco F, Muzykantov VR. Pecam-directed immunotargeting of catalase: specific, rapid and transient protection against hydrogen peroxide. Free Radic Biol Med 2003; 34(8): 1035-46.

[214] Kozower BD, Christofidou-Solomidou M, Sweitzer TD, Muro S, Buerk DG, Solomides CC, et al. Immunotargeting of catalase to the pulmonary endothelium alleviates oxidant stressand reduces acute lung transplantation injury. Nat Biotechnol 2003; 21(4): 392-8.

[215] Yajima Y, Kawashima S. Calpain function in the differentiation of mesenchymal stem cells. Biol Chem 2002; 383(5): 757-64.

[216] Gil-Parrado S, Popp O, Knoch TA, Zahler S, Bestvater F, Felgentrager M, et al. Subcellular localization and *in vivo* subunit interactions of ubiquitous mu -calpain. J Biol Chem 2003; 278: 1636-46.

[217] Gregoriou M, Willis AC, Pearson MA, Crawford C. The calpain cleavage sites in the epidermal growth factor receptor kinase domain. Eur J Biochem 1994; 223(2): 455-64.

[218] Guttmann RP, Baker DL, Seifert KM, Cohen AS, Coulter DA, Lynch DR. Specific proteolysis of the NR2 subunit at multiple sites by calpain. J Neurochem 2001; 78(5): 1083-93.

[219] Fox JE. Cytoskeletal proteins and platelet signaling. Thromb Haemost 2001; 86(1): 198-213.

[220] Huttenlocher A, Palecek SP, Lu Q, Zhang W, Mellgren RL, Lauffenburger DA, et al. Regulation of cell migration by the calcium-dependent protease calpain. J Biol Chem 1997; 272(52): 32719-22.

[221] Potter DA, Tirnauer JS, Janssen R, Croall DE, Hughes CN, Fiacco KA, et al. Calpain regulates actin remodeling during cell spreading. J Cell Biol 1998; 141(3): 647-62.

[222] Dunlop RA, Rodgers KJ, Dean RT. Recent developments in the intracellular degradation of oxidized proteins. Free Radic Biol Med 2002; 33(7): 894-906.

[223] Tanaka K, Kasahara M. The MHC class I ligand-generating system: roles of immunoproteasomes and the interferon-gamma-inducible proteasome activator PA28. Immunol Rev 1998; 163: 161-76.

[224] Groettrup M, Khan S, Schwarz K, Schmidtke G. Interferon-gamma inducible exchanges of 20S proteasome active site subunits: why? Biochimie 2001; 83(3-4): 367-72.

[225] Gruenberg J. The endocytic pathway: a mosaic of domains. Nat Rev Mol Cell Biol 2001; 2(10): 721-30.

[226] Stoorvogel W, Strous GJ, Geuze HJ, Oorschot V, Schwartz AL. Late endosomes derive from early endosomes by maturation. Cell 1991; 65(3): 417-27.

[227] Reaves BJ, Banting G, Luzio JP. Lumenal and transmembrane domains play a role in sorting type I membrane proteins on endocytic pathways. Mol Biol Cell 1998; 9(5): 1107-22.

[228] Mellman I. Endocytosis and molecular sorting. Annu Rev Cell Dev Biol 1996; 12: 575-625.

[229] Knight A, Hughson E, Hopkins CR, Cutler DF. Membrane protein trafficking through the common apical endosome compartment of polarized Caco-2 cells. Mol Biol Cell 1995; 6(5): 597-610.

[230] Fuchs R, Male P, Mellman I. Acidification and ion permeabilities of highly purified rat liver endosomes. J Biol Chem 1989; 264(4): 2212-20.

[231] Mellman I. The importance of being acid: the role of acidification in intracellular membrane traffic. J Exp Biol 1992; 172: 39-45.

[232] Warnock DG. Regulation of endosomal acidification via Gi-type protein. Kidney Int 1999; 55(6): 2524-5.

[233] Gille L, Nohl H. The existence of a lysosomal redox chain and the role of ubiquinone. Arch Biochem Biophys 2000; 375(2): 347-54.

[234] Killisch I, Steinlein P, Romisch K, Hollinshead R, Beug H, Griffiths G. Characterization of early and late endocytic compartments of the transferrin cycle. Transferrin receptor antibody blocks erythroid differentiation by trapping the receptor in the early endosome. J Cell Sci 1992; 103 (Pt 1): 211-32.

[235] Futai M, Oka T, Moriyama Y, Wada Y. Diverse roles of single membrane organelles: factors establishing the acid lumenal pH. J Biochem (Tokyo) 1998; 124(2): 259-67.

[236] Kornfeld S, Mellman I. The biogenesis of lysosomes. Annu Rev Cell Biol 1989; 5: 483-525.

[237] Pillay CS, Elliott E, Dennison C. Endolysosomal proteolysis and its regulation. Biochem J 2002; 363(Pt 3): 417-29.

[238] Fukuda M. Lysosomal membrane glycoproteins. Structure, biosynthesis, and intracellular trafficking. J Biol Chem 1991; 266(32): 21327-30.

[239] Storer AC, Menard R. Catalytic mechanism in papain family of cysteine peptidases. Methods Enzymol 1994; 244: 486-500

[240] de Bruyn PP, Cho Y, Michelson S. *In vivo* endocytosis by bristle coated pits of protein tracers and their intracellular transport in the endothelial cells lining the sinuses of the liver. II. The endosomal-lysosomal transformation. J Ultrastruct Res 1983; 85(3): 290-9.

[241] Sheff DR, Daro EA, Hull M, Mellman I. The receptor recycling pathway contains two distinct populations of early endosomes with different sorting functions. J Cell Biol 1999; 145(1): 123-39.

[242] Mellman IS, Plutner H, Steinman RM, Unkeless JC, Cohn ZA. Internalization and degradation of macrophage Fc receptors during receptor-mediated phagocytosis. J Cell Biol 1983; 96(3): 887-95.

[243] Pitt A, Mayorga LS, Schwartz AL, Stahl PD. Transport of phagosomal components to an endosomal compartment. J Biol Chem 1992; 267(1): 126-32.

[244] Mayorga LS, Bertini F, Stahl PD. Fusion of newly formed phagosomes with endosomes in intact cells and in a cell-free system. J Biol Chem 1991; 266(10): 6511-7.

[245] Hewlett LJ, Prescott AR, Watts C. The coated pit and macropinocytic pathways serve distinct endosome populations. J Cell Biol 1994; 124(5): 689-703.

[246] Desjardins M, Huber LA, Parton RG, Griffiths G. Biogenesis of phagolysosomes proceeds through a sequential series of interactions with the endocytic apparatus. J Cell Biol 1994; 124(5): 677-88.

[247] Parton RG, Lindsay M. Exploitation of major histocompatibility complex class I molecules and caveolae by simian virus 40. Immunol Rev 1999; 168: 23-31.

[248] Norkin LC. Simian virus 40 infection via MHC class I molecules and caveolae. Immunol Rev 1999; 168: 13-22.

[249] Kamen BA, Johnson CA, Wang MT, Anderson RG. Regulation of the cytoplasmic accumulation of 5-methyltetrahydrofolate in MA104 cells is independent of folate receptor regulation. J Clin Invest 1989; 84(5): 1379-86.

[250] Haasemann M, Cartaud J, Muller-Esterl W, Dunia I. Agonist-induced redistribution of bradykinin B2 receptor in caveolae. J Cell Sci 1998; 111 (Pt 7): 917-28.

[251] Chun M, Liyanage UK, Lisanti MP, Lodish HF. Signal transduction of a G protein-coupled receptor in caveolae: colocalization of endothelin and its receptor with caveolin. Proc Natl Acad Sci USA 1994; 91(24): 11728-32.

[252] Dessy C, Kelly RA, Balligand JL, Feron O. Dynamin mediates caveolar sequestration of muscarinic cholinergic receptors and alteration in NO signaling. EMBO J 2000; 19(16): 4272-80.

[253] Muro S, Cui X, Gajewski C, Muzykantov VR, Koval M. Slow intracellular trafficking of catalase nanoparticles targeted to endothelial ICAM-1 protects endothelial cells from oxidative stress. Am J Physiol Cell 2003; 285(5): 1339-47.

[254] Bomsel M, Parton R, Kuznetsov SA, Schroer TA, Gruenberg J. Microtubule- and motor-dependent fusion *in vitro* between apical and basolateral endocytic vesicles from MDCK cells. Cell 1990; 62(4): 719-31.

[255] Palade GE, Simionescu M, Simionescu N. Structural aspects of the permeability of the microvascular endothelium. Acta Physiol Scand Suppl 1979; 463: 11-32.

[256] Majno G. Maude Abbott Lecture--1991. The capillary then and now: an overview of capillary pathology. Mod Pathol 1992; 5(1): 9-22.

[257] McDonald DM, Thurston G, Baluk P. Endothelial gaps as sites for plasma leakage in inflammation. Microcirculation 1999; 6(1): 7-22.

[258] Schnitzer JE, Oh P, McIntosh DP. Role of GTP hydrolysis in fission of caveolae directly from plasma membranes. Science 1996; 274(5285): 239-42.

[259] Niles WD, Malik AB. Endocytosis and exocytosis events regulate vesicle traffic in EC. J Membr Biol 1999; 167(1): 85-101.

[260] Minshall RD, Tiruppathi C, Vogel SM, Niles WD, Gilchrist A, Hamm HE, et al. Endothelial cell-surface gp60 activates vesicle formation and trafficking via G(i)-coupled Src kinase signaling pathway. J Cell Biol 2000; 150(5): 1057-70.

[261] Vogel SM, Easington CR, Minshall RD, Niles WD, Tiruppathi C, Hollenberg SM, et al. Evidence of transcellular permeability pathway in microvessels. Microvasc Res 2001; 61(1): 87-101.

[262] Volker W, Hess S, Vischer P, Preissner KT. Binding and processing of multimeric vitronectin by vascular endothelial cells. J Histochem Cytochem 1993; 41(12): 1823-32.

[263] John TA, Vogel SM, Tiruppathi C, Malik AB, Minshall RD. Quantitative analysis of albumin uptake and transport in the rat microvessel endothelial monolayer. Am J Physiol Lung Cell Mol Physiol 2003; 284(1): L187-96.

[264] Dvorak AM, Feng D. The vesiculo-vacuolar organelle (VVO). A new endothelial cell permeability organelle. J Histochem Cytochem 2001; 49(4): 419-32.

[265] Simionescu N, Siminoescu M, Palade GE. Permeability of muscle capillaries to small heme-peptides. Evidence for the existence of patent transendothelial channels. J Cell Biol 1975; 64(3): 586-607.

[266] Schnitzer JE, Oh P, Pinney E, Allard J. Filipin-sensitive caveolae-mediated transport in endothelium: reduced transcytosis, scavenger endocytosis, and capillary permeability of select macromolecules. J Cell Biol 1994; 127(5): 1217-32.

[267] Predescu D, Predescu S, McQuistan T, Palade GE. Transcytosis of alpha1-acidic glycoprotein in the continuous microvascular endothelium. Proc Natl Acad Sci USA 1998; 95(11): 6175-80.

[268] Horvat R, Palade GE. Thrombomodulin and thrombin localization on the vascular endothelium; their internalization and transcytosis by plasmalemmal vesicles. Eur J Cell Biol 1993; 61(2): 299-313.

[269] Vasile E, Simionescu M, Simionescu N. Visualization of the binding, endocytosis, and transcytosis of low-density lipoprotein in the arterial endothelium in situ. J Cell Biol 1983; 96(6): 1677-89.

[270] Robinson CS, Wagner RC. Differential endocytosis of lipoproteins by capillary endothelial vesicles. Microcirc Endothelium Lymphatics 1985; 2(3): 313-29.

[271] Tiruppathi C, Song W, Bergenfeldt M, Sass P, Malik AB. Gp60 activation mediates albumin transcytosis in endothelial cells by tyrosine kinase-dependent pathway. J Biol Chem 1997; 272(41): 25968-75.

[272] Predescu D, Predescu S, Malik AB. Transport of nitrated albumin across continuous vascular endothelium. Proc Natl Acad Sci USA 2002; 99(21): 13932-7.

[273] Terasaki T, Pardridge WM. Targeted drug delivery to the brain; (blood-brain barrier, efflux, endothelium, biological transport). J Drug Target 2000; 8(6): 353-5.

[274] Prokai-Tatrai K, Nguyen V, Zharikova AD, Braddy AC, Stevens SM, Prokai L. Prodrugs to enhance central nervous system effects of the TRH-like peptide pGlu-Glu-Pro-NH(2). Bioorg Med Chem Lett 2003; 13(6): 1011-4.

[275] Stins MF, Nemani PV, Wass C, Kim KS. Escherichia coli binding to and invasion of brain microvascular endothelial cell derived from humans and rats of different ages. Infect Immun 1999; 67(10): 5522-5.

[276] Muruganandam A, Tanha J, Narang S, Stanimirovic D. Selection of phage-displayed llama single-domain antibodies that transmigrate across human blood-brain barrier endothelium. FASEB J 2002; 16(2): 240-2

[277] Wengenack TM, Curran GL, Olson EE, Poduslo JF. Putrescine-modified catalase with preserved enzymatic activity exhibits increased permeability at the blood-nerve and blood-brain barriers. Brain Res 1997; 767(1): 128-35.

[278] Scherphof GL, Romero EL, Velinova MJ, Kamps JAAM, Koning GA, Meijer DKF, Swart P, Daemen T, editor. Endothelial and transendothelial delivery of pharmaceutically active agents; potential of liposomes. Leiden. The Netherlands.: Kupffer Cell Foundation; 1999.

[279] Tsukita S, Furuse M, Itoh M. Multifunctional strands in tight junctions. Nat Rev Mol Cell Biol 2001; 2(4): 285-93.

[280] Fanning AS, Mitic LL, Anderson JM. Transmembrane proteins in the tight junction barrier. J Am Soc Nephrol 1999; 10(6): 1337-45.

[281] Nitta T, Hata M, Gotoh S, Seo Y, Sasaki H, Hashimoto N, et al. Size-selective loosening of the blood-brain barrier in claudin-5-deficient mice. J Cell Biol 2003; 161(3): 653-60.

[282] Hopkins AM, Li D, Mrsny RJ, Walsh SV, Nusrat A. Modulation of tight junction function by G protein-coupled events. Adv Drug Deliv Rev 2000; 41(3): 329-40.

[283] Nourry C, Grant SG, Borg JP. PDZ domain proteins: plug and play! Sci STKE 2003; 2003(179): RE7.

[284] Pawson T, Nash P. Assembly of cell regulatory systems through protein interaction domains. Science 2003; 300(5618): 445-52.

[285] Martin TA, Mansel RE, Jiang WG. Antagonistic effect of NK4 on HGF/SF induced changes in the transendothelial resistance (TER) and paracellular permeability of human vascular endothelial cells. J Cell Physiol 2002; 192(3): 268-75.

[286] Stevens T, Garcia JG, Shasby DM, Bhattacharya J, Malik AB. Mechanisms regulating endothelial cell barrier function. Am J Physiol Lung Cell Mol Physiol 2000; 279(3): L419-22.

[287] Lum H, Malik AB. Regulation of vascular endothelial barrier function. Am J Physiol 1994; 267(3 Pt 1): L223-41.

[288] McDonald DM, Thurston G, Baluk P. Endothelial gaps as sites for plasma leakage in inflammation. Microcirculation 1999; 6(1): 7-22.

[289] Hashizume H, Baluk P, Morikawa S, McLean JW, Thurston G, Roberge S, et al. Openings between defective endothelial cells explain tumor vessel leakiness. Am J Pathol 2000; 156(4): 1363-80.

[290] Hobbs SK, Monsky WL, Yuan F, Roberts WG, Griffith L, Torchilin VP, et al. Regulation of transport pathways in tumor vessels: role of tumor type and microenvironment. Proc Natl Acad Sci USA 1998; 95(8): 4607-12.

[291] Feng D, Nagy JA, Pyne K, Hammel I, Dvorak HF, Dvorak AM. Pathways of macromolecular extravasation across microvascular endothelium in response to VPF/VEGF and other vasoactive mediators. Microcirculation 1999; 6(1): 23-44.

[292] Haselton FR, Alexander JS, Mueller SN. Adenosine decreases permeability of *in vitro* endothelial monolayers. J Appl Physiol 1993; 74(4): 1581-90.

[293] Dejana E. Endothelial adherens junctions: implications in the control of vascular permeability and angiogenesis. J Clin Invest 1996; 98(9): 1949-53.

[294] Moore TM, Norwood NR, Creighton JR, Babal P, Brough GH, Shasby DM, et al. Receptor-dependent activation of store-operated calcium entry increases endothelial cell permeability. Am J Physiol Lung Cell Mol Physiol 2000; 279(4): L691-8.

[295] Lum H, Malik AB. Regulation of vascular endothelial barrier function. Am J Physiol 1994; 267(3 Pt 1): L223-41.

[296] Verin AD, Csortos C, Durbin SD, Aydanyan A, Wang P, Patterson CE, et al. Characterization of the protein phosphatase 1 catalytic subunit in endothelium: involvement in contractile responses. J Cell Biochem 2000; 79(1): 113-25.

[297] Cho MM, Ziats NP, Pal D, Utian WH, Gorodeski GI. Estrogen modulates paracellular permeability of human endothelial cells by eNOS- and iNOS-related mechanisms. Am J Physiol 1999; 276(2 Pt 1): C337-49.

[298] Wu J, Akaike T, Maeda H. Modulation of enhanced vascular permeability in tumors by a bradykinin antagonist, a cyclooxygenase inhibitor, and a nitric oxide scavenger. Cancer Res 1998; 58(1): 159-65.

[299] Maeda H, Sawa T, Konno T. Mechanism of tumor-targeted delivery of macromolecular drugs, including the EPR effect in solid tumor and clinical overview of the prototype polymeric drug SMANCS. J Control Release 2001; 74(1-3): 47-61.

[300] Drab M, Verkade P, Elger M, Kasper M, Lohn M, Lauterbach B, et al. Loss of Caveolae, Vascular Dysfunction, and Pulmonary Defects in Caveolin-1 Gene-Disrupted Mice. Science 2000; 293: 2449-2452.

[301] Schlegel A, Pestell RG, Lisanti MP. Caveolins in cholesterol trafficking and signal transduction: implications for human disease. Front Biosci 2000; 5: D929-37.

ICAM-1 recycling in endothelial cells: a novel pathway for sustained intracellular delivery and prolonged effects of drugs

Silvia Muro, Christine Gajewski, Michael Koval, and Vladimir R. Muzykantov

Intercellular adhesion molecule-1 (ICAM-1) is a target for drug delivery to endothelial cells (ECs), which internalize multivalent anti-ICAM nanocarriers (anti-ICAM/NCs) within 15 to 30 minutes. The concomitant ICAM-1 disappearance from the EC surface transiently inhibited subsequent binding and uptake of anti-ICAM/NCs. Within 1 hour, internalized ICAM-1 diverged from anti-ICAM/NCs into prelysosomal vesicles, resurfaced, and enabled uptake of a subsequent anti-ICAM/NC dose. Thus, internalized ICAM-1 was able to recycle back to the plasma membrane. In vivo pulmonary targeting of a second anti-ICAM/NC dose injected 15 minutes after the first dose was decreased by 50% but recovered between 30 minutes and 2.5 hours, comparable to cultured ECs. Anti-ICAM/NCs affected neither EC viability nor fluid-phase endocytosis and traffic to lysosomes. However, lysosomal trafficking of the second dose of anti-ICAM/NCs was decelerated at least 2-fold versus the first dose; hence the major fraction of anti-ICAM/NCs resided in prelysosomal vesicles for at least 5 hours without degradation. Two successive doses of anti-ICAM/NC/catalase protected ECs against H_2O_2 for at least 8 hours versus 2 hours afforded by a single dose, suggesting that recurrent targeting to ICAM-1 affords longer effects. ICAM-1 recycling and inhibited lysosomal traffic/degradation of subsequent doses may help to prolong activity of therapeutic agents delivered into ECs by anti-ICAM/NCs. (Blood. 2005;105:650-658)

Introduction

Intercellular adhesion molecule-1 (ICAM-1) is an Ig family transmembrane glycoprotein constitutively exposed on the luminal surface of endothelial cells (ECs).[1-3] ICAM-1 represents an attractive target for drug delivery to ECs, since it is up-regulated and functionally involved in vascular inflammation, oxidant stress, and thrombosis.[4-7] Antibodies to ICAM-1 are being explored as therapeutics and affinity carriers in cell cultures, animal models, and early clinical studies.[8-13] In addition to acting as delivery vehicles, antibody blocking of ICAM-1 suppresses leukocyte adhesion to ECs, providing an anti-inflammatory benefit to the effects of drugs.[14,15]

Targeting nanocarriers (NCs) to EC determinants decreases the clearance of drugs from the bloodstream and permits site-specific delivery, increasing therapeutic capacity and reducing side effects (Muzykantov[16]). Internalization and proper subcellular processing of drugs also are critical in the rational design of drug delivery systems (Muro et al[17]). For instance, intracellular targeting of antioxidants in ECs may help to detoxify oxidants produced within the cell body and decrease elimination of drugs that otherwise shed from the EC surface.[18-22]

ICAM-1 targeting offers the possibility of intracellular drug delivery, given that ECs internalize multimeric anti-ICAM conjugates and anti-ICAM/NCs via a unique, newly defined pathway, cell adhesion molecule (CAM)–mediated endocytosis.[23] ICAM-1 engagement by multimeric ligands triggers signaling via protein kinase C, Src family kinases, and Rho-dependent kinase, also involves dynamin and amiloride-sensitive Na^+/H^+ exchangers, leading to rapid reorganization of the actin cytoskeleton and formation of endocytic compartments.[23]

Intracellular delivery of an antioxidant enzyme, catalase, to ECs via CAM-mediated endocytosis may help contain vascular oxidant stress by minimizing catalase shedding from the cell surface. Endocytosed catalase does not escape endosomes but retains enzymatic activity within these organelles. Due to the high diffusion rate of H_2O_2 across cellular membranes, catalase within endocytic vesicles intercepts intracellular oxidants and provides antioxidant protection. Decay of this antioxidant effect occurs approximately 2-3 hours after internalization, due to pH-dependent proteolytic degradation following delivery to lysosomes.[13] This time frame is sufficient to protect lung vasculature from acute oxidant stress in animal models.[11,24,25]

By analogy with classical endocytic receptors, internalized ICAM-1 could follow nanoparticle trafficking to lysosomes or dissociate from anti-ICAM in a sorting prelysosomal compartment. The latter scenario, including recycling of internalized ICAM-1 molecules to the cell surface, could provide a pathway for recurrent drug delivery permitting sustained effects. However, the fate of ICAM-1 molecules involved in endocytosis is not known. The only pathway for endothelial ICAM-1 turnover identified to date is shedding from the plasma membrane, a negative feedback mechanism reducing leukocyte adhesion.[21,22]

In the present study we characterized intracellular trafficking of ICAM-1 after CAM-mediated anti-ICAM/NC endocytosis in ECs

From the Institute for Environmental Medicine and Departments of Physiology and Pharmacology University of Pennsylvania School of Medicine, Philadelphia, PA.

Submitted May 4, 2004; accepted August 30, 2004. Prepublished online as *Blood* First Edition Paper, September 14, 2004; DOI 10.1182/blood-2004-05-1714.

Supported by National Institutes of Health grants HL/GM 71175-01 (V.R.M), GM61012 (M.K.), and P01 HL019737-26; Project 3 (M.K.); Department of Defense grant PR 012262 (V.R.M.); and American Heart Association grant 0435481N (S.M.).

Reprints: Silvia Muro, IFEM, University of Pennsylvania School of Medicine, 1 John Morgan Building, 3620 Hamilton Walk, Philadelphia, PA 19104-6068; e-mail: silvia@mail.med.upenn.edu.

The publication costs of this article were defrayed in part by page charge payment. Therefore, and solely to indicate this fact, this article is hereby marked "advertisement" in accordance with 18 U.S.C. section 1734.

and ICAM-1 availability for retargeting. The effects of 2 consecutive doses of anti-ICAM/NCs on the internalization capacity, intracellular trafficking, and the fate of anti-ICAM/NCs were examined. Results from cell culture and in vivo animal model studies showed that a large fraction of ICAM-1 molecules dissociated from internalized anti-ICAM/NCs, recycled to EC surface, and permitted recurrent, sustained targeting of anti-ICAM/NCs, providing a prolonged therapeutic effect.

Materials and methods

Antibodies and reagents

Monoclonal antibodies recognizing the extracellular domain of human or murine ICAM-1 were mAb R6.5[26] and mAb YN1,[27] respectively. An antibody to the cytoplasmic domain of human ICAM-1 (LB-2) was from Santa Cruz Biotechnology (Santa Cruz, CA). Secondary antibodies were from Molecular Probes (Eugene, OR). Polystyrene latex microspheres, 100 nm in diameter, were from Polysciences (Warrington, PA). Unless otherwise stated, all other reagents were from Sigma (St Louis, MO).

Preparation of anti-ICAM nanocarriers

For fluorescence microscopy in cell cultures, latex nanospheres were coated with anti-ICAM alone (anti-ICAM/NC) or anti-ICAM and catalase (anti-ICAM/NC/catalase), as described previously.[13] Radiolabeled nanocarriers for in vivo studies were prepared using anti-ICAM and ^{125}I-IgG (95:5) or a mix of IgG and ^{125}I-IgG (95:5). The effective diameter of coated nanocarriers ranged from 200 to 300 nm, as determined by dynamic light scattering.[28]

Cell culture

Pooled human umbilical vein endothelial cells (HUVECs) were purchased from Clonetics (San Diego, CA) and cultured in supplemented M199 medium as described.[13] For experiments, HUVECs (passage 4 to 5) were seeded onto 12-mm^2 gelatin-coated coverslips in 24-well plates and then activated by overnight incubation with tumor necrosis factor–α (TNF-α), unless otherwise stated.

Detection of surface ICAM-1 during nanocarrier internalization

TNF-α–activated HUVECs were treated with 50 μg/mL cyclohexamide for 30 minutes to inhibit protein synthesis, then all further incubations were done in medium containing 10 μg/mL cyclohexamide. The cells were incubated at 4°C for 10 minutes with anti-ICAM/NCs to enable binding, then washed and warmed to 37°C to permit internalization. Surface ICAM-1 was determined by incubation with ^{125}I-labeled anti-ICAM at 4°C, followed by elution with acid glycine solution and quantification in a gamma counter.[29] The results were normalized by constitutive ICAM-1 turnover, determined in HUVECs treated with cyclohexamide but not anti-ICAM/NCs, and total cell protein in the samples. In parallel experiments, nanocarrier uptake by either resting or TNF-α–activated cells was quantified by fluorescence microscopy as described previously.[23] Cells incubated at 4°C were used as controls.

Recycling experiments

TNF-α–activated HUVECs were incubated for a 10-minute pulse at 37°C in the presence of fluorescein isothiocyanate (FITC)–labeled anti-ICAM/NCs and 2 mg/mL amine-fixable Texas Red dextran (10 000 molecular weight [MW]) to permit internalization of both counterparts within common endocytic vesicles. The cells were then washed, incubated at 37°C to enable intracellular trafficking, and fixed and incubated with goat anti–mouse IgG conjugated to blue Alexa Fluor 350 (Excitation: 350 nm, Emission: 450 nm) to label surface-bound nanocarriers. Alternatively, HUVECs were incubated with only FITC-labeled anti-ICAM/NCs, and ICAM-1 intracellular trafficking was followed by permeabilization and immunolabeling of ICAM-1 cytoplasmic tail in red. The samples were analyzed by fluorescence microscopy (Eclipse TE2000-U, Nikon, Melville, NY) using filters optimized for Alexa Fluor 350, FITC, and Texas Red, and a 60×/NA1.4 PlanApo objective (Nikon, Melville, NY). Images were obtained with Orca-1CCD camera (Hamamatsu, Bridgewater, NJ) and analyzed using ImagePro 3.0 software (Media Cybernetics, Silver Spring, MD).

Uptake and intracellular trafficking of anti-ICAM nanocarriers

HUVECs, either resting or activated with TNF-α, were incubated first with a dose of anti-ICAM/NCs, followed by a second dose of FITC-labeled anti-ICAM/NCs, varying the amount of time between the application of the first and the second dose of nanocarriers. Finally, ECs were washed, fixed, and treated with Texas Red goat anti–mouse IgG to label surface-bound anti-ICAM/NCs. Merged micrographs were analyzed automatically to determine the percentage of anti-ICAM/NCs internalized by the cells with respect to the total number of nanocarriers associated to these.[23]

To follow intracellular trafficking of anti-ICAM/NCs, ECs were incubated for 1 hour at 37°C with Texas Red dextran to label lysosomes,[13] washed, and incubated with a first and a second dose of anti-ICAM/NCs as described above for uptake studies. At varying periods of time after internalization, the cells were fixed and the colocalization of anti-ICAM/NCs within dextran-labeled compartments was determined. The results were confirmed by labeling lysosomes with phycoerythrin-conjugated rabbit anti–human LAMP-1.

Effects of internalized nanocarriers on endocytic trafficking and cell viability

To evaluate the effect of nanocarriers on the uptake of Texas Red dextran, HUVECs were untreated or pretreated with FITC anti-ICAM/NCs and then incubated with the fluid phase marker for 15 minutes at 37°C, washed, and fixed. To identify the endocytic pathways employed by HUVECs in this study, the cells were treated with inhibitors of clathrin-coated pits (monodansyl cadaverine [MDC]), caveoli (filipin), or macropinocytosis (amiloride), as previously described.[23]

The number of dextran-labeled vesicles and the percentage of these that trafficked to lysosomal compartments preloaded with nanocarriers were determined from fluorescent micrographs. Trafficking of Texas Red dextran to FITC-labeled anti–LAMP-1–positive compartments by unloaded cells was used as a control. Also, HUVECs were incubated for 48 hours after internalization of anti-ICAM/NCs, then cells were stained using the Live/Dead kit described in "Antioxidant protection of anti-ICAM/NC/catalase" to determine the fraction of cells retaining intracellular nanocarriers, morphological appearance of the cell monolayer, total number of cells per sample, and cell viability.

Antioxidant protection of anti-ICAM/NC/catalase

HUVECs were treated with a single dose or 2 sequential doses of control anti-ICAM/NCs or anti-ICAM/NC/catalase. At varying periods of time after internalization, the cells were incubated with a 5 mM H_2O_2 solution to induce oxidative injury. The cells were then washed, incubated with 0.1 μM calcein AM and 1 μM ethidium (Live/Dead kit, Molecular Probes) and finally scored as percentage of surviving cells (calcein positive/ethidium negative).[13]

Recurrent targeting to pulmonary vasculature in mice

A single dose of ^{125}I-labeled anti-ICAM/NCs or control ^{125}I-IgG/NCs was injected intravenously to anesthetized C57BL/6 mice, and lungs were collected 30 minutes after injection to determine the uptake (percent of injected dose ID per gram of lung).[12] In the next series, ^{125}I-labeled anti-ICAM/NCs (second dose) were injected either 15 minutes, 30 minutes, or 150 minutes after injection of nonlabeled anti-ICAM/NCs or nonlabeled IgG/NCs (first dose). A second dose of ^{125}I-labeled IgG/NCs was injected into a separate group to control for mechanical retention of second-dose nanocarriers in the pulmonary vasculature.

Statistics

Unless otherwise stated, the data were calculated as the mean ± standard deviation, where statistical significance was determined by Student *t* test.

Results

Recycling of internalized ICAM-1 by endothelial cells

Binding of anti-ICAM/NCs (hereafter referred to as "nanocarriers") to ICAM-1 on the surface of activated HUVECs at 4°C partially inhibited the subsequent binding of ^{125}I–anti-ICAM (Figure 1A). Warming ECs to 37°C caused nanocarriers to be rapidly internalized, which reached a maximum level at 30 minutes (Figure 1B). Anti-ICAM/NCs also bound to quiescent ECs, although at a lower extent than to TNF-α–activated cells (3.9 ± 1.4-fold less) due to lower ICAM-1 expression. Given lower nanocarrier binding, the absolute amount of nanocarriers internalized by resting HUVECs also was lower than in activated cells. However, the rate and relative extent of nanocarrier internalization was comparable for quiescent and TNF-α–activated cells (82.1% ± 4.1% vs 82.8% ± 2.0% [30 minutes], 92.9% ± 3.6% vs 89.5% ± 1.7% [1 hour], and 90.1% ± 5.5% vs 97.9% ± 0.6% [3 hours]).

Probing with ^{125}I-anti-ICAM revealed a rapid disappearance of ICAM-1 from the EC surface, coinciding with the internalization of anti-ICAM/NCs at 37°C (Figure 1B). However, in contrast with the plateau value of 20% to 25% blockage for ^{125}I–anti-ICAM by anti-ICAM/NCs at 4°C, CAM-mediated endocytosis was followed by a rapid reappearance of ICAM-1 on the endothelial surface (Figure 1B). In this experiment, cells were pretreated with cyclohexamide to inhibit protein synthesis and rule out the appearance of newly synthesized ICAM-1. The reappearance of ICAM-1 on the cell surface implies that approximately 50% of internalized ICAM-1 recycled to the plasma membrane in a relatively intact form, within less than one hour after anti-ICAM/NC uptake.

We examined the intracellular itinerary of FITC-labeled anti-ICAM/NCs and the target ICAM-1 using monoclonal antibodies to its cytosolic domain, which is not blocked by nanocarriers. Multilabel fluorescence microscopy revealed that ICAM-1 rapidly clustered in the vicinity of nanocarriers bound to the cell surface, where the white "ICAM-1" color in Figure 2A shows its colocalization with surface-bound nanocarriers. Texas Red dextran did not bind directly to anti-ICAM/NCs, since it did not label surface-bound nanocarriers. However, as a fluid phase marker, Texas Red dextran entered cells concomitantly to nanocarrier internalization (Figure 2A). Both ICAM-1 and Texas Red dextran colocalized with nanocarriers in nascent vesicles negative for EEA-1 and LAMP-1 (Figure 2A). However, 1 hour after internalization, when practically all nanocarriers reside in EEA-1–positive endosomal compartments, about 50% of the dextran-labeled vesicles and 40% of ICAM-1–positive vesicles did not colocalize with the nanocarriers (Figure 2B,D), likely representing the fraction of vesicles containing ICAM-1 that will recycle to the plasma membrane. At 3 hours after internalization, nanocarriers reside almost exclusively in lysosomes that are partially positive for the ICAM-1 cytosolic domain and contain the fluid phase tracer; hence, a fraction of the target ICAM-1 antigen cannot escape lysosomal traffic driven by the nanocarriers.

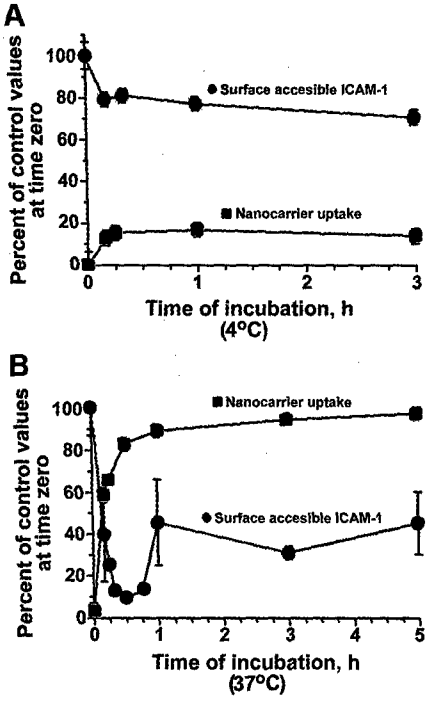

Figure 1. ICAM-1 reappears on HUVEC surface after internalization of anti-ICAM nanocarriers. Kinetics of FITC-labeled anti-ICAM/NC internalization (uptake, squares) and accessibility of ICAM-1 on EC surface to ^{125}I-labeled anti-ICAM (circles) were evaluated in cyclohexamide-treated HUVECs at 4°C (A) or at 37°C (B). Cells were activated with TNF-α in all experiments shown in the figures. Data represent M ± SEM for n = 9 wells from 3 independent experiments.

Recurrent targeting of anti-ICAM nanocarriers to endothelium in vitro and in vivo

In theory, the reappearance of ICAM-1 on the endothelial surface could be used for sustained or recurrent intracellular delivery of nanocarriers, thus, exceeding initial saturating dose and duration of a drug effect. To test this possibility, we treated cells with 2 subsequent doses of nanocarriers, imitating recurrent injections. Indeed, binding of second-dose anti-ICAM/NCs to TNF-α–activated cells was reduced by 50% when applied 30 minutes after internalization of the first dose, but recovered to the control level when applied 3 hours after the first dose (Figure 3A). Also, the amount of internalized second-dose anti-ICAM/NCs decreased 30 minutes after the first dose, but recovered to the control value by 3 hours, both in the case of TNF-α–activated HUVECs (Figure 3A) and quiescent cells (68.2% ± 3.9% and 101.2% ± 4.2% of the control value 30 minutes and 3 hours after the first dose, respectively). Furthermore, in the case of quiescent cells, the binding capacity of anti-ICAM/NCs even increased to 134.2% ± 12.5% of the control level 3 hours after the first dose. Perhaps because of maximal surface expression of ICAM-1 already induced by cytokine treatment, this "overshoot" effect was not seen in TNF-α–activated cells. Anti-ICAM/NC internalization kinetics, which were significantly decreased when the second dose was added 30 minutes following the first dose, recovered to a markedly more rapid rate of internalization when the second dose was applied 3 hours after the initial dose (Figure 3B).

We tested EC targeting in vivo by a single versus repetitive dose of intravenously injected ^{125}I-labeled anti-ICAM/NCs, which bind to pulmonary ECs and preferentially accumulate in the pulmonary vasculature.[11,12,30,31] We observed a highly specific pulmonary uptake of anti-ICAM/NCs after intravenous injection in mice, 137% ± 10.7% versus 12.9% ± 4% ID/g of control IgG/NC counterpart (Figure 3C). Similar to the increased targeting of anti-ICAM/NCs to cytokine-activated HUVECs in culture, the pulmonary uptake of anti-ICAM/NCs was further increased in mice pre-injected with lipopolysaccharide prior to nanocarriers (173.6% ± 21% of the value obtained in control mice). Also, in agreement with cell culture data, pulmonary targeting of ^{125}I-labeled anti-ICAM/NCs injected 15 minutes after nonlabeled anti-ICAM/NCs was markedly inhibited (55.6% ± 7.8% of control

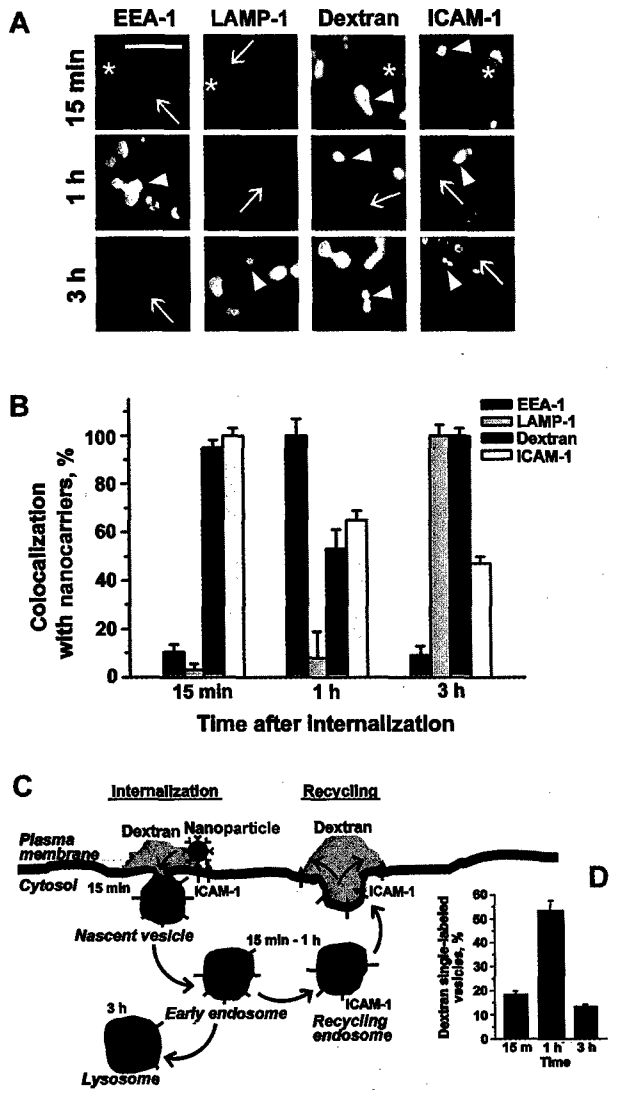

Figure 2. Dissociation of ICAM-1 from internalized anti-ICAM nanocarriers. (A) Fluorescence microscopy of green FITC-labeled anti-ICAM/NCs in HUVECs at indicated time at 37°C. In 4 columns, red labeling depicts markers of early endosomes (anti–EEA-1), lysosomes (anti–LAMP-1), Texas Red dextran, or ICAM-1 cytosolic domain. Yellow color, vesicles in which anti-ICAM/NC particles colocalize with indicated markers (arrowhead); green color, anti-ICAM/NC–containing vesicles negative for indicated markers (arrow); red color, anti-ICAM/NC–free vesicles positive for indicated markers; blue color, noninternalized anti-ICAM/NCs (asterisk); white color, sites of ICAM-1 clustering by anti-ICAM/NC at the cell surface. Bar = 1 μm. (B) Percentage of localization of the markers (EEA-1, LAMP-1, Texas Red [TR] dextran, or cytosolic ICAM-1) to anti-ICAM/NC–containing vesicles, quantified by image analysis and plotted as a function of the time after anti-ICAM/NC internalization. (C) Schema of ICAM-1 recycling. ICAM-1 enters ECs via nascent vesicles along with anti-ICAM/NCs. Anti-ICAM/NCs traffic to lysosomes via early endosomes, whereas ICAM-1 partially escapes lysosomal pathway and recycles to the plasma membrane. The fluid phase TR dextran labels both the lysosomal and the recycling route. (D) Single-labeled dextran-containing vesicles, diverging from anti-ICAM/NC–containing vesicles, can be detected 1 hour after internalization and disappear by 3 hours, likely due to release from recycling compartments. Data in panels B and D are shown as M ± SD for n > 10 cells from 2 independent experiments.

level), yet gradually recovered (84.5% ± 10% and 128.2% ± 10% of control level) when administered 30 minutes and 150 minutes after injection of the first dose, respectively. In contrast, the level of pulmonary accumulation of ^{125}I-anti-ICAM/NCs did not differ from control values when animals had received a first dose of nonspecific IgG/NCs regardless of the time interval between the nanocarrier injection (Figure 3C). Pulmonary targeting of second-dose of anti-ICAM/NCs was not due to mechanical uptake or other nonspecific effects, since second doses of control IgG/NCs did not accumulate in lungs after the administration of nonlabeled anti-ICAM/NCs (Figure 3C).

The second dose of anti-ICAM nanocarriers persists in a prelysosomal compartment

Nanocarriers internalized at 2 subsequent doses trafficked as 2 separate pools within the cell, and only a minor fraction (24.9% ± 13.2%) colocalized 3 hours after internalization of the second dose, regardless of the time interval between the first and second doses (not shown). The second dose, applied either 30 minutes or 1 hour after the first one, did not affect delivery of the first dose to lysosomes, which occurred between 2 and 3 hours after internalization (Figure 4A). However, lysosomal trafficking of the second-dose nanocarriers was markedly decreased: 3 hours after internalization, only 21.4% ± 14.4% of the second-dose nanocarriers could be detected in lysosomes versus 70.7% ± 7% of the

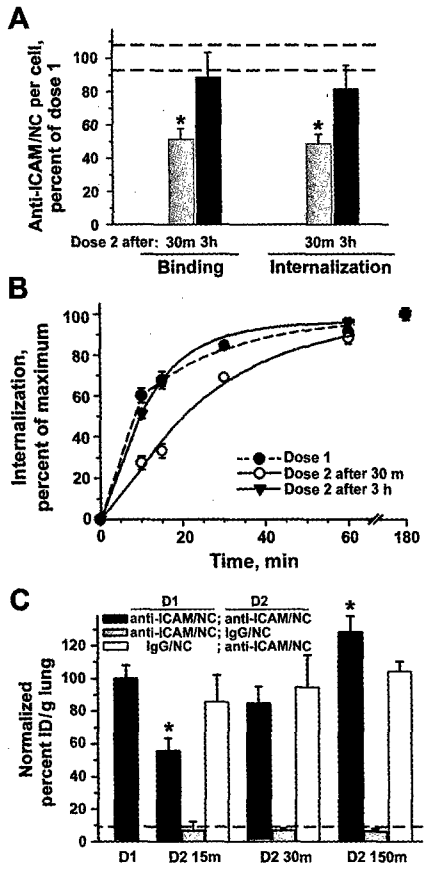

Figure 3. Recurrent targeting of anti-ICAM nanocarriers to endothelium in vitro and in vivo. (A) Sequential targeting of 2 doses of anti-ICAM/NCs into TNF-α–activated HUVECs. The number of surface-bound and internalized anti-ICAM/NCs in the first dose is taken as 100% (dashed lines represent the standard deviation of this control value). Binding and internalization of the second dose anti-ICAM/NCs were inhibited at 30 minutes after the internalization of the first dose, yet recovered to 100% by 3 hours. (B) Internalization kinetics for the first dose and second dose at 30 minutes versus 3 hours, determined as percent of internalized nanocarriers. Data are means ± SEM for n > 20 cells from 2 independent experiments. (C) Control mice received a single injection intravenously of either ^{125}I-labeled anti-ICAM/NCs (first dose, D1) or IgG/NCs (dashed line) to test targeting to the lungs. In other groups, mice were injected with nonlabeled anti-ICAM/NCs followed by a similar dose of ^{125}I-labeled anti-ICAM/NCs (black bars) or ^{125}I-IgG/NCs (gray bars) either 15, 30, or 150 minutes later (second dose, D2). In a separate group, mice were injected with a first dose of nonlabeled IgG/NCs and a second dose of ^{125}I-labeled anti-ICAM/NCs (white bars). Lung uptake was calculated as percent of injected dose per gram and plotted as percent of the level obtained with a single dose of anti-ICAM/NCs (D1) as M ± SEM, n = 4-5.

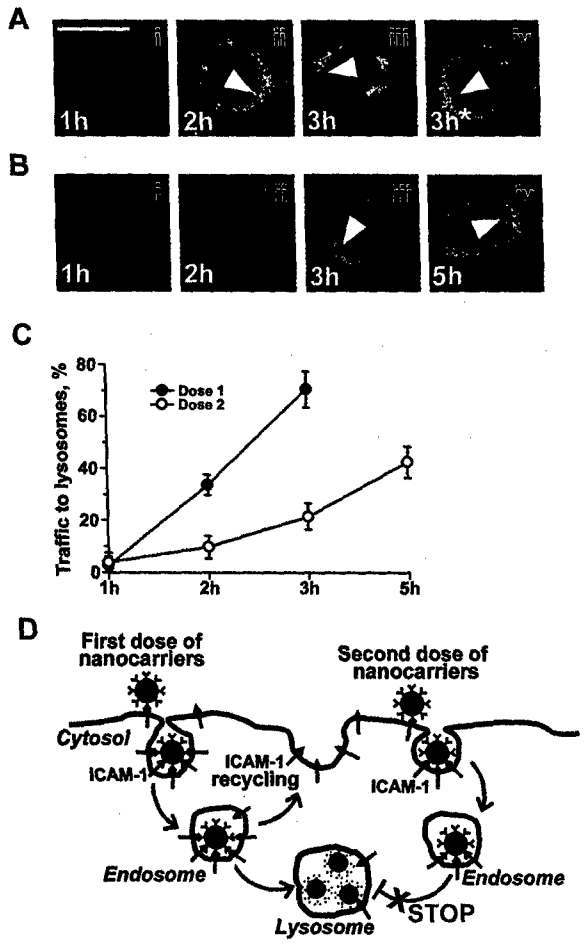

Figure 4. Decelerated intracellular traffic of second dose of anti-ICAM nanocarriers. Cells prelabeled with Texas Red dextran were incubated with FITC-labeled anti-ICAM/NCs (A) or nonlabeled anti-ICAM/NCs (B) for 1 hour at 4°C, warmed to 37°C after washing of nonbound materials, incubated for indicated time at 37°C, and counterstained with secondary labeled antibodies, which would stain surface-bound nanocarriers in blue. The first dose was followed by the same dose of FITC-labeled anti-ICAM/NCs at the indicated time (B). The absence of blue staining in panels A and B indicates that both first and second doses are internalized. Yellow color shows colocalization (arrowhead) of anti-ICAM/NCs with red-labeled lysosomes. Bar = 10 μm. (C) Anti-ICAM/NC colocalization with lysosomes is plotted as a function of time after internalization of the corresponding dose. Data are M ± SEM for n > 10 cells from 2 independent experiments. (D) Schema of recurrent intracellular traffic and deceleration of lysosomal delivery of the second dose of anti-ICAM/NCs.

first-dose nanocarriers (Figure 4B-C). Thus, loading of lysosomes by nanocarriers inhibits lysosomal delivery of the second dose (Figure 4D).

To test whether anti-ICAM/NCs affect constitutive endocytosis and lysosomal traffic, we used fluorescent dextran as a fluid phase marker. HUVECs treated with either single or double combinations of pharmacological inhibitors of internalization via clathrin-coated pits (MDC), caveoli (filipin), or macropinocytosis (amiloride) were still able to internalize dextran (Figure 5A). The fact that dextran uptake could only be inhibited by simultaneous treatment with drugs affecting all 3 pathways confirms that it enters ECs through all these classical endocytic mechanisms. Furthermore, dextran was similarly internalized and delivered to lysosomes by control cells and cells that had internalized a saturating dose of anti-ICAM/NCs (Figure 5B-C). Therefore, anti-ICAM/NC internalization via CAM-mediated endocytosis does not affect other endocytic pathways in ECs.

Furthermore, anti-ICAM/NCs still resided in intracellular vesicular compartments 48 hours after uptake by HUVECs (Figure 6A); 97% ± 12% of the cells still contained nanocarriers at this time (Figure 6B). Neither cell number nor morphology of the endothelial monolayer nor cellular viability was affected by the prolonged intracellular retention of nanocarriers (Figure 6B-C). Interestingly, an almost equal share of intracellular nanocarriers could be identified in dividing endothelial cells (Figure 6A, insert).

Delivery of 2 sequential doses of anti-ICAM/NC/catalase provides sustained protection against oxidant stress

To evaluate the potential therapeutic implications of our findings, we employed anti-ICAM/NC/catalase in a model of H_2O_2-induced oxidative injury in HUVECs, as previously described.[13] Cells were transiently protected against H_2O_2 injury by anti-ICAM/NC/catalase, but protection was markedly diminished after 2 hours (Figure 7). However, if a second dose of anti-ICAM/NC/catalase was delivered by this time, the cells were protected from oxidative injury for at least 6 more hours; hence continuous protection by 2

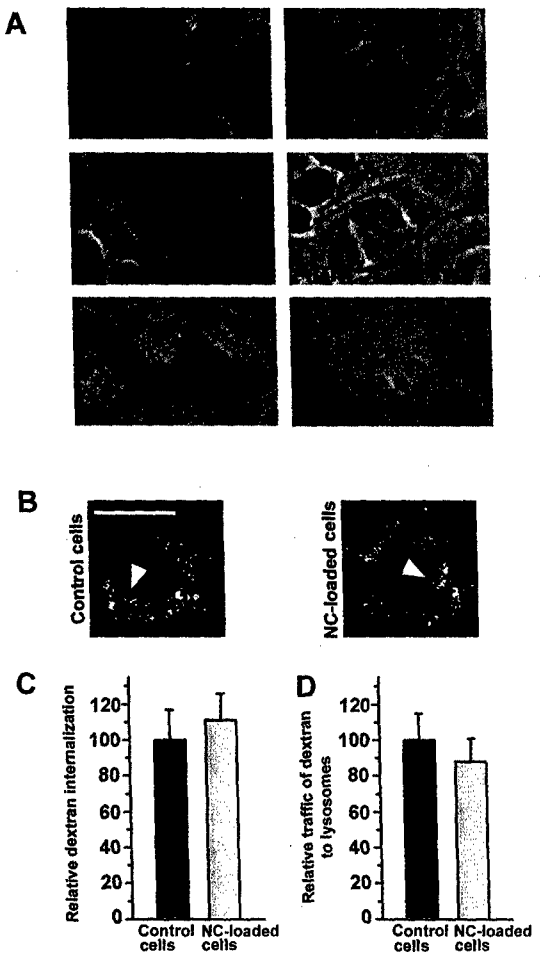

Figure 5. Loading cells with anti-ICAM nanocarriers does not affect endocytosis and trafficking of dextran. (A) Internalization of a fluid phase marker, fluorescent Texas Red dextran, by either control HUVECs or cells treated with pharmacological inhibitors of internalization by clathrin-coated pits (MDC), caveoli (Filipin = Fil), or macropinocytosis (Amiloride = Amil). Note that TR dextran enters cells via diverse endocytic pathways. (B) HUVECs, either control or preloaded with a saturating dose anti-ICAM/NCs, were incubated with TR dextran and traffic to lysosomes was tested. Yellow color (arrowhead): colocalization of TR dextran with lysosomes labeled in green by FITC–anti–LAMP-1 (control cells) or FITC–anti-ICAM/NCs (particle-loaded cells). Bar = 10 μm. (C) The number of TR dextran-labeled endocytic vesicles per cell and (D) percent of these localizing to lysosomal compartments was determined by fluorescence microscopy. Data are M ± SEM from n > 10 cells.

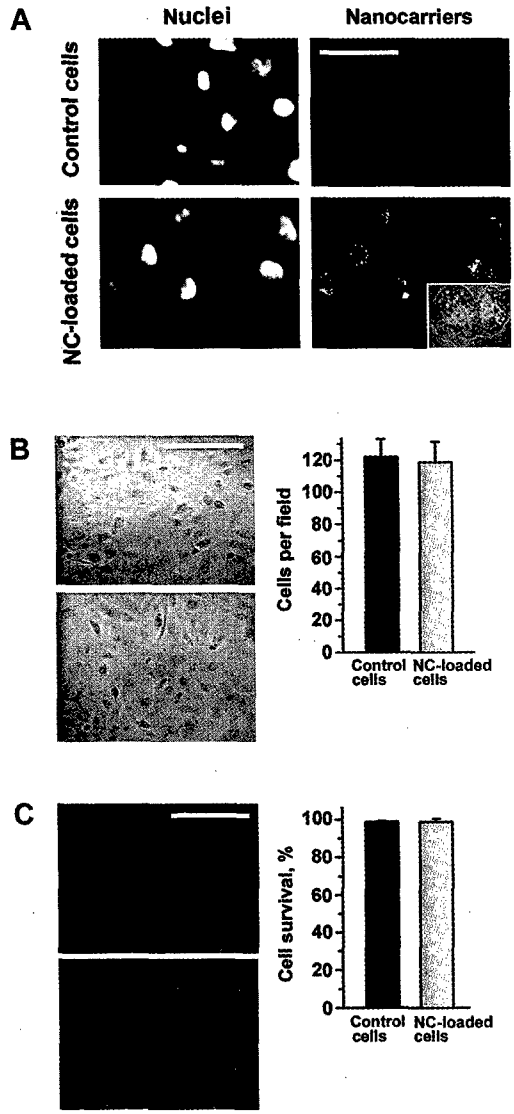

Figure 6. Anti-ICAM nanocarriers do not compromise endothelial cell viability. Both control and FITC–anti-ICAM/NC–treated HUVECs were maintained in culture for 48 hours. (A) Cells, visualized by nuclear staining with DAPI (4′6-diamidino-2-phenylindole 2HCl), retain intracellular anti-ICAM/NCs, which distribute between dividing cells (inset). Bar = 30 μm. (B) The morphology of the HUVEC monolayer and cell number is not affected by anti-ICAM/NC retention in cells. Magnification bar = 50 μm. (C) Intracellular anti-ICAM/NCs do not affect HUVEC survival revealed by fluorescent staining of alive (green) and dead (red) cells. Bar = 50 μm. Data are M ± SEM from at least 500 cells per condition.

sequential doses of anti-ICAM/NC/catalase lasted for at least 8 hours versus 2 hours afforded by a single dose.

Protection by the second dose of anti-ICAM/NC/catalase applied after catalase-free anti-ICAM/NCs also lasted for at least 5 hours after internalization, indicating that, in good agreement with data shown in Figure 4, the synergistic character of the increased duration of protection was not simply due to delivery of twice the amount of catalase, but rather, due to the inhibited lysosomal trafficking and degradation of the second dose of anti-ICAM/NC/catalase.

Discussion

We found that ICAM-1 trafficking in ECs has 2 key features that increase the efficacy of recurrent drug targeting using anti-ICAM/NCs. First, after mediating internalization of nanocarriers, ICAM-1 recycles to the cell surface, indicating that a single ICAM-1 molecule can participate in multiple rounds of nanocarrier binding and internalization. Second, the capacity of lysosomal trafficking of anti-ICAM/NCs in ECs is limited, for example, delivery of a second dose of nanocarriers to lysosomes is markedly inhibited. These new aspects of the recently described CAM-mediated endocytic pathway[23] further enhance its potential use for drug targeting into ECs.

Most studies of uptake and trafficking in ECs have been focused on known receptors for endocytosis and transcytosis, for example, transferrin receptor and albondin endocytosed via clathrin-coated pits and caveoli, respectively.[32-34] Surface cell adhesion molecules are less characterized in this context, since their initially identified natural ligands (white blood cells) appear too large to be internalized by ECs.[28,35] However, recent work has examined the internalization and trafficking of an inducible cell adhesion molecule, E-selectin, which has been suggested to be a potential receptor for endothelial drug targeting strategies since it is internalized by clathrin-mediated endocytosis.[36-38]

ICAM-1 belongs to a different family of EC adhesion molecules, Ig-superfamily CAM. Neither ICAM-1 nor another member of this superfamily, PECAM-1, is constitutively internalized or significantly internalize monomolecular ligands.[12,28,39] However, binding of multimeric ICAM-1 or PECAM-1 ligands (eg, anti-ICAM or anti-PECAM nanocarriers) induces internalization by ECs via a mechanism that differs from all previously described endocytic pathways and requires CAM cross-linking (CAM-mediated endocytosis[23]). Thus, CAM-endocytosis may represent a specific case of activating EC signaling by multivalent ICAM-1 ligands (Hubbard and Rothlein[40]). In contrast, pre-activation of ECs (eg, by TNF-α) is not required to induce CAM-mediated endocytosis.[23] In fact, we found that internalization induced by anti-ICAM/NCs occurs with a similar kinetics by both activated and quiescent ECs.

At 37°C, ICAM-1 rapidly disappears from the plasma membrane concomitantly to anti-ICAM/NC internalization. The extent of ICAM-1 disappearance (~ 90%) in this process exceeds the extent of ICAM-1 blocking by anti-ICAM/NCs at 4°C in the absence of internalization (~ 20%). One possibility is that ICAM-1 is clustered by anti-ICAM/NCs at 37°C (Figure 2C), similar to the "zipperlike" mechanism observed when phagocytic receptors are

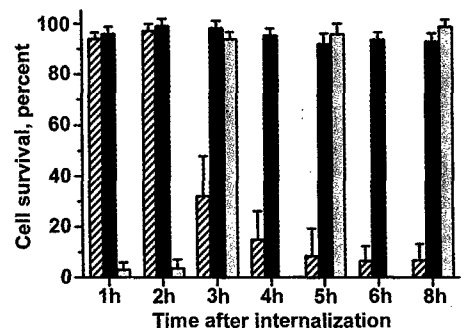

Figure 7. Recurrent catalase targeting by anti-ICAM nanocarriers provides prolonged antioxidant protection of EC. HUVECs were treated with first-dose "empty" anti-ICAM/NCs (gray bars) or anti-ICAM/NC/catalase (hatched and black bars) and 170 minutes later with a second-dose anti-ICAM/NC/catalase (black and gray bars). As determined by a cell viability assay, the first-dose anti-ICAM/NC/catalase protected cells from H_2O_2-induced injury for 2 hours, while double-dose treated cells remained protected for at least 8 hours. Data were quantified by fluorescence microscopy from at least 500 cells per condition and represent M ± SD as percent of cell survival.

clustered by particulate ligands.[41] A quantitative analysis correlating anti-ICAM/NC concentration and surface density of anti-ICAM on nanocarriers to ICAM-1 internalization remains to be determined. However, a rough estimation of these parameters under the conditions used in this study (~ 300 anti-ICAM molecules per particle × 2 ICAM-1 molecules engaged per antibody × ~ 2×10^7 particles/well = 1.2×10^{10} anti-ICAM molecules/well[28,42]) implies that anti-ICAM/NCs have the theoretical capacity to cluster most of ICAM-1 molecules expressed on the EC surface (~ 10^5 cells/well × ~ $1\text{-}2 \times 10^5$ ICAM-1 molecules/cell = $1\text{-}2 \times 10^{10}$ ICAM-1 molecules/well[17]). Noteworthy, a significant reduction (~ 20%) of anti-ICAM/NC binding also was observed in HUVECs pretreated with anti-PECAM/NC, which is targeted to an unrelated ligand (S.M., M.K., V.M. unpublished data, June, 2004), implying that a fraction of ICAM-1 not engaged by its ligands may be passively internalized from the plasmalemma into the numerous induced endocytic vesicles. Free ICAM-1, associated directly or via adaptor or cytoskeleton molecules with ICAM-1 engaged by anti-ICAM/NCs, also may be involved in nanocarrier-masked membrane domains and endocytic vesicles. These factors may account for the massive disappearance of ICAM-1 from the EC surface concomitant to anti-ICAM/NC internalization at 37°C.

The notion that multivalent ligands induce CAM-mediated endocytosis and trafficking is of interest in the context of vascular pathophysiology, since ICAM-1 mediates internalization of multivalent pathogens (Hopkins et al[43]), including HIV,[44] rhinoviruses, poliovirus,[45,46] and plasmodium-infected erythrocytes.[47] ICAM-1 and VCAM-1 clustering induced by cells too large to be internalized also helps promote endothelial cell signaling and actin remodeling in response to leukocyte adhesion and transmigration.[35,48]

We provide the first evidence that internalized ICAM-1 has the capacity to be recycled to the plasma membrane in ECs. Recently, it has been shown that there is a PECAM-1 pool that recycles from an endothelial submembrane storage compartment to the plasma membrane to support leukocyte transmigration at the cell borders.[49] However, this PECAM-1 storage compartment is accessible to small tracer molecules in the extracellular milieu, which suggests that it is distinct from a bona fide endocytic compartment, as opposed to internalized ICAM-1 that moves via endocytic vesicles. Recycling of internalized ICAM-1 might be more analogous to the recycling pathway taken by endocytosed receptors, such as transferrin receptor.[50] However, transferrin receptor recycling is rapid (eg, 5-15 minutes),[51] while the kinetics for recycling of ICAM-1 internalized by multivalent nanocarriers (1 hour) is more comparable to the slower recycling kinetics for multivalent, cross-linked transferrin.[52] Recruitment of ICAM-1 from the secretory pathway seems unlikely, since ICAM-1 reappeared at the plasma membrane in the absence of new protein synthesis. Also, to date, EC secretory vesicles containing ICAM-1 have not been described, as opposed to vesicles such as Weibel-Palade bodies, which mediate stimulated secretion of other cell adhesion molecules, P-selectin, within 2 minutes.[53]

ICAM-1 recycling provides a pathway for recurrent drug targeting, for example, continuous or subsequent doses of nanocarriers can be efficiently delivered to the same cell. ECs in the lung vessels represent a privileged vascular target, because lungs (1) contain approximately 30% of total endothelial surface in the body; (2) represent the first pass extended vascular bed after intravenous injections; (3) receive 100% cardiac venous blood output at each systole; and, (4) experience a relatively slow perfusion rate via high-capacity, low-resistance vascular bed, which favors binding of EC ligands. These factors explain why anti-ICAM/NCs, as well as other carriers directed against pan-endothelial surface determinants, accumulate preferentially in the pulmonary vasculature after intravenous injections in animals and humans.[16] We employed anti-ICAM pulmonary targeting to verify our findings in vivo.

Rapid and effective restoration of the pulmonary uptake of a second dose of anti-ICAM/NCs injected into mice (Figure 3C) strongly supports physiological and potential therapeutic significance of cell culture findings (Figures 1-2 and 3A-B). It appears that nanocarriers provide an important advantage in targeting, since amplitude of the targeting exceeds that of anti-ICAM itself by an order of magnitude (> 30 vs < 5% ID in lungs, Murciano et al[12]). Reappearance of ICAM-1 on the luminal surface of pulmonary ECs in mice occurs relatively quickly, which would argue against the reappearance of ICAM-1 due to de novo synthesis, as this is expected to require a lag of 2 to 4 hours.[54] Interestingly, we observed that at later time points (eg, 150 minutes after the first administration of nanocarriers), pulmonary uptake of second-dose anti-ICAM/NCs overshoots the basal level of uptake (Figure 3C). The nature of this enhancement remains to be determined. The absence of this effect in animals injected with a first dose of control IgG/NCs rules out the possibility that ICAM-1 expression is up-regulated as a consequence of a systemic release of cytokines in response to FcR-mediated uptake of IgG/NCs and activation of reticulo endothelial system (RES) macrophages. It is possible, however, that ICAM-1 engagement by first-dose anti-ICAM/NCs results in a positive feedback loop, leading to up-regulation of ICAM-1 expression.[40] This hypothesis would agree with the finding that there was enhanced binding of anti-ICAM/NCs applied 3 hours after the first dose in quiescent cells in culture. However, a comparable overshoot was not observed in TNF-α–activated cells, most likely due to the maximal level of ICAM-1 expression by these cells. Also, lack of pulmonary uptake of IgG/NCs injected after anti-ICAM/NC counterpart suggests that anti-ICAM/NCs rapidly disappear from the lumen and rules out the possibility that lung uptake of the second dose is merely due to vessel occlusion and mechanical entrapment.

In addition to opportunities of sustained or recurrent targeting provided by ICAM-1 recycling, lysosomal trafficking of internalized nanocarriers was retarded due to loading of the first dose (Figure 5). Under normal conditions, lysosomes freely intermix and exchange contents.[55] However, accumulation of nondegradable material in lysosomes (eg, the latex nanocarriers in this study) can inhibit the delivery of subsequent doses of nanocarriers to these compartments and, as a secondary consequence, decelerate degradation of the nanocarrier protein cargo. A similar effect has been previously observed in macrophage lysosomes and has been largely considered to be a pathological condition that diminishes macrophage defensive function and is related to lysosomal storage diseases.[56] Nevertheless, we have found that macromolecules (eg, 10 000 MW dextran) that enter ECs by classical endocytic mechanisms can still traffic to lysosomes containing nondegraded nanocarriers (Figure 5). The difference in trafficking of fluid phase markers versus multimeric anti-ICAM/NCs may reflect that multimeric ligands traffic more slowly to lysosomal compartments. This is the case for oligomerized transferrin, which is retained in an early endocytic compartment resistant to degradation.[52] However, the slow degradation of a second dose of anti-ICAM/NCs, due to delayed lysosomal trafficking, had a therapeutic benefit since it had the capacity to prolong the efficacy of catalase nanocarriers for protection against oxidative injury from 2 hours to at least 8 hours (Figure 7), providing an alternative to pharmacological means that block lysosomal traffic and degradation of anti-ICAM/NCs.[13]

The goal of prolonging the therapeutic effects of drugs delivered to target cells (eg, endothelial cells) is critical. Gene therapy strategies that, in theory, can afford prolonged therapeutic interventions are risky and cannot afford an immediate effect that is desirable in acute settings, such as oxidant stress in acute lung injury, ischemia reperfusion, or organ transplantation. On the other hand, the duration of the effect for the short time period afforded by a single bolus of nanocarriers targeted to ICAM-1 or PECAM-1 may be insufficient for successful containment of the stress.

Multiple injections of anti-ICAM/NCs, as with any repetitive protein therapy (eg, enzyme replacement therapies), require a rigorous safety study to avoid potential immune responses. It is unlikely, however, that injection of the second and perhaps even third dose within a 5- to 50-hour time period would elicit more severe immune reactions than a single injection (in most cases, such immunization requires a second boost by the sixth or seventh day). Use of "stealth" nanocarriers coated with polyethylene glycol, which provides prolonged circulation and reduced immune recognition, may offer even safer interventions.[57-60] In theory, a long-circulating pool of stealth anti-ICAM/NCs could serve as a source of sustained intake by ECs via recycling ICAM-1, providing prolonged therapeutic effects.

Acknowledgments

The authors express their deep gratitude to Ms Tanya Krasik and Mr John Leferovich for invaluable help in animal experiments.

References

1. Springer TA. Traffic signals for lymphocyte recirculation and leukocyte emigration: the multistep paradigm. Cell. 1994;76:301-314.
2. Almenar-Queralt A, Duperray A, Miles LA, Felez J, Altieri DC. Apical topography and modulation of ICAM-1 expression on activated endothelium. Am J Pathol. 1995;147:1278-1288.
3. Diamond MS, Staunton DE, Marlin SD, Springer TA. Binding of the integrin Mac-1 (CD11b/CD18) to the third immunoglobulin-like domain of ICAM-1 (CD54) and its regulation by glycosylation. Cell. 1991;65:961-971.
4. Diamond MS, Staunton DE, de Fougerolles AR, et al. ICAM-1 (CD54): a counter-receptor for Mac-1 (CD11b/CD18). J Cell Biol. 1990;111: 3129-3139.
5. Dustin ML, Rothlein R, Bhan AK, Dinarello CA, Springer TA. Induction by IL 1 and interferon-gamma: tissue distribution, biochemistry, and function of a natural adherence molecule (ICAM-1). J Immunol. 1986;137:245-254.
6. Kumasaka T, Quinlan WM, Doyle NA, et al. Role of the intercellular adhesion molecule-1 (ICAM-1) in endotoxin-induced pneumonia evaluated using ICAM-1 antisense oligonucleotides, anti-ICAM-1 monoclonal antibodies, and ICAM-1 mutant mice. J Clin Invest. 1996;97:2362-2369.
7. Panes J, Perry MA, Anderson DC, et al. Regional differences in constitutive and induced ICAM-1 expression in vivo. Am J Physiol. 1995;269: H1955-H1964.
8. Mastrobattista E, Storm G, van Bloois L, et al. Cellular uptake of liposomes targeted to intercellular adhesion molecule-1 (ICAM-1) on bronchial epithelial cells. Biochim Biophys Acta. 1999;1419: 353-363.
9. Bloemen PG, Henricks PA, van Bloois L, et al. Adhesion molecules: a new target for immunoliposome-mediated drug delivery. FEBS Lett. 1995;357:140-144.
10. Villanueva FS, Jankowski RJ, Klibanov S, et al. Microbubbles targeted to intercellular adhesion molecule-1 bind to activated coronary artery endothelial cells. Circulation. 1998;98:1-5.
11. Atochina EN, Balyasnikova IV, Danilov SM, Granger DN, Fisher AB, Muzykantov VR. Immunotargeting of catalase to ACE or ICAM-1 protects perfused rat lungs against oxidative stress. Am J Physiol. 1998;275:L806-L817.
12. Murciano JC, Muro S, Koniaris L, et al. ICAM-directed vascular immunotargeting of antithrombotic agents to the endothelial luminal surface. Blood. 2003;101:3977-3984.
13. Muro S, Cui X, Gajewski C, Murciano JC, Muzykantov VR, Koval M. Slow intracellular trafficking of catalase nanoparticles targeted to ICAM-1 protects endothelial cells from oxidative stress. Am J Physiol Cell Physiol. 2003;285:C1339-C1347.
14. Broide DH, Sullivan S, Gifford T, Sriramarao P. Inhibition of pulmonary eosinophilia in P-selectin- and ICAM-1–deficient mice. Am J Respir Cell Mol Biol. 1998;18:218-225.
15. DeMeester SR, Molinari MA, Shiraishi T, et al. Attenuation of rat lung isograft reperfusion injury with a combination of anti-ICAM-1 and anti-beta2 integrin monoclonal antibodies. Transplantation. 1996;62:1477-1485.
16. Muzykantov V. Targeting pulmonary endothelium. In: Biomedical Aspects of Drug Targeting. Muzykantov V and Torchilin V, eds. Boston-Dodrecht-London: Kluwer Academic Publishers; 2003:129-148.
17. Muro S, Koval M, Muzykantov V. Endothelial endocytic pathways: gates for vascular drug delivery. Current Vasc Pharm. 2004;2:281-299.
18. Muzykantov VR. Delivery of antioxidant enzyme proteins to the lung. Antioxid Redox Signal. 2001; 3:39-62.
19. Muzykantov VR. Targeting of superoxide dismutase and catalase to vascular endothelium. J Control Release. 2001;71:1-21.
20. Fisher AB, Al-Mehdi AB, Muzykantov V. Activation of endothelial NADPH oxidase as the source of a reactive oxygen species in lung ischemia. Chest. 1999;116:25S-26S.
21. Robledo O, Papaioannou A, Ochietti B, et al. ICAM-1 isoforms: specific activity and sensitivity to cleavage by leukocyte elastase and cathepsin G. Eur J Immunol. 2003;33:1351-1360.
22. Melis M, Pace E, Siena L, et al. Biologically active intercellular adhesion molecule-1 is shed as dimers by a regulated mechanism in the inflamed pleural space. Am J Respir Crit Care Med. 2003; 167:1131-1138.
23. Muro S, Wiewrodt R, Thomas A, et al. A novel endocytic pathway induced by clustering endothelial ICAM-1 or PECAM-1. J Cell Sci. 2003;116: 1599-1609.
24. Kozower BD, Christofidou-Solomidou M, Sweitzer TD, et al. Immunotargeting of catalase to the pulmonary endothelium alleviates oxidative stress and reduces acute lung transplantation injury. Nat Biotechnol. 2003;21:392-398.
25. Christofidou-Solomidou M, Scherpereel A, Wiewrodt R, et al. PECAM-directed delivery of catalase to endothelium protects against pulmonary vascular oxidative stress. Am J Physiol Lung Cell Mol Physiol. 2003;285:L283-L292.
26. Marlin SD, Springer TA. Purified intercellular adhesion molecule-1 (ICAM-1) is a ligand for lymphocyte function-associated antigen 1 (LFA-1). Cell. 1987;51:813-819.
27. Jevnikar AM, Wuthrich RP, Takei F, et al. Differing regulation and function of ICAM-1 and class II antigens on renal tubular cells. Kidney Int. 1990; 38:417-425.
28. Wiewrodt R, Thomas AP, Cipelletti L, et al. Size-dependent intracellular immunotargeting of therapeutic cargoes into endothelial cells. Blood. 2002; 99:912-922.
29. Muro S, Muzykantov VR, Murciano J-C. Characterization of endothelial internalization and targeting of antibody-enzyme conjugates in cell cultures and in laboratory animals. In: Bioconjugation protocols: strategies and methods. Niemeyer CM, ed. Totowa, NJ: Humana Press; 2004;21-36.
30. Panes J, Perry MA, Anderson DC, et al. Portal hypertension enhances endotoxin-induced intercellular adhesion molecule 1 up-regulation in the rat. Gastroenterology. 1996;110:866-874.
31. Danilov SM, Gavrilyuk VD, Franke FE, et al. Lung uptake of antibodies to endothelial antigens: key determinants of vascular immunotargeting. Am J Physiol Lung Cell Mol Physiol. 2001;280:L1335-L1347.
32. Lee HJ, Engelhardt B, Lesley J, Bickel U, Pardridge WM. Targeting rat anti-mouse transferrin receptor monoclonal antibodies through blood-brain barrier in mouse. J Pharmacol Exp Ther. 2000;292:1048-1052.
33. Roberts RL, Fine RE, Sandra A. Receptor-mediated endocytosis of transferrin at the blood-brain barrier. J Cell Sci. 1993;104:521-532.
34. Schnitzer JE, Oh P, Pinney E, Allard J. Filipin-sensitive caveolae-mediated transport in endothelium: reduced transcytosis, scavenger endocytosis, and capillary permeability of select macromolecules. J Cell Biol. 1994;127:1217-1232.
35. Barreiro O, Yanez-Mo M, Serrador JM, et al. Dynamic interaction of VCAM-1 and ICAM-1 with moesin and ezrin in a novel endothelial docking structure for adherent leukocytes. J Cell Biol. 2002;157:1233-1245.
36. Kuijpers TW, Raleigh M, Kavanagh T, et al. Cytokine-activated endothelial cells internalize E-selectin into a lysosomal compartment of vesiculotubular shape: a tubulin-driven process. J Immunol. 1994;152:5060-5069.
37. von Asmuth EJ, Smeets EF, Ginsel LA, Onderwater JJ, Leeuwenberg JF, Buurman WA. Evidence for endocytosis of E-selectin in human endothelial cells. Eur J Immunol. 1992;22:2519-2526.
38. Everts M, Koning GA, Kok RJ, et al. In vitro cellular handling and in vivo targeting of E-selectin–directed immunoconjugates and immunoliposomes used for drug delivery to inflamed endothelium. Pharm Res. 2003;20:64-72.
39. Muzykantov VR, Christofidou-Solomidou M, Balyasnikova I, et al. Streptavidin facilitates internalization and pulmonary targeting of an anti-endothelial cell antibody (platelet-endothelial cell adhesion molecule 1): a strategy for vascular immunotargeting of drugs. Proc Natl Acad Sci U S A. 1999;96:2379-2384.
40. Hubbard AK, Rothlein R. Intercellular adhesion

molecule-1 (ICAM-1) expression and cell signaling cascades. Free Radic Biol Med. 2000;28: 1379-1386.

41. Griffin FM, Griffin JA, Leider JE, Silverstein SC. Studies on the mechanism of phagocytosis, I; requirements for circumferential attachment of particle-bound ligands to specific receptors on the macrophage plasma membrane. J Exp Med. 1975;142:1263-1282.
42. Koval M, Preiter K, Adles C, Stahl PD, Steinberg TH. Size of IgG-opsonized particles determines macrophage response during internalization. Exp Cell Res. 1998;242:265-273.
43. Hopkins AM, Baird AW, Nusrat A. ICAM-1: targeted docking for exogenous as well as endogenous ligands. Adv Drug Deliv Rev. 2004;56:763-778.
44. Liu NQ, Lossinsky AS, Popik W, et al. Human immunodeficiency virus type 1 enters brain microvascular endothelia by macropinocytosis dependent on lipid rafts and the mitogen-activated protein kinase signaling pathway. J Virol. 2002; 76:6689-6700.
45. Greve JM, Davis G, Meyer AM, et al. The major human rhinovirus receptor is ICAM-1. Cell. 1989; 56:839-847.
46. Rieder E, Gorbalenya AE, Xiao C, et al. Will the polio niche remain vacant? Dev Biol (Basel). 2001;105:111-122.
47. Berendt AR, Simmons DL, Tansey J, Newbold CI, Marsh K. Intercellular adhesion molecule-1 is an endothelial cell adhesion receptor for Plasmodium falciparum. Nature. 1989;341:57-59.
48. Carman CV, Jun CD, Salas A, Springer TA. Endothelial cells proactively form microvilli-like membrane projections upon intercellular adhesion molecule 1 engagement of leukocyte LFA-1. J Immunol. 2003;171:6135-6144.
49. Mamdouh Z, Chen X, Pierini LM, Maxfield FR, Muller WA. Targeted recycling of PECAM from endothelial surface–connected compartments during diapedesis. Nature. 2003;421: 748-753.
50. Sheff D, Pelletier L, O'Connell CB, Warren G, Mellman I. Transferrin receptor recycling in the absence of perinuclear recycling endosomes. J Cell Biol. 2002;156:797-804.
51. Sheff DR, Daro EA, Hull M, Mellman I. The receptor recycling pathway contains two distinct populations of early endosomes with different sorting functions. J Cell Biol. 1999;145:123-139.
52. Marsh EW, Leopold PL, Jones NL, Maxfield FR. Oligomerized transferrin receptors are selectively retained by a lumenal sorting signal in a long-lived endocytic recycling compartment. J Cell Biol. 1995;129:1509-1522.
53. Kameda H, Morita I, Handa M, et al. Re-expression of functional P-selectin molecules on the endothelial cell surface by repeated stimulation with thrombin. Br J Haematol. 1997;97:348-355.
54. Scholz D, Devaux B, Hirche A, et al. Expression of adhesion molecules is specific and time-dependent in cytokine-stimulated endothelial cells in culture. Cell Tissue Res. 1996;284:415-423.
55. Ferris AL, Brown JC, Park RD, Storrie B. Chinese hamster ovary cell lysosomes rapidly exchange contents. J Cell Biol. 1987;105:2703-2712.
56. Montgomery RR, Webster P, Mellman I. Accumulation of indigestible substances reduces fusion competence of macrophage lysosomes. J Immunol. 1991;147:3087-3095.
57. Photos PJ, Bacakova L, Discher B, Bates FS, Discher DE. Polymer vesicles in vivo: correlations with PEG molecular weight. J Control Release. 2003;90:323-334.
58. Li Y, Pei Y, Zhang X, et al. PEGylated PLGA nanoparticles as protein carriers: synthesis, preparation and biodistribution in rats. J Control Release. 2001;71:203-211.
59. Park JW, Hong K, Kirpotin DB, et al. Anti-HER2 immunoliposomes: enhanced efficacy attributable to targeted delivery. Clin Cancer Res. 2002;8: 1172-1181.
60. Moghimi SM. Chemical camouflage of nanospheres with a poorly reactive surface: towards development of stealth and target-specific nanocarriers. Biochim Biophys Acta. 2002;1590:131-139.

Penn

University of Pennsylvania

10th Annual Respiration Research Retreat

June 11, 2004

Items # 7 and 8

Program and Abstracts

Sugarloaf Conference Center • Philadelphia, PA

33

Sustained endothelial delivery of catalase via ICAM-1 recycling pathway. Silvia Muro, Christine Gajewski, Michael Koval and Vladimir R. Muzykantov. Institute for Environmental Medicine. University of Pennsylvania School of Medicine. Philadelphia. PA.

Affinity nanocarriers (NC) can be designed to improve vascular drug delivery. InterCellular Adhesion Molecule (ICAM)-1, which is up-regulated and functionally involved in pathological processes including oxidative stress, is a good target for NC delivery. Anti-ICAM/NC deliver catalase into endothelial cells and protect against H_2O_2-induced injury. However, protection is transient (2 h) due to lysosomal degradation of catalase. To determine whether the therapeutic window could be expanded using sustained delivery of anti-ICAM/NC, we studied fate of the target molecule, ICAM-1, after uptake of anti-ICAM/NC. We found that ICAM-1 disappears from the cell surface concomitantly to anti-ICAM/NC internalization, but partially recycles to the plasma membrane 1 h after NC uptake. This enables a second dose of anti-ICAM/NC to bind to and be internalized by endothelial cells both in culture and in vivo after IV injection in mice. Pulmonary targeting of a second dose of anti-ICAM/NC injected 15 min after the first dose was decreased by 50%, but recovered between 30 min and 2.5 h, comparable to cultured endothelial cells. Internalized anti-ICAM/NC did not affect cell viability or fluid phase endocytosis and trafficking. However, lysosomal trafficking of the second dose of anti-ICAM/NC was decelerated minimum two folds, thus the major fraction resided in pre-lysosomal vesicles for at least 5 h without degradation. As a result, successive administration of two doses of anti-ICAM/NC/catalase to endothelial cells prolonged anti-oxidant protection by at least four folds, mainly due to delayed intracellular processing of the second dose of NC. These results indicate that ICAM-1 recycling maintains the capacity for recurrent intracellular targeting of catalase to endothelial cells. This maneuver (administration of either multiple doses or long circulating anti-ICAM/NC/catalase) will enhance protective potency in acute pathological conditions associated to vascular oxidative stress, including acute lung injury and ischemia-reperfusion injury.

34

The innate immune molecule surfactant protein (SP)-D is upregulated in the lung following cigarette smoke (CS) exposure in a murine model. Y Cao[1], M. Grous[2], ST Scanlon[1], MF Beers[1], RA Panettieri[1], M. Salmon[2], A. Haczku[1] [1]University of Pennsylvania, Philadelphia, PA, [2]GSK Pharmaceuticals, King of Prussia, PA

RATIONALE: SP-D a mediator between the innate and adaptive immune system may play an important protective role during inflammatory changes of the lung. We have previously shown that Pneumocystis Carinii infection as well as allergic airway inflammation resulted in significant increases in production of SP-D, but the underlying mechanisms remain to be clarified. METHODS: To investigate the effect of a non-antigen related inflammatory challenge such as cigarette smoke on SP-D production, C57BL/6 mice received exposure to cigarette smoke 3 times a day for a 3-day period (day 0-day 3). A group of mice (n=6) was studied on days 1, 2, 3, 4, 5 and 6. Total protein levels, inflammatory cell influx and proinflammatory cytokine profile were assessed in the BAL. The BAL fluid was fractionated into small (SA) and large (LA) surfactant fractions and the levels of SP-D were quantified using Western blot and ELISA. RESULTS: CS elicited a significant neutrophilia that coincided with the peak of protein levels and KC (IL-8) release into the airways on day 2 after starting the CS exposure. In spite of continuing CS exposure however, on day 3 the inflammatory changes declined and were completely back to baseline by day 5. Interestingly, the pulmonary surfactant protein SP-D that started to raise on day 2, reached peak levels on day 3 (23ng/ug total protein, $p<0.001$, vs. non-exposed controls, n=6). Further, although the majority of the proinflammatory cytokine IL-6 was released on Day 1, its levels showed a strong positive correlation ($r=0.7$, $p<0.01$) with levels of SP-D in the same BAL samples suggesting either a causal relationship or common regulatory pathways. CONCLUSIONS: Our results indicate that acute CS exposure elicited transient inflammatory changes, the resolution of which coincided with emergence of SP-D. We speculate that this lung collectin may play a modulatory role in CS-induced airway inflammation. Funded by: GSK Pharmaceuticals (AH, RAP), R-21-AI055593-01 (AH)

41

PECAM-targeted delivery of superoxide dismutase to endothelium protects against xanthine oxidase-induced oxidant stress and angiotensin II-induced hypertension. Vladimir V.Shuvaev[1], Samira Tliba[1], Karine Laude[2], David G.Harrison[2], and Vladimir R.Muzykantov[1] Institute for Environmental Medicine[1], University of Pennsylvania School of Medicine, Philadelphia, PA; Division of Cardiology[2], Emory University School of Medicine, Atlanta, GA 30322.

Superoxide anion, a free radical produced in cells by several enzymes as a by-product of substrate oxidation, can directly inactivate a key vasodilating agent NO and indirectly cause oxidant stress via formation of peroxinitrate and H_2O_2 that can further convert into strong oxidants. Superoxide dismutase (SOD) accelerates superoxide conversion into H_2O_2 and thus maintains NO effects and helps to protect cells against oxidant stress. Using streptavidin as a cross-link for biotinylated proteins we prepared immunoconjugate containing anti-PECAM antibody and SOD that retained 50% of its initial enzymatic activity after biotinylation and conjugation. Anti-PECAM/SOD conjugate, but not non-immune IgG/SOD counterpart, significantly increased survival of umbilical vein endothelial cells exposed to hypoxanthine-xanthine oxidase. Anti-PECAM/^{125}I-SOD showed 12-times higher pulmonary uptake 1 h post IV injection in mice that non-immune counterpart, and roughly 30% of injected SOD was found in other organs including the heart, reflecting specific binding to vascular endothelium. Functional activity of anti-PECAM/SOD was studied in a mouse model of hypertension induced by chronic angiotensin II (Ang II) infusion. Micropump was implanted subcutaneously in mouse and Ang II was infused at a constant rate during 14 days. Thoracic aorta was harvested 15 min post IV injection of immunoconjugates. H_2O_2 level in the tissue was measured with Amplex Red assay and vasorelaxation by acetylcholine was measured on 5-mm ring aorta segments. Anti-PECAM/catalase, but neither anti-PECAM/SOD nor free SOD decreased H_2O_2 level in aorta. However, injection of 20 μg of anti-PECAM/SOD normalized the vasorelaxation (Ang II infusion significantly impaired vasorelaxation compared to control), whereas free SOD had little effect and anti-PECAM/catalase did not have any effect. Thus, SOD immunotargeting may be a useful protective tool in pathological states where overproduced superoxide anion plays a role in pathogenesis, such as NO inactivation in hypertension.

42

Lung injury and mortality with hyperoxia are increased in Peroxiredoxin 6 gene-targeted mice. Yan Wang[1], Sheldon I. Feinstein[1], Yefim Manevich[1], Ye Shih Ho[2], and Aron. B. Fisher[1] Institute for Environmental Medicine, University of Pennsylvania Medical Center[1], and Institute of Environmental Health Sciences, Wayne State University[2]

Overexpression of peroxiredoxin 6 (Prdx6) has been shown to protect lungs of mice against hyperoxia-mediated injury. In this study, we evaluated whether genetic inactivation of Prdx6 in mice increases sensitivity to oxygen toxicity. We evaluated mouse survival, lung histopathology, total protein and nucleated cells in bronchoalveolar lavage fluid (BALF), and oxidation of lung protein and lipids by measurement of protein carbonyls and thiobarbituric reactive substances (TBARS). The duration of survival for Prx6 -/- mice was significantly shorter than that observed in wild-type mice on exposure to 85% or 100% O_2; survival of Prdx6 +/- mice was intermediate. After 72h exposure to 100% O_2, lungs of Prdx6-/- mice showed more severe injury compared to wild-type control with increased wet/dry weight, epithelial cell necrosis and alveolar edema on microscopic examination, increased protein and nucleated cells in BALF, and higher content of TBARS and protein carbonyls in lung homogenate. These findings show that Prdx6 -/- mice have increased sensitivity to hyperoxia and provide *in vivo* evidence that Prdx6 is an important anti-oxidant enzyme. Keywords: 1-cys peroxiredoxin; bronchoalveolar lavage fluid; protein carbonyls; lipid peroxidation; oxidant stress

Silvia Muro

LESLIE DAN FACULTY OF pharmacy
University of Toronto

MOLECULAR DESIGN IN DRUG DISCOVERY & DEVELOPMENT SYMPOSIUM SERIES

Toronto 2004

BIOMOLECULAR DESIGNS AND DRUG DISCOVERY

DELIVERY OF MACROMOLECULES INTO CELLS USING NON-VIRAL VECTORS

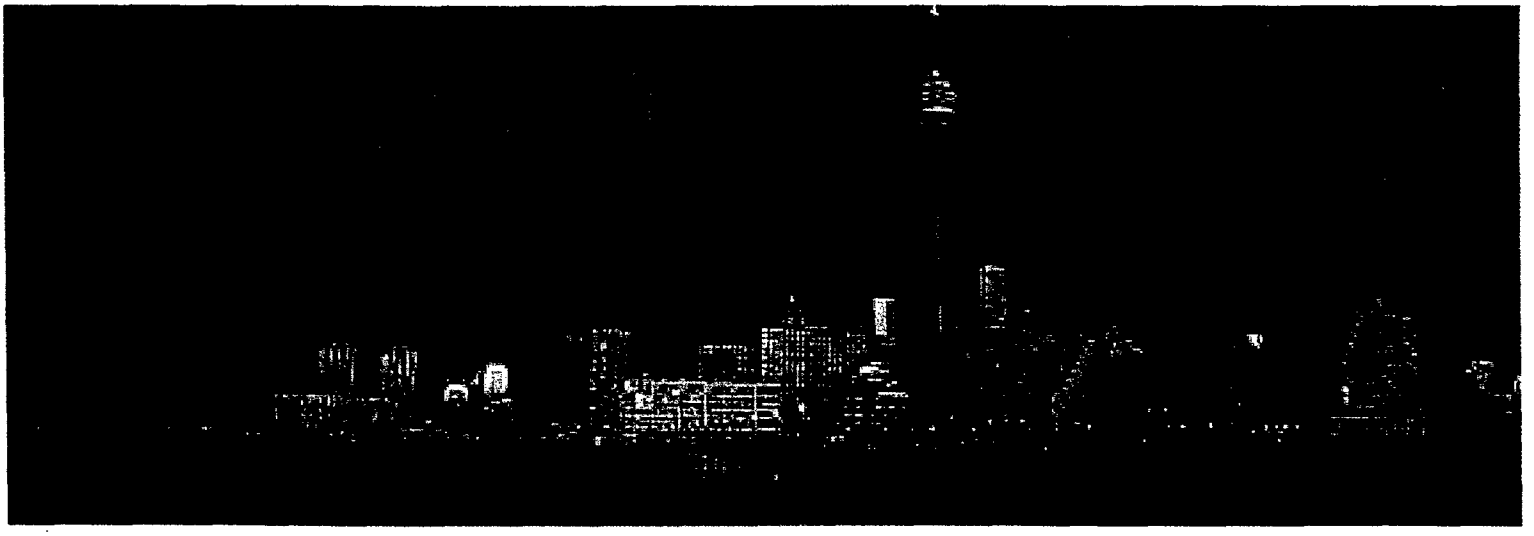

JULY 8-10, 2004 **TORONTO, CANADA**

SUSTAINED DRUG DELIVERY INTO ENDOTHELIUM VIA RECYCLING ICAM-1

[redacted]o, Christine Gajewski, Michael Koval and Vladimir R. Muzykantov

University of Pennsylvania School of Medicine,
Philadelphia, PA, USA

Silvia@mail.med.upenn.edu

Endothelial cells (EC) internalize multivalent nanoparticles (NP) targeted to InterCellular Adhesion Molecule 1 (ICAM-1), a plasma membrane protein up-regulated in altered EC and functionally involved in pathological conditions, including vascular oxidative stress. Immunotargeting NP to ICAM-1 has been shown to provide intracellular delivery of anti-oxidant enzymes (e.g., catalase) and protect endothelial cells from H2O2-induced oxidative injury. However, the anti-oxidant protection decayed after 2 h following NP uptake, consistent with intracellular degradation of internalized enzymes within lysosomes. Fluorescence microscopy and radiotracer studies in human umbilical vein EC (HUVEC) revealed that target ICAM-1 molecules disappear within 15 min from the cell surface, concomitantly to NP internalization, but partially recycle to the plasma membrane 1 h later. Consistent with this pattern of ICAM-1 accessibility, binding and uptake of a second dose of anti-ICAM/NP administered 15 or 30 min following internalization of the first dose was markedly decreased, but recovered to normal levels 1 h later. Similarly, targeting of 125I-anti-ICAM/NP to the pulmonary endothelium was reduced by 50% when particles were injected in mice 15 min after the same dose of non-labeled counterpart, but completely recovered by 2.5 h post injection of the first dose. The second dose of anti-ICAM/NP did not affect intracellular traffic of the first dose to lysosomal degradative compartments, but lysosomal traffic of the second dose was markedly decelerated. However, presence of particles within lysosomes did not affect cell viability or fluid phase endocytosis and lysosomal trafficking. We tested the therapeutic potential of repetitive targeting of anti-ICAM/NP loaded with catalase to HUVEC. Cells treated with a single dose lost anti-oxidant protection 3 h after NP internalization, but administration of the second dose conferred a marked prolongation of the protection (at least to 8 h), consistent with the slow lysosomal trafficking of the second dose. These results indicate that recurrent targeting to ICAM-1 has a potential for sustained intracellular delivery to enhance therapeutic interventions in acute pathological conditions associated to vascular oxidative stress.

Supported by National Institutes of Health grants HL/GM 71175-01 (V.R.M), GM61012 (M.K.) and P01 HL019737-26, Project 3 (M.K.) and Department of Defense Grant PR 012262 (V.R.M.).

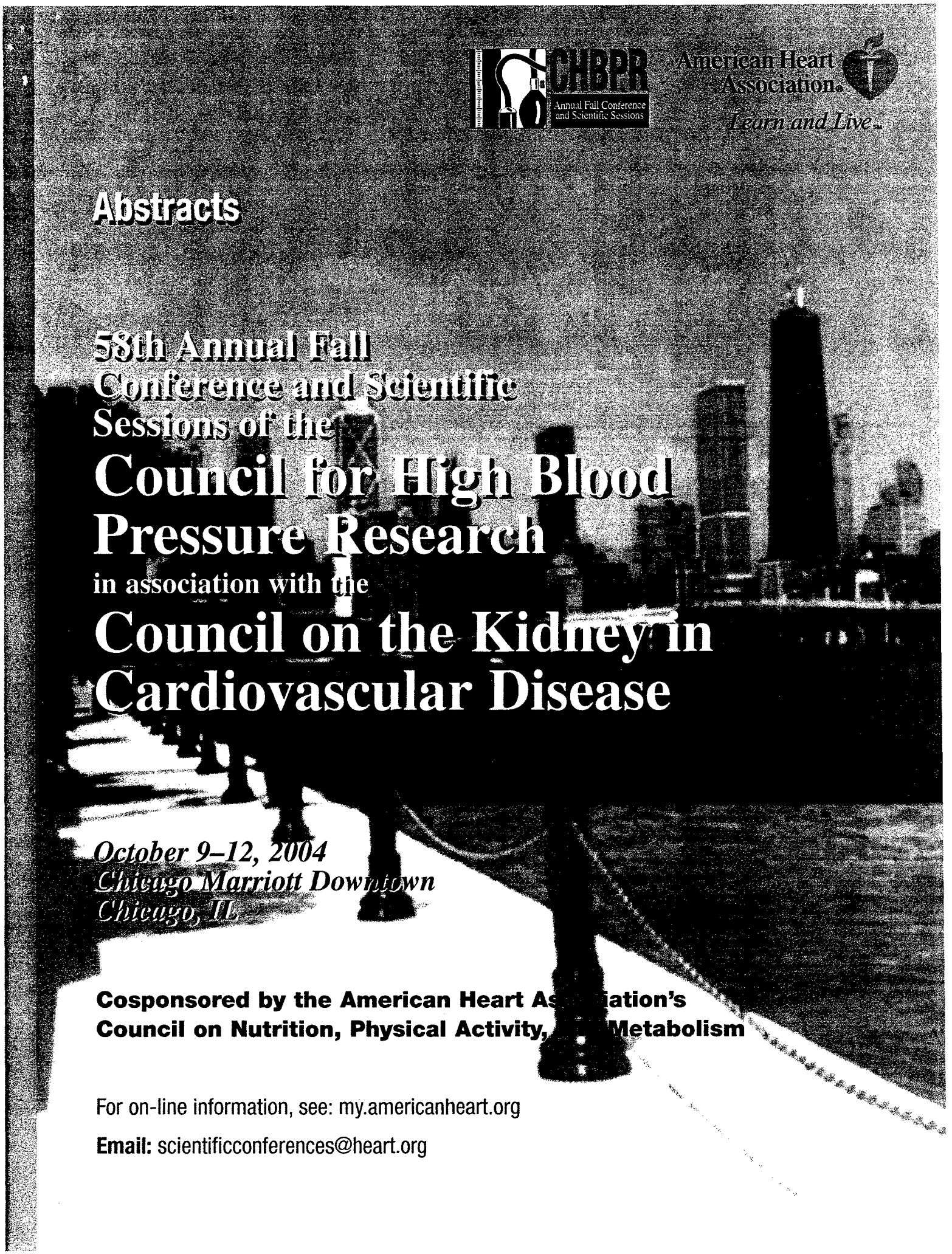

Abstracts

58th Annual Fall Conference and Scientific Sessions of the

Council for High Blood Pressure Research

in association with the

Council on the Kidney in Cardiovascular Disease

October 9–12, 2004
Chicago Marriott Downtown
Chicago, IL

Cosponsored by the American Heart Association's Council on Nutrition, Physical Activity, and Metabolism

For on-line information, see: my.americanheart.org

Email: scientificconferences@heart.org

Hypertension, Vol 44, #4, October 2004

P200

Exaggerated Hypertensive Target Organ Damage in Mice Lacking Peripheral Serotonin

Claudia S Wilhelm, Luciana A Campos, Volkmar Gross, Ovidiu Baltatu, Max-Delbrück-Center, Berlin, Germany; Diego J Walther, Max-Planck-Institut für Molekulare Genetik, Berlin, Germany; Michael Bader, Max-Delbrück-Center, Berlin, Germany

Serotonin is not only a prominent neurotransmitter but also a hormone active in the cardiovascular system. We have recently shown that mice lacking tryptophan hydroxylase (TPH) 1 lack serotonin in the blood but exhibit normal levels of the hormone in the central nervous system due to the presence of the previously unknown neuronal isoenzyme, TPH2. These mice are ideal models to study the peripheral functions of serotonin. In first experiments we could show that TPH1 knockout (KO) mice have an impaired hemostasis due to attenuated secretion of von-Willebrand factor from platelets. In the present study we have induced hypertension in these mice by the DOCA/salt regimen. TPH1-KO mice on C57Bl/6 background and controls (WT) did not differ in their basic blood pressure values measured by telemetry (111.8 ± 0.8 mmHg in TPH1-KO vs 108.1 ± 3.0 mmHg in WT) and developed equally increased mean arterial pressures after three weeks of DOCA/salt treatment (134.8 ± 1.1 mmHg in TPH1-KO, $p<0.0001$, vs 132.3 ± 2.4 mmHg in WT, $p<0.005$). However, cardiac hypertrophy induced by DOCA/salt treatment was with 143% of basal cardiac weight (basic relative left ventricular weight: 3.19 ± 0.10 mg/g vs after DOCA: 4.55 ± 0.18 mg/g, $p<0.00005$) significantly ($p<0.005$) more pronounced in the mice lacking peripheral serotonin than in WT mice with 123% (basal: 3.00 ± 0.05 mg/g vs after DOCA: 3.67 ± 0.07 mg/g, $p<0.0002$). Furthermore, kidney damage assessed by histology and albumin excretion into the urine (urinary albumine: 1200.1 ± 152.8 μg/24h in TPH1-KO vs 174.4 ± 103.4 μg/24h in WT, $p<0.01$) was markedly exaggerated in these mice. In conclusion, serotonin in the circulation is not involved in the development of hypertension in the DOCA/salt model but protects animals from target organ damage induced by the treatment. Immunomodulatory actions of peripheral serotonin, for which we also collected evidence in TPH1-KO mice, may be involved in these effects.

P201

Endothelial immunotargeting of superoxide dismutase corrects endothelial dysfunction in angiotensin II-induced hypertension

Karine LAUDE, Hua Cai, Emory University School of Medicine, Atlanta, GA; Vladimir V Shuvaev, University of Pennsylvania, Philadelphia, PA; Alfiya Bikineyeva, Sergey Dikalov, Emory University School of Medicine, Atlanta, GA; Vladimir Muzykantov, University of Pennsylvania, Philadelphia, PA; David G Harrison, Emory University School of Medicine, Atlanta, GA

Angiotensin II (AII)-induced hypertension increases vascular superoxide ($O_2^{\cdot-}$) production and causes endothelial dysfunction due to inactivation of NO by $O_2^{\cdot-}$. It remains unclear whether increased $O_2^{\cdot-}$ production is predominantly in the endothelium or in the vascular smooth muscle. To examine this question and to target therapy more precisely, we measured aortic $O_2^{\cdot-}$ in mice with AII-induced hypertension via HPLC detection of oxy-ethidium, the reaction product of dihydroethidium and $O_2^{\cdot-}$. To evaluate specifically the role of $O_2^{\cdot-}$, we conjugated superoxide dismutase (SOD) or catalase to PECAM antibody to target the endothelium. AII-infusion increased aortic $O_2^{\cdot-}$ production and this was abolished by endothelial denudation (figure), suggesting that the endothelium is the source of $O_2^{\cdot-}$. Tetrahydrobiopterin (BH4) and to a further extent apocynin (NADPH oxidase inhibitor) decreased AII-induced $O_2^{\cdot-}$ production, suggesting that both the NADPH oxidase and uncoupled NO synthase were sources of $O_2^{\cdot-}$. AII-induced hypertension reduced endothelium-dependent vasodilatation, and this was corrected by IV anti-PECAM/SOD (maximal relaxation to Ach: 97±0% vs 72±4% in untreated AII, $P<0.05$). Anti-PECAM/SOD also completely normalized aortic $O_2^{\cdot-}$ production. In contrast, anti-PECAM/catalase had no effects on vasoreactivity and $O_2^{\cdot-}$ production. We conclude that chronic AII stimulates endothelial $O_2^{\cdot-}$ production from both NADPH oxidases and uncoupled eNOS. The subsequent endothelial dysfunction can be prevented by immunotargeting of SOD to endothelial cells. Immunotargeting with anti- PECAM/SOD represents a promising approach for treatment of vascular oxidative stress.

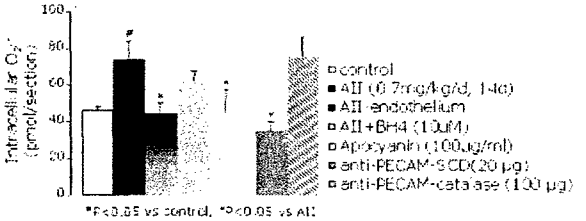

P202

Induction of Renal 20-Hydroxyeciosatetraenoic Acid (20-HETE) Prevents Angiotensin II (Ang-II) Dependent Hypertension in Mice

Trinity Vera, Montoya Taylor, University of Mississippi Medical Center, Jackson, MS; Richard Roman, Medical College of Wisconsin, Milwaukee, WI; David Stec, University of Mississippi Medical Center, Jackson, MS

Recently, we found that the activity of CYP enzymes that produce 20-HETE are similar in the liver of mice and rats but that the activity in the in the kidney is 10-fold less in mice. Since 20-HETE has been reported to be a major natriuretic factor in the kidney, we wanted to test the hypothesis that induction of renal 20-HETE production could prevent the development of Ang II -dependent hypertension. Mice were divided into 4 groups, Control (Con), Fenofibrate (FF), angiotensin II treated (Ang II), and Ang II + FF. Fenofibrate treatment (90 mg/kg/day, IP) was started two days prior to implantation of an osmotic minipump which delivered Ang II at a rate of 1000 ng/kg/min, SQ. Mean arterial blood pressure (MAP) averaged 107 ± 3 and 109 ± 6 mmHg in Con and FF treated mice (n=4). MAP was significantly increased in the Ang II treated mice to 144 ± 4 mmHg (n=7). However, FF treatment prevented the development of Ang II-dependent hypertension with MAP averaging 115 ± 5 mmHg in mice treated with both Ang II + FF (n=6). Renal 20-HETE production was very low in Con (n=4) and Ang II (n=7) treated mice averaging 32 ± 6 and 25 ± 2 pmoles/min/mg protein in each respective group. Renal 20-HETE production increased by over 3 fold in FF (n=4) and Ang II + FF (n=3) treated mice averaging 76 ± 14 and 98 ± 14 pmoles/min/mg protein, respectively. The expression of the Cyp4A10, 4A12, and 4A14 mRNAs were determined using real-time PCR with isoform specific primers. FF treatment caused more than a 100 fold induction of all 3 Cyp4A isoforms in the kidney; whereas, Ang II + FF treatment lead to induction of just the Cyp4A10 and Cyp4A14 isoforms but at lower levels as compared to FF treatment alone. These results demonstrate that increased renal tubular production of 20-HETE may be a viable pathway for treatment of Ang II- dependent hypertension.

P203

Human heme oxygenase gene transfer into newborn rats prevents hyperglycemia-mediated superoxide production and attenuates endothelial cell sloughing

Rita Rezzani, Luigi Rodella, University of Brescia, Brescia, Italy; Giovanni Li Volti, University of Catania, Catania, Italy; Rossella Bianchi, University of Brescia, Brescia, Italy; Alvin I Goodman, Nader G Abraham, New York Medical College, Valhalla, NY

Heme oxygenase-1 (HO-1) is a stress protein, which has been implicated as a key defense mechanism against oxidative injury in the vascular endothelium. Hyperglycemia has been directly linked to increased oxidative stress, leading to endothelial dysfunction, delayed cell replication and apoptosis. We examined the effect of HO-1 overexpression and underexpression on the vascular endothelium in Type I diabetic rats by measuring the level of oxidants and endothelial cell sloughing. The effect of streptozotocin (STZ)-induced hyperglycemia on aortic HO activity and heme content, the number of circulating endothelial cells, and urinary 8-epi-isoprostane was measured in control rats (LXSN), transgenic rats overexpressing HO-1 (LSN-human-HO-1) and transgenic rats underexpressing HO-1 (LSN-rat-HO-1-AS). HO-1 protein expression was unchanged, but HO activity was decreased in hyperglycemic rats compared to control rats ($p<0.05$). Hyperglycemia increased urinary 8-epi-isoprostane in control rats (n=5; 159 ± 16 pg./min). The increase in urinary 8-epi-isoprostane was significantly augmented ($p<0.05$) in diabetic rats underexpressing HO-1, LSN-rat-HO-1-AS rats (n=5; 321 ± 24 pg/min), but was attenuated in rats overexpressing human HO-1 (LSN-human-HO-1). The number of differentiated sloughed endothelial cells in blood was increased in hyperglycemic rats and was magnified in rats underexpressing HO-1, but was diminished in rats overexpressing HO-1. The number of circulating endothelial cells in control rats, control hyperglycemic rats, hyperglycemic rats overexpressing human HO-1 (LSN-human-HO-1), and hyperglycemic rats underexpressing rat HO-1 (LSN-rat-HO-1-AS) was 2.5 ± 1.5, 16.0 ± 4.3, 7.0 ± 3.5, and 29.5 ± 5.5 per ml of whole blood, respectively. Taken together, these data demonstrate that delivery of HO-1 gene to the vascular system during development brings about a reduction in 8-epi-isoprostane and decreased endothelial cell sloughing in diabetes. Upregulation of HO-1 may provide a pharmacological means to decrease oxidants, endothelial cell shedding, and hyperglycemia-induced cardiovascular complications.

P204

Regulation of Connexin Expression After Balloon Injury: Mechanism for Antiproliferative Effect of Statins?

Lihong Wang, Michigan State University, East Lansing, MI; Junzhu Chen, Yilan Sun, Furong Zhang, Jianhua Zhu, Shengjiang Hu, College of Medicine, Zhejiang University, Hangzhou, Zhejiang, China; Donna H Wang, Michigan State University, East Lansing, MI

Statins, the HMG-CoA reductase inhibitors, have been shown to inhibit the migration of macrophages and smooth muscle cell proliferation leading to an antiproliferative effect. Although this beneficial effect of statins has been suggested to be independent of lipid lowering properties, the possible mechanisms responsible for this action is largely unknown. Gap junctions, which serve as channels for direct intercellular exchange of ions, secondary messengers, and small signaling molecules, play an important role in tissue homeostasis and regulation of growth, differentiation, and development. This study was designed to test the hypothesis that the expression of the component proteins of gap junctions, connexins 40 and 43 (Cx40 and 43), is up-regulated in arteries subjected to balloon injury, which can be suppressed by statin therapy. Male New Zealand white rabbits were subjected to injury in which angioplasty catheter was introduced into the right iliac artery from the femoral artery under fluoroscopic guidance. Five groups of rabbits (n=7) were treated for 2 weeks with: balloon injury (BL), BL+lovastatin (BL+L, 10 mg/kg/day), BL+fluvastatin (BL+F, 10 mg/kg/day), sham operation (Sham), and control (Con). Immunohistochemistry studies showed that Cx40 and Cx43 were expressed in normal smooth muscle cells (SMCs) throughout the media. RT-PCR and Western blot analysis showed that Cx40 and Cx43 mRNA and protein expression were elevated after injury ($p<0.001$ for both proteins and both assays) and these elevations were suppressed by lovastatin and fluvastatin to a similar degree ($p<0.05$ for both drugs and both assays). Consistently, immunostaining of Cx40 and Cx43 was enhanced in the neointimal area after injury and lovastatin and fluvastatin reduced staining of these proteins in the lessened neointimal layer. Transmission electron microscopy revealed that there were abundant gap junctions between neointimal SMCs and fewer and smaller gap junctions after statin treatment. Therefore, balloon injury causes up-regulation of Cx40 and Cx 43 in neointimal SMCs. Lovastatin and fluvastatin reduce neointimal proliferation and suppress upregulated Cx40 and Cx 43 expression, suggesting that Cx40 and Cx43 play a role in statin-induced antiproliferative effect.

The Department of Defense

Military Health Research Forum

Sponsored by the US Army Medical Research and Materiel Command's Peer Reviewed Medical Research Program

25-28 April 2004

Best Viewed in Microsoft Internet Explorer

Click on the links below for more information about the Military Health Research Forum:

- **Agenda**
- **General Information**
- **Continuing Medical Education**
- **Abstracts and Poster Assignments**

All of the documents on this CD have been created in PDF format. In order to view these documents, you must have Adobe Acrobat Reader 3.0 or greater installed on your machine. If you already have this program, then you may begin browsing the documents. If you do not have this program, click the icon below to download and install the latest version of Adobe Acrobat Reader on your computer.

Note: If you encounter an error during the installation of Adobe Acrobat, which says "Authenticode Signature Not Found," you may ignore it and proceed. This is an error that occurs in Microsoft Internet Explorer and is normal when trying to install Adobe Acrobat.

33

Sustained endothelial delivery of catalase via ICAM-1 recycling pathway. [redacted], Christine Gajewski, Michael Koval and Vladimir R. Muzykantov. Institute for Environmental Medicine. University of Pennsylvania School of Medicine. Philadelphia. PA.

Affinity nanocarriers (NC) can be designed to improve vascular drug delivery. InterCellular Adhesion Molecule (ICAM)-1, which is up-regulated and functionally involved in pathological processes including oxidative stress, is a good target for NC delivery. Anti-ICAM/NC deliver catalase into endothelial cells and protect against H_2O_2-induced injury. However, protection is transient (2 h) due to lysosomal degradation of catalase. To determine whether the therapeutic window could be expanded using sustained delivery of anti-ICAM/NC, we studied fate of the target molecule, ICAM-1, after uptake of anti-ICAM/NC. We found that ICAM-1 disappears from the cell surface concomitantly to anti-ICAM/NC internalization, but partially recycles to the plasma membrane 1 h after NC uptake. This enables a second dose of anti-ICAM/NC to bind to and be internalized by endothelial cells both in culture and in vivo after IV injection in mice. Pulmonary targeting of a second dose of anti-ICAM/NC injected 15 min after the first dose was decreased by 50%, but recovered between 30 min and 2.5 h, comparable to cultured endothelial cells. Internalized anti-ICAM/NC did not affect cell viability or fluid phase endocytosis and trafficking. However, lysosomal trafficking of the second dose of anti-ICAM/NC was decelerated minimum two folds, thus the major fraction resided in pre-lysosomal vesicles for at least 5 h without degradation. As a result, successive administration of two doses of anti-ICAM/NC/catalase to endothelial cells prolonged anti-oxidant protection by at least four folds, mainly due to delayed intracellular processing of the second dose of NC. These results indicate that ICAM-1 recycling maintains the capacity for recurrent intracellular targeting of catalase to endothelial cells. This maneuver (administration of either multiple doses or long circulating anti-ICAM/NC/catalase) will enhance protective potency in acute pathological conditions associated to vascular oxidative stress, including acute lung injury and ischemia-reperfusion injury.

34

The innate immune molecule surfactant protein (SP)-D is upregulated in the lung following cigarette smoke (CS) exposure in a murine model. Y Cao[1], M. Grous[2], ST Scanlon[1], MF Beers[1], RA Panettieri[1], M. Salmon[2], A. Haczku[1] [1]University of Pennsylvania, Philadelphia, PA, [2]GSK Pharmaceuticals, King of Prussia, PA

RATIONALE: SP-D a mediator between the innate and adaptive immune system may play an important protective role during inflammatory changes of the lung. We have previously shown that Pneumocystis Carinii infection as well as allergic airway inflammation resulted in significant increases in production of SP-D, but the underlying mechanisms remain to be clarified. METHODS: To investigate the effect of a non-antigen related inflammatory challenge such as cigarette smoke on SP-D production, C57BL/6 mice received exposure to cigarette smoke 3 times a day for a 3-day period (day 0-day 3). A group of mice (n=6) was studied on days 1, 2, 3, 4, 5 and 6. Total protein levels, inflammatory cell influx and proinflammatory cytokine profile were assessed in the BAL. The BAL fluid was fractionated into small (SA) and large (LA) surfactant fractions and the levels of SP-D were quantified using Western blot and ELISA. RESULTS: CS elicited a significant neutrophilia that coincided with the peak of protein levels and KC (IL-8) release into the airways on day 2 after starting the CS exposure. In spite of continuing CS exposure however, on day 3 the inflammatory changes declined and were completely back to baseline by day 5. Interestingly, the pulmonary surfactant protein SP-D that started to raise on day 2, reached peak levels on day 3 (23ng/ug total protein, $p<0.001$, vs. non-exposed controls, n=6). Further, although the majority of the proinflammatory cytokine IL-6 was released on Day 1, its levels showed a strong positive correlation ($r=0.7$, $p<0.01$) with levels of SP-D in the same BAL samples suggesting either a causal relationship or common regulatory pathways. CONCLUSIONS: Our results indicate that acute CS exposure elicited transient inflammatory changes, the resolution of which coincided with emergence of SP-D. We speculate that this lung collectin may play a modulatory role in CS-induced airway inflammation. Funded by: GSK Pharmaceuticals (AH, RAP), R-21-AI055593-01 (AH)

AMERICAN JOURNAL OF

Respiratory and Critical Care Medicine

Volume 169 • Number 7 • April 2004

Abstracts

2004 INTERNATIONAL CONFERENCE

May 21–26, ORLANDO, FLORIDA
AMERICAN THORACIC SOCIETY

This is a supplement of the *American Journal of Respiratory and Critical Care Medicine*

AN OFFICIAL JOURNAL OF THE AMERICAN THORACIC SOCIETY

Role of Parenchymal and Inflammatory Cell TNF Receptors in the Development of PCP Induced Lung Injury

C.J. Johnston[1], T.W. Wright[1], G.S. Pryhuber[1], M.A. O'Reilly[1], J.P. Williams[1], F. Gigliotti[1], J.N. Finkelstein[1]. [1]University of Rochester, Rochester, NY.

Rationale: Host immune-mediated response to P. carinii (Pc) leads to epithelial damage and progressive loss of epithelial functions. Early synthesis of TNFα appears to control Pc proliferation and initial infection. TNFα activity is mediated by two distinct receptors. Our hypothesis is that ablation of TNF receptors on inflammatory cells will lessen CD 8^- T cell mediated inflammation and subsequent lung injury. Methods: Female (F), Wild Type (WT), B6.129 mice were irradiated using a split whole body dose (2 x 6 Gy) with a 4 hr interval. Immediately following the second dose, mice received 1 x 10^7 bone marrow cells from male (M) TNFR1/R2-/- or WT mice. Animals were allowed to reconstitute for 45 days. TNFR1/R2-/-, WT or chimera mice were then $CD4^-$ cell depleted and inoculated with Pc and sacrificed 21, 28 or 35 days post-inoculation. Breathing rates, inflammatory cell recruitment and gene expression were analyzed. Results: WT and WT chimera (M) WT into (F) WT) responded similarly with increased inflammatory cell infiltrate, decreased respiratory rates and elevated mRNA abundance of RANTES, TNFα, IL-1β and SPA 35 days post-inoculation. TNFR1/R2 -/- mice demonstrated similar responses to WT mice but changes were to a lesser extent. TNFR1/R2-/- (M) into B6/129 (F) chimera mice did not develop an inflammatory response similar to TNFR1/R2-/- mice. Breathing rates and mRNA levels were similar to age matched sham controls. Conclusions: Lack of TNF receptors on bone-marrow derived cells dramatically reduces epithelial injury and delays the inflammatory response associated with Pc infection.

This Abstract is Funded by: Supported by P01 HL-071659 and P30 ES-01247.

Biliverdin Administration Protects Against Endotoxin-Induced Acute Lung Injury

J.K. Sarady[1], A.M.K. Choi[1], L.E. Otterbein[1]. [1]University of Pittsburgh, Pittsburgh, PA. Email: saradyj@msx.upmc.edu

Inflammation associated with sepsis continues to have high morbidity and mortality rates so introducing new therapeutic modalities to prevent acute respiratory distress remain a major clinical focus. The enzyme heme oxygenase-1 (HO-1) has been shown to provide potent cytoprotection against lung injury, however the mechanism by which it does so is just beginning to be explored. HO-1 catabolizes heme into biliverdin (BV), which is then rapidly converted to bilirubin by biliverdin reductase. We tested the hypothesis that BV administration could substitute for the effects observed with HO-1. Using the well-described rat model of lipopolysaccharide (LPS)-induced shock, we demonstrate that exposure to 5mg/kg BV, a dose that raises the serum bilirubin levels only 2 fold, can impart a potent defense against lethal endotoxemia and effectively abrogate the inflammatory response. BV administration 16 hrs prior to a lethal dose of LPS leads to long-term survival of more than 80% of animals versus 20% survival in controls. Assessment of lung injury showed that BV suppressed LPS-induced lung alveolitis and associated edema formation. BAL protein and neutrophil content was lower (50%) in the BV-pretreated group vs. controls. BV-treated animals also showed significantly reduced serum levels of LPS-induced expression of pro-inflammatory cytokines TNF-α and IL-6 and augmented production of the anti-inflammatory cytokine IL-10 vs. control animals. Similar effects were observed *in vitro* in mouse endothelial (MLEC) and RAW 264.7 cells treated with 1 μg/ml LPS. BV significantly inhibited LPS-induced TNF-α and IL-6 levels, while elevated IL-10 levels measured in the media.

Taken together these data support the hypothesis that BV can modulate the inflammatory response and supports the possibility that BV might mediate protection in inflammatory disease states and therefore may have potential therapeutic application.

This Abstract is Funded by: RO1-HL60234

Vascular Immunotargeting of Catalase and SOD Using an Anti-PECAM Antibody Carrier Ameliorates Oxidative Lung Injury in a Double Hit Mouse Model

M. Christofidou-Solomidou[1], V. Shuvaev[1], A. Scherpereel[1], E. Arguiri[1], S. Tilba[1], V.R. Muzykantov[1]. [1]University of Pennsylvania, Philadelphia, PA. Email: melpo@mail.med.upenn.edu

REATIONALE: Vascular oxidative stress plays an important role in pulmonary diseases including Acute Lung Injury (ALI/ARDS). We have previously shown that vascular immunotargeting of antioxidant enzyme (AOE) catalase, using coupling of AOE to antibodies against surface endothelial antigens, such as PECAM-1, is effective in ameliorating ALI in an artificial model of targeted pulmonary oxidant stress. In this study, we wanted a) to extent those findings to a more complex model of double hit oxidative injury caused by glucose oxidase (GOX) immunotargeting/ Hyperoxia and b) to test simultaneous targeting of twoAOEs, catalase and superoxide dismutase (SOD) to endothelial PECAM. **METHODS & RESULTS:** Mice were injected iv with 100μg of either anti-PECAM/catalase or anti-PECAM/Catalase/SOD conjugates followed by a low dose (1 μg/g) anti-TM/GOX and exposed to hyperoxia (PO_2=80%) for 4 h prior to sacrifice. Lung injury was characterized by BAL protein, and WBC differentials. The groups were: 1) untreated control; 2) 80% O_2 + anti-TM/GOX (double-hit); 3) double hit and anti-PECAM/catalase; and 4) double hit and anti-PECAM/CAT/SOD. BAL proteins were 0.1, 3.14±0.75, 0.95±0.23, and 0.78±0.21, respectively. Percent BAL PMN for the same groups were 0, 21.25±7.11, 2.11±0.49 and 0.4±0.4, respectively. Therefore, targeted tandem AOE conjugate ameliorated edematous injury induced by combined oxidant stress and prevented PMN influx. **CONCLUSION:** Vascular immunotargeting of AOEs to the pulmonary endothelium is a promising strategy for treatment oxidant lung injury and can be further optimized by delivery of diverse AOE.

This Abstract is Funded by: AHA (MCS) Department of Defense (VM)

Conditional Activation of NF-κB in Airway Epithelium Causes Acute Lung Injury in Transgenic Mice

D.S. Cheng[1], W. Han[1], V.V. Polosukhin[1], F.E. Yull[1], J.W. Christman[1], T.S. Blackwell[1]. [1]Vanderbilt University School of Medicine, Nashville, TN. Email: timothy.blackwell@vanderbilt.edu

Rationale: Airway epithelial cells are thought to participate in airway inflammation and innate immunity, but a decisive role has not been proven. We hypothesized that activation of NF-κB in airway epithelial cells is a principal mechanism for generation of acute lung injury. Therefore, we developed a transgenic mouse model based on the tetracycline inducible system (tet-on) to selectively activate NF-κB in epithelial cells. **Methods**: A line of double transgenic mice was produced by co-injecting the following constructs: tetracycline operator/minimal CMV promoter driven FLAG-tagged constitutively active IκB kinase 2 [(tet-o)--cIKK2], and Clara cell specific promoter (CC10) driven tetracycline-controlled transcriptional silencer. Double transgenic mice were identified by Southern Blot and cross-bred with mice expressing a reverse tetracycline transactivator under the control of the rat CC10 promoter. The resulting triple transgenic mice were treated with 1 mg/ml doxycycline (dox) in drinking water to induce transgene expression. **Results**: Expression of cIKK2 was not identified in the absence of dox treatment but was induced exclusively in lung epithelium of triple transgenic mice by 3 days of dox. At 7 days of dox treatment, high level expression of NF-κB dependent genes, including TNFα, MIP-2, RANTES was identified in lung tissue. Increased inflammatory cells and total protein were present in lung lavage. Lung histology showed hemorrhage, edema, and a marked inflammatory cell influx. At 2 weeks of dox treatment, mortality reached 80%, compared to no mortality in wild type or double transgenic mice treated with dox. **Conclusion**: Sustained activation of NF-κB in airway epithelium results in an ARDS-like acute lung injury that is associated with a high mortality. These data suggest that airway epithelial cells play a critical role in regulating inflammation and host derived lung injury.

This Abstract is Funded by: HL66196, HL 61419, HL68121

Targeted Inactivation of CD11b Induced in Trangenic Mice Protects Against Sepsis-Induced PMN Sequestration and Acute Lung Injury

Q.H. Liu*[1], X.P. Gao*[1], E.S. Ong[1], D. Predescu[1], X.M. Zhou[1], M. Broman[1], N. Xu[1], A. Rahman[1], A.B. Malik[1]. [1]Department of Pharmacology, College of Medicine, University of Illinois at Chicago, Chicago, IL. Email: qliu@uic.edu

We generated transgenic mice expressing the specific CD11b-antagonist, Neutrophil Inhibitory Factor (NIF), to assess the *in vivo* effects of CD11b/CD18 blockade in sepsis-induced acute lung injury. As NIF cDNA was driven by cytomegalovirus promoter, the protein was expressed in all organs and was abundant in the circulation. Binding of NIF to CD11b resulted in decreased CD11b cell surface expression in polymorphonuclear leukocytes (PMNs), whereas CD11a did not serve as *in vivo* ligand for NIF. Presence of the CD11b ligand caused neutrophilia (~40% increase in PMN count). PMN migration across the pulmonary endothelial-alveolar epithelial barriers was markedly reduced in the CD11b-blocked transgene mice after *E. coli* challenge. PMN sequestration in lungs and production of oxygen free radicals induced by sepsis were blocked. Pulmonary microvessel filtration coefficient (K_{fc}) and lung wet weight gain, indicators of lung vascular injury measured *ex vivo* the mouse sepsis model, were also significantly reduced in these the CD11b-blocked transgene mice . Thus, targeted inactivation of CD11b induced transgenic mice by expression of a CD11b-binding antagonist peptide prevents PMN-mediated lung inflammation and acute lung injury. (* Qinghui Liu and Xiao-pei Gao contributed equally to this work.)

This Abstract is Funded by: This work was supported by NIH grants T32 HL-07829, HL-45638, HL-60678, and HL-27016

Hyperoxia-Induced Acute Lung Injury Is Mediated by an Imbalance between CXCR2 and CXCR3 Receptor and Ligand Expressions

R.D. Sue[1], L.A. Murray[1], J.A. Belperio[1], M.D. Burdick[1], Y.Y. Xue[1], J.J. Kwon[1], M.P. Keane[1], R.M. Strieter[1]. [1]Division of Pulmonary and Critical Care Medicine, David Geffen School of Medicine at UCLA, Los Angeles, CA. Email: rsue@mednet.ucla.edu

Rationale: The fibroproliferative phase of ARDS is characterized by persistent inflammation leading to dysregulated repair with denudation of basement membrane, excessive matrix deposition, and parenchymal fibrosis. In addition, increased levels of BALF procollagen III have been demonstrated to be a marker of acute lung injury and early mortality. Hyperoxia may promote ARDS and perpetuate lung injury. Hyperoxia-induced lung injury is characterized by infiltration of activated leukocytes, in conjunction with endothelial and epithelial cell injury followed by fibrogenesis. We hypothesized that the fibrogenesis demonstrated during hyperoxia-induced lung injury is mediated, in part, by an imbalance in angiogenic and angiostatic chemokines. **Methods:** Balb/c mice were continuously exposed to 80% oxygen for 6 days. Animals were subsequently sacrificed and lungs analyzed for leukocyte infiltration, collagen gene expression and deposition, angiogenic activity, chemokine generation and chemokine receptor expression. **Results:** Hyperoxia-induced lung injury was associated with excessive fibrogenesis as measured by an increase in total lung collagen content and increased gene expression of procollagen III and procollagen I. The increased fibrosis was paralleled by an increase in leukocyte number, elevation in lung levels of CXCR2 ligands, a decrease in CXCR3 ligand generation, and a trend for increased angiogenesis as measured by FACS analysis of endothelial cells. Moreover, real-time quantitative RT-PCR demonstrated elevated CXCR2 expression in hyperoxia challenged animals, as compared with room air controls while CXCR3 expression trended down in the hyperoxia group. **Conclusions:** These results suggest that the excessive fibrosis seen in hyperoxia-induced lung injury may be associated with aberrant angiogenesis due, in part, to an imbalance in ELR+ and ELR- CXC chemokines.

This Abstract is Funded by: NIH HL67665

Department of Defense

Peer Reviewed Medical Research Program

US Army Medical Research and Materiel Command

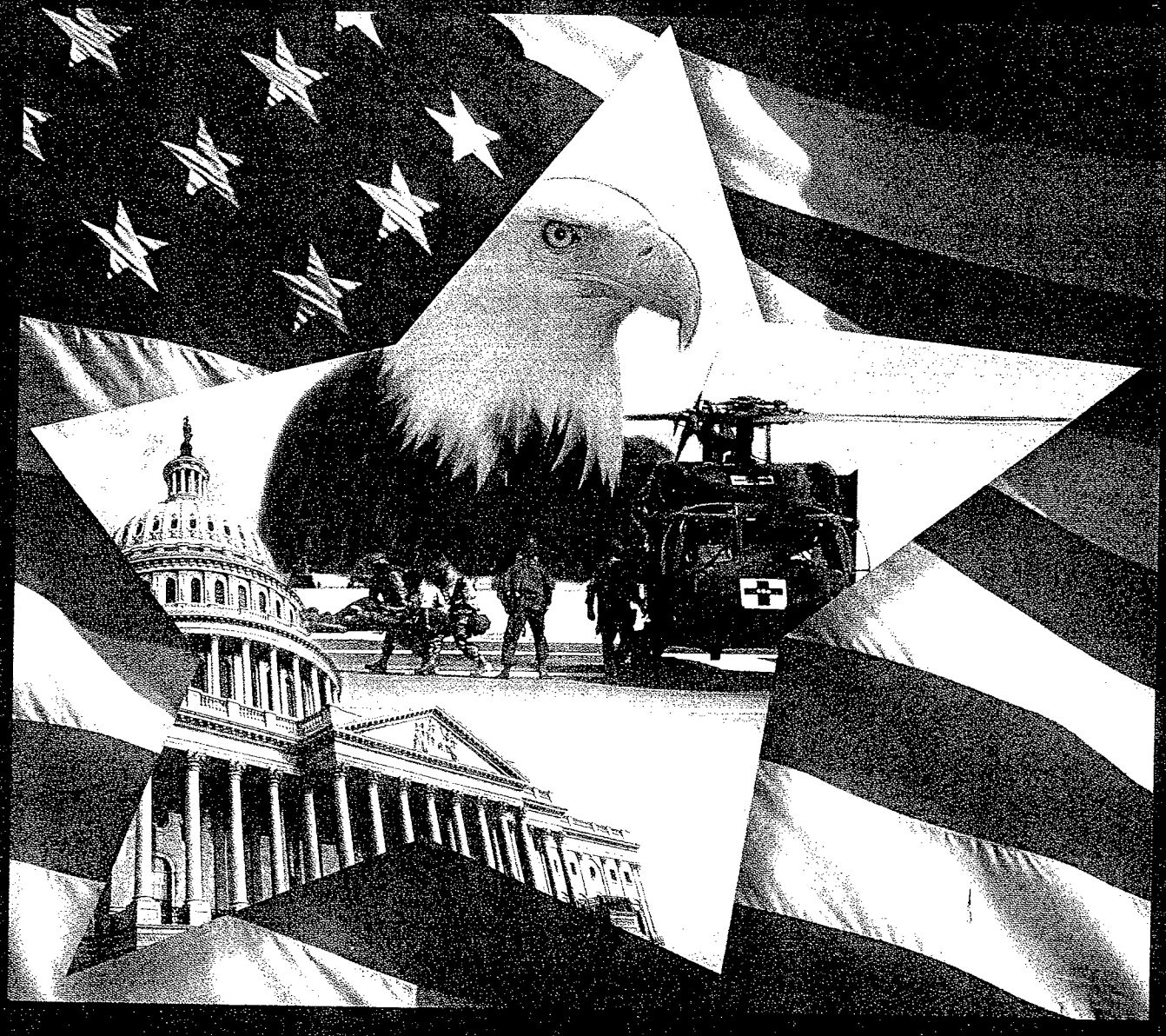

PRMRP Military Health Research Forum

25-28 April 2004
Caribe Hilton Hotel
San Juan, Puerto Rico

PROCEEDINGS

The Department of Defense

Military Health Research Forum

PROCEEDINGS

Caribe Hilton Hotel
San Juan, Puerto Rico

25-28 April 2004

TARGETING OF DRUGS TO CELL ADHESION MOLECULES FOR TREATMENT OF ACUTE LUNG INJURY

Muro S, Murciano JC, Christofidou M, and Muzykantov V

Department of Pharmacology, University of Pennsylvania Medical Center, Philadelphia, PA

BACKGOUND/PURPOSE: Trauma, hemorrhage, and sepsis (e.g., associated with military casualties) may lead to acute lung injury (ALI), a condition that involves pulmonary thrombosis and oxidative stress. In theory, anti-thrombotic agents (e.g., plasminogen activators, tPA) and antioxidant enzymes (e.g., catalase) could be used for ALI therapy, but their use is restricted by inadequate vascular delivery and side effects. The purpose of this study is to improve their utility for treatment of ALI via targeted delivery to the pulmonary endothelium.

METHODS: We conjugated these drugs with monoclonal antibodies to InterCellular Adhesion Molecule-1 (ICAM-1, endothelial determinant) using bi-functional chemical cross-linkers. Fluorescent and electron microscopy, radioisotope tracing, and determination of enzymatic activity of tPA and catalase have been used to study binding, internalization, metabolism, and effects of the conjugates in cell cultures, mice, and rats.

RESULTS: (1) Conjugates accumulate in the pulmonary endothelium after injection in animals. (2) Pulmonary targeting of conjugates is increased in pathological conditions associated with ALI (e.g., inflammation). (3) Endothelial cells do not internalize monomer ICAM antibodies and conjugates larger than 500 nm diameter, which can be utilized for delivery of tPA to the endothelial lumen, providing dissolution of pulmonary thrombi. (4) Endothelial cells internalize anti-ICAM conjugates of 100-350 nm diameter via a novel endocytotic pathway regulated by protein kinase C, NHE-1 ion exchanger in the plasma membrane, and rearrangements of actin cytoskeleton in endothelium. (5) Internalized anti-ICAM/catalase slowly traffics into lysosomes retaining its activity for several hours. (6) Auxiliary drugs disrupting lysosomal traffic and degradation prolong antioxidant effect of anti-ICAM/catalase. (7) Internalized ICAM-1 recycles to the cell surface, permitting sustained intracellular delivery and effects of catalase with repetitive administration or prolonged infusion of conjugates.

CONCLUSION: Immunotargeting ICAM-1 permits selective delivery of drugs to endothelial lumen or intracellular compartments. Delivery of tPA to the pulmonary vascular lumen will permit safe and effective fibrinolysis, while intracellular endothelial targeting of catalase will protect against oxidant stress. Further development of these delivery strategies will help to improve treatment of ALI/acute respiratory distress syndrome.

MECHANISTIC MODEL OF THE INTERNAL RESPIRATORY CONDITIONS AND ITS RELATION TO PULMONARY PRESSURE-VOLUME CURVE

Narusawa U, Amini R, and Creeden K

Northeastern University, Boston, MA

BACKGROUND/PURPOSE: This study reports (1) results of validity tests of a pulmonary pressure-volume (P-V) model equation, and (2) a development of a mechanistic model of the internal respiratory conditions and its relation to P-V curves as well as the model equation.

METHODS: Over 70 P-V curves are used to test overall accuracy of a continuous P-V model equation by statistical error analyses, and a mechanistic model of the total respiratory system (TRS) is constructed as an ensemble of a large number of elements to relate the internal TRS conditions to the parameters of P-V model equation through computational applications of principles of statistical mechanics.

RESULTS: Through statistical analyses, it is confirmed that the error function P-V model equation represents clinical P-V curves accurately and that the magnitudes of its four parameters quantify differences and similarities that exist among various P-V data sets. An element in the mechanistic model, an ensemble of which constitutes the TRS, is simulated as a piston-cylinder subsystem. Since the piston displacement varies with the pressure, P, the distribution of elements over the piston displacement depends on the magnitudes of the parameters of the P-V model equation, thus making it possible to relate the P-V curve characteristics to such intrarespiratory conditions as a degree of alveolar recruitment and of the tissue distension.

CONCLUSION: The study has generated a new method for quantitative interpretations of clinical P-V curves, which will help optimize ventilator strategy for patients with acute lung injury, as well as monitor both patients with chronic respiratory diseases and the state of health of the respiratory system in general.

TARGETING OF DRUGS TO CELL ADHESION MOLECULES FOR TREATMENT OF ACUTE LUNG INJURY

Muro S, Murciano JC, Christofidou M, and Muzykantov V

Department of Pharmacology, University of Pennsylvania Medical Center, Philadelphia, PA

BACKGOUND/PURPOSE: Trauma, hemorrhage, and sepsis (e.g., associated with military casualties) may lead to acute lung injury (ALI), a condition that involves pulmonary thrombosis and oxidative stress. In theory, anti-thrombotic agents (e.g., plasminogen activators, tPA) and antioxidant enzymes (e.g., catalase) could be used for ALI therapy, but their use is restricted by inadequate vascular delivery and side effects. The purpose of this study is to improve their utility for treatment of ALI via targeted delivery to the pulmonary endothelium.

METHODS: We conjugated these drugs with monoclonal antibodies to InterCellular Adhesion Molecule-1 (ICAM-1, endothelial determinant) using bi-functional chemical cross-linkers. Fluorescent and electron microscopy, radioisotope tracing, and determination of enzymatic activity of tPA and catalase have been used to study binding, internalization, metabolism, and effects of the conjugates in cell cultures, mice, and rats.

RESULTS: (1) Conjugates accumulate in the pulmonary endothelium after injection in animals. (2) Pulmonary targeting of conjugates is increased in pathological conditions associated with ALI (e.g., inflammation). (3) Endothelial cells do not internalize monomer ICAM antibodies and conjugates larger than 500 nm diameter, which can be utilized for delivery of tPA to the endothelial lumen, providing dissolution of pulmonary thrombi. (4) Endothelial cells internalize anti-ICAM conjugates of 100-350 nm diameter via a novel endocytotic pathway regulated by protein kinase C, NHE-1 ion exchanger in the plasma membrane, and rearrangements of actin cytoskeleton in endothelium. (5) Internalized anti-ICAM/catalase slowly traffics into lysosomes retaining its activity for several hours. (6) Auxiliary drugs disrupting lysosomal traffic and degradation prolong antioxidant effect of anti-ICAM/catalase. (7) Internalized ICAM-1 recycles to the cell surface, permitting sustained intracellular delivery and effects of catalase with repetitive administration or prolonged infusion of conjugates.

CONCLUSION: Immunotargeting ICAM-1 permits selective delivery of drugs to endothelial lumen or intracellular compartments. Delivery of tPA to the pulmonary vascular lumen will permit safe and effective fibrinolysis, while intracellular endothelial targeting of catalase will protect against oxidant stress. Further development of these delivery strategies will help to improve treatment of ALI/acute respiratory distress syndrome.

CALL CENTER-BASED DISEASE MANAGEMENT (CBDMP) OF PEDIATRIC ASTHMATICS

Quinn JM, Rathkopf M, Edwards HF, Terry RM, Blamire G, Napoli DC, Stritmatter F, and Grissom J

59th Medical Group, Wilford Hall Medical Center, Lackland Air Force Base, TX

BACKGROUND/PURPOSE: The goal of CBDMP is motivating patients to take charge of their condition rather than relying on the MHS to control acute episodes of care. The CBDMP will be a population-based intervention using preventive measures to control asthmatics through the use of proactive education and monitoring. This study will attempt to determine if CBDMP, applied to asthma will: improve patient and caregiver quality of life (QOL); reduce disease severity, as measured by reduced inhaled short acting beta agonist use; improve patient condition as measured by Peak Expiratory Flow and/or FEV1; reduce Emergency Department (ED) visits and hospital admissions, and/or reduced costs.

METHODS: Subjects 7 to 16 years of age with the diagnosis of asthma are eligible to enroll. Subjects are being recruited from three TRICARE Prime Military Treatment Facility (MTF) communities with similar resources—Fort Sill, Oklahoma; Tinker Air Force Base, Oklahoma; and Sheppard Air Force Base, Texas. Patients are randomly assigned to either and intervention group or a control group at each site. All subjects receive an electronic peak flow meter along with written instructions for self-monitoring of peak expiratory flow. All subjects are assessed for their appropriate National Heart Lung and Blood Institute (NHLBI) classification and all will receive the DoD/VA standardized asthma education materials.

The intervention group is entered into a CBDMP for 12 months. Only the intervention group is contacted by the CBDMP. The intervention is predetermined and timed education calls that assess, monitor, and educate asthmatics on a variety of health and environmental factors related to asthma control as developed and applied by the CBDMP contractor—National Jewish Medical and Research Center. The CBDMP allows unlimited patient initiated contact through 24-hour telephone access.

All control and intervention subjects have retrospective and prospective ED visits, hospital admissions, and beta-agonist utilization collected. Specific retrospective utilization, cost, and compliance data are collected from all subjects. Prospective ED and hospital admissions, peak flow values, short-acting rescue medication, FEV1, and QOL data are collected at baseline, 6 months, and 12 months. QOL data is also being collected from caregivers. Junipers Quality of Life instrument is used for the study. The asthmatic subjects are randomized into control and intervention groups. Utilization data will be collected from Managed Care Support Contract (MCSC) claims, MHS encounter, and self-reported data. Analysis of variance (ANOVA) and Chi-Square analysis will be used to test for changes over the course of the study, to compare the intervention and control groups, and to compare the four asthma severity level groups. All statistical testing will be performed at the 0.05 alpha level.

RESULTS: To date, 420 patients have been enrolled and enrollment continues through December 2003.

CONCLUSION: Subjects are continuing to enroll. No outcome data has been finalized or analyzed at this time.

The US Army Medical Research and Materiel Command supported this work.

American Heart Association®
Learn and Live℠

Final Program

Grover Conference on the Pulmonary Circulation:

Genetic and Environmental Determinants of Pulmonary Endothelial Cell Function

September 9-12, 2004
Lost Valley Ranch and Conference Center
Sedalia, Colorado

Sponsored by the American Heart Associationís Council on Cardiopulmonary, Perioperative & Critical Care

Co-sponsored by the American Thoracic Society, the American Physiological Society, and the Pulmonary Circulation Foundation

For online information, see www.my.americanheart.org and click on the Conferences and Education tab
Email: scientificconferences@heart.org

12

Sustained Drug Delivery into Endothelium via ICAM-1

Silvia Muro, Vladimir R. Muzykantov, University of Pennsylvania School of Medicine, Philadelphia, PA

Inter-Cellular Adhesion Molecule-1 (ICAM) is up-regulated in EC (endothelial cells) and functionally involved in many disease conditions including vascular oxidative stress. EC do not internalize monomer anti-ICAM, but internalize multivalent anti-ICAM nanoparticles via a new pathway, CAM-endocytosis. Anti-ICAM nanoparticles deliver catalase into and protect EC from oxidative injury for ~2-3 h after their uptake, consistent with kinetics of lysosomal traffic and degradation of catalase. Target ICAM molecules disappear from EC lumen within 15 min of nanoparticles internalization, yet recycle to the surface 1 h later. Binding and uptake of anti-ICAM nanoparticles administered 15 min after uptake of the first dose was markedly decreased, but recovered to normal level by 1 h. Targeting of ^{125}I-anti-ICAM nanoparticles to the pulmonary EC was reduced by 50% if they were injected in mice 15 min after the same dose of non-labeled counterpart, but recovered by 1 h. The second dose of anti-ICAM nanoparticles did not affect intracellular traffic of the first dose, yet lysosomal traffic and degradation of the second dose was decelerated. However, prolonged lysosomal residence of nanoparticles did not affect EC viability, fluid phase endocytosis and lysosomal trafficking. EC lost anti-oxidant protection 3 h after delivery of a single dose of anti-ICAM/catalase nanoparticles, but the second dose afforded prolongation of the protection for at least to 8 h, consistent with its slow lysosomal trafficking. ICAM recycling, permitting recurrent drug delivery into endothelial cells, provides a strategy to achieve sustained specific therapeutic interventions in endothelium.

13

Co-Localization of Adenylyl Cyclase 6 and Phosphodiesterase 4D4 to Caveolin- Enriched Fractions Defines a Membrane-Delimited cAMP Pool in Lung Microvascular Endothelium

J. Creighton, B. Zhu, T. Stevens, University of South Alabama, Mobile, AL

Pulmonary microvascular endothelial cells (PMVECs) and pulmonary macrovascular endothelial cells (PAECs) express calcium-inhibited type 6 adenylyl cyclase (AC6) and cAMP specific type 4 phosphodiesterase (PDE4). However, apparent cAMP hydrolysis is higher in PMVECs. We hypothesized that AC6 and PDE4 form a functional microdomain in PMVECs that coordinates cAMP synthesis with degradation. Caveolin-enriched membrane fractions--where AC6 is localized—were utilized to resolve PDE4 activity associated with AC6. Results indicate selective enhancement of rolipram-sensitive PDE4 activity in PMVECs compared to PAECs. Western blot analysis revealed enrichment of a 116 kDa protein band in PMVECs that co-immunoprecipitated with non-erythroid spectrin suggesting the PDE4D4 splice variant (that binds spectrin) localized to caveolin-enriched membranes in PMVECs but not in PAECs. Furthermore, adenylyl cyclase studies indicate greater calcium inhibition in PMVECs compared to PAECs, suggesting greater AC6 specific activity in PMVEC membranes. PDE4 inhibition (rolipram) increased cAMP accumulation more in PMVEC membranes than in PAEC membranes, confirming the presence of a PDE4 enzyme in PMVEC caveolin-enriched regions. Thus, when compared with PAECs, PMVECs possess both enhanced membrane-associated calcium inhibition of AC6 and higher PDE4 activity, creating a functional microdomain that precisely controls membrane-associated cAMP concentrations.

14

Soluble Adenylyl Cyclase Generates a cAMP Pool that Disrupts the Pulmonary Microvascular Endothelial Barrier

Sarah L. Sayner, University South Alabama, Mobile, AL; Carmen W. Dessauer, University of Texas, Houston, TX; Troy Stevens, University South Alabama, Mobile, AL

In vivo and in vitro studies illustrate barrier protective effects of elevated cAMP. Evidence suggests membrane-associated cAMP, not global rises in cAMP, is sufficient to promote endothelial cell barrier function. However, Pseudomonas aeruginosa injects an adenylyl cyclase, ExoY, into the cytosol of eukaryotic cells, elevating intracellular cAMP in pulmonary microvascular endothelial cells (PMVECs). In contrast to barrier protective effects of endogenous cAMP synthesis, ExoY-cAMP induced endothelial gaps. Therefore, we tested the hypothesis that relocalizing endogenous transmembrane adenylyl cyclase to the cytosolic compartment generates a cAMP pool that disrupts the endothelial cell barrier. Linking catalytic regions of mammalian adenylyl cyclase type I and II generates a soluble adenylyl cyclase. Basal cAMP concentration was unaltered in PMVECs infected with adenovirus expressing this fusion protein. While forskolin activated endogenous adenylyl cyclases, cells infected with the fusion protein exhibited a concentration-dependent increase in cAMP above soluble GFP infected and uninfected controls. The elevated cytosolic cAMP pool overwhelmed barrier protective effects of endogenous plasmalemma cAMP to induce endothelial gap formation. These studies demonstrate the subcellular localization of cAMP is a critical determinant of its downstream effects; while membrane-associated cAMP protects the barrier, rises in cytosolic cAMP disrupt the barrier.

15

Role of p38 and Signal Transducer and Activator of Transcription-1 in the Synergistic Induction of Inducible Nitric Oxide Synthase by Endotoxin and Interferon in Macrovascular Endothelial Cells

Hong Huang, Robin Buerki, Dale G. Hoyt, Ohio State University, Columbus, OH

Inducible NO synthase (iNOS) is induced in many cell types by pro-inflammatory agents, such as bacterial lipopolysaccharide (LPS) and cytokines. In contract to macrophages, murine aortic endothelial cells (MAEC) produce no NO in response to either LPS or interferon-gamma (IFN) alone. Combined treatment is highly synergistic, however. The murine iNOS promoter has sites for signal transducer and activator of transcription-1 (STAT1), nuclear factor kB (NFkB), and activating protein-1 (AP1). Based on in vitro DNA binding, IFN activated STAT1, but not NFkB or AP1, while LPS activated NFkB and AP1, but not STAT1. LPS also activated p38 mitogen-activated protein kinase. The p38 inhibitor, SB202190, blocked NO production with an IC50 of 13.4 uM, suggesting that p38 alpha and/or beta were involved. While SB202190 inhibited phosphorylation of STAT1 at serine727 and its DNA binding, activation of NFkB and AP1 were not blocked. The critical role of STAT1 was confirmed by the lack of iNOS induction in LPS/IFN-treated STAT1 knockout MAEC, whereas, transfection with STAT1 cDNA reconstituted the induction. As expected mutation of tyrosine701 to phenylalanine, a site required for IFN-induction dimerization of STAT1, did not support NO production in transfected knockout cells. Furthermore, NO production was restored only to 50% of the wildtype effect if serine727 was mutated to alanine. Although other factors, such as NFkB and AP1, may be required, the results demonstrate a critical role of STAT1, its

The 21st Annual

Penn
Graduate Group *in*
Pharmacological Sciences
www.med.upenn.edu/pharmgg

Pharmacological Sciences Student Symposium

Keynote Speaker:

Tamas Bartfai, Ph. D.

The Scripps Research Institute

"Ethical Challenges in Drug Development:
Large and Small Indications,
Offlabel Use and the Use of Pharmacogenomics"

October 8, 2004
Gregg Conference Center
Bryn Mawr, PA

Items #15 and 16

Graduate Group in the Pharmacological Sciences
University of Pennsylvania

Twenty-First Annual

Student Pharmacology Symposium

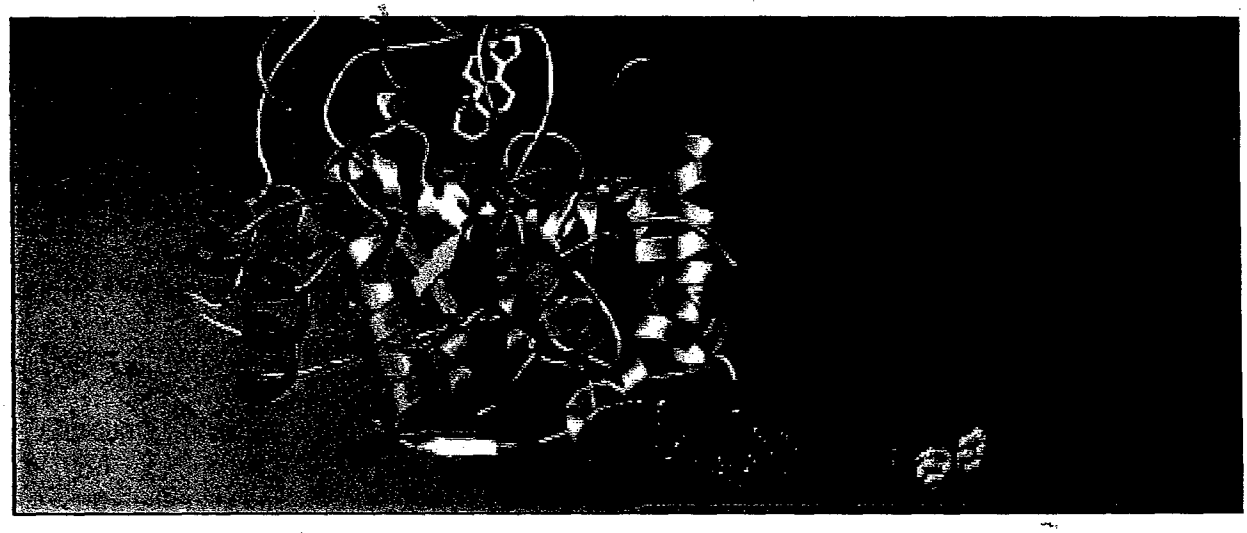

Friday, October 8, 2004

The Gregg Conference Center
at the
American College
270 South Bryn Mawr Avenue
Bryn Mawr, Pennsylvania

Analysis of Conjugated Estrogens in Plasma by Liquid Chromatography/Electron Capture Atmospheric Pressure Chemical Ionization/Mass Spectrometry

Xingpin Cui, Seon Hwa Lee, Peter O'Dwyer, Peter Moate, Ray Boston, Ian A. Blair
Center for Cancer Pharmacology, Department of Pharmacology
University of Pennsylvania, Philadelphia, PA 19104

We have recently developed a stable isotope dilution liquid chromatography/electron capture atmospheric pressure chemical ionization/tandem mass spectrometry (LC/ECAPCI/MS/MS) method for analyzing free estradiol and its metabolites in human plasma. This method was used to quantify estrogens in plasma after sublingual dosing with estradiol. The major circulating metabolites were estrone and 2-methoxy-estrone. Estradiol concentrations were very low, which suggested that substantial metabolism had occurred in the buccal epithelial system. Methodology was developed to analyze the plasma conjugates by coupling LC/ECAPCI/MS/MS analysis with enzymatic hydrolysis using arylsulfatase/b-glucuronidase. The limit of detection for estrogen metabolites was 4 pg on column. This assay revealed that substantial pre-systemic conversion of estradiol to estrone occurred and that both estradiol and estrone were conjugated. Therefore, the buccal epithelial cells must contain a substantial capacity to oxidize estradiol (through 17b-hydroxysteroid dehydrogenase) and to conjugate both estrogens (through sulfotransferase and/or UDP glucuoronosyl transferase). Supported by NIH grant PO1CA082707.

A genetically engineered anti-PECAM/urokinase fusion construct for targeting fibrinolysis to pulmonary vasculature

Bi-Sen Ding[1], Claudia Gottstein[2], Douglas B. Cines[3], Alice Kuo[3], Sergei Zaitsev[1], Tanya Krasik[1], Kumkum Ganguly[1] and Vladimir R. Muzykantov[1]
1- Department of Pharmacology and Institute For Environmental Medicine, University of Pennsylvania, 2- University of Cologne, 3- Department of Laboratory Pathology, University of Pennsylvania

Plasminogen activators have been widely used in the treatment of thrombosis. Their clinical applications, nevertheless, were limited by severe side effects. Vascular immunotargeting, the administration of drugs coupled to antibodies to endothelial surface antigens, has the potential for prophylactic thrombolysis. Platelet endothelial cell adhesion molecule-1 (PECAM-1), which is highly expressed on the surface of endothelial cells, represents an ideal candidate for vascular targeting. Here, we report a recombinant fibrinolytic agent, consisting of low molecular weight urokinase (Leu 144-Leu 411) fused to a single chain variable fragment (scFv) of antibody P-390 specific to mouse PECAM-1. Fusion protein was constructed with recombinant DNA technology. Schneider S2 cells were transfected and stable transfectants were used to express the recombinant protein. Fibrinolytically active fusion protein was purified by affinity chromatography, and the homogeneity was tested by SDS-PAGE. Binding assay on human mesothelioma REN cells transfected with cDNA encoding murine PECAM-1 confirmed binding activity of 390scFv-lmw UK. Competition ELISA with P-390 whole molecule indicated specific binding to mouse PECAM-1. After IV injection, 24.4±0.97 % of the injected dose per gram tissue (%ID/g) of ^{125}I-labeled fusion protein was detected in lungs of C57 BL6 mice within 60 min vs < 4%ID/g in lungs of PECAM-1 knockout mice. By virtue of the high level of PECAM-1 in pulmonary vasculature, lung uptake of fusion protein didn't reach plateau even at the dose of 300 ug. In a mouse pulmonary embolism model, 300 and 100 ug of fusion proteins yielded 87.8±0.4% and 67.5±1.9% fibrinolysis *vs* 59.6±1.7% and 43.7±5.2% by equivalent doses of non-targeted urokinase. Construction of recombinant fusion protein could avert several apparent disadvantages of chemical conjugation such as random coupling and possibility to interfere with the functional properties, as well as reducing immunogenicity. Vascular targeting of genetically engineered fusion protein represents a promising strategy for the treatment of acute pulmonary vascular diseases.

Acute Ras expression induces apoptosis in THYROID cells

A. Fikaris[1], A. Lewis[2], G. Cheng[1], J. Meinkoth[1]
[1]Department of Pharmacology, University of Pennsylvania, Philadelphia, PA [2]Department of Biomedicine, University of Bergen, Norway

Activating Ras mutations are commonly detected in thyroid adenomas and carcinomas, and are thought to be initiating factors in thyroid cell transformation. Recently, acute activation of Ras has been implicated in triggering genomic instability and apoptosis in thyroid cells. These findings highlight that cell proliferation and cell death are tightly linked. Moreover, evidence has emerged that the critical switch between cell cycle progression and apoptosis is governed by differential regulation of cell cycle proteins. Cell death may be a consequence of an aberrant increase in cell cycle progression involving cyclin A and CDK-2. We have previously shown that chronic expression of activated Ras enhanced sensitivity to suspension-, LY-, and PD-mediated apoptosis in Wistar rat thyroid cells. Acute expression of activated Ras induced S and G2 phase progression, with subsequent apoptosis. Our goal is to elucidate the mechanism by which acute expression of Ras stimulates apoptosis. Preliminary data revealed that acute Ras expression induced caspase-3 cleavage in detached, apoptotic cells. Immunostaining of adherent cells revealed an increase in active caspase-3 by day 2 post-infection, demonstrating that apoptosis was not a consequence of detachment. Further, Ras induced DNA laddering. Together, these data confirm that the observed cell death was apoptosis. Acute expression of Ras induced CDK-2 activity in attached and detached cells, with kinetics that correlated with apoptosis rather than S phase entry. To determine the mechanism of CDK-2 activation, we examined CDK-2 expression as well as the expression of three important CDK-2 regulators, cyclins A and E, and p27. Ras upregulated CDK-2 and cyclins A and E, and downregulated p27 expression in a time-dependent manner. Cyclin A and p27 were cleaved in detached cells. Together, these data suggest that acute expression of activated Ras triggers apoptosis in thyroid cells via the deregulation of important cell cycle regulatory proteins.

Sustained endothelial delivery of catalase via ICAM-1 recycling pathway

Christine M. Gajewski[1], Silvia Muro[1], Michael Koval[1,3] and Vladimir R. Muzykantov[1,2]
Institute for Environmental Medicine[1]. Departments of Pharmacology[2] and Physiology[3]. University of Pennsylvania School of Medicine. Philadelphia. PA.

Affinity nanocarriers (NC) can be designed to improve vascular drug delivery. InterCellular Adhesion Molecule (ICAM)-1, which is up-regulated and functionally involved in pathological processes including oxidative stress, is a good target for NC delivery. Anti-ICAM/NC deliver catalase into endothelial cells and protect against H_2O_2-induced injury. However, protection is transient (2 h) due to lysosomal degradation of catalase. To determine whether the therapeutic window could be expanded using sustained delivery of anti-ICAM/NC, we studied fate of the target molecule, ICAM-1, after uptake of anti-ICAM/NC. We found that ICAM-1 disappears from the cell surface concomitantly to anti-ICAM/NC internalization, but partially recycles to the plasma membrane 1 h after NC uptake. This enables a second dose of anti-ICAM/NC to bind to and be internalized by endothelial cells both in culture and *in vivo* after IV injection in mice. Pulmonary targeting of a second dose of anti-ICAM/NC injected 15 min after the first dose was decreased by 50%, but recovered between 30 min and 2.5 h, comparable to cultured endothelial cells. Internalized anti-ICAM/NC did not affect cell viability or fluid phase endocytosis and trafficking. However, lysosomal trafficking of the second dose of anti-ICAM/NC was decelerated minimum two folds, thus the major fraction resided in pre-lysosomal vesicles for at least 5 h without degradation. As a result, successive administration of two doses of anti-ICAM/NC/catalase to endothelial cells prolonged anti-oxidant protection by at least 4 fold, mainly due to delayed intracellular processing of the second dose of NC. These results indicate that ICAM-1 recycling maintains the capacity for recurrent intracellular targeting of catalase to endothelial cells. This maneuver (administration of either multiple doses or long circulating anti-ICAM/NC/catalase) will enhance protective potency in acute pathological conditions associated to vascular oxidative stress, including acute lung injury and ischemia-reperfusion injury.

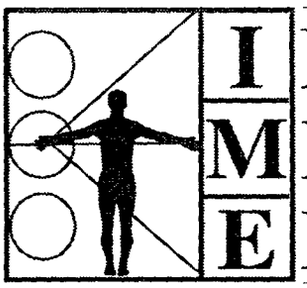

INSTITUTE FOR MEDICINE AND ENGINEERING

UNIVERSITY OF PENNSYLVANIA

I
M
E

2004 Symposium

December 2, 2004

Biomedical Research Building
421 Curie Boulevard
University of Pennsylvania
Philadelphia

Items 17-19

Endothelial Adhesion Molecules as Therapeutic Targets

Vladimir Muzykantov, M.D., Ph.D.
Silvia Muro, Tom Dziubla, Vladimir Shuvaev
Department of Pharmacology and Institute for Environmental Medicine

Many enzymes currently available in highly purified and/or recombinant forms could find therapeutic use, yet sub-optimal bioavailability and delivery to target cells restrict their utility. In order to achieve more effective and specific protection against vascular oxidative stress, we optimize delivery to endothelial cells of anti-oxidant enzymes such as catalase decomposing H_2O_2. To facilitate catalase binding to endothelium, we couple it with monoclonal antibodies against PECAM-1 and ICAM-1, cell adhesion molecules expressed on the endothelial surface. These determinants are involved in inflammation, oxidative stress and thrombosis; hence their inhibition by targeted drugs might provide secondary benefits. Endothelium does not internalize ICAM-1 or PECAM-1, which thus represent good determinants for targeting of monomolecular conjugates and fusion proteins to the luminal surface. However, endothelial cells internalize multivalent anti-CAM conjugates via a peculiar endocytotic pathway distinct from clathrin- and caveoli-mediated mechanisms. This pathway affords intracellular immunotargeting of antioxidant enzymes to endothelium, thus permitting to detoxify harmful reactive oxygen species formed by or/and diffusing into endothelial cells in cell culture and animal experiments. Intracellularly delivered catalase retains enzymatic activity for several hours prior to lysosomal degradation. Auxiliary drugs that delay lysosomal traffic and degradation prolong protective effects of internalized catalase. Furthermore, loading of catalase into PLGA-PEG polymer carriers (diameter 200-400 nm, which is within the range of CAM endocytotic capacity) restricts proteolysis of the cargo catalase that effectively decomposes H_2O_2 diffusing through the polymer shell. Deciphering of molecular and cellular mechanisms of targeted recognition of endothelial cells and sub-cellular traffic and rational design of polymer nanocarriers minimizing degradation of cargo enzymes en route and in site of destination represent key components of novel drug delivery systems for treatment of a plethora of disease conditions involving acute vascular oxidative stress.

B.Kozower, M.Christofidou-Solomidou, T.Sweitzer, S.Muro, D.Buerk, C.Solomides, S.Albelda, G.A.Patterson and V.Muzykantov (2003) Immunotargeting of catalase to the pulmonary endothelium alleviates oxidative stress and reduces acute transplantation lung injury. *Nature Biotech.*, 21:392-398

S.Muro, R.Wiewrodt, A.Thomas, L.Koniaris, S.Albelda, V.Muzykantov and M.Koval (2003) A novel endocytic pathway induced by clustering endothelial ICAM-1 or PECAM-1. *J Cell Sci.*, 116:1599-1609

M.Christofidou-Solomidou, A.Scherpereel, R.Wiewrodt, K.Ng, T.Sweitzer, E.Argiri, V.Shuvaev, C.Solomides, S.Albelda and V.Muzykantov (2003) PECAM-directed immunotargeting of catalase to endothelium protects against pulmonary vascular oxidative stress. *Am.J.Physiol. Lung Mol.Cell.Physiol.*, 285:L283-L292

S.Muro, X.Cui, C.Gajewski, V.Muzykantov and M.Koval (2003) Slow intracellular trafficking of catalase nanoparticles targeted to ICAM-1 protects endothelial cells from oxidative stress. *Am.J.Physiol., Cell Physiol.*, 285(5):C1339-47

Microscale Tissue Engineering: Lessons in Form and Function

Qiu, Weining
Predoctoral

Characterization of Surface-Adsorbed Antibody Particle Binding to the Endothelium

Weining Qiu[1], Silvia Muro[2], Thomas Dziubla[2], Vladmir Muzykantov[1,2]
[1]Department of Bioengineering
[2]Institute for Environmental Medicine (IFEM)

Vascular immunotargeting of nanocarriers may provide a useful drug delivery method for many therapeutic indications such as antioxidant and enzyme replacement therapy. Previous work in our laboratory has shown that the binding of latex nanocarriers (100nm diameter) using anti-ICAM antibodies resulted in a high level (~200 beads/cell) of binding to endothelial cells (HUVEC). Data from other labs show that binding of 5•m microspheres coated with the same antibody to HUVEC under flow was dramatically less effective (<1bead/cell). In order to elucidate the reason for this disparity in binding efficiency, we have conducted a series of experiments determining the relative contributions of key parameters, including antibody surface density, particle concentration and particle size. At a particle concentration of 683,000 beads/cell, beads coated with different surface antibody densities (7000/•m^2, 4300/•m^2 and 2500/•m^2) displayed different binding efficiency to HUVEC cells (174, 129, 39 beads/cell, respectively). In addition, dose-dependent curves corresponding to the 3 different antibody surface densities indicate that at higher particle concentrations, one can reach a maximum binding level (~280 beads/cell). We also saw larger size beads (500nm) coated with the same antibody surface density (4300/•m^2 and 2500/•m^2) displayed higher binding efficiency (155 beads/cell and 57 beads/cell, respectively). These experimental results will also be compared to first principle models describing interactions of particles with endothelium.

Shuvaev, Vladimir
Postdoctoral

INSTITUTE FOR MEDICINE AND ENGINEERING
UNIVERSITY OF PENNSYLVANIA

Targeted delivery of superoxide dismutase via immunoconjugation to endothelium protects against xanthine oxidase-induced oxidant stress and angiotensin II-induced hypertension.

Vladimir V.Shuvaev[1], Samira Tliba[1], Karine Laude[2], David G.Harrison[2], and Vladimir R.Muzykantov[1]
Institute for Environmental Medicine[1], School of Medicine, Philadelphia, PA; Division of Cardiology[2], Emory University School of Medicine, Atlanta, GA 30322.

Superoxide anion, a free radical produced in cells by several enzymes as a by-product of substrate oxidation, can directly inactivate a key vasodilating agent NO and indirectly cause oxidant stress via formation of peroxinitrate and H_2O_2 that can further convert into strong oxidants. Superoxide dismutase (SOD) accelerates superoxide conversion into H_2O_2 and thus maintains NO effects and helps to protect cells against oxidant stress. Using streptavidin as a cross-link for biotinylated proteins we prepared immunoconjugate containing anti-PECAM antibody and SOD that retained 50% of its initial enzymatic activity after biotinylation and conjugation. Anti-PECAM/SOD conjugate, but not non-immune IgG/SOD counterpart, significantly increased survival of umbilical vein endothelial cells exposed to hypoxanthine-xanthine oxidase. Anti-PECAM/^{125}I-SOD showed 12-times higher pulmonary uptake 1 h post IV injection in mice that non-immune counterpart, and roughly 30% of injected SOD was found in other organs including the heart, reflecting specific binding to vascular endothelium. Functional activity of anti-PECAM/SOD was studied in a mouse model of hypertension induced by chronic angiotensin II (Ang II) infusion. Micropump was implanted subcutaneously in mouse and Ang II was infused at a constant rate during 14 days. Thoracic aorta was harvested 15 min post IV injection of immunoconjugates. H_2O_2 level in the tissue was measured with Amplex Red assay and vasorelaxation by acetylcholine was measured on 5-mm ring aorta segments. Anti-PECAM/catalase, but neither anti-PECAM/SOD nor free SOD decreased H_2O_2 level in aorta. However, injection of 20 μg of anti-PECAM/SOD normalized the vasorelaxation (Ang II infusion significantly impaired vasorelaxation compared to control), whereas free SOD had little effect and anti-PECAM/catalase did not have any effect. Thus, SOD immunotargeting may be a useful protective tool in pathological states where overproduced superoxide anion plays a role in pathogenesis, such as NO inactivation in hypertension.